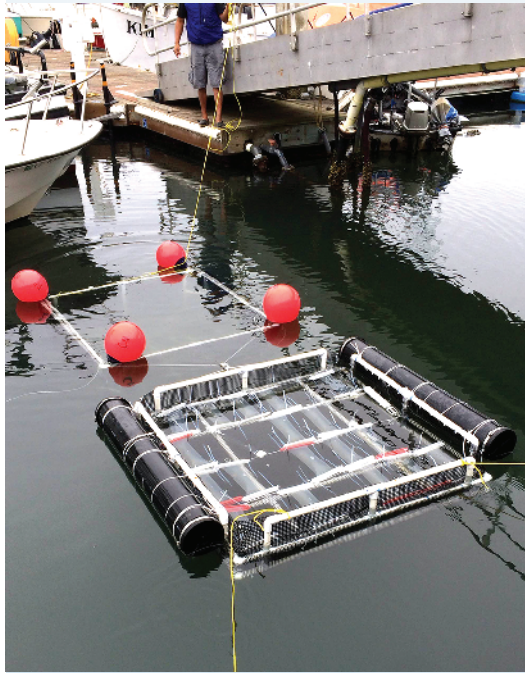


Determination of DNA-based Fecal Marker Aging Characteristics for Use in Quantitative Microbial Source Tracking



Yiping Cao
Gary L. Andersen
Alexandria A. Boehm
Patricia A. Holden
Jennifer A. Jay
John F. Griffith

Southern California Coastal Water Research Project

SCCWRP Technical Report 978

Determination of DNA-based Fecal Marker Aging Characteristics for Use in Quantitative Microbial Source Tracking

Yiping Cao¹, Gary L. Andersen², Alexandria A. Boehm³, Patricia A. Holden⁴,
Jennifer A. Jay⁵, John F. Griffith¹

¹*Southern California Coastal Water Research Project*

²*University of California, Berkeley*

³*Stanford University*

⁴*University of California, Santa Barbara*

⁵*University of California, Los Angeles*

April 2017

SCCWRP Technical Report 978

TABLE OF CONTENTS

Executive Summary	1
Project Overview	4
Methods	5
Overall Project Design	5
In-situ Field Studies	6
Sediment Effect Laboratory Investigation.....	8
Water Matrix Effect Laboratory Investigation.....	9
Decay Data Analysis.....	9
Results	10
Field Decay Studies	10
Sewage-Marine water	15
Sewage-Brackish water	15
Sewage-Freshwater.....	16
Cow-Freshwater	16
Gull-freshwater	17
Community Analysis Results	17
Sediment Effect Investigation.....	18
Water Matrix Effect Investigation.....	19
Discussion	20
Regarding Relative Degradation	20
Regarding MST Data Interpretation	20
Ratio Model	20
Human Fecal Score	21
Literature Cited.....	23
Appendix A: Relative Decay of Sewage Fecal Material in Marine Waters	27
Introduction.....	27
Methods	28
Study Design	28
Physical Measurements.....	30
Culture-based Fecal Indicator Bacteria Enumeration	30
Salmonella.....	30
Results	34

Decay Models	36
Human-Associated Fecal Markers Versus General FIB	38
Culture-Based Versus Molecular-Based General FIB	38
Impact of UVB Exposure and Season	40
Enteric Pathogen Decay	41
Bag Effects on Nutrient and Chlorophyll Concentrations	42
Quality Assurance/Quality Control	42
Additional Methods and Results	42
Literature Cited.....	43
Supporting Information	46
Methods.....	46
Results.....	46
SI References	55
Appendix B: Relative Decay of Sewage Fecal Material in Brackish Waters.....	56
Introduction.....	56
Materials and Methods	57
Study Area.....	57
Field Deployments	57
Sampling Procedures.....	57
Laboratory Analyses	58
Decay Modeling and Statistical Analyses.....	59
Results	60
qPCR Quality Assurance and Controls	60
Physical Lagoon and Chamber Characteristics.....	61
Nutrient Availability in Raw Sewage, Ambient Lagoon Water and Chambers.....	63
FIB, Fecal DNA Markers, and Pathogens in Raw Sewage and Ambient Lagoon Water	65
FIB Decay Kinetics.....	66
Literature Cited.....	73
Supplementary Information.....	76
Equations.....	76
Fecal DNA Marker Decay Kinetics	76
Bacterial Pathogen and Virus Decay Kinetics	77
Decay Comparison between FIB, Fecal DNA Markers and Pathogens	78
Appendix C: Relative Decay of Fecal Material in Fresh Waters.....	92
Introduction.....	92

Methods.....	92
Results	98
Sewage field studies	98
Cow fecal field studies	102
Gull fecal field studies	106
Literature Cited.....	110
Appendix D: Community Analysis of Fecal Material Degradation in Marine, Brackish and Fresh Waters	111
Introduction.....	111
Material and Methods	111
Illumina sequencing	111
PhyloChip array	111
Statistical analysis	111
Results	112
Tracking the decay of the microbial community over time	113
Fecal contamination methodology comparison	114
Preliminary conclusions	116
Literature Cited.....	117
Appendix E. Sediment Effect Investigation.....	118
Introduction.....	118
Methods	118
Sediment Collection and Characterization	118
Microcosm Setup	119
Sampling and Analysis.....	119
Culturable Pathogens and Fecal Indicator Bacteria (FIB) Analysis.....	120
Marker Analysis	120
Data analysis and Statistical Analysis	121
Results	121
Sediment Characteristics	121
Decay in Sediment.....	122
Markers.....	127
Decay in the Different Sediments.....	128
Decay in Water Column	133
Literature Cited.....	135
Appendix F. Water Matrix Effect Investigation.....	137

Introduction.....	137
Methods	137
Field water collection	137
Sewage.....	138
Outdoor mesocosms.....	138
Mesocosm setup.....	138
Sample collection.....	139
Sample processing and analysis.....	139
Decay modeling.....	139
Results	140
Decay rates	140
Relationships between decay rates and water matrices.....	143
Supporting Information	145
Appendix G. Ratio Model: The Effect of Aging on the Use of the Source Allocation Model	146
Introduction.....	146
Methods	146
Results	148
Marine waters	148
Freshwaters.....	150
Brackish site	151
Summary.....	152
Literature Cited.....	155
Appendix H. Human Fecal Score (HFS).....	156
Background	156
Completed Work Task 1: Model description.....	156
Completed Work Task 2: Sensitivity analysis results	158
Completed Work Task 3: Model use recommendation for site ranking.....	160
Effect of Marker Degradation	162
Literature Cited.....	163

EXECUTIVE SUMMARY

Escherichia coli and enterococci are fecal indicator bacteria (FIB) used to assess surface water quality around the world. In California's built environment, their presence in bathing water is associated with human illness when the bacteria arise from sources such as faulty sewer infrastructure, wastewater and urban runoff. However, FIB can originate from many other fecal and non-fecal sources, including animal feces, beach wrack, sands, and submerged vegetation, with little or reduced risk of human illness.

Identifying FIB sources through microbial source tracking (MST) is therefore essential for two important management scenarios: remediating contaminated surface waters and determining potential health risks to swimmers.

MST approaches have greatly advanced with the advent of fecal source-associated assays (i.e., qPCR quantification of DNA-based markers) able to identify the presence of an increasing number of animal sources of FIB, but implementation of MST in the two essential management scenarios remains difficult. This difficulty is due to serious limitations in the ability to accurately interpret DNA-based marker information. One major limitation is that knowledge of marker prevalence and performance has been obtained mostly from "fresh" fecal material in the laboratory, and it is not clear how aging of fecal material in the environment affects marker performance and data interpretation. During "aging," various environmental processes (e.g., inactivation, predation, adsorption to particles) may change the relative abundance of the different constituent microorganisms found in feces from that of the "fresh" sample.

The goals of this study were to answer two main questions surrounding DNA-based MST markers:

1. What are the relative decay rates of DNA-based markers, FIB (*E. coli* and enterococci), and representative pathogens, as well as the whole microbial community, from sewage, cow feces, and bird feces, under environmental conditions relevant to the California coast?
2. Given the assessed patterns of DNA-based marker aging in fecal contamination, juxtaposed against FIB aging patterns, how can water quality managers best use MST data to diagnose the presence and amount of contamination from specific fecal hosts for a sampled site (i.e., beach or site along an MST sampling transect)?

To answer these questions, this project examined relative degradation of FIB, DNA-based markers, and pathogens through both *in-situ* field experiments as well as *ex-situ* laboratory experiments.

The *in-situ* field aging studies were conducted at three sites representing the typical surface water types in California: a freshwater site, a brackish water coastal lagoon site, and a marine, nearshore site. The design utilized diffusive dialysis bags that allow equilibrium of environmental conditions inside and outside the bags, thus allowing the decay of fecal microbes (inside the bags) to be monitored under realistic field conditions. The effects of environmental factors such as season and sunlight were assessed through replicating the study at each site during winter, summer with no shading, and summer with shading. Sewage, cow feces, and gull feces served as microbial seeds for these experiments.

The laboratory experiments expanded what could be assessed in the field by individually examining the effect of the water matrix and sediment on relative degradation of sewage fecal organisms. In the water matrix effect investigation, sewage aging in 12 waters (i.e., 3 from each of the 4 California regions represented by the project PIs) was investigated via an outdoor mesocosm study. In the sediment effect investigation, sewage aging in the presence of each of three types of sediment (i.e., freshwater, brackish and marine water sediment from the three sites of the *in-situ* field aging study) was investigated via a separate outdoor microcosm study. In all experiments, representative FIB, MST markers and pathogens, as well as the entire microbial communities, were measured for each fecal source.

Overall, there was no universal trend regarding degradation of MST markers relative to FIB and pathogens observed in this project. Whether the three target groups experienced differential degradation, and to what extent, depended on the combination of environmental conditions (i.e., field site, season, sunlight) and fecal source, whether the MST markers were *Bacteroidales* or *Catelliboccus*.

Nevertheless, while the *Bacteroidales* MST markers did not always show higher decay rates than pathogens and cultivable FIB, these MST markers rarely showed decay rates lower than the other two groups. The gram-positive *Catelliboccus* gull MST marker appeared to be a more conservative marker than the gram-negative *Bacteroidales* human, cow and dog MST markers, showing decay rates more similar to those of pathogens and *Enterococcus* DNA markers. While non-specific, the *Enterococcus* DNA markers generally appeared to be a conservative marker for indicating fecal contamination and potential human health risk.

In practice, our results demonstrate that commonality regarding relative degradation may not be expected across sites, although similar decay between certain targets might be assumed under certain conditions. This was likely because different abiotic and biotic factors were the dominant factors affecting decay at different field sites. A holistic model integrating these various factors, if achievable, might be most useful for beach managers in predicting degradation behaviors at their local sites. A preliminary model integrating sunlight intensity, color and depth of environmental water has been developed, representing one step forward towards such a goal.

To assist managers interpreting results, two quantitative MST models were developed:

- 1) A ratio model for potential fecal source allocation
- 2) A human fecal score for assessing the extent of human fecal contamination at a site

Theoretically, the proportion of fecal contamination in a water sample attributable to a single source can be determined using a ratio method. However, the accuracy of this model relies on all markers decaying at a similar rate. As there is currently no simple method available for estimating the fecal contamination age, source allocation models must either be restricted to use on fresh fecal contamination scenarios or used with analytes that decay at a similar rate in the environment. Based on the results of our field studies, there are only certain rare conditions when decay rates are close enough to make this model viable. The ratio source allocation model therefore may only be used in environmental conditions where decay constants of FIB and MST markers are not expected to be different.

Quantitatively characterizing a site regarding its extent of human fecal contamination for site remediation prioritization and effectiveness evaluation generally requires integrating human marker results across multiple samples from a site. Previously, this was mostly done via the best professional judgement (BPJ) available within the premise of each individual project. Recent research has demonstrated tremendous variability/uncertainty/inconsistency in the BPJ approaches for MST data interpretation, and it was concluded that a mathematically defined standardized algorithm was needed. Thus, a human fecal score (HFS) was developed to provide such an assessment based on HF183 qPCR measurements.

The application of HFS is based on the collective results from daily morning water samples from a beach site. Model sensitivity analysis was conducted to demonstrate how HFS can be used to optimize study design parameters such as sample size (i.e., number of days sampled at the beach site) and qPCR replication (i.e., number of qPCR replicates analyzed per sample) HFS. Decision charts on sample size and PCR replication were developed for the management application of site prioritization (Appendix H).

However, it is important to consider how HF183 marker degradation may affect application of HFS. A wide range of decay rates ($k = <1 \text{ day}^{-1}$ to 6 day^{-1} , in $C = C_0 e^{-kt}$) were observed for the HF183 marker in this project: marine waters ($k = 1-2$), brackish waters ($k = 1-6$), freshwater ($k = 1-5$), water matrix laboratory

study ($k=1-5$), sediment ($k=1-2$). These rates translate to <0.5 to $<3 \log_{10}$ reduction per day. Assuming a starting concentration of HF183 from fresh sewage input to be $6 \log_{10}$ copy per 100ml (5% sewage measured in this project averaged $6.7 \log_{10}$ copies of HF183 per 100ml), the HF183 signal would disappear in two days under the fastest decay rates observed in this project. If the sewage fecal source is introduced locally at the beach with a daily sampling scheme, the HFS would be integrating both the fresh and aged HF183 signals under most decay conditions. Nevertheless, with a less frequent sampling scheme (e.g., only once every two days), it would be possible to miss the HF183 signals under environmental conditions enabling the highest decay rates. It is therefore important for managers to consider the extent of potential decay on the spectrum of rates observed in this project, and adjust sampling design accordingly (more details in Appendix H).

This project is the first ever to determine decay constants for such a large number of MST markers, FIB, and pathogens under environmental conditions. Although the Ratio Model may not be useful under most conditions, valuable information about how microbes behave in a range of environmental conditions was gleaned from this study. Even outside the context of a model, this information will help beach managers and researchers as they take on the arduous task of microbial source identification. Further, the Human Fecal Score Model will allow managers to prioritize beaches for remediation or Quantitative Microbial Risk Assessment studies.

PROJECT OVERVIEW

Escherichia coli and enterococci are fecal indicator bacteria (FIB) used to assess surface water quality around the world. In California's built environment, their presence in bathing water is associated with human illness when the bacteria arise from sources such as faulty sewer infrastructure, wastewater and urban runoff (Wade et al. 2003, Kay et al. 1994, Haile et al. 1999, Cabelli et al. 1982). However, FIB can originate from a number of other fecal and non-fecal sources with little or reduced risk of human illness including animal feces, beach wrack, sands, and submerged vegetation (Imamura et al. 2011, Yamahara et al. 2007, Boehm et al. 2003, Desmarais et al. 2002, Yamahara et al. 2009, Gast et al. 2011, Halliday and Gast 2011, Ferguson and Signoreto 2011, Valiela et al. 1991, Anderson et al. 1997, Badgley et al. 2010, Whitman et al. 2003, USEPA 2007).

Identifying FIB sources through microbial source tracking (MST) is therefore essential for two important management scenarios: remediating contaminated surface waters and determining potential health risks to swimmers.

However, while MST approaches have greatly advanced with fecal source-associated assays (i.e., qPCR quantification of DNA-based markers) now available to identify the presence of an increasing number of animal sources of FIB (Bernhard et al. 2000, Dick et al. 2005, Dick et al. 2005, Layton et al. 2006, Reischer et al. 2006, Kildare et al. 2007, Okabe et al. 2007, Shanks, et al. 2008, Shanks et al. 2009, Jeter et al. 2009, Lamendella et al. 2009, Sike and Nelson 2009, Mieszkin et al. 2009, Mieszkin et al. 2010, Lu et al. 2008, Shibata et al. 2010, Seurinck et al. 2005, Haugland et al. 2010, Johnston et al. 2010, Reischer et al. 2007, Lee et al. 2010), implementation of MST in the two essential management scenarios remains difficult. This is due to serious limitations in accurately interpreting DNA-based marker information acquired through field sampling and sample analysis. One major limitation is that knowledge of marker prevalence and performance has been obtained mostly from "fresh" fecal material in the laboratory, and it is not clear how aging of fecal material in the environment affects marker performance and data interpretation. Here, "aging" refers to the time lapse from when fecal material is released into the environment, migrates through various matrices, and is subsequently detected in ambient water. During "aging", various environmental processes (e.g., inactivation, predation, absorption to particles) may change the relative abundance of the different constituent microorganisms found in feces from that of the "fresh" sample.

For instance, FIB source allocation is greatly useful for remediating contaminated surface waters and assessing potential public health risks. However, source allocation is hampered by the disconnection between water quality monitoring (based on FIB) and MST (based on markers) and is further complicated by fecal aging. As fecal material from different hosts varies greatly in its FIB (i.e. enterococci) content, as well as in its host-associated DNA-based marker content, greater marker concentrations may signal different relative enterococci contributions from each host. Currently, no sound method is available for inferring how many enterococci arise from each possible source, e.g. on the basis of DNA-based marker concentration, even if marker abundance can be related back (e.g. through a ratio method) to the host fecal material's proportional enterococci content. This is because the current understanding of relative enterococci contributions from different hosts is based on DNA-based marker abundance for "fresh" feces. Yet DNA-based markers and enterococci from different sources are known to decay in the environment – albeit at unknown rates. Therefore, the use of MST data for FIB source allocation cannot be validated until the relative degradation characteristics of FIB and MST markers are understood.

Similarly, being able to distinguish between fecal sources (e.g. human vs. non-human) with high certainty has great value for prioritizing remediation efforts and assessing potential public health risk, because fecal sources differ in their potential to cause human illnesses. Yet, efforts to link sources to risk are hampered by the disconnect between MST (based on markers) and risk assessment (based on pathogens) and is further complicated by fecal aging in the environment. MST marker assays have varied sensitivity (i.e.,

ability to reliably produce a positive result when the target source is present) and specificity (i.e. ability to produce a negative result when the target source is absent), mainly due to variations in marker prevalence (in target and non-target sources) and in assay design (e.g. primer, probe and reaction conditions). As marker assays have shown relatively high sensitivity and specificity in laboratory evaluation studies, detection and high concentrations of human markers should signal the presence of human fecal material (i.e. and pathogens by inference). However, because such marker performance has previously been assessed using only “fresh” fecal sources, it is unclear if an absence of detection of human markers in the field indeed reflects absence of human fecal material (and therefore pathogens). The validity of using MST data to infer fecal (or pathogen) presence cannot be established until the relative degradation characteristics of MST markers and pathogens under environmental conditions are understood.

Our study therefore is aimed at gathering urgently needed data and knowledge regarding how DNA-based fecal markers change in ambient environments. Specifically, we investigated the relative degradation characteristics of FIB, DNA-based markers, and pathogens. Understanding how this information can be used to improve MST implementation for management applications is critical for establishing the applicability of quantitative MST tools for high priority management applications.

Our research questions for the overall project are:

1. What are the relative decay rates of DNA-based markers, FIB (*E. coli* and enterococci), and representative pathogens, as well as the whole microbial community, from sewage, cow feces, and bird feces under environmental conditions relevant to the California coast?
2. Given the assessed patterns of DNA-based marker aging in fecal contamination, juxtaposed against FIB aging patterns, how can water quality managers best use MST data to diagnose the presence and amount of contamination from specific fecal hosts for a sampled site (i.e., beach or site along an MST sampling transect)?

Methods

Overall Project Design

This project examined relative degradation of FIB, DNA-based markers, and pathogens through both *in-situ* field experiments, as well as *ex-situ* laboratory experiments.

The *in-situ* field aging studies were conducted at three sites representing the typical surface water types in California: a freshwater site, a brackish water coastal lagoon site, and a marine, nearshore site. The design utilized diffusive dialysis bags that allow equilibrium of environmental conditions inside and outside of the bags, thus allowing the decay of fecal microbes (inside the bags) to be monitored under realistic field conditions. The effect of environmental factors such as season and sunlight were assessed through replicating the study at each site during winter, summer with no shading, and summer with shading. Sewage, cow feces, and gull feces served as microbial seeds for these experiments.

The laboratory experiments expanded what could be assessed in the field by individually examining the effect of the water matrix and sediment on relative degradation of sewage fecal organisms. In the water matrix effect investigation, sewage aging in 12 waters (i.e., 3 from each of the 4 California regions represented by the project PIs) was investigated via an outdoor mesocosm study. In the sediment effect investigation, sewage aging in the presence of each of three types of sediment (i.e., freshwater, brackish and marine water sediment from the three sites of the *in-situ* field aging study) was investigated via a separate outdoor microcosm study.

For all experiments, representative FIB, MST markers and pathogens, as well as the entire microbial communities, were measured for each fecal source.

***In-situ* Field Studies**

A total of 17 field experiments were conducted representing 17 combinations of water type (field site), fecal source, and environmental condition (Table 1).

Table 1. Description of the 17 *in-situ* field experiments. These deployments at different depths (3cm, 15cm, and 99cm below the water surface) at the marine site served as an analog to the “summer with shading vs. no shading” at fresh and brackish water sites. The sunlight is expected to attenuate with increasing depth, therefore providing a “shading” effect.

Field site	Fecal source	Environmental condition	Number of field replicates	Number of time points analyzed
Freshwater site	sewage	winter	2	7-10
		summer no shading	2	7-10
		summer with shading	2	7-10
	cattle	winter	2	7-10
		summer no shading	2	7-10
		summer with shading	2	7-10
	gull	winter	2	7-10
		summer no shading	2	7-10
		summer with shading	2	7-10
Brackish water lagoon site	sewage	winter	2	7
		summer no shading ^a	2	7
		summer with shading	2	7
Marine site	sewage	winter surface	2	7
		winter medium depth ^a	2	7
		winter depth ^a	2	7
		summer surface	2	7
		summer depth ^a	2	7

The three field sites were Pillar Point Harbor (PPH, Half Moon Bay, CA, 37.502467° N, 122.4838829° W), Arroyo Burro Lagoon (ABL, Santa Barbara, CA, 34.4045167°N, 119.7405944°W), and San Joaquin Marsh (SJM, Irvine, CA, 33° 39' 57.9" N, 117° 50' 46.8" W) for marine, brackish and freshwater, respectively. ABL has a sand berm that periodically breaches, allowing discharge to the surf zone and changes in the salinity of the lagoon. SJM receives mostly urban runoff from and discharges into the adjacent San Diego Creek. Ambient water at the experiment site is similar to that in the creek, but experiments were conducted at SJM instead of the creek itself because of the ease of public access to the creek and potential for vandalism to the experiment.

The 7 or 10-day decay experiments were conducted *in situ* using dialysis bags (6-8 kDa, Spectra/Por®4, Spectrum Labs, Rancho Dominguez, CA) containing a single fecal source (primary influent sewage (5% v/v), cow (1% w/v) or gull (0.1% v/v) feces) seeded into unaltered ambient water from the field site. Dialysis bags were suspended from PVC frames placed in ambient water so that the bags floated at a pre-designated depth, similar to that done in previous studies (Korajkic et al.2013, Korajkic et al. 2013), in the water based on the study design at each field site (Table 1). To provide the “summer no shading vs. summer with shading treatment” contrast at SJM and ABL, half of the PVC frames were covered with one layer of the shade cloth (Easy Gardener Heavy Black Sun Screen Shade Cloth, Home Depot) (Figure 1). To provide the various depth treatments at PPH, the dialysis bags were simply secured at different depths to the PVC frames.



Figure 1. Summer Field deployment photos (from left to right: San Joaquin Marsh freshwater site, Arroyo Burro Lagoon brackish water site, and Pillar Point Harbor marine water site).

The summer deployments were on August 18-28, 2014 at SJM and on September 8-18, 2014 at ABL and PPH. The winter deployments were on January 9-19 at SJM, on February 2-12, 2015 at ABL, and on February 13-20, 2015 at PPH. Primary influent sewage was collected from local wastewater treatment plants, except in the case of the Arroyo Burro Lagoon, where raw wastewater was substituted. Cow and gull fecal material were collected from farms and beaches, respectively, in Orange County.

For each field deployment, daily samples were collected with duplicate dialysis bags, providing two biological replicates. Sample water from within the bags was processed for measurements of three categories of organisms (FIB, MST marker, and pathogens) by culture- and/or PCR-based methods (Table 2). Microbial community analyses, targeting the entire prokaryotic community were also conducted using Illumina MiSeq DNA sequencing and PhyloChip, a DNA microarray method. Details on the field deployments at each site, as well as microbiological and physicochemical measurements are provided in Appendices A, B, and C for PPH, ABL, and SJM, respectively.

Table 2. Summary of microbiological analyses for each fecal source in the field experiments. *Campylobacter* and *Salmonella* analysis by culture were not done for winter deployment at the freshwater site as summer data were mostly non-detectable and provided little value.

Category	Analysis	Sewage	Cattle	Birds
FIB by culture or qPCR/ddPCR	Enterococcus by culture	X	X	X
	<i>E. coli</i> by culture	X	X	X
	Enterol1a	X	X	X
	GenBac3	X	X	X
MST markers by qPCR/ddPCR	HF183	X		
	HumM2	X		
	BacHum	X		
	CowM2		X	
	Catelicoccus			X
Pathogen by culture or qPCR/ddPCR	Norovirus	X		
	<i>Campylobacter</i> by culture ^a	X	X	X
	<i>Salmonella</i> by culture ^a	X	X	X
	<i>Campylobacter</i> by qPCR	X	X	X
	<i>Salmonella</i> by qPCR	X	X	X
Community analysis	PhyloChip	X	X	X
	Illumina	X	X	X

Sediment Effect Laboratory Investigation

A total of six experimental treatments were examined, each with four replicate microcosms. Each microcosm contained high (50% v/v) or low (10% v/v) primary influent sewage in the presence of each of the three sediments. Sediments (top 0-5cm) were collected from each of the three field study sites within 72 hours of the microcosm experiments.

Each microcosm (2L glass pyrex beakers) contained 400ml sewage-seeded sediments and 400ml corresponding artificial water (artificial fresh, brackish and marine waters for the sediments from the fresh, brackish and marine water field sites, respectively). Beakers were covered with polyethylene film secured with Parafilm to limit water loss due to evaporation and to prevent the addition of foreign particles from the environment to the microcosms. Beakers were set up under ambient light conditions in a plexiglass water bath on top of Boelter Hall, UCLA. Throughout the experiment, temperature was maintained at 20 °C using two water chillers, and oxygen content of beakers was maintained by using an airstone in each beaker.

Microcosms were sampled, for both the sediments and overlaying waters, once a day for eight consecutive days for decay of FIB, DNA-based markers, and pathogens. Following removal of the overlying water, approximately 25 g sediment was collected at each time point using a sterile core. 20 g sediment was washed with PBS per standard protocol (Boehm et al. 2009) and eluate processed for FIB and representative pathogens by culture-based methods. For PCR-based analyses, nucleic acid extraction was performed directly on frozen sediment samples (for additional method details see Appendix E).

Water Matrix Effect Laboratory Investigation

A total of 12 treatments were examined, each with duplicate microcosms. Water samples were collected from three sites from each of the four regions: San Mateo County, Santa Barbara County, Los Angeles County, and Orange County. The three sites included a freshwater and a marine water site, plus a site with expected in-between salinity. Microcosms contained primary sewage influent seeded (5% v/v) into each of the 12 waters.

Each treatment microcosm (rectangular glass aquaria) contained 30L of sewage-seeded ambient water. One control microcosm containing 30L ambient water only was set up for each of the 12 waters. The microcosms were setup on the patio of Kerckhoff Marine Laboratory (Newport Beach, CA). All aquariums were placed in six large trays containing circulating seawater to ensure mesocosm water temperature at ambient seawater temperature during the experiments. Each aquarium was equipped with two airstones for mixing and a sterile siphon tube for sampling. The aquariums were not covered, but the depth of the water was monitored to account for evaporation.

Samples were collected at six time points during the 4-day experiment: hour 0 (8am) and hour 6 (2pm) on 4/23/2015, then daily at 8 am till 4/27/2015. Samples were processed and analyzed for FIB, DNA-based markers and representative pathogens (for additional method details see Appendix F).

Decay Data Analysis

In general, quantitative results from culture- or PCR-based assays were analyzed by the GinaFit decay modeling tool (Geeraed et al 2015). Briefly, the classic log linear (LL) decay model and its variations (LL+Shoulder, LL+Tail, LL+Shoulder+Tail, Biphasic, Biphasic+Shoulder) were fit to each time series data set and best fit model was selected. Decay profiles of the different targets were compared by comparing decay rates and/or correlation of time evolution of relevant targets. Statistical comparisons were made using standard statistics software packages (STATA, SPSS, R, etc). More details on decay data analysis are provided in the corresponding Appendices.

Results

Field Decay Studies

Summary of best fit decay models and estimated decay rates are presented in Figures 2 – 6. Figures 2, 3, and 4 summarized sewage decay in marine, brackish, and fresh water field studies, respectively. Figures 5 and 6 summarize cow and gull fecal decay, respectively, in freshwater field studies. *Enterococcus* and *E. coli* were measured by culture-based methods unless otherwise specified in the figure legends. Detailed model fitting results are presented in corresponding appendices (Appendices A, B, and C for marine, brackish and fresh water sites, respectively).

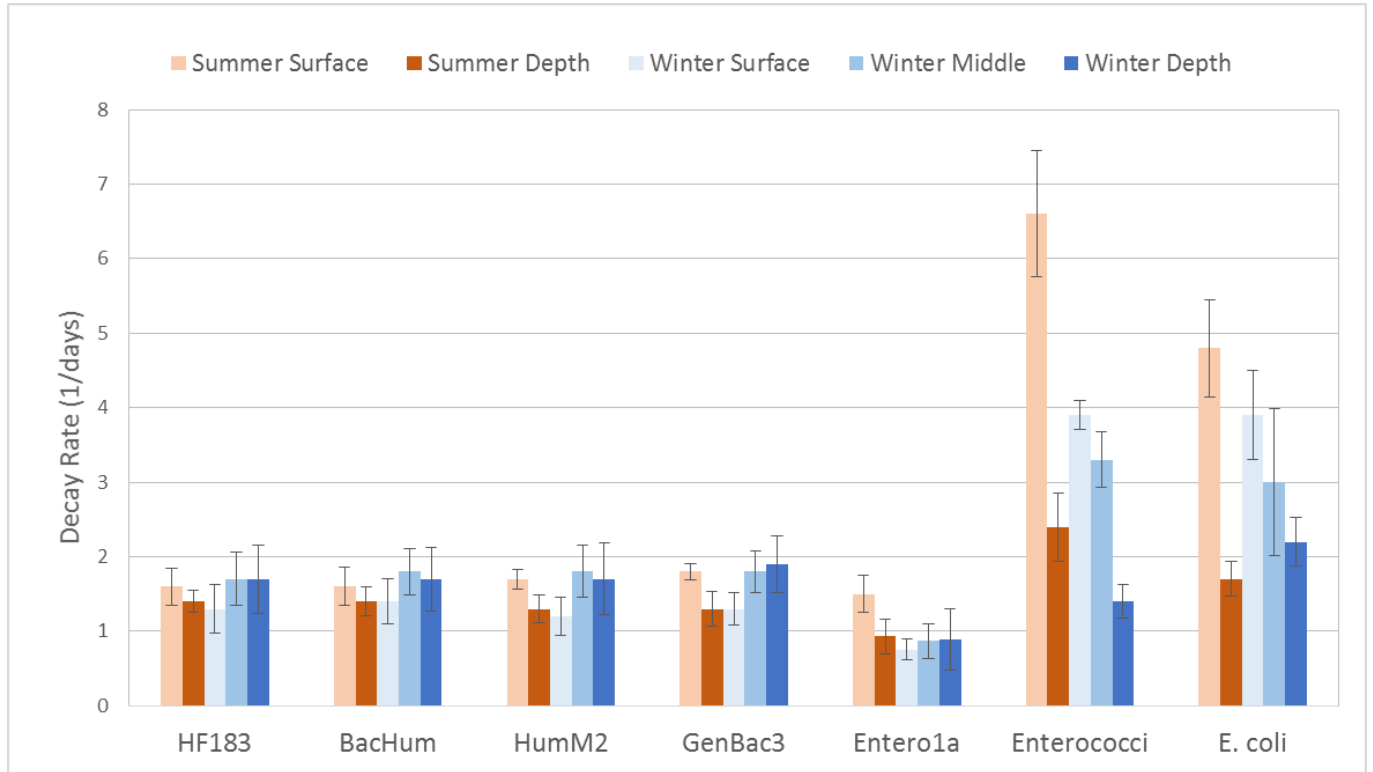


Figure 2. Marine water field studies with sewage: Modeled decay rate coefficients for FIB and MST markers during two seasons (summer and winter) and at three depths. Surface, middle, and depth correspond to the dialysis bags floating 3, 15, and 99 cm below the water surface. All genetic markers (Entero1a, GenBac3, HF183, BacHum, and HumM2) in winter were modeled with LL+Shoulder models while the rest were simple LL models. *Salmonella* (qPCR & culture), *Campylobacter*, and Norovirus GII were too low in starting sewage mixture to model decay. Error bars represent the 95% confidence interval.

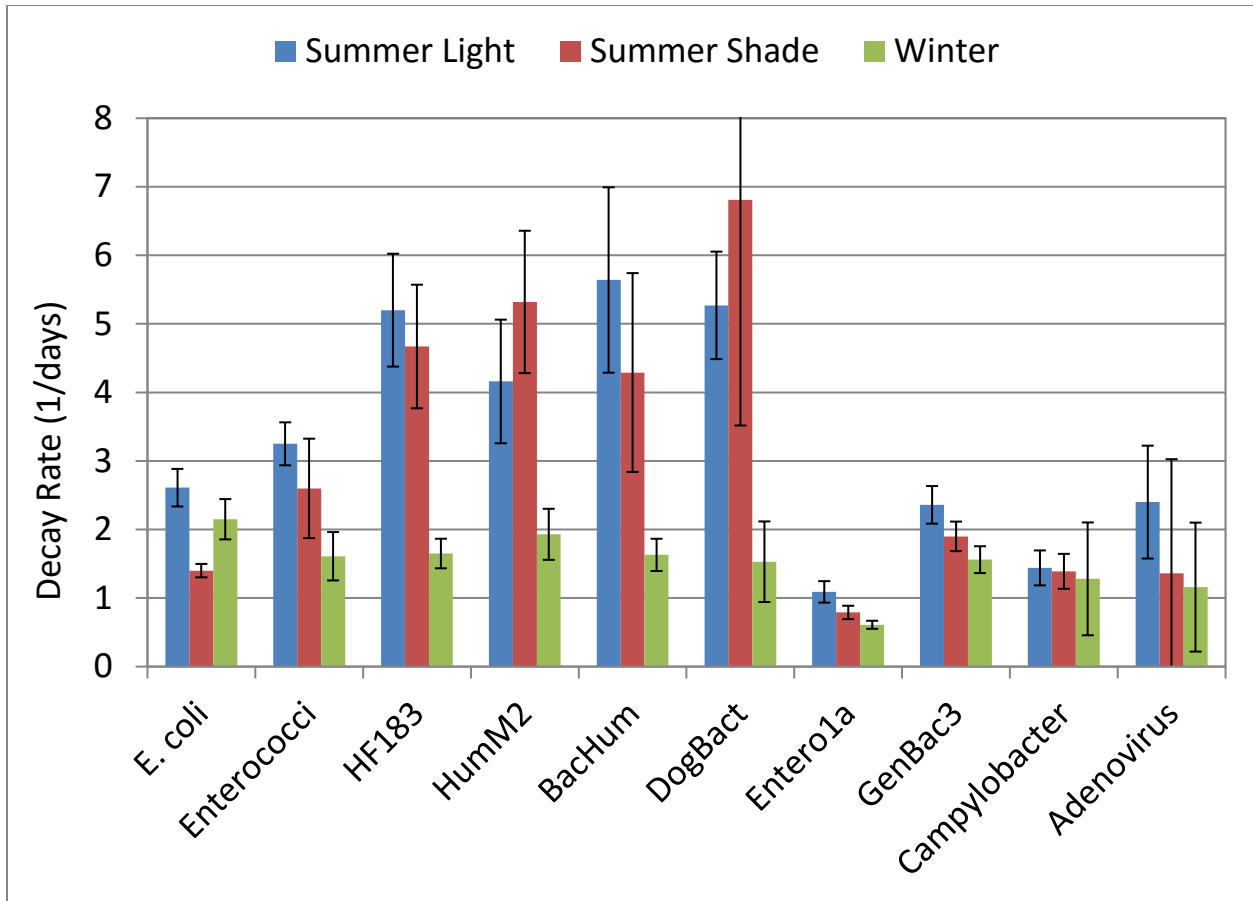


Figure 3. Brackish water field studies with sewage: Modeled decay rate coefficients for FIB, MST markers, and pathogens during two seasons. During the summer, a light vs. shade contrast was examined by applying a shade cloth over half of the dialysis bags. During winter, no shade cloth was applied. All MST markers were modeled with LL+Shoulder models, while most other assays were modeled with simple LL models. Error bars represent the 95% confidence interval.

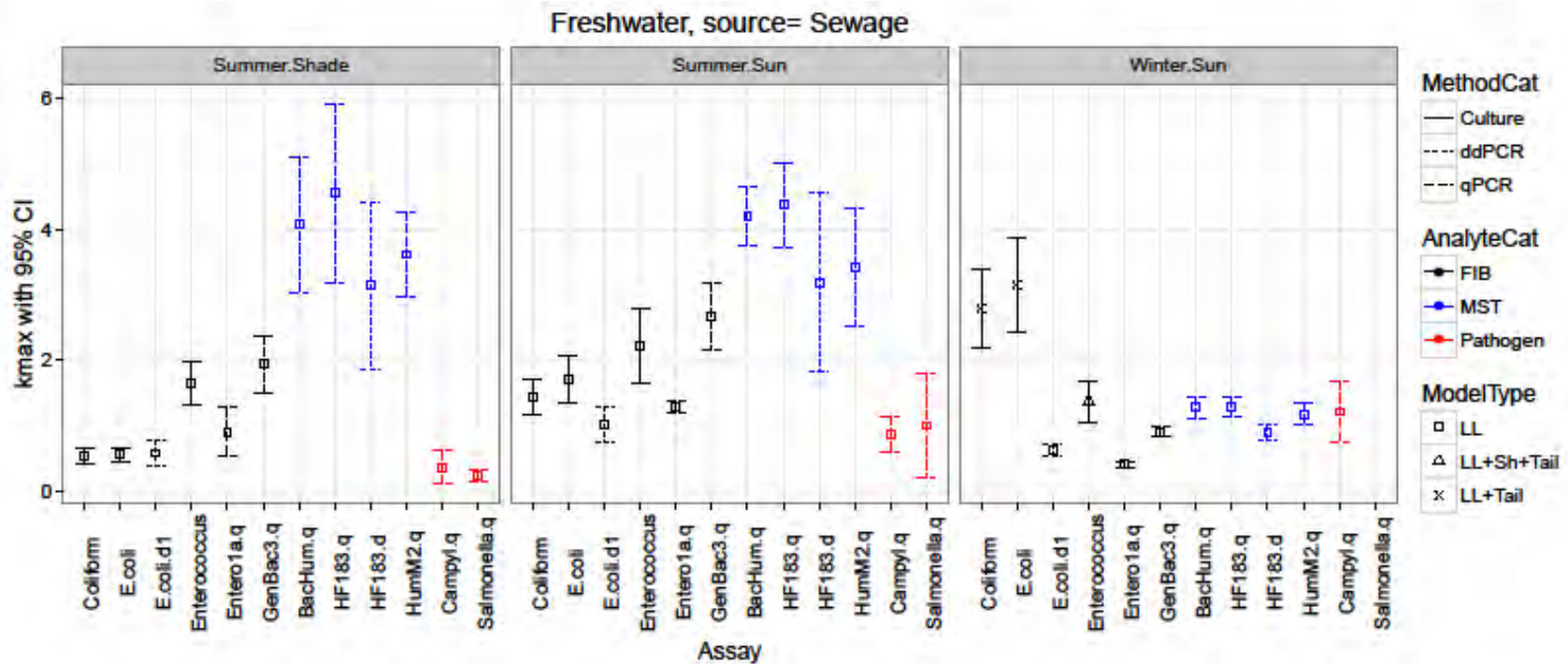


Figure 4. Freshwater water field studies with sewage: Modeled decay rate coefficients for FIB (black), MST markers (blue), and pathogens (red) during two seasons. During the summer, a light vs. shade contrast was examined by applying a shade cloth over half of the dialysis bags, while no shade cloth was applied during winter, resulting in three experiments: Summer.Shade, Summer.Sun, and Winter.Sun. Each subpanel represents one of the experiments as labeled in the banner. Assays with suffixes .q and .d indicate measurement by qPCR and digital PCR, respectively. Assays without suffixes are measured by IDEXX. Error bars represent the 95% confidence interval of decay rates (day^{-1}).

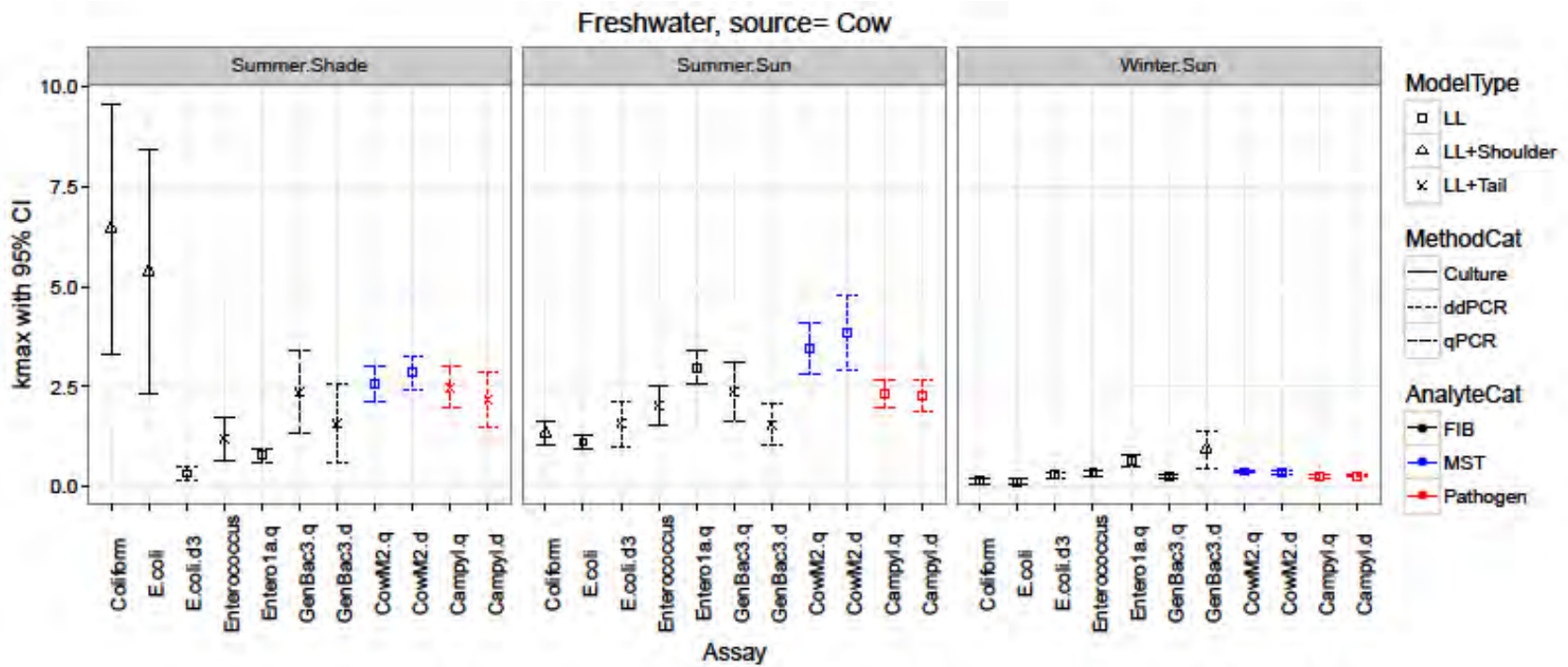


Figure 5. Freshwater water field studies with cow feces: Modeled decay rate coefficients for FIB (black), MST markers (blue), and pathogens (red) during two seasons. During the summer, a light vs. shade contrast was examined by applying a shade cloth over half of the dialysis bags, while no shade cloth was applied during winter, resulting in three experiments: Summer.Shade, Summer.Sun, and Winter.Sun. Each subpanel represents one of the experiments as labeled in the banner. Assays with suffixes .q and .d indicate measurement by qPCR and digital PCR, respectively. Assays without suffixes are measured by IDEXX. Error bars represent the 95% confidence interval of decay rates (day^{-1}).

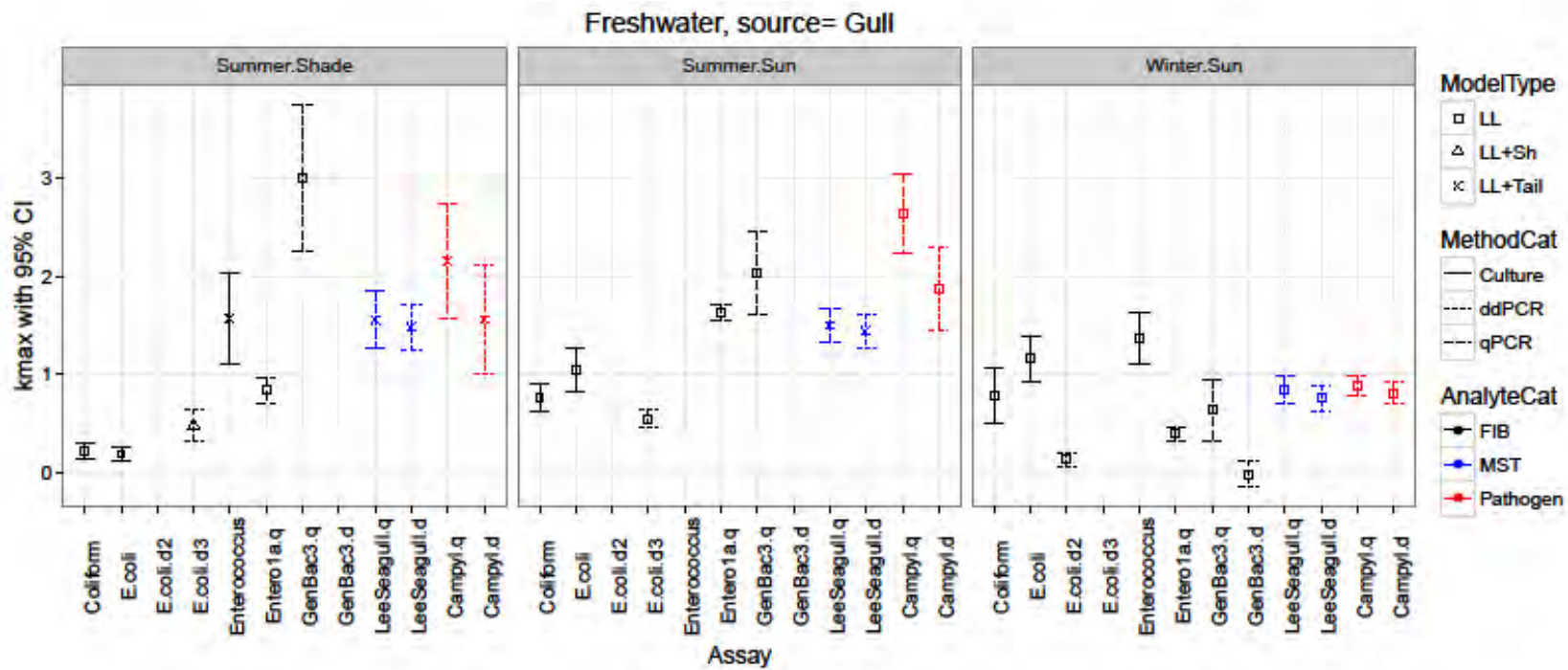


Figure 6. Freshwater water field studies with gull feces: Modeled decay rate coefficients for FIB (black), MST markers (blue), and pathogens (red) during two seasons. During the summer, a light vs. shade contrast was examined by applying a shade cloth over half of the dialysis bags, while no shade cloth was applied during winter, resulting in three experiments: Summer.Shade, Summer.Sun, and Winter.Sun. Each subpanel represents one of the experiments as labeled in the banner. Assays with suffixes .q and .d indicate measurement by qPCR and digital PCR, respectively. Assays without suffixes are measured by IDEXX. Error bars represent the 95% confidence interval of decay rates (day^{-1}).

Sewage-Marine water

Differential decay was observed between cultivable FIB (*Enterococcus*, *E.coli*) and molecular *Bacteroidales* markers (human and general, i.e., HF183, BacHum, HumM2, GenBac3). Only at the lowest UVB intensities (winter deployment in the deepest bags) did the cultivable FIB (*E. coli* and enterococci) decay at the same rate as the molecular *Bacteroidales* markers (human and general); otherwise, the culture-based FIB decayed at a significantly greater rate than the *Bacteroidales* molecular targets.

However, *Bacteroidales* markers themselves (human-specific and general) decayed at the same rate in seawater during both summer and winter seasons and at various depths. Additionally, the human-specific and general *Bacteroidales* marker decay rates did not change with depth or season, while *E. coli* and enterococci (cultivable and molecular marker) decay rates significantly changed with season and depth and were significantly associated with UVB intensity.

The pathogens measured in our experiments (*Salmonella* by culture and molecular methods and norovirus GII) did not persist as long as cultivable FIB; therefore, in both of our deployments and at all depths, the cultivable FIB were conservative indicators of pathogen presence.

A significant and statistically similar shoulder, or lag phase, was seen only in the decay of the molecular markers during the winter deployment (Appendix A).

Sewage-Brackish water

The MST molecular *Bacteroidales* markers (human and dog) decayed more rapidly in the summer compared to FIB (cultivable and molecular), general *Bacteroidales* markers, and pathogens. This was different from the marine water experiments in that cultivable FIB showed the greatest decay rates in marine waters compared to molecular *Bacteroidales* markers and that source-associated and general *Bacteroidales* decayed at similar rates.

The relatively rapid decay of human and dog-associated markers during the summer deployment suggests that these markers are an effective MST tool for the detection of recent inputs of human or dog fecal contamination in a lagoon environment. However, use of these markers to identify and allocate cultivable FIB sources may be limited due to rapid decay of the MST marker and persistence of FIB (cultivable and molecular measurements). Additionally, use of these markers to infer human health risk in such lagoon systems may be limited due to their more rapid decay compared to the bacterial and viral pathogens evaluated in these lagoon field studies.

The pathogens measured in this study (*Campylobacter* and adenovirus) also showed increased persistence compared to cultivable FIB and MST markers, suggesting that health risks could be present even in the absence of indicator and marker organisms. Thus, water monitoring for health risk assessment should likely be conducted as close to the source as possible.

Nevertheless, the general DNA fecal markers, particularly the *Enterococcus* DNA marker (less so the total *Bacteroidales* measured by qPCR, i.e., GenBac3), decayed slower compared to the MST markers and pathogens. The *Enterococcus* DNA marker (Entero1a), which has been allowed for routine recreational water monitoring (USEPA 2012) may represent a more conservative estimate of fecal contamination and potential health risk.

Many of the organisms investigated in this study, including the human fecal markers, were best modeled by including shoulder and/or tail parameters (Appendix B).

Sewage-Freshwater

The MST *Bacteroidales* markers (human) had much greater decay rates than FIB (cultivable and molecular), the general *Bacteroidales* marker, and pathogens during the summer freshwater field studies, regardless of the shading condition. However, such differentiation degradation was not observed during the winter when decay of all measured organisms slowed down. In the winter, the human markers had similar decay rates to *Campylobacter* (by qPCR) and the general *Bacteroidales* marker. This suggests that relative degradation characteristics may not be extrapolated between seasons.

However, decay of the three human *Bacteroidales* markers was similar to each other regardless of season. This was largely consistent with observations during the marine and brackish water field studies. It was also consistent with general expectations. Although the three markers (BacHum, HF183, HumM2) showed different diagnostic sensitivity and specificity in MST method evaluation studies (Layton et al. 2013), they targeted closely-related, if not the same, species of *Bacteroidales*.

Contrary to findings in marine waters, but similar to that in brackish waters, decay rates of the general *Bacteroidales* marker (GenBac3) were generally lower than that of the human *Bacteroidales* markers.

The *Enterococcus* DNA marker (Enterol1a) appeared to be a conservative marker of fecal contamination and potential human health risk, exhibiting generally lower (or similar) decay rates than the MST markers and pathogens. This increased persistence of the *Enterococcus* DNA marker was also observed in marine and brackish water field studies. The *E. coli* DNA marker (only measured in freshwater studies) may also be a conservative marker, exhibiting a similar trend as the *Enterococcus* DNA marker.

Additionally, cultivable FIB decayed much faster than genetic FIB markers or MST markers and pathogens during the winter, suggesting cultivable FIB could underestimate fecal contamination and potential human health risk.

Comparing among the experiments during summer and winter, a majority of the assays showed the lowest decay rates in winter. Also, shading had little effect on decay characteristics during the summer at this site, particularly for all the genetic measurements (Appendix C), indicating sunlight didn't play an important role in fecal degradation at the freshwater site.

The majority of the decay curves (32 out of 35) were best modeled with log linear models. However, during the winter, the three cultivable (by IDEXX) FIB were best described by log linear models with a tail or both a tail and a shoulder component.

Cow-Freshwater

There was a lack of general trend among experiments (summer with or no shading, winter) with respect to relative degradation of the cow MST *Bacteroidales* marker to FIB and pathogens. The cow marker (CowM2) decay rates were significantly higher and slower than that of *Enterococcus* and *E. coli* DNA markers during summer and winter, respectively. The cow marker generally decayed faster than pathogens (*Campylobacter*) in summer no shading, similar to pathogens in summer with shading, but slower than pathogens in winter. It is important to note that all decay rates in winter were much lower than those in summer, so the absolute difference in decay rates among organisms/markers was much less prominent in winter than in summer.

Generally, the cow MST *Bacteroidales* marker had similar decay rates to that of the general *Bacteroidales* across experiments. This was consistent with the sewage-marine experiments where human MST *Bacteroidales* marker had similar decay rates to that of the general *Bacteroidales* across experiments, but different than the sewage-freshwater and sewage-brackish water experiments where general *Bacteroidales*

marker showed slower decay rates compared to MST *Bacteroidales* marker. This may indicate site and source difference.

Whether the *Enterococcus* DNA marker was a conservative marker or not differed among experiments, as its decay rates were significantly lower than, similar to, and higher than a pathogen (Campylobacter by qPCR) and the cow MST marker in summer with shading, summer with no shading, and winter, respectively. However, the *E. coli* DNA markers appeared to be a conservative marker across freshwater experiments, as it showed significantly lower (summer with shading) or similar (summer with no shading and winter) decay rates than the pathogen and MST markers.

Comparing among the experiments during summer and winter, nearly all the assays (including Campylobacter) exhibited the lowest decay rates in winter. Also, decay rates were generally not significantly different between shading vs. no shading treatments in summer for nearly all assays. This was consistent with observations from sewage decay experiments at the same site, indicating sunlight didn't play as an important role in fecal degradation at this site.

Slightly more than half of the decay curves (20 out of 33) were modeled with a LL model. The general *Bacteroidales* marker often required a tail component regardless of experiment, while Campylobacter (by qPCR) during summer with shading was best described with a log linear model with a tail as well.

Gull-freshwater

The gull MST *Catelicoccus* gull marker had similar decay rates to that of a pathogen (Campylobacter by qPCR) regardless of experiment. The *Catelicoccus* marker decay rates ($<2 \text{ day}^{-1}$ in summer, $<1 \text{ day}^{-1}$ in winter) were also generally much lower than *Bacteroidales* MST marker decay rates (e.g. cow and human), and much closer to *Enterococcus* DNA marker decay rates than the *Bacteroidales* MST markers. The *Catelicoccus* gull marker decay rates were slightly higher than those of the *Enterococcus* DNA marker in summer with shading and in winter; similar to those of the *Enterococcus* DNA marker in summer with no shading.

The *Enterococcus* DNA marker appeared to be a conservative indicator, as its decay rates were either similar to or lower than that of Campylobacter. The *E. coli* DNA marker also appeared to be a conservative indicator, as its k rates were lower than both the gull MST marker and Campylobacter.

Comparing among the experiments, nearly all assays showed lowest decay rates in winter. Generally no significant difference was observed for shade vs. no shading in summer for nearly all assays (including the general *Bacteroidales* and *E. coli* DNA markers, the *Catelicoccus* MST marker, and molecular Campylobacter targets). This was consistent with findings in sewage and cow fecal decay field studies at the same site.

More than half of the decay curves (22 out of 30) were modeled with LL model. However, the gull MST *Catelicoccus* marker during summer field studies was best described by LL with a tail component.

Community Analysis Results

Overall, community analysis demonstrated a clear evolution of the microbial community from the raw fecal material to the raw and control water samples of each experiment, reflecting the decay of the fecal contamination. Detailed analysis also indicated that different taxonomic groups had distinctly different decay rates.

Among the environmental factors, the salinity of the water matrix (compared across three field sites) had the strongest influence on overall microbial community composition. In the marine and freshwater water samples, season (summer vs. winter) also significantly affected the microbial community (ANOSIM:

R=0.63, p=0.001), while the light exposure (shading vs. no shading in summer) did not (ANOSIM: R=0.11, p=0.001).

There were some differences in decay rates of microbes between different levels of light exposure. PhyloChip analysis detected a faster decay under unshaded conditions for the ocean and creek water. The Illumina data detected differences between seasons, with changes being slower during winter. The freshwater water presented lower decay rates than the lagoon and ocean water, exhibiting a higher fecal contamination signal at the end of the experiments.

Sediment Effect Investigation

Differences were observed between relative decay amongst the three sediments (i.e. sediments from the marine, brackish and freshwater field study sites), illustrating that assumptions regarding the fate of bacteria within the sediment compartment cannot be applied universally (Figure 7). Commonalities between indicator decay rates across the sediment types were uncommon. Nevertheless, similar decay rates were observed at 10% and 50% sewage-inoculated microcosms for the different assays. Detailed results are presented in Appendix E.

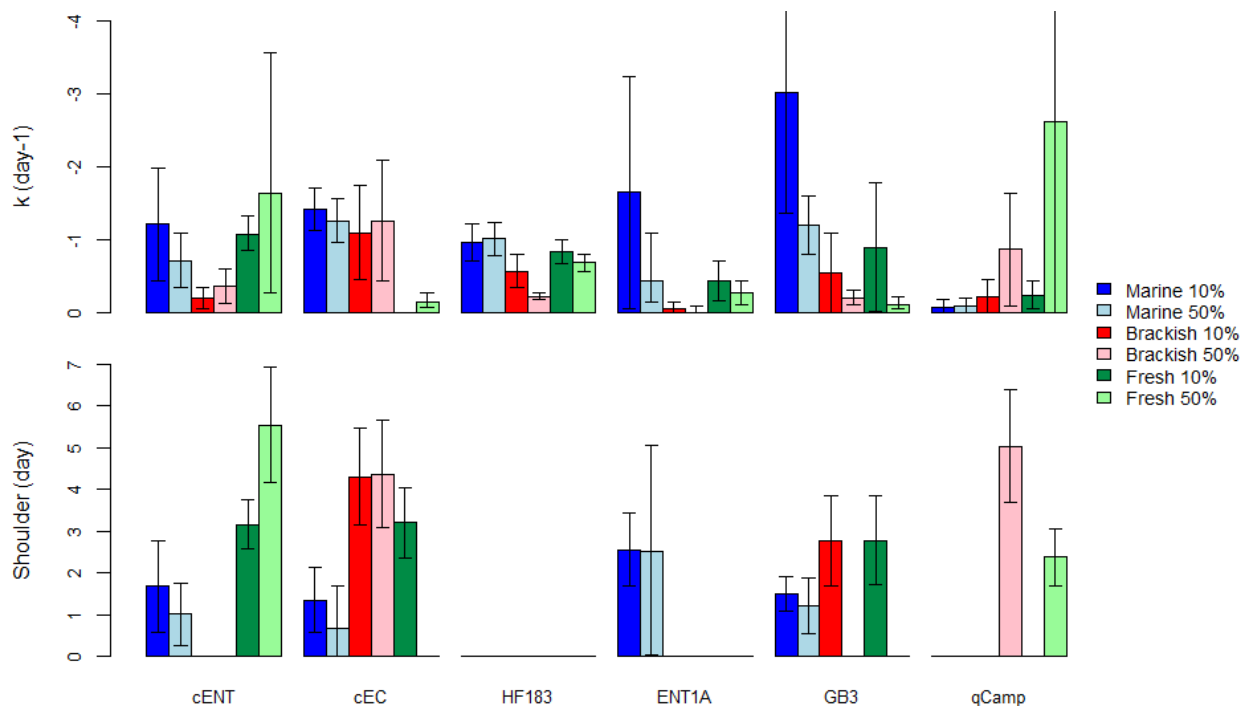


Figure 7. Sediment laboratory studies with 10% and 50% sewage inoculum. Decay rates (upper panel) and length of shoulder (lower panel) estimated by decay modeling are presented with error bars denoting 95% confidence intervals.

Generally, the human marker (HF183) did not show the ability to grow in sediments, increasing the applicability of this marker to source tracking of recent inputs of human fecal contamination in sediment and making it less likely for detection of false positives. However, the HF183 marker fell below the limit of quantification by day four in the marine water sediment with 10% sewage inoculum, despite cultivable

Salmonella and all other indicators being detected through day seven, making it a less conservative marker when applied to beach sand.

The *Enterococcus* DNA marker exhibited increased persistence and slower decay rates versus the other markers and FIB, suggesting it may be useful as a more conservative, though less specific, marker of fecal contamination.

Potential for regrowth was observed for the general *Bacteroidales* marker and cultivable *Enterococcus* and *E. coli* in the freshwater sediment microcosms. Presence of a shoulder was a common characteristic for cultivable FIB amongst the three sediments tested, whereas a shoulder was not observed for the HF183 marker in any of the treatments, with the exception of brackish water sediment with 10% sewage.

Water Matrix Effect Investigation

Differential decay rates were prominent, as *Enterococcus* and *E. coli* measured by growth-based methods decayed much faster than genetic markers for general (i.e., Enterol1a, GenBac3) and human-associated fecal markers (i.e., HF183). Growth-based *Enterococcus* and *E. coli* signals in all 12 waters disappeared by day 2 and 3, respectively, while all genetic markers were still above detection limits by the end of the mesocosm experiments (i.e. day 4). Because of the fast decay of cultivable *Enterococcus* and *E. coli*, decay modeling of these targets could not be performed on all waters due to lack of data.

However, decay rates of the genetic markers (Enterol1a, GenBac3, HF183) were highly correlated (correlation coefficients: 0.73 to 0.91), indicating potentially similar water matrix effects on different genetic markers. Decay rates of the genetic markers also exhibited significant relationships with salinity and absorbance of UV light by the water. The higher the salinity (Figure 8) and UV absorbance (Appendix F), the slower was the decay.

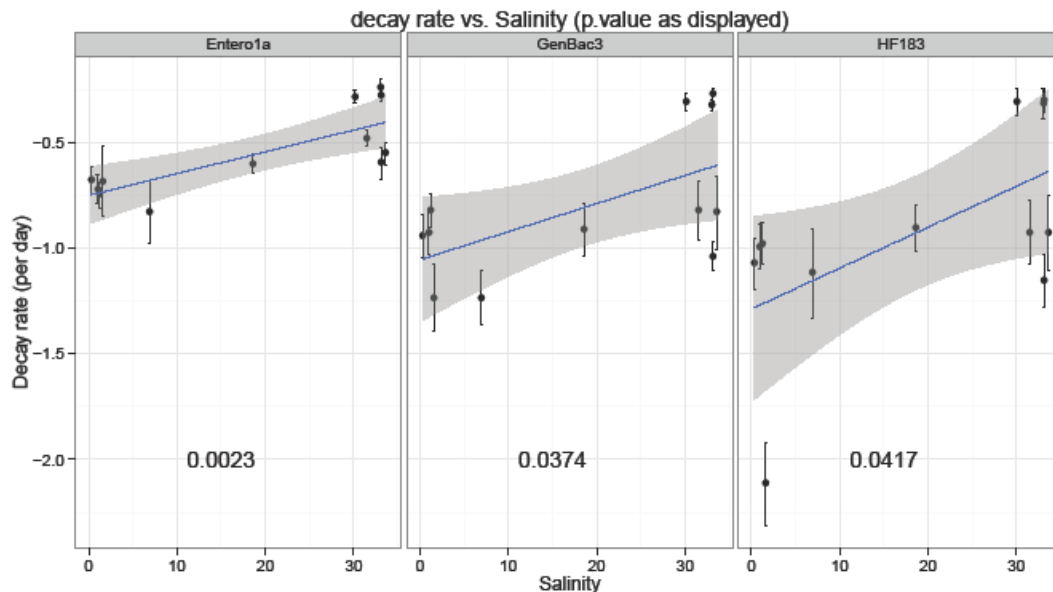


Figure 8. Water matrix effect investigation: Relationship between decay rates and salinity. Error bars represent 95% confidence intervals.

Discussion

Regarding Relative Degradation

Overall, there was no universal trend regarding degradation of MST markers relative to FIB and pathogens as observed in this project. Whether the three target groups experienced differential degradation, and to what extent, depended on the combination of environmental conditions (i.e., field site, season, sunlight) and fecal source, whether the MST markers were *Bacteroidales* or *Catelliboccus*.

Nevertheless, while the *Bacteroidales* MST markers did not always show higher decay rates than pathogens and cultivable FIB, these MST markers rarely showed decay rates lower than the other two groups. The gram-positive *Catelliboccus* gull MST marker appeared to be a more conservative marker than the gram-negative *Bacteroidales* human, cow and dog MST markers, showing decay rates more similar to those of pathogens and *Enterococcus* DNA markers. While non-specific, the *Enterococcus* DNA markers generally appeared to be a conservative marker for indicating fecal contamination and potential human health risk.

In practice, commonality regarding relative degradation may not be expected across sites, although similar decay between certain targets might be assumed under certain conditions. This was likely because different abiotic and biotic factors were the dominant factors affecting decay at different field sites. A holistic model integrating these various factors, if achievable, might be most useful for beach managers in predicting degradation behaviors at their local sites. A preliminary model integrating sunlight intensity, color and depth of environmental water has been developed, representing one step forward towards such a goal.

Regarding MST Data Interpretation

Two quantitative MST models were developed and are described in detail in Appendix G (the ratio model for potential fecal source allocation) and Appendix F (the human fecal score for assessing the extent of human fecal contamination at a site). Brief descriptions of the models and their application are discussed below.

Ratio Model

Theoretically, the proportion of fecal contamination in a water sample attributable to a single source can be determined using a ratio method developed by Wang et al (2013). Briefly, this method calculates the proportion of FIB (for example, *E. coli*) in water from a specific fecal source by dividing the ratio of the source-associated MST marker concentration to the FIB concentration in the water sample by the ratio of that MST marker concentration to FIB concentration in the fecal source. The equation for this method is as follows:

$$P_i = \frac{R_M}{R_{i_feces}(t)} \quad (1)$$

where P_i is the proportion of fecal contamination from source, i . R_M is the ratio of the concentration of the source-specific MST marker to the concentration of FIB being allocated in the ambient water sample, and $R_{i_feces}(t)$ is the ratio of the concentrations of MST marker to FIB in feces aged time t in the environment. The age of the feces refers to the time from when feces is released into the environment, migrates through various matrices, and is subsequently detected in ambient water. During aging, the concentration of the MST markers and FIB in feces can decay due to factors such as inactivation, predation, or absorption to particles. Therefore, if the MST source-specific markers and FIB do not decay at the same rate in the environment, the age of the fecal pollution must be known to utilize the ratio source appointment method.

As there is currently no simple method available for estimating the fecal contamination age, source allocation models must either be restricted to use on fresh fecal contamination scenarios or used with analytes that decay at a similar rate in the environment. Taken all field studies results together, there are only certain conditions when k values are the same (Table 3). One cannot assume a priori that they are. The ratio source allocation model therefore may only be used in certain environmental conditions where k values of FIB and MST markers are not expected to be different.

Overall, commonalities in relative degradation across sites and water types were rare, suggesting whether source allocation models could be applicable may need to be evaluated at each site of interest through fecal decay studies.

Table 3. Summary of experimental treatments from all field studies when k did not differ between each class of FIB and each MST marker.

	HF183	BacHum	HumM2	CowM2	LeaSeaGull
cENT	marine winter depth, freshwater summer sun & winter sun, brackish winter sun	marine winter depth, freshwater summer sun & winter sun, brackish winter sun	marine winter depth, freshwater summer sun, brackish winter sun & summer sun	fresh summer shaded & winter sun	fresh summer sun, fresh winter sun
tENT	marine summer surface	marine summer surface	marine summer surface	freshwater summer sun & winter sun	freshwater summer sun
EC	marine winter depth, freshwater winter sun	marine winter depth & summer depth, freshwater winter sun	marine winter depth, brackish winter sun, freshwater summer sun & winter sun		freshwater summer sun & summer shade

Human Fecal Score

To quantitatively characterize a site regarding its extent of human fecal contamination, for site remediation prioritization and effectiveness evaluation, generally requires integrating human marker results across multiple samples from a site. Previously, this was mostly done via best professional judgement (BPJ) available within the premise of each individual project. Recent research demonstrated tremendous variability/uncertainty/inconsistency in the BPJ approaches for MST data interpretation, and it was concluded that a mathematically defined standardized algorithm was needed (Cao et al. 2013). A human fecal score (HFS) was developed to provide such an assessment based on HF183 qPCR measurements.

Briefly, the HFS takes into account all data from a given site by dividing data into two categories: the MPN range including non-detect and detected but not quantifiable qPCR results, and the ROQ range including the quantifiable qPCR results. Previously, the MPN range could not be integrated and utilized to characterize a site in a quantitative fashion. The HFS utilizes the Poisson probabilistic distribution to quantify samples in the MPN range, which is then combined with sample results from the ROQ ranges to provide a weighted average of all measurements. The calculation is achieved via Bayesian statistics and the HFS is reported as copies of HF183 marker per 100 ml of water. Detailed descriptions of the equations are provided in Appendix H.

The application of HFI is based on results from daily morning water samples from a beach site. Model sensitivity analysis was conducted to evaluate how sample size (i.e. number of days sampled at the beach

site) and qPCR replication (i.e. number of qPCR replicates analyzed per sample) affect accuracy and precision of HFSI. Decision charts on sample size and PCR replication were developed for the management application of site prioritization (Appendix H).

However, it is important to consider how HF183 marker degradation may affect application of HFS. A wide range of decay rates ($k < 1 \text{ day}^{-1}$ to 6 day^{-1} , in $C = C_0 e^{-kt}$) were observed for the HF183 marker in this project: marine waters ($k = 1-2$), brackish waters ($k = 1-6$), freshwater ($k = 1-5$), water matrix laboratory study ($k < 1 - 5$), sediment ($k < 1-2$). These rates translate to < 0.5 to $< 3 \log_{10}$ reduction per day. Assuming a starting concentration of HF183 from fresh sewage input to be $6 \log_{10}$ copy per 100ml (5% sewage measured in this project averaged $6.7 \log_{10}$ copies of HF183 per 100ml), the HF183 signal would disappear in two days under the fastest decay rates observed in this project. If the sewage fecal source is introduced locally at the beach, with a daily sampling scheme, the HFS would be integrating both the fresh and aged HF183 signals under most decay conditions. Nevertheless, with a less frequent sampling scheme (e.g. only once every two days), it would be possible to miss the HF183 signals under environmental conditions enabling the highest decay rates. It is therefore important for managers to consider the extent of potential decay on the spectrum of rates observed in this project, and adjust sampling design accordingly (more details in Appendix H).

Additionally, although proof-of-concept work has been done to interpret human marker concentration in a risk-based framework (Boehm et al. 2015), no attempt is currently made to infer human health risk from the HFS because relative degradation of HF183 vs. a suite of pathogens would need to be incorporated into such a risk-based framework first.

Conclusion

Field aging studies determined the relative rates of fecal marker, FIB and pathogen decay, laboratory studies added verified field results and facilitated interpretation of field results, and probabilistic and ratio models were completed and their utility demonstrated.

Despite the successful completion of all the field and laboratory tasks, the project did not result in a simple source apportionment model for fecal contamination. Although there were some observable trends, most often associated with the level of sunlight and salinity of the water, we found that decay characteristics of the different markers, FIB and pathogens varied by site, season and physico-chemical conditions. This level of variability in decay rates confounded the ratio model, which requires decay rates to be constant across analytes to produce viable source apportionment estimates. This said, the model is still viable when fecal sources are known to be fresh.

In contrast, the probabilistic model for human contamination was shown to be workable and robust, with the caveat that sufficient data with a usable range of positive values must be collected. This model will be a valuable tool in determining the level of human contamination present at beaches, will allow managers to prioritize mitigation efforts and determine if beach sites are eligible for developing site specific objectives using QMRA.

This project is the first ever to determine decay constants for such a large number of MST markers, FIB, and pathogens under environmental conditions. Although the Ratio Model, may have limited utility under most conditions, valuable information about how microbes behave in a range of environmental conditions was gleaned from this study. Even outside the context of a model, this information will help beach managers and researchers as they take on the arduous task of microbial source identification. Further, the Human Fecal Score Model will allow managers to prioritize beaches for remediation or Quantitative Microbial Risk Assessment studies.

Literature Cited

- Anderson, S.A., S.J. Turner, G.D. Lewis. Enterococci in the New Zealand environment: Implications for water quality monitoring. *Water Sci. Technol.* 1997, 35, 325-331.
- Badgley, B.D., F.I.M. Thomas, V.J. Harwood. The effects of submerged aquatic vegetation on the persistence of environmental populations of *Enterococcus* spp. *Environ. Microbiol.* 2010, 12, 1271-1281.
- Bernhard, A.E. and K.G. Field. A PCR assay to discriminate human and ruminant feces on the basis of host differences in *Bacteroides-Prevotella* genes encoding 16S rRNA. *Appl Environ Microbiol* 2000, 66, 4571-4574.
- Boehm, A.B., J.A. Fuhrman, R.D. Mrse, S,B, Grant. Tiered approach for identification of a human fecal pollution source at a recreational beach: Case study at Avalon Cay, Catalina Island, California. *Environ. Sci. Technol.* 2003, 37, 673-680.
- Boehm, A.B., J. Griffith, C. McGee, T.A. Edge, H.M. Solo-Gabriele, R. Whitman, Y. Cao, M. Getrich, J.A. Jay, D. Ferguson, K.D. Goodwin, C.M. Lee, M. Madison, S.B. Weisberg. Fecal indicator bacteria enumeration in beach sand: a comparison study of extraction methods in medium to coarse sands. *J. Appl. Microbiol.* 2009, 107, 1740-1750.
- Boehm, A.B., J.A. Soller, O.C. Shanks. Human-Associated Fecal Quantitative Polymerase Chain Reaction Measurements and Simulated Risk of Gastrointestinal Illness in Recreational Waters Contaminated with Raw Sewage. *Environmental Science & Technology Letters* 2015, 2, 270-275.
- Cabelli, V.J., A.P. Dufour, L.J. McCabe, M.A. Levin. Swimming-associated gastroenteritis and water quality. *Am. J. Epidemiol.* 1982, 115, 606-616.
- Cao, Y., C. Hagedorn, O.C. Shanks, D. Wang, J. Ervin, J.F. Griffith, B.A. Layton, C.D. McGee, T.E. Riedel, S.B. Weisberg. Towards establishing a human fecal contamination index in microbial source tracking. *Int. J. Environ. Eng. Syst.* 2013, 4, 46-58.
- Desmarais, T.R., H.M. Solo-Gabriele, C.J. Palmer. Influence of soil on fecal indicator organisms in a tidally influenced subtropical environment. *Applied And Environmental Microbiology* 2002, 68, 1165-1172.
- Dick, L.K., A.E. Bernhard, T.J. Brodeur, J.W.S. Domingo, J.M. Simpson, S.P. Walters, K.G. Field. Host distributions of uncultivated fecal *Bacteroidales* bacteria reveal genetic markers for fecal source identification. *Appl. Environ. Microbiol.* 2005, 71, 3184-3191.
- Dick, L. K., M.T. Simonich, K.G. Field. Microplate Subtractive Hybridization To Enrich for *Bacteroidales* Genetic Markers for Fecal Source Identification *Applied and Environmental Microbiology* 2005, 71, 3179-3183.
- Ferguson, D. and C. Signoretto. *Environmental Persistence and Naturalization of Fecal Indicator Organisms*, Springer, 233 Spring Street, New York, Ny 10013, United States, 2011.
- Gast, R.J., L. Gorrell, B. Raubenheimer, S. Elgar. Impact of erosion and accretion on the distribution of enterococci in beach sands. *Cont. Shelf Res.* 2011, 31, 1457-1461.
- Haile, R.W., J.S. Witte, M. Gold, R. Cressey, C. McGee, R.C. Millikan, A. Glasser, N. Harawa, C. Ervin, P. Harmon, J. Harper, J. Dermand, J. Alamillo, K. Barrett, M. Nides, G.Y. Wang. The health effects of swimming in ocean water contaminated by storm drain runoff. *Epidemiology* 1999, 10, 355-363.

Halliday, E. and R.J. Gast. Bacteria in Beach Sands: An Emerging Challenge in Protecting Coastal Water Quality and Bather Health. *Environ. Sci. Technol.* 2011, 45, 370-379.

Haugland, R.A., M. Varma, M. Sivaganesan, C. Kelty, L. Peed, O.C. Shanks. Evaluation of genetic markers from the 16S rRNA gene V2 region for use in quantitative detection of selected Bacteroidales species and human fecal waste by qPCR. *Systematic and Applied Microbiology* 2010, 33, 348-357.

Imamura, G.J., R.S. Thompson, A.B. Boehm, J.A. Jay. Wrack promotes the persistence of fecal indicator bacteria in marine sands and seawater. *FEMS Microbiol. Ecol.* 2011, 77, 40-49.

Jeter, S.N., C.M. McDermott, P.A. Bower, J.L. Kinzelman, M.J. Bootsma, G.W. Goetz, S.L. McLellan. Bacteroidales diversity in Ring-Billed Gulls (*Larus delawarensis*) residing at Lake Michigan beaches. *Appl. Environ. Microbiol.* 2009, 75, 1525-1533.

Johnston, C., J.A. Ufnar, J.F. Griffith, J.A. Gooch, J.R. Stewart. A real-time qPCR assay for the detection of the *nifH* gene of *Methanobrevibacter smithii*, a potential indicator of sewage pollution. *J. Appl. Microbiol.* 2010, 109, 1946-1956.

Kay, D., F. Jones, M.D. Wyer, J.M. Fleisher, R.L. Salmon, A.F. Godfree, A. Zelenauch-Jacquotte, R. Shore. Predicting likelihood of gastroenteritis from sea bathing: results from randomised exposure. *The Lancet* 1994, 344, 905-909.

Kildare, B.J., C.M. Leutenegger, B.S. McSwain, D.G. Bambic, V.B. Rajal, S. Wuertz. 16S rRNA-based assays for quantitative detection of universal, human-, cow-, and dog-specific fecal Bacteroidales: A Bayesian approach. *Water Research* 2007, 41, 3701-3715.

Korajkic, A., B.R. McMinn, V.J. Harwood, O.C. Shanks, G.S. Fout, N.J. Ashbolt. Differential decay of enterococci and *Escherichia coli* originating from two fecal pollution sources. *Appl. Environ. Microbiol.* 2013, 79, 2488-92.

Korajkic, A., P. Wanjugi, V.J. Harwood. Indigenous microbiota and habitat influence *Escherichia coli* survival more than sunlight in simulated aquatic environments. *Appl. Environ. Microbiol.* 2013, 79, 5329-37.

Lamendella, R., J.W.S. Domingo, A.C. Yannarell, S. Ghosh, G. Di Giovanni, R.I. Mackie, D.B. Oerther. Evaluation of Swine-Specific PCR Assays Used for Fecal Source Tracking and Analysis of Molecular Diversity of Swine-Specific "Bacteroidales" Populations. *Applied and Environmental Microbiology* 2009, 75, 5787-5796.

Layton, B.A., Y. Cao, D.L. Ebentier, K. Hanley, E. Ballesté, J. Brandão, M. Byappanahalli, R. Converse, A.H. Farnleitner, J. Gentry-Shields, M.L. Gidley, M. Gourmelon, C.S. Lee, J. Lee, S. Lozach, T. Madi, W.G. Meijer, R. Noble, L. Peed, G.H. Reischer, R. Rodrigues, J.B. Rose, A. Schriewer, C. Sinigalliano, S. Srinivasan, J. Stewart, L.C. Van De Werfhorst, D. Wang, R. Whitman, S. Wuertz, J. Jay, P.A. Holden, A.B. Boehm, O. Shanks, J.F. Griffith. Performance of human fecal anaerobe-associated PCR-based assays in a multi-laboratory method evaluation study. *Water Res.* 2013, 47, 6897-6908.

Layton, A., L. M Lamendella, Kay, D. Williams, V. Garrett, R. Gentry, G. Sayler. Development of Bacteroides 16S rRNA gene TaqMan-based real-time PCR assays for estimation of total, human, and bovine fecal pollution in water. *Appl. Environ. Microbiol.* 2006, 72, 4214-4224.

Lee, D. Y., W.C. Weir, H. Lee, J.T. Trevors. Quantitative identification of fecal water pollution sources by TaqMan real-time PCR assays using Bacteroidales 16S rRNA genetic markers. *Appl. Microbiol. Biotechnol.* 2010, 88, 1373-1383.

- Lu, J. R., J.W. Santo Domingo, R. Lamendella, T. Edge, S. Hill. Phylogenetic diversity and molecular detection of bacteria in gull feces. *Appl. Environ. Microbiol.* 2008, 74, 3969-3976.
- Mieszkin, S., J.P. Furet, G. Corthier, M. Gourmelon. Estimation of Pig Fecal Contamination in a River Catchment by Real-Time PCR Using Two Pig-Specific Bacteroidales 16S rRNA Genetic Markers. *Applied and Environmental Microbiology* 2009, 75, 3045-3054.
- Mieszkin, S., J.F. Yala, R. Joubrel, M. Gourmelon. Phylogenetic analysis of Bacteroidales 16S rRNA gene sequences from human and animal effluents and assessment of ruminant faecal pollution by real-time PCR. *J. Appl. Microbiol.* 2010, 108, 974-984.
- Okabe, S., N. Okayama, O. Savichtcheva, T. Ito. Quantification of host-specific Bacteroides-Prevotella 16S rRNA genetic markers for assessment of fecal pollution in freshwater. *Appl. Microbiol. Biotechnol.* 2007, 74, 890-901.
- Reischer, G. H., D.C. Kasper, R. Steinborn, R.L. Mach, A.H. Farnleitner. Quantitative PCR Method for Sensitive Detection of Ruminant Fecal Pollution in Freshwater and Evaluation of This Method in Alpine Karstic Regions *Applied and Environmental Microbiology* 2006, 72, 5610-5614.
- Reischer, G. H., D.C. Kasper, R. Steinborn, A.H. Farnleitner, R.L. Mach. A quantitative real-time PCR assay for the highly sensitive and specific detection of human faecal influence in spring water from a large alpine catchment area. *Lett. Appl. Microbiol.* 2007, 44, 351-356.
- Seurinck, S., T. Defoirdt, W. Verstraete, S.D. Siciliano. Detection and quantification of the human-specific HF183 Bacteroides 16S rRNA genetic marker with real-time PCR for assessment of human faecal pollution in freshwater. *Environ. Microbiol.* 2005, 7, 249-259.
- Shanks, O. C., E. Atikovic, A.D. Blackwood, J.R. Lu, R.T. Noble, J.S. Domingo, S. Seifring, M. Sivaganesan, R.A. Haugland. Quantitative PCR for detection and enumeration of genetic markers of bovine fecal pollution. *Applied and Environmental Microbiology* 2008, 74, 745-752.
- Shanks, O. C., C.A. Kelty, M. Sivaganesan, M. Varma, R.A. Haugland. Quantitative PCR for genetic markers of human fecal pollution. *Appl. Environ. Microbiol.* 2009, 75, 5507-5513.
- Shibata, T., H.M. Solo-Gabriele, C.D. Sinigalliano, M.L. Gidley, L.R.W. Plano, J.M. Fleisher, J.D. Wang, S.M. Elmir, G. He, M.E. Wright, A.M. Abdelzaher, C. Ortega, D. Wanless, A.C. Garza, J. Kish, T. Scott, J. Hollenbeck, L.C. Backer, L.E. Fleming. Evaluation of conventional and alternative monitoring methods for a recreational marine beach with nonpoint source of fecal contamination. *Environ. Sci. Technol.* 2010, 44, 8175-8181.
- Silkie, S. S. and K.L. Nelson. Concentrations of host-specific and generic fecal markers measured by quantitative PCR in raw sewage and fresh animal feces. *Water Research* 2009, 43, 4860-4871.
- USEPA. "Recreational Water Quality Criteria," Office of Water 820-F-12-058, 2012.
- USEPA. Report of the Expert Scientific Workshop on Critical Research Needs for the Development of New or Revised Recreational Water Quality Criteria (Airlie Workshop). EPA-823-R-07-006. 2007.
- Valiela, I., M.C. Alber, M. Lamontagne. Fecal-coliform loadings and stocks in Buttermilk Bay, Massachusetts, USA and management implications. *Environ. Manage.* 1991, 15, 659-674.
- Wade, T.J., N. Pai, J.N.S. Eisenberg, J.M.J. Colfor. Do U.S. Environmental Protection Agency water quality guidelines for recreational waters prevent gastrointestinal illness? A systematic review and meta-analysis. *Environmental Health Perspectives* 2003, 111, 1102-1109.

Wang, D., A.H. Farnleitner, K.G. Field, H.C. Green, O.C. Shanks, A.B. Boehm. Enterococcus and Escherichia coli Apportionment At Recreational Beaches Using Fecal Source Identification Genetic Markers – Is It Feasible? *Water Res.* 2013.

Whitman, R.L., D.A. Shively, H. Pawlik, M.B. Nevers, M.N. Byappanahalli. Occurrence of Escherichia coli and enterococci in Cladophora (Chlorophyta) in nearshore water and beach sand of Lake Michigan. *Applied and Environmental Microbiology* 2003, 69, 4714-4719.

Yamahara, K.M., B.A. Layton, A.E. Santoro, A.B. Boehm. Beach sands along the California coast are diffuse sources of fecal bacteria to coastal waters. *Environ. Sci. Technol.* 2007, 41, 4515-4521.

Yamahara, K. M., S.P. Walters, A.B. Boehm. Growth of Enterococci in unaltered, unseeded beach sands subjected to tidal wetting. *Appl. Environ. Microbiol.* 2009, 75, 1517-1524.

APPENDIX A: RELATIVE DECAY OF SEWAGE FECAL MATERIAL IN MARINE WATERS

Introduction

(Field Site: Pillar Point Harbor)

Culturable fecal indicator bacteria (FIB), namely *Escherichia coli* and enterococci, have been used for the last 60 years to evaluate the microbial quality of recreational water. The presence of these microorganisms is indicative of fecal contamination in environmental waters because they are commensal bacteria present in high numbers within intestinal tracts of animals. However, because FIB are shed by all warm-blooded (and to a lesser extent, cold-blooded) animals, FIB presence in water does not provide any information as to the source of the fecal contamination (Field and Samadpour 2007). Identifying the source of fecal contamination is important because the health risks associated with microbial pollution in recreational waters depends on the source of pollution (Soller et al. 2010). In addition, the use of FIB to assess microbial water quality and human health risks has been called into question due to their variability in coastal waters on multiple time scales (Boehm et al. 2009) (Boehm et al. 2002), as well as their presence (and potential growth) within environmental reservoirs such as algae, wrack, and sand (Russell et al. 2012, Yamahara et al. 2012, Byappanahali et al. 2003).

Microbial source tracking (MST) is used to track sources of FIB in water. MST incorporates fecal source-associated MST markers to differentiate animal hosts contributing FIB to waters. Fecal source-associated MST markers are genetic sequences unique to bacteria from specific hosts, many of which are genetic sequences from *Bacteroidales* (Boehm et al. 2013). By determining major fecal pollution sources, water resource managers and public health officials can evaluate the health risks posed to recreational water users and target major pollution sources for remediation (Harwood et al. 2014). For example, if the contamination were primarily human in origin, this would suggest a sewage spill or leak in area, but if the contamination were primarily livestock-associated, this might point toward potential upstream agricultural run-off sources and present different health risks from possible zoonotic pathogens. For this reason, the 2012 US Environmental Protection Agency (USEPA) Recreational Water Quality Criteria recommends the use of source tracking tools for confirming presumed sources of fecal contamination in a watershed and prioritizing clean-up efforts (USEPA 2012).

Theoretically, the proportion of fecal contamination in a water sample attributable to a single source can be determined using a ratio method developed by Wang et al. (2013). Briefly, this method calculates the proportion of FIB (for example, *E. coli*) in water from a specific fecal source by dividing the ratio of the source-associated MST marker concentration to the FIB concentration in the water sample by the ratio of that MST marker concentration to FIB concentration in the fecal source. The equation for this method is as follows:

$$P_i = \frac{R_M}{R_{i \text{ feces}}(t)} \quad (1)$$

where P_i is the proportion of fecal contamination from source, i . R_M is the ratio of the concentration of the source-specific MST marker to the concentration of FIB being allocated in the ambient water sample, and $R_{i \text{ feces}}(t)$ is the ratio of the concentrations of MST marker to FIB in feces aged time t in the environment. The age of the feces refers to the time from when feces is released into the environment, migrates through various matrices, and is subsequently detected in ambient water. During aging, the concentration of the MST markers and FIB in feces can decay due to factors such as inactivation, predation, or absorption to particles. Therefore, if the MST source-specific markers and FIB do not decay at the same rate in the environment, the age of the fecal pollution must be known to utilize the ratio source appointment method.

Determining the age of fecal pollution in the environment is often not feasible in most practical applications. However, the ratio method for source allocation can be used without this information so long as the decay of the MST markers and FIB is the same. Presently, there is a striking lack of knowledge on how aging of fecal contamination affects concentrations of both source-associated MST markers. While several studies have been conducted to look at the decay of fecal indicators in environmental waters (Walters et al. 2009, Green et al. 2011, Sinton et al. 1999, Sinton et al. 1994), these studies have rarely looked at source-associated genetic markers and FIB concurrently. In addition, there is little information on the concurrent decay of fecal markers (both host-specific and general) and associated enteric pathogens. This makes it difficult to determine if the decay of fecal markers is representative of the decay of pathogens and, in turn, good indicators for risk assessment.

The goal of this study is to test the hypothesis that human-associated MST markers, pathogens, and FIB from sewage decay at the same rate in marine waters. Decay rates were measured using an in situ, microcosm design seeded with untreated sewage to emulate human fecal pollution in marine waters. The results of this work will inform the interpretation of MST measurements for source allocation, the identification of human-impacted beaches, and the evaluation of health risk associated with recreational waters.

Methods

Study Design

Field microcosm experiments were conducted at Pillar Point Harbor (37.502467° N, 122.4838829° W) in Half Moon Bay, CA, USA during September 2014 (summer deployment) and February 2015 (winter deployment). To simulate sewage pollution in marine waters, experiments were conducted in dialysis bags (120 mm flat width) with a 6-8 kDa molecular weight cutoff (~1 nm pore size, Spectra/Por Standard RC Tubing, Spectrum Laboratories Inc., Rancho Dominguez, CA) containing 95% by volume raw ocean water from the deployment site mixed with 5% by volume raw sewage from the Palo Alto Regional Water Quality Control Plant (Palo Alto, California). The plant services 220,000 residents and processes 22 million gallons of wastewater a day, according to the City of Palo Alto Regional Water Quality Control Plant website (<http://www.cityofpaloalto.org/gov/depts/pwd/rwqcp/default.asp>). Both the ocean water and raw sewage were collected the morning of the initiation of the experiments.

The dialysis tubing was filled to a total volume of 1 L (~30 cm length of dialysis tube) of the ocean water-raw sewage mixture and closed on both ends using polypropylene clamps (Spectra/Por closures, Spectrum Laboratories Inc., Rancho Dominguez, CA). The pore size of the dialysis bags allowed the passage of nutrients and water, but prevented the passage of microorganisms and genetic materials greater than 6-8 kDa. The spectral absorbance of the dialysis bag material was measured using a spectrophotometer (Uvikon XL Spectrophotometer, BioTek Instruments, Winooski, VT) and is reported elsewhere (Maraccini et al. 2016).

The dialysis bags were deployed by securing them to floating rigs constructed of polyvinylchloride (PVC) pipes attached to air-filled plastic cylinders that acted as buoys. The placement of the cylinder on two sides of each rig determined the depth of the rig. Plastic polyethylene mesh (pore size 0.625 cm, Industrial Netting Inc., Minneapolis, MN) was attached to the sides and the bottom of the PVC frame of the rig to provide a surface that the bags could be attached to and to protect the bags from marine life and debris. The bags were attached to the mesh using plastic zip-ties connected to the clamps sealing the bag ends. The bags were oriented in the horizontal direction with the largest surface area of the bag perpendicular to the sky to maximize light exposure. In order to evaluate the impact of sunlight irradiation at depth, separate rigs were constructed to float at the following depths: 5 cm and 99 cm during the summer deployment and 5 cm, 18 cm, and 99 cm depths during the winter deployment (measurements represent

the distance from the water surface to the top of the bag). The average bag thickness was 6 cm when filled. Photos of a floating deployment rigs are shown in Figure 1.

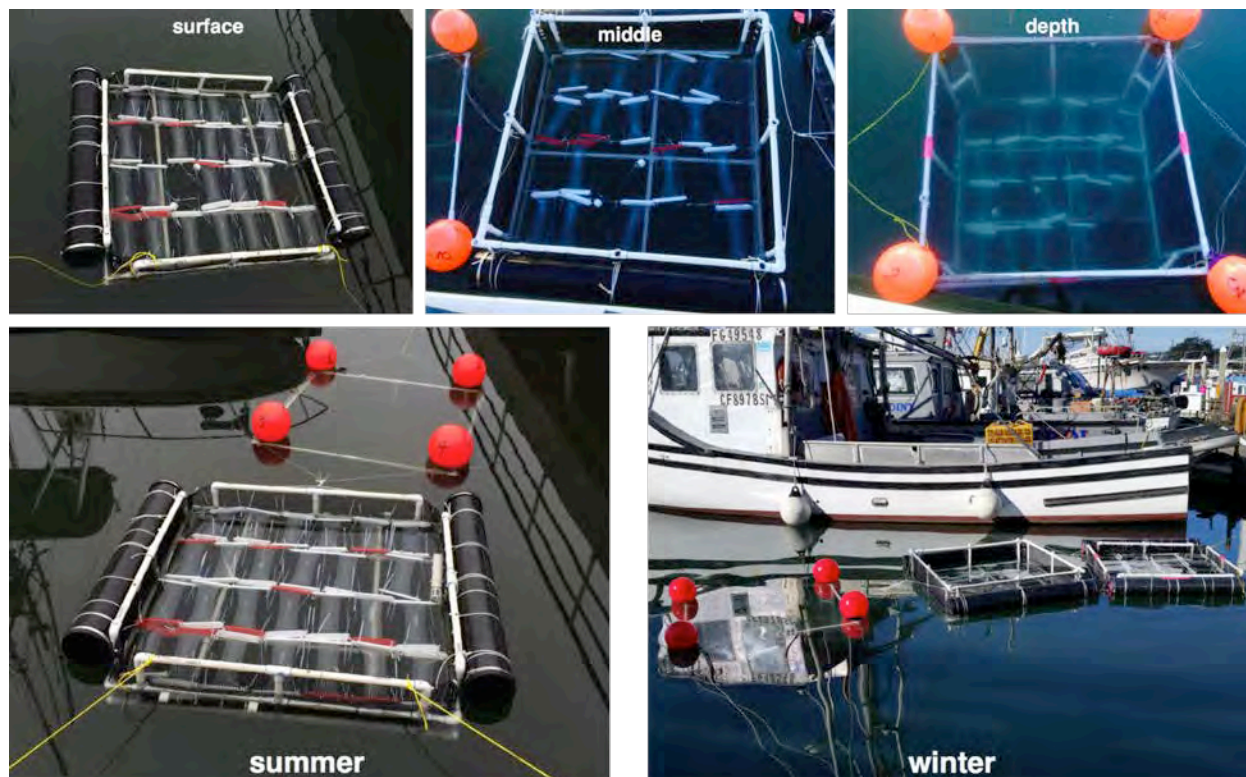


Figure 1. Pictures of the in-situ field microcosms during the summer (bottom left) and winter (bottom right). The dialysis bags were floated at 3 cm (surface, top left) and 99 cm (depth, top right) below the water surface during the summer deployment and at 3 cm, 15 cm (middle, top middle), and 99 cm below the surface during the winter deployment.

Each day of the experiment, two dialysis bags representing biological replicates were destructively sampled from each depth at approximately 8:00 h. Three bags were collected from each depth on one day during both the summer and winter deployments. The summer and winter deployments were conducted for 10 and 7 days, respectively. Control bags containing only ocean water were placed at each depth and were collected on days 5 and 10 for the summer deployment and day 7 for the winter. Additional control bags containing only molecular grade water were placed at 3 and 99 cm for both deployments and collected on the same days as other control bags to evaluate the ability of the dialysis bags to prevent genetic materials and microorganisms from entering the bag while deployed in the ocean or during sample collection in the field and processing in the lab.

The salinity, temperature, and dissolved oxygen (DO) of the environmental waters were measured upon sample collection using a handheld YSI-30 system (YSI, Yellow Springs, OH). A thermistor (SBE 39 Temperature Recorder, Sea-Bird Electronics, Inc., Bellevue, Washington) was attached to the shallowest rig to continuously measure ocean water temperature for the duration of the experiment. A 1 L sample of the ambient ocean water was also collected in a sterile 1 L bottle at the time of sampling. Water from the dialysis bags was aseptically poured into a sterile bottle, stored in the dark at 4°C, and processed within 4 h of collection at Stanford University (Stanford, CA, USA).

Physical Measurements

The turbidity (DRT-15CE Turbidimeter, HF Scientific Inc., Fort Myers, FL), chlorophyll *a* concentration, and water absorbance (Uvikon XL Spectrophotometer, BioTek Instruments, Winooski, VT) of the ambient water were measured within 12 h of sampling. Chlorophyll *a* was measured following the United States Environmental Protection Agency (USEPA) Method 445.0 (Arar and Collins 1997). The non-purgeable organic carbon (NPOC, TOC-L Autoanalyzer, Shimadzu Corp., Kyoto, Japan) and nutrients (NO_2^- , $\text{NO}_3^- + \text{NO}_2^-$, NH_4^+ , PO_4^{3-}) (QuikChem 8000, Lachat Instruments Div., Zellweger Analytics, Inc., Loveland, CO) of both the bag water and ambient ocean water were measured by standard methods within weeks of collection. To prepare water samples for non-purgeable organic carbon and nutrient measurements, approximately thirty milliliters of water were filtered through a 0.2 μm pore size PES syringe filter (Millipore, Billerica, MA) and stored in the dark at -20°C until analysis.

The UVB intensity at each site was obtained in 30 minute intervals for the duration of the deployment using the Simple Model of the Atmospheric Radiative Transfer of Sunshine (SMARTS, Table S1) (Khan and Edge 2007). There was little variation in the incident UVB between days of each experiment (data not shown) so data from the middle day of each experiment was used to represent each day of the experiment. Incident UVB was used to find the UVB transmitted to the middle of the deployed dialysis bags within the water column following methods described in Maraccini et al. (2016). Briefly, the method accounts for screening of UVB by the water column as well as the dialysis bag. The daily-average UVB was calculated across the entire day, including the time of day when it was dark.

Culture-based Fecal Indicator Bacteria Enumeration

Enterococci and *Escherichia coli* were enumerated using a colorimetric-liquid-defined substrate assay (Enterolert® and Colilert®, respectively; IDEXX, Westbrook, ME) (Budnick et al. 1996, Standard Methods for the Examination of Water and Wastewater 2005). Samples were 10-fold diluted and multiple dilutions were assayed. In some cases, dilutions were assayed in duplicate. All dilutions that yielded measurements within the assay range of quantification (ROQ) were averaged to find the concentration of each biological replicate. If all replicates for a particular biological replicate were below the assay detection limit (BDL, typically 10 MPN/100 ml), then <10 MPN/100 ml was retained. These data are previously reported by Maraccini et al. (2016) and are included here to compare with the MST marker and pathogen data as described in the introduction.

Salmonella

The presence of culturable *Salmonella* in each water sample was assessed using a modified version of EPA method 1682 for enumeration in biosolids by the MPN method (Yamahara et al.) (USEPA 1997). Briefly, 100 ml of sample was filtered onto 47 mm, 0.45 μm -pore size nitrocellulose filters (HA type filters, Millipore, Billerica, MA). The filters were then placed in 25 ml of tryptic soy broth (TSB) at 37°C for 24 h for enrichment. Six 30 μl aliquots of each TSB enrichment were spotted onto modified semisolid Rappaport-Vassiliadis medium (MSRV) agar (BD Diagnostic, Franklin Lakes, NJ) and incubated at 42°C for 16-18 h. Organisms exhibiting mobility in the MSRV plates were streaked onto xylose lysine deoxycholate agar (XLD) (BD Diagnostic) and incubated at 37°C for 24 h. The biochemical characteristics of colonies displaying typical *Salmonella* morphology (red-pink colonies with or without black centers) were tested on both lysine iron agar (BD Diagnostic) and triple-sugar iron agar (BD Diagnostic). Putative positive isolates were archived in 250 μl of molecular grade water and stored at -20°C for confirmation by PCR. DNA was obtained by lysing isolates at 100°C for 10 min followed by centrifugation and collection of the supernatant. Lysate supernatants and 1:10 dilutions of supernatants were tested for the *Salmonella* genus-specific *invA* gene using Qiagen HotStar Plus Master Mix (Qiagen Inc., Valencia, CA) following the PCR conditions in Malorny et al. (2004).

Campylobacter

The presence of culturable *Campylobacter* was detected using a modified version (Yamahara et al. 2012) of the method of Khan and Edge (2007) in which 100 ml of water sample was filtered through HA filters and then placed in 25 ml of Bolton broth (Remel, Lenexa, KS) supplemented with Oxoid Bolton Broth Selective Supplement (Remel) and Laked Horse Blood (Remel) for enrichment under microaerophilic conditions (42°C for 48 h) using GasPak 100 systems with EZ Campy Container System sachets (BD Diagnostic). Bolton broth enrichments were streaked onto modified Karmali agar (Remel) supplemented with Oxoid *Campylobacter* Selective Supplement Karmali (Remel) and again incubated under microaerophilic conditions (42°C for 48 h). Colonies displaying typical *Campylobacter* morphology (white to gray colonies) were picked as presumptive positives, and DNA was extracted as described above for *Salmonella*, with PCR confirmation targeting *Campylobacter* 16S rRNA (Linton and Stanley 1996).

Molecular Detection of General Bacteroidales, Total Enterococci, *Salmonella enterica*, Human-associated MST markers, and Norovirus GII. For the detection of enterococci, human MST markers, and *Salmonella*, 100 ml from each bag or ambient ocean water sample was filtered through three separate (300 ml in total) 47 mm, 0.45 µm-pore size polycarbonate (PC) filters (Millipore, Billerica, MA). The PC filters were immediately flash frozen in liquid nitrogen and stored at -80 °C. For the detection of norovirus GII, 100 ml of each sample was filtered through two separate (200 ml total) 47 mm, 0.45 µm-pore size HA filters. Prior to filtering, 0.5 ml of 2.5 M MgCl₂ was added to every 50 ml of water sample filtered through the HA filters to facilitate the capture of virus particles (Victoria et al. 2009). After filtration, HA filters were treated with 500 µL of the RNA/DNA stabilizing agent RNeasy (Qiagen, Germantown, MD), allowed to sit for 5 minutes, and then vacuum aspirated (Keating et al. 2008). Filters were stored at -20°C for 24 hours and then placed at -80°C for up to 2 months until further molecular processing. Filtration blanks were run daily for each filter type.

Nucleic acid extraction

DNA was extracted from PC filters for the quantification of bacterial molecular markers using the GeneRite DNA-EZ kit (catalog no. K200-02C-50, GeneRite, North Brunswick, NJ) following manufacturer's instructions with a 100 µl final elution volume. The eluent from the three replicate PC filter extractions (each with 100 ml of sample filtered) were pooled (300 µl total extract eluent) and then separated into 50 µl aliquots and stored at -80°C for subsequent molecular analyses. DNA concentrations and purities were determined on a Nanodrop[®] ND-1000 UV-Vis spectrophotometer (Nanodrop Technologies, Wilmington, DE).

Total RNA and DNA were extracted simultaneously from the two replicate HA filters for the quantification of norovirus GII using a modified MoBio PowerWater[®] RNA Isolation Kit (Mo Bio Laboratories Inc., Carlsbad, CA) with a final elution volume of 100 µl (see SI for details on modifications) (Mattioli et al. 2014) (Viau et al. 2011). Extraction blanks were run with every seventeen samples. Separate 30 µL aliquots of extracted RNA/DNA were stored at -80°C for subsequent molecular analyses. All RNA and DNA aliquots underwent a maximum of one freeze-thaw cycle prior to molecular analysis.

Molecular assays

Molecular markers for were measured using quantitative polymerase chain reaction (qPCR) or reverse transcriptase qPCR (RT-qPCR) on an Applied Biosystems StepOnePlus[™] thermocycler (Applied Biosystems (ABI), Carlsbad, CA). The human-associated *Bacteroidales* were quantified using three different qPCR assays: BacHum (Kildare et al. 2007), HumM2 (Shanks et al. 2009), and HF183/BacR287 (Green et al. 2014). General fecal indicator bacteria were measured using (USEPA 2012) the general *Bacteroidales* assay, GenBac3 (Shanks et al. 2012), and the enterococci assay, entero1a (USEPA 2012).

The two enteric pathogens assayed were *Salmonella* spp. targeting the *ttr* locus (Malorny et al. 2004) using qPCR and norovirus genotype II (NVGII) targeting the ORF1-ORF2 gene (Viau et al. 2011) using RT-qPCR.

All qPCR assays used Environmental MasterMix 2.0 (Life Technologies, Grand Island, NY), and AgPath-ID One-Step RT-PCR MasterMix (Life Technologies, Grand Island, NY) was used for the RT-qPCR assay. Twenty-five μ l reactions were run for all (RT-) qPCR assays, and each reaction contained 2 μ l extract and 6 μ l of extract for each qPCR and RT-qPCR, respectively. The Taqman probe (Life Technologies, Grand Island, NY) and primer concentrations and sequences for each (RT-) qPCR assay are listed in Table S1, as well as the final bovine serum albumin fraction V (Life Technologies, Grand Island, NY) concentration in each reaction. The thermal cycling parameters for all qPCR assays were as follows: 10 minutes at 95°C and then 45 cycles of 95 ° for 15 seconds and 60 °C for 1 minute. The thermal cycling parameters for the RT-qPCR assay were a 30-minute reverse transcription step at 50°C, followed by a 10 minute denaturation step at 95°C and then 45 cycles of 95°C for 15 seconds and 60°C for 60 seconds.

The same linearized DNA plasmid standard was used as the standard for the HF183/BacR287 and the HumM2 assays (Green et al. 2014). A different non-linearized DNA plasmid, B9 (Walters et al. 2009), was used for the BacHum assay, and genomic DNA was used as the standards for the entero1a and *Salmonella* spp. qPCR assays using the American Type Culture Collection (ATCC Manassas, VA) *Enterococcus faecalis* strain 29212 and *Salmonella enterica* subsp. *enterica* serovar Typhimurium LT2 (ATCC 19585), respectively. A synthetic single stranded RNA standard, Synthetic Norovirus G2 (II) RNA (ATCC VR3200SD) was used for the NVGII assay. Seven, 10-fold serial dilutions (10^6 down to 10^0 per reaction) of (RT-) qPCR standards were run in triplicate with every 96-well plate. A master standard calibration curve was generated from eleven independent standard dilution series (Sivaganesan et al. 2010). Details of the standard curves and assay efficiencies for each molecular assay are provided in Table S1 of the SI.

All standards and samples were run in triplicate (RT-) qPCR reactions on 96-well plates (ABI, Carlsbad, CA). Triplicate no template controls (NTC) were included in every run with every plate. The amplification threshold for the enterococci (entero1a) and the three assays human-specific *Bacteroidales* assays (HF183/ BacR287, HumM2, and BacHum) was set to 0.03 Δ Rn units. The amplification threshold for the general *Bacteroidales* assay (GenBac3) and the two enteric pathogen assays (NVGII and *Salmonella* spp.) was 0.025 and 0.02 Δ Rn units, respectively. Raw data were processed using StepOnePlus™ version 2.3 software (Life Technologies, Grand Island, NY).

Copy number per (RT-) qPCR reaction were calculated for all samples with amplification prior to a quantification cycle (Cq) of 40, even those with a Cq above that of the lowest concentration standard, also known as the lower limit of quantification (LLOQ). For those samples with a Cq above the LLOQ, copy number estimates were obtained by extrapolating from the linear fit of the log-transformed standard copy number versus Ct (see Table S1 for standard curve parameters of each assay). The number of gene copies in all three sample replicates were averaged, normalized by the volume of sample in each (RT-) qPCR reaction, and then multiplied by the volume eluted in each extraction and the volume of water filtered per sample to obtain concentration in units of copies per 100 ml (Viau et al. 2011).

The theoretical lowest detectable concentration (LDC) was calculated assuming that 1 copy of the nucleic acid target amplifies in a reaction. Samples were considered below the LDC if two of the three replicates had Cq values greater than that associated with 1 copy/reaction. Based on the 200 ml combined filtration volume from the two HA filters, the LCD of NVGII assay was 25 copies per 100 ml. The LDC of the bacterial molecular markers and the *Salmonella* spp. molecular marker were 50 copies per 100 ml based on combined filtration volume of 300 ml through the three separate PC filters.

Potential amplification interference present in the molecular assays was tested in two ways. The first interference testing method was to run the HF183/BacR287 and HumM2 assays in multiplex with an internal amplification control (IAC) (Green et al. 2014). Each qPCR was spiked with 500 copies of the IAC (2 μ l of IAC template added to each reaction). The interference threshold was determined by averaging the C_q value of the IAC spiked into qPCR without template ($n = 24$). Amplification interference was defined as the interference threshold C_q value ± 1.5 . The second interference testing method was to run 1:10 dilutions of a subset of samples in triplicate for each (RT-) qPCR assay. The samples tested for interference by dilution were from the first two days of the deployments, including the 100% raw sewage and one control sample ($n = 9$ for the summer and $n = 7$ for the winter). If the difference in C_q values between the diluted and undiluted sample was less than 2.3, then amplification interference was considered present in the sample (Boehm et al. 2013).

Modeling decay

The Geeraerd and Van Impe inactivation model fitting tool (GInaFit) was used in Excel 2013 (Microsoft Inc., Redmond, WA) to determine the decay rates (Geeraerd et al. 2005). The shoulder-log linear model was used to fit the decay data (Geeraerd et al. 2005):

$$C(t) = C_0 \cdot e^{-k \cdot t} \cdot \left(\frac{e^{-k \cdot S}}{1 + (e^{k \cdot S} - 1) \cdot e^{-k \cdot t}} \right) \quad (2)$$

where t is time (d, days), C (MPN/100 ml for the culture-based assays or copies/100 ml for (RT-) qPCR assays) is the measured concentration at time t , C_0 is the fitted initial concentration at time 0, S (d) is the shoulder or lag time over which there is minimal decay or inactivation of the nucleic acid targets or culturable bacteria, respectively, and k (d⁻¹) is the decay rate constant for the log-linear portion of the decay curve after the shoulder. If the 95% confidence interval for the fitted shoulder parameter, S , crossed zero, the shoulder was considered insignificant, and the decay curve was fit to a log-linear model following Chick's Law (Chick 1910):

$$C(t) = C_0 \cdot e^{-k \cdot t} \quad (3)$$

where C is the culturable bacteria or molecular target concentration (MPN or copies/100 ml) at time, t (d), C_0 is the model fitted initial concentration (MPN or copies/100 ml), and k (d⁻¹) is the decay or inactivation constant rate. It should be noted that Eqn (2) simplifies to Eqn (3) when the shoulder is equal to 0.

For all decay models, concentration measured in each biological replicate was treated as a separate data point; therefore, each day had two data points per experimental depth. In addition, only days with measurements above the lower limit of detection and after the shoulder, only the decreasing portion of the data was included in modeling the log-linear decay rate. For the molecular data, this resulted in modeling data collected on days 0 through 5 for the summer deployment and days 0 through 7 for the winter deployment. For modeling culturable enterococci inactivation in the summer, days 0 through 1 and days 0 through 3 were used to model inactivation at surface (5 cm) and depth (99 cm), respectively. Days 0 through 1, days 0 through 2, and days 0 through 5 were used to model culturable enterococci inactivation in the winter at surface (5 cm), middle (18 cm), and depth (99 cm), respectively. For the culturable *E. coli* inactivation in the summer, days 0 through 3 and days 0 through 6 were used to model inactivation at surface (5 cm) and depth (99 cm), respectively. Days 0 through 5, days 0 through 6, and days 0 through 10 were used to model culturable *E. coli* inactivation in the winter at surface (5 cm), middle (18 cm), and depth (99 cm), respectively.

Fitted decay/inactivation rates were statistically compared between target within a season and depth using a z -test of the differences assuming a normal distribution for the fitted rate, k , and associated standard error (SE) outputted from the GInaFit model. A generalized linear model (GLM) was used to determine

the association between specific fecal indicator decay rate, sunlight intensity (represented by UVB transmitted as a continuous variable), and season (as a binary variable with winter as the reference). The GLM results are reported in the form of coefficients (β), 95% confidence intervals, and P values. An analysis of variance (ANOVA) test was used to evaluate differences in nutrient and chlorophyll a concentrations between depths and between inside the bags and the ambient ocean water. Results are considered statistically significant at a level of $P \leq 0.05$.

Results

A summary of the environmental parameters for the two deployments at Pillar Point Harbor is presented in Table 1. The ambient ocean water quality parameters described are the average (\pm standard deviation): maximum daily ambient ocean water temperature, dissolve oxygen, salinity, chlorophyll a , turbidity, and non-purgeable organic carbon (NPOC). The daily average UVB (280-320 nm) irradiance within the dialysis bags at each depth is also included in Table 1.

Table 1. Field deployment information and physical properties of ambient Pillar Point Harbor water (Half Moon Bay, CA USA) (mean \pm standard deviation) during the summer (10 days) and winter (7 days) deployments.

Season	Study Period	Depth	Daily UVB	Chlorophyll a	Avg. Max. Daily Temp	Dissolved Oxygen	Salinity	Turbidity	NPOC
		[cm]	[W/m ²]	[μ g/L]	[$^{\circ}$ C]	mg/ml	[ppt]	[NTU]	[mg/L]
Summer	8 Sept - 18 Sept 2014	5	0.337	11.8 \pm 7.9	19.7 \pm 1.3	6.46 \pm 0.3	33.5 \pm 0.2	2.97 \pm 1.8	2.16 \pm 0.6
		99	4.33x10 ⁻⁴						
Winter	13 Feb - 20 Feb 2015	5	0.198	2.07 \pm 3.2	16.5 \pm 1.3	7.42 \pm 0.3	32.9 \pm 0.5	2.84 \pm 0.5	1.87 \pm 0.5
		18	8.04 x10 ⁻²						
		99	3.33x10 ⁻⁴						

Decay Models

The fitted decay rates of each target measured during the summer and winter deployments at different depths are presented in Table 2. Figures S1-S7 display the plots for each of the targets, as well as the fitted decay models during the summer and winter deployments at each depth. Culturable enterococci and *E. coli* inactivation fit a log-linear model for both the summer and winter deployments. The molecular-based fecal indicator assays (HF183/BacR287, BacHum, HumM2, GenBac3, and entero1a) fit a log-linear model for the summer deployment and a shoulder log-linear model for the winter deployment.

Table 2. Decay rates of fecal indicator bacteria in marine waters during two seasons (summer and winter) and at three depths, modeled using a shoulder log-linear or log-linear model (Geeraerd et al. 2005). Surface, middle, and depth correspond to the dialysis bags floating 3, 15, and 99 cm below the water surface. *k* and *S* (\pm 95% confidence interval) are the fitted decay rate ($-d^{-1}$) and shoulder (*d*) parameters, respectively.*

Assay	Summer ^{a,b}		Winter					
	Surface	Depth	Surface		Middle		Depth	
	<i>k</i>	<i>k</i>	<i>k</i>	<i>S</i>	<i>k</i>	<i>S</i>	<i>k</i>	<i>S</i>
HF183/BacR287	1.6 (0.25)	1.4 (0.15)	1.3 (0.32)	2.0 (1.21)	1.7 (0.36)	3.0 (0.76)	1.7 (0.46)	2.7 (1.04)
BacHum	1.6 (0.26)	1.4 (0.20)	1.4 (0.30)	2.1 (1.02)	1.8 (0.31)	3.0 (0.64)	1.7 (0.43)	2.5 (1.04)
HumM2	1.7 (0.13)	1.3 (0.18)	1.2 (0.25)	1.7 (1.14)	1.8 (0.35)	2.8 (0.73)	1.7 (0.48)	2.7 (1.11)
GenBac3	1.8 (0.11)	1.3 (0.23)	1.3 (0.21)	1.8 (0.85)	1.8 (0.28)	3.0 (0.56)	1.9 (0.38)	2.8 (0.75)
entero1a	1.5 (0.25)	0.93 (0.23)	0.75 (0.14)	2.4 (0.90)	0.87 (0.23)	3.2 (1.03)	0.89 (0.41)	3.9 (1.42)
Enterococci ^{b,c}	6.6 (0.85)	2.4 (0.46)	3.9 (0.20)	-	3.3 (0.37)	-	1.4 (0.22)	-
<i>E. coli</i> ^{b,c}	4.8 (0.65)	1.7 (0.23)	3.9 (0.60)	-	3.0 (0.98)	-	2.2 (0.33)	-

^a When value was not significantly different from 0 ($p \leq 0.05$), log-linear decay models were used (Chick's Law)

^b Assayed by culture-based methods

^c Only first 5 days were used to fit decay curve because the concentration stayed constant afterward

* *Salmonella* (qPCR & culture), *Campylobacter*, and Norovirus GII were too low in starting sewage mixture to model decay (see Table 4)

Human-Associated Fecal Markers Versus General FIB

The decay rates of the three human-specific fecal molecular markers (HF183/BacR287, HumM2, and BacHum) were not significantly different from one another within each deployment (summer and winter) and each depth (Summer: mean k of human-specific markers = 1.66 d^{-1} surface, 1.36 d^{-1} depth; Winter: mean k = 1.30 d^{-1} surface, 1.75 d^{-1} middle, 1.73 d^{-1} depth; $P > 0.05$). The decay rates of the three human-specific fecal molecular markers were also not significantly different than GenBac3 (GenBac3 Summer: k = 1.84 d^{-1} surface, 1.33 d^{-1} depth; GenBac3 Winter: k = 1.80 d^{-1} surface, 1.80 d^{-1} middle, 1.92 d^{-1} depth; $P > 0.05$) within each deployment and depth ($P > 0.05$). In addition, the lengths of the fitted shoulders (S , days) during the winter deployment were not significantly different between the three human-specific fecal markers or between the human-specific markers and GenBac3 at each depth (Winter: mean S = 1.88 d surface, 2.96 d middle, 2.65 d depth; $P > 0.05$).

Enterol1a k was significantly smaller than the three human-specific fecal markers during both deployments and at all depths (enterol1a summer: k = 1.50 d^{-1} surface, 0.93 d^{-1} depth; enterol1a winter: k = 0.75 d^{-1} surface, 0.87 d^{-1} middle, 0.89 d^{-1} depth; $P < 0.05$) except during the summer deployment at the surface (highest sunlight intensity) when the rates were not significantly different (average human marker k = 1.66 d^{-1} , $P > 0.05$). Enterol1a k was 0.4 d^{-1} less than the average decay rate of the three human-specific molecular markers (average human marker k = 1.36 d^{-1}) during the summer deployment in the deep bags (99 cm). During the winter deployment, the enterol1a decay rate was 0.55 d^{-1} , 0.88 d^{-1} , and 0.84 d^{-1} less than the average decay rate of the three human-specific molecular markers (surface = 1.30 d^{-1} , middle = 1.75 d^{-1} , depth = 1.73 d^{-1}) in the surface, middle, and deep bags, respectively.

Culturable enterococci k was significantly greater than the k of the three human-specific molecular markers during both deployments (summer and winter) and at all depths (5 cm, 18 cm, and 99 cm) except in the deepest bags during the winter deployment (lowest sunlight) when the culturable enterococci decay rate (k = 1.47 d^{-1}) was not statistically different ($P > 0.05$) than the human-specific molecular markers' decay rate (mean k = 1.73 d^{-1}). During the summer deployment, culturable *E. coli* decay rate was significantly greater ($P < 0.05$) than the three human-specific markers at both depths except in the deep bags where the BacHum marker decay rate was (k = 1.40 d^{-1}) not significantly different from culturable *E. coli* (k = 1.66 , $P = 0.09$). During the winter deployment, culturable *E. coli* k was significantly greater ($P < 0.05$) than the three human-specific markers in the surface and middle depth bags. In the deep bags (99 cm) during the winter (lowest sunlight intensity), the culturable *E. coli* k was not significantly different than any of the three human-specific molecular maker decay rates ($P > 0.05$).

Culture-Based Versus Molecular-Based General FIB

The decay rate for culturable *Escherichia coli* was significantly smaller than for culturable enterococci during the summer deployment at both depths (surface: difference = 1.79 d^{-1} , $P = 0.001$; depth: difference = 0.74 d^{-1} , $P = 0.004$). During the winter deployment, culturable *E. coli* k was not significantly different from culturable enterococci k at the surface (5 cm) (difference = 0.02 d^{-1} , $P = 0.95$) and middle (18 cm) (difference = 0.29 d^{-1} , $P = 0.59$) depths. However, at the deepest depth (99 cm) in the winter (lowest sunlight intensity), culturable *E. coli* k was significantly greater than culturable enterococci k (difference = 0.69 d^{-1} , $P = 0.005$).

Figure 2 displays enterococci data and fitted models during the summer and winter deployments measured by both culture-based and molecular-based methods. The culturable enterococci decayed significantly faster than the molecular enterococci target, enterol1a, during both deployments and at all depths (Summer—surface: difference = 5.06 d^{-1} , $P < 0.001$; depth: difference = 1.48 d^{-1} , $P < 0.001$; Winter— surface: difference = 3.22 d^{-1} , $P < 0.001$; middle: difference = 2.46 d^{-1} , $P < 0.001$; depth: difference = 0.58 d^{-1} , $P = 0.03$). During the summer deployment, the culturable enterococci decay rate, k , was 4.4 times greater than the enterol1a k at the surface (5 cm deep) and 2.6 times greater at depth (99 cm

deep). During the winter deployment, culturable enterococci k was 5.2 times greater than entero1a at the surface, 3.8 times greater at the middle depth (18 cm), and 1.6 times greater at depth. The culturable enterococci and entero1a data did not display a shoulder during the summer deployment. During the winter deployment, the culturable enterococci data did not display a shoulder but entero1a did display a significant shoulder at all three depths (surface = 2.4 d, middle = 3.2 d, and depth = 3.9 d).

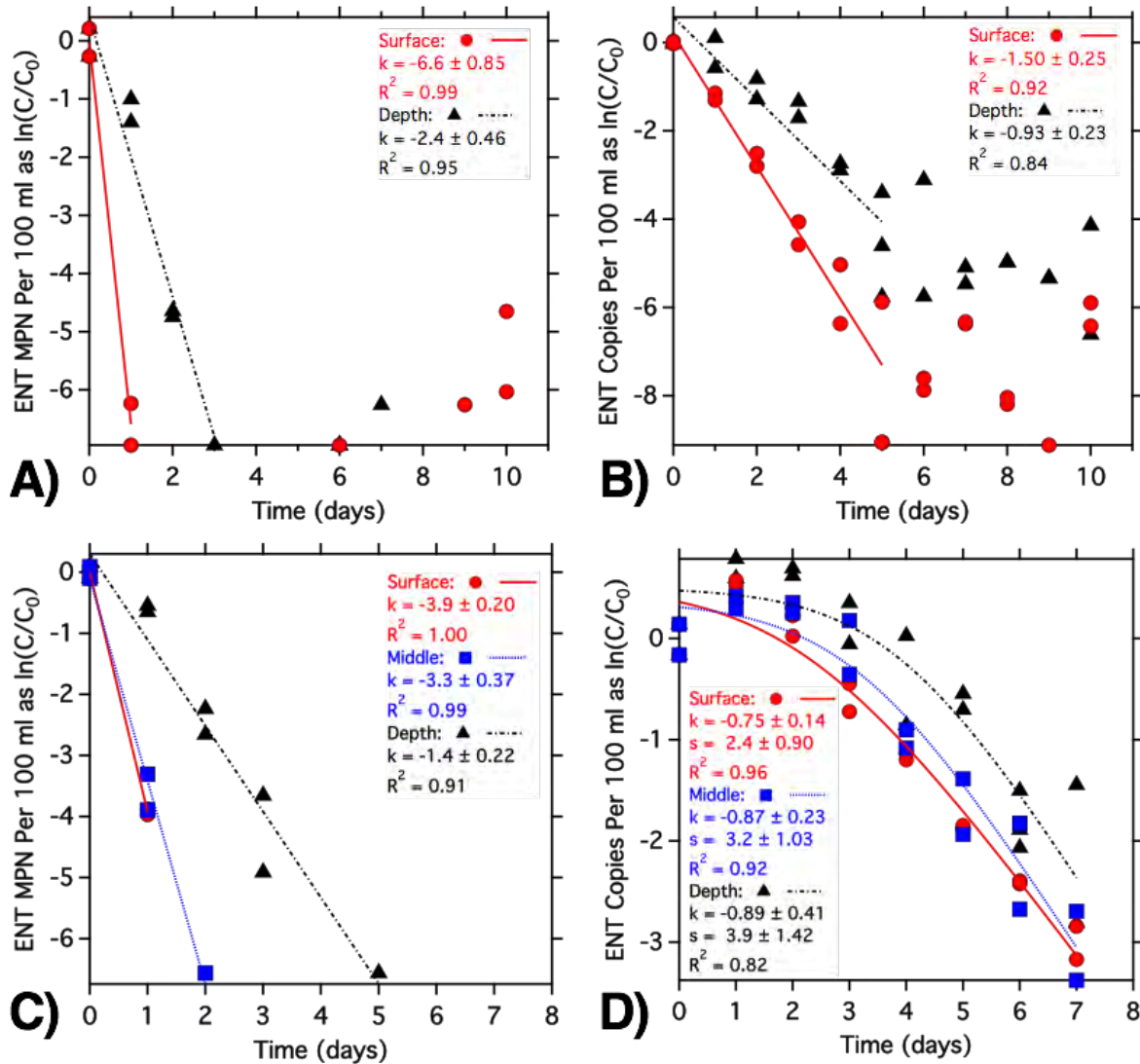


Figure 2. Enterococci decay curves for the summer (A and B) and winter (C and D) deployments measured by culture-based (A and C) and molecular-based (B and D) methods. The modeled shoulder log-linear or log-linear decay rate (k , day⁻¹), shoulder (s , d), and model fit (R^2). Surface, middle, and depth correspond to the dialysis bags floating 3, 15, and 99 cm below the water surface.

Impact of UVB Exposure and Season

A generalized linear model was used to evaluate the relationship between k , season, and sunlight intensity, as represented by the daily average UVB (Table 3). The decay rates of the three human-specific molecular fecal markers and GenBac3 were not significantly associated with UVB or season. These markers were also not independently, linearly associated with UVB. The enterol1a decay rate was positively associated with UVB ($\beta = 1.07 \text{ (day}^{-1}) \text{ (W/m}^2\text{)}^{-1}$, $P = 0.02$) and season ($\beta = 0.30$, $P = 0.02$), meaning that enterol1a k increases as sunlight intensity increases and during the summer season (versus the winter season). Enterococci and *E. coli* k were also positively associated with UVB (enterococci: $\beta = 12.3$, $P < 0.001$; *E. coli*: $\beta = 9.14$, $P = < 0.001$), but UVB had an over 10-fold greater effect on the decay rates of culturable FIB than the molecular FIB target, enterol1a. Culturable enterococci k was positively associated with season ($\beta = 0.65$, $P = 0.03$), while *E. coli* k was negatively associated with season ($\beta = -0.50$, $P < 0.001$). Therefore, enterol1a and culturable enterococci decay rates were 0.3 and 0.65 d^{-1} greater, respectively, in the summer than in the winter at the same sunlight intensity, and *E. coli* k was 0.5 d^{-1} greater in the winter than summer at the same sunlight intensity. The seasonal effect on enterol1a k was not statistically different than the effect on culturable enterococci k ($P = 0.27$), and though in opposite directions, the magnitude of the seasonal effect on *E. coli* k was not statistically different than the seasonal effect on culturable enterococci or enterol1a decay rates ($P = 0.62$ and $P = 0.14$, respectively).

Table 3. Generalized linear models of decay rates, k , as a function of daily average UVB in W/m^2 and season. UVB was modeled as a continuous variable, and season was modeled as a binary variable with winter as the reference. Separate models were run for each assay. Coefficients, β , 95% confidence intervals, and P-values are presented.

Assay	UVB (280-320)			Season		
	β	\pm 95% CI	P	β	\pm 95% CI	P
HF183/BacR287	0.037	1.213	0.953	-0.092	0.319	0.571
BacHum	0.033	1.056	0.951	-0.118	0.278	0.406
HumM2	0.093	1.682	0.914	-0.054	0.442	0.812
GenBac3	0.290	1.857	0.759	-0.107	0.488	0.668
enteor1a	1.071	0.931	0.024	0.295	0.245	0.018
ENT	12.246	2.226	<0.0001	0.653	0.585	0.029
<i>E. coli</i>	9.138	0.487	<0.0001	-0.503	0.128	<0.0001

Enteric Pathogen Decay

Salmonella (qPCR & culture), *Campylobacter*, and human norovirus GII (NVGII) were too low in starting sewage mixture to model decay. Table 4 describes the number of days each enteric pathogen (*Salmonella* and NVGII) was detected during the experiments. The enteric pathogens could not be fitted to a decay model because the pathogens concentrations were too close to the detection limit in the starting 5% sewage mixture. The initial concentration of *Salmonella* by qPCR was 194 copies/100 ml and 141 copies/100 ml (LOD 50 copies/100 ml) during the summer and winter deployments, respectively. *Salmonella* by both culture and molecular methods was only detected in the initial 5% sewage mixture for the surface bags during both the summer and winter deployments. *Salmonella* was detected only by culture for the first two days of the summer deployment in the deep bags (99 cm). During the winter, culturable *Salmonella* was present through day 1 in the deepest bags (99 cm), and *Salmonella* by qPCR was detectable through day two during the winter deployment in the middle and depth bags only. The *Salmonella* molecular target concentration data during each deployment is shown in Figure S6.

Norovirus GII was not detected in the initial 5% sewage mixture during the summer deployment. The initial concentration of NVGII during the winter deployment was 69 copies/100 ml (LOD 25 copies/100 ml). NVGII was detected at all three depths for the first two days of the winter deployment. Culturable *Campylobacter* was not detected in the initial 5% sewage mixture during either the summer or winter deployments. The NVGII data during each deployment is shown in Figure S7 of the SI.

Table 4. The number of days each enteric pathogen was detected during the field deployments. A value of zero means the pathogen was only detected in the starting 5% sewage-95% seawater mixture. NA indicates the pathogen was not detected in the starting sewage-seawater mixture.

Assay	Summer		Winter		
	Surface	Depth	Surface	Middle	Depth
<i>Salmonella</i> by culture	0	2	0	0	1
<i>Salmonella</i> by qPCR	0	0	0	2	2
Norovirus GII†	NA	NA	2	2	2
<i>Campylobacter</i> β	NA	NA	NA	NA	NA

† Pathogen was detected in raw sewage for summer and winter deployments

β *Campylobacter* was not detected in the raw sewage for either deployment but was detected in ambient ocean on day 6 in the winter.

Bag Effects on Nutrient and Chlorophyll Concentrations

Nutrient (NO_3^- , NH_4^+ , PO_4^{3-}) and chlorophyll *a* concentrations were measured inside the dialysis bags and in the ambient ocean water each day to evaluate how well the bag environments emulated the natural ocean environment. Figure S8 and S9 show the nutrient concentrations within the bags and in the ambient ocean water. After the initial nutrient spike on day zero from the sewage, the nutrients were always lower inside the bag than in the ambient ocean water (average difference between nutrients in the ocean and inside bags (standard deviation) - summer: $\text{NO}_3^- = 2.90$ (1.94) μM , $\text{NH}_4^+ = 3.39$ (2.34) μM , $\text{PO}_4^{3-} = 0.78$ (0.93) μM ; winter: $\text{NO}_3^- = 2.41$ (3.17) μM , $\text{NH}_4^+ = 3.17$ (2.03) μM , $\text{PO}_4^{3-} = 0.43$ (0.69) μM), and there was no difference between nutrient concentrations inside the bags by depth (F-statistic (*P* value): $\text{NO}_3^- = 0.60$ (0.56), $\text{NH}_4^+ = 0.46$ (0.63), $\text{PO}_4^{3-} = 0.54$ (0.59)). Seasonal differences in nutrients concentrations is described in the SI.

The chlorophyll *a* concentrations during the two deployments are shown in Figures S10 and S11. Chlorophyll *a* spiked at day 5 of 10 (113.63 $\mu\text{g/L}$ in surface bags) during the summer deployment and at day 7 of 7 (38.74 $\mu\text{g/L}$ in surface bags) during the winter deployment, both corresponding to visible algal blooms inside the bags. The ambient ocean water chlorophyll *a* concentration also spiked at days 5 (17.82 $\mu\text{g/L}$) and 7 (10.00 $\mu\text{g/L}$) during the summer and winter deployments, respectively. In addition, the control bags (ocean water only) showed chlorophyll *a* concentrations similar to the study bags at the same depth that day (days 5 and 7 in the summer and day 7 in the winter). In general, throughout the deployments the ambient ocean water chlorophyll *a* concentrations followed the same trend as inside the bags but at lower concentrations.

Quality Assurance/Quality Control

The control and molecular grade water bags collected during the summer and winter deployments had no detectable culturable or molecular fecal markers. Amplification interference was not detected in any of the (RT-) qPCR reactions by either the internal amplification control (IAC) spike or evaluating the ΔCq from diluted samples. The IAC interference threshold Cq for HumM2 and HF183/BacR287 were 28.93 and 29.34, respectively. All qPCR reactions were within the IAC interference threshold $\text{Cq} \pm 1.5$ ranges. The average ΔCq of the 1:10 diluted to undiluted samples for the molecular assays were as follows: BacHum = 3.35, entero1A = 3.41, GenBac3 = 3.61, HF183/BacR287 = 3.52, and HumM2 = 3.00. All extraction blanks, filtration blanks, and NTCs were negative, and duplicate samples generally agreed for culture-based FIB analyses.

Additional Methods and Results

Additional methods and results can be found in the Supporting Information section at the end of this appendix:

Table S1: Primer and probe sequences used in qPCR and reverse transcriptase (RT)-qPCR assays

Figures S1-S7: Decay plots and model fits for HF183/BacR287, BacHum, HumM2, GenBac3, *E. coli*, *Salmonella*, and Norovirus GII during the summer and winter deployments

Figures S8 and S9: Nutrient concentrations inside the bags and in the ambient ocean water during the summer and winter deployments

Figures S10 and S11: Chlorophyll *a* concentrations inside the bags and in the ambient ocean during the summer and winter deployments.

Literature Cited

- Arar, E.J., and G.B. Collins, *Method 445.0: In Vitro Determination of Chlorophyll a and Pheophytin a in Marine and Freshwater Algae by Fluorescence*. U.S. Environmental Protection Agency National Exposure Research Laboratory, Office of Research and Development.: Cincinnati, Ohio, 1997.
- Boehm, A.B., N.J. Ashbolt, J.M. Colford, Jr., L.E. Dunbar, L.E. Fleming, M.A. Gold, J.A. Hansel, P.R. Hunter, A.M. Ichida, C.D. McGee, J.A. Soller, S.B. Weisberg. A sea change ahead for recreational water quality criteria. *Journal of Water and Health* **2009**, 7, (1), 9-20.
- Boehm, A.B., S.B. Grant, J.H. Kim, S.L. Mowbray, C.D. McGee, C.D. Clark, D.M. Foley, D.E. Wellman. Decadal and shorter period variability of surf zone water quality at Huntington Beach, California. *Environ Sci Technol* **2002**, 36, (18), 3885-92.
- Boehm, A.B., L.C. Van De Werfhorst, J.F. Griffith, P.A. Holden, J.A. Jay, O.C. Shanks, D. Wang, S.B. Weisberg. Performance of forty-one microbial source tracking methods: a twenty-seven lab evaluation study. *Water Research* **2013**, 47, (18), 6812-28.
- Budnick, G.E., R.T. Howard, D.R. Mayo. Evaluation of Enterolert for enumeration of enterococci in recreational waters. *Applied and Environmental Microbiology* **1996**, 62, (10), 3881-4.
- Byappanahalli, M.N., D.A. Shively, M.B. Nevers, M.J. Sadowsky, R.L. Whitman. Growth and survival of *Escherichia coli* and enterococci populations in the macro-alga *Cladophora* (Chlorophyta). *FEMS Microbiology Ecology* 2003, 46, (2), 203-11.
- Field, K.G. and M. Samadpour. Fecal source tracking, the indicator paradigm, and managing water quality. *Water Research* 2007, 41, (16), 3517-38.
- Geeraerd, A.H., V.P. Valdramidis, J.F. Van Impe. GInaFit, a freeware tool to assess non-log-linear microbial survivor curves. *International Journal of Food Microbiology* 2005, 102, (1), 95-105.
- Green, H.C., R.A. Haugland, M. Varma, H.T. Millen, M.A. Borchardt, K.G. Field, W.A. Walters, R. Knight, M. Sivaganesan, C.A. Kelty, O.C. Shanks. Improved HF183 quantitative real-time PCR assay for characterization of human fecal pollution in ambient surface water samples. *Applied and Environmental Microbiology* 2014, 80, (10), 3086-94.
- Green, H.C., O.C. Shanks, M. Sivaganesan, R.A. Haugland, K.G. Field. Differential decay of human faecal *Bacteroides* in marine and freshwater. *Environmental Microbiology* 2011, 13, (12), 3235-49.
- Harwood, V.J., C. Staley, B.D. Badgley, K. Borges, A. Korajkic. Microbial source tracking markers for detection of fecal contamination in environmental waters: relationships between pathogens and human health outcomes. *FEMS Microbiology Reviews* 2014, 38, (1), 1-40.
- Keating, D.T., A.P. Malizia, D. Sadlier, C. Hurson, A.E. Wood, J. McCarthy, L. Nolke, J.J. Egan, P.P. Doran. Lung tissue storage: optimizing conditions for future use in molecular research. *Exp Lung Res* 2008, 34, (8), 455-66.
- Khan, I.U. and T.A. Edge. Development of a novel triplex PCR assay for the detection and differentiation of thermophilic species of *Campylobacter* using 16S-23S rDNA internal transcribed spacer (ITS) region. *Journal of Applied Microbiology* 2007, 103, (6), 2561-9.

- Kildare, B.J., C.M. Leutenegger, B.S. McSwain, D.G. Bambic, V.B. Rajal, S. Wuertz. 16S rRNA-based assays for quantitative detection of universal, human-, cow-, and dog-specific fecal Bacteroidales: a Bayesian approach. *Water Research* 2007, 41, (16), 3701-15.
- Linton, D., R.K. Owen, J. Stanley. Rapid identification by PCR of the genus *Campylobacter* and of five *Campylobacter* species enteropathogenic for man and animals. *Research in Microbiology* 1996, 147, (9), 707-18.
- Malorny, B., E. Paccassoni, P. Fach, C. Bunge, A. Martin, R. Helmuth. Diagnostic real-time PCR for detection of *Salmonella* in food. *Applied and Environmental Microbiology* 2004, 70, (12), 7046-52.
- Maraccini, P.A., M.C. Mattioli, L.M. Sassoubre, Y. Cao, J.F. Griffith, J.S. Ervin, L.C. Van De Werfhorst, A.B. Boehm. Solar inactivation of enterococci and *Escherichia coli* in natural waters: effects of water absorbance and depth. In Review.
- Mattioli, M.C., A.B. Boehm, J. Davis, A.R. Harris, M. Mrisho, A.J. Pickering. Enteric pathogens in stored drinking water and on caregiver's hands in Tanzanian households with and without reported cases of child diarrhea. *PloS one* 2014, 9, (1), e84939.
- Russell, T.L., K.M. Yamahara, A.B. Boehm. Mobilization and transport of naturally occurring enterococci in beach sands subject to transient infiltration of seawater. *Environmental Science & Technology* 2012, 46, (11), 5988-96.
- Shanks, O.C., C.A. Kelty, M. Sivaganesan, M. Varma, R.A. Haugland. Quantitative PCR for genetic markers of human fecal pollution. *Applied and Environmental Microbiology* 2009, 75, (17), 5507-13.
- Shanks, O.C., M. Sivaganesan, L. Peed, C.A. Kelty, A.D. Blackwood, M.R. Greene, R.T. Noble, R.N. Bushon, E.A. Stelzer, J. Kinzelman, T. Anan'eva, C. Sinigalliano, D. Wanless, J. Griffith, Y. Cao, S. Weisberg, V.J. Harwood, C. Staley, K.H. Oshima, M. Varma, R.A. Haugland. Interlaboratory comparison of real-time PCR protocols for quantification of general fecal indicator bacteria. *Environmental Science & Technology* 2012, 46, (2), 945-53.
- Sinton, L.W., R.J. Davies-Colley, R.G. Bell. Inactivation of enterococci and fecal coliforms from sewage and meatworks effluents in seawater chambers. *Applied and Environmental Microbiology* 1994, 60, (6), 2040-8.
- Sinton, L. W., R.K. Finlay, P.A. Lynch. Sunlight inactivation of fecal bacteriophages and bacteria in sewage-polluted seawater. *Applied and Environmental Microbiology* 1999, 65, (8), 3605-13.
- Sivaganesan, M., R.A. Haugland, E.C. Chern, O.C. Shanks. Improved strategies and optimization of calibration models for real-time PCR absolute quantification. *Water Research* 2010, 44, (16), 4726-35.
- Soller, J.A., M.E. Schoen, T. Bartrand, J.E. Ravenscroft, N.J. Ashbolt. Estimated human health risks from exposure to recreational waters impacted by human and non-human sources of fecal contamination. *Water Research* 2010, 44, (16), 4674-91.
- Standard Methods for the Examination of Water and Wastewater. In *Standard Method 9223 B-97*, 21st Edition ed., American Public Health Association: 2005.
- USEPA Method 1611: Enterococci in Water by TaqMan® Quantitative Polymerase Chain Reaction (qPCR) Assay, United States Environmental Protection Agency: Washington, D.C., 2012.

USEPA Method 1682: *Salmonella* in sewage sludge (biosolids) by modified semisolid Rappaport-Vassiliadis (MSRV) medium., Office of Water and Hazardous Materials, US Environmental Protection Agency: Washington, D.C., 1997.

USEPA: *Recreational Water Quality Criteria*, United States Environmental Protection Agency: Washington, D.C., 2012.

Viau, E.J., D. Lee, A.B. Boehm, Swimmer risk of gastrointestinal illness from exposure to tropical coastal waters impacted by terrestrial dry-weather runoff. *Environmental Science and Technology* **2011**, *45*, (17), 7158-65.

Victoria, M., F. Guimaraes, T. Fumian, F. Ferreira, C. Vieira, J.P. Leite, M. Miagostovich. Evaluation of an adsorption-elution method for detection of astrovirus and norovirus in environmental waters. *J Virol Methods* **2009**, *156*, (1-2), 73-6.

Wang, D., A.H. Farnleitner, K.G. Field, H.C. Green, O.C. Shanks, A.B. Boehm. Enterococcus and Escherichia coli fecal source apportionment with microbial source tracking genetic markers--is it feasible? *Water Research* **2013**, *47*, (18), 6849-61.

Walters, S.P., K.M. Yamahara, A.B. Boehm. Persistence of nucleic acid markers of health-relevant organisms in seawater microcosms: implications for their use in assessing risk in recreational waters. *Water Res* **2009**, *43*, (19), 4929-39.

Yamahara, K. M., L.M. Sassoubre, K.D. Goodwin, A.B. Boehm. Occurrence and persistence of bacterial pathogens and indicator organisms in beach sand along the California coast. *Applied and Environmental Microbiology* **2012**, *78*, (6), 1733-45.

Supporting Information

Methods

RNA/DNA Extraction Using Mobio PowerWater Kit

To increase RNA/DNA yields, the maximum volume of supernatant was recovered at each step; reagent volumes in subsequent steps were increased accordingly. Initial viral capsid lysis used vortex agitation with 1 mm silicon carbide beads (Biospec Products Inc., Bartlesville, OK). To improve inhibitor removal, incubations with Inhibitor Removal Technology® (IRT) solution were increased to 10 min at 4°C. After the second incubation step and the addition of the supernatant to the PWR3 and PWR4 mixture, the supernatant from the two replicate HA filters (100 ml each from the same water sample) were loaded onto the same the Spin Filter in order to concentrate the 200 ml filtered into the same extraction. To obtain DNA with the RNA kit, the on-filter DNA degradation and subsequent DNase buffer wash steps were eliminated. Final RNA/DNA elution was performed by adding 50 µL molecular grade water (preheated to 95°C) to the silica filter and incubating the filter for 1 min at room temperature before centrifugation. RNA/DNA elutions from the silica filter were performed twice in series.

Results

Nutrient and Chlorophyll Concentrations

There was not a significant difference between PO_4^{3-} concentrations inside the bags in the summer compared to the winter (F-statistic = 2.16, $P = 0.15$), but the average NO_3^- and NH_4^+ concentrations within the bags were significantly higher in the winter than in the summer (F-statistic (P -value): $\text{NO}_3^- = 7.50$ (0.01); $\text{NH}_4^+ = 4.53$ (0.04)). Conversely, the average PO_4^{3-} concentration in the ocean was significantly greater during the summer deployment compared to the winter the winter (F-statistic = 7.77, $P = 0.02$), but there was not a significant difference in NO_3^- or NH_4^+ concentrations between deployments (F-statistic (P -value): $\text{NO}_3^- = 0.64$ (0.44); $\text{NH}_4^+ = 1.66$ (0.22)). Chlorophyll *a* concentrations were significantly different by depth each day during the summer (F-statistic = 7.82, $P = 0.02$) with the highest concentrations occurring in the shallowest bags, but the same was not true of the winter deployment (F-statistic = 2.46, $P = 0.13$).

Table S1. Primer and probe sequences used in qPCR and reverse transcriptase (RT)-qPCR assays.

Target Organism	Gene	Primer/ Probe Name ^a	Primer/Probe Sequence (5' to 3' Direction) ^b	Primer/ Probe Ref	Final Primer Concentration (μM)	BSA per qPCR reaction (mg/ml) ^c	Pooled curve slope, intercept (R ²) ^d	qPCR Efficiency
Norovirus GII ²	ORF1-ORF2	QNIF2d	ATGTTCAGRTGGATGAGRTTCTCWGA	2	0.4			
		COG2R	TCGACGCCATCTTCATTCACA	3	0.4	0.2	-3.31, 37.78 (1.00)	100.4%
		QNIFSP	FAM-AGCACGTGGGAGGGCGATCG-TAMRA	3	0.12			
<i>Salmonella</i> spp. ⁴	ttrBCA	tt4-6	CTCACCAGGAGATTACAACATGG		0.4			
		tt4-4	AGCTCAGACCAAAAGTGACCATC	4	0.4	0.01	-3.84, 38.51 (0.98)	97.46%
		tt4-5	FAM- CACCGACGGCGAGACCGACTTT-TAMRA		0.24			
General <i>Bacteroidales</i> (GenBac3) ⁶	16S rRNA	GenBactF3	GGGGTTCTGAGAGGAAGGT	6	1			
		GenBactR4	CCGTCATCCTTCACGCTACT	7	1	0.2	-3.39, 38.67 (1.00)	98.21%
		GenBactP2	FAM-CAATATTCCTCACTGCTGCCTCCCGTA-TAMRA	6	0.08			
Enterococci (entero1a) ⁷	23S rRNA	EnteroF1a	GAGAAATCCAAACGAACTTG	8	1			
		EnteroR1	CAGTGCTCTACCTCCATCATT	9	1	0.2	-3.27, 39.25 (0.99)	102.4%
		GPL813TQ	FAM-TGG TTCTCTCCGAAATAG CTTTAGGGCTA-TAMRA	9	0.08			
Human-specific <i>Bacteroidales</i> (HF183 /BacR287) ¹	16S rRNA	HF183	ATCATGAGTTCACATGTCCG	11	1			
		BacR287	CTTCCTCTCAGAACCCCTATCC	10	1			
		BacP234 MGB	FAM-CTAATGGAACGCATCCC-MGB	10	0.08	0.2	-3.43, 37.94 (0.99)	95.73%
		Bac234IAC	VIC-AACACGCCGTTGCTACA-MGB	10	0.08			
		HumM2F	CGTCAGGTTTGT TTCGGTATTG	12	1	0.2		103.4%

Human-specific <i>Bacteroidales</i> (HumM2) ⁵	<i>Bacteroidales</i> -like putative σ factor	HumM2R	TCATCACGTAAC TTATTTATATGC ATTAGC	1				
		HumM2P	FAM-TATCGAAAATCTCACGGATTA ACTCTTGTGTACG C-TAMRA	0.08		-3.24, 38.83 (0.99)		
		UC1P1	VIC-CCTGCCGTCTCGTGCTCCTCA-TAMRA	0.08				
Human-specific <i>Bacteroidales</i> (BacHum) ³	16s rRNA	BacHum160f	TGAGTTCACATGTCCGCATGA	0.4				
		BacHum241r	CGTTACCCCGCCTACTATCTAATG	0.4	13	0.05	-3.38, 37.89 (0.98)	97.52%
		BacHum193p	FAM-TCCGGTAGACGATGGGGATGCGTT-TAMRA	0.08				

^a Primers and probes are listed in the following order: forward (F), reverse (R), hydrolysis probe (P), and then internal amplification control (IAC).

^b Mixed bases in degenerate primers and probe are as follows: R, A or G; W, A or T. The TaqMan probes were labeled at the 5' end with the reporter dye FAM (6-carboxyfluorescein) or VICTM and at the 3' end with the quencher dye TAMRA (6-carboxytetramethyl-rhodamine).

^c BSA is bovine serum albumin Fraction V in phosphate-buffered saline (Life Technologies, Grand Island, NY)

^d Concentrations were determined with the following formula: $Cq = \text{slope} \times \log_{10}(\text{concentration}) + y\text{-intercept}$. PCR efficiency = $10^{-1/\text{slope}+1}$

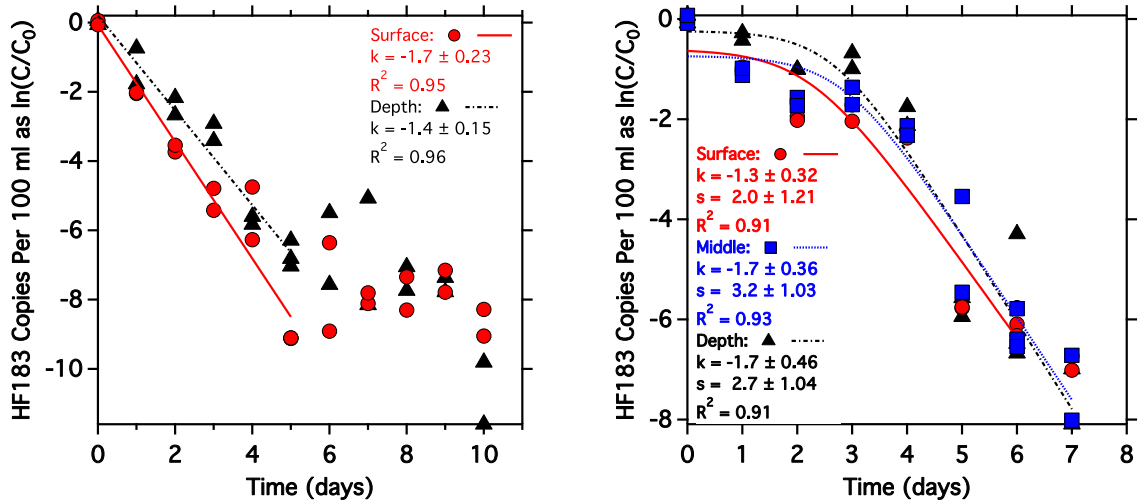


Figure S1. HF183/BacR287 decay curves for the summer (left) and winter (right) deployments. The modeled decay rate (k , d^{-1}), shoulder (s , d), and model fit (R^2) are displayed for each depth.

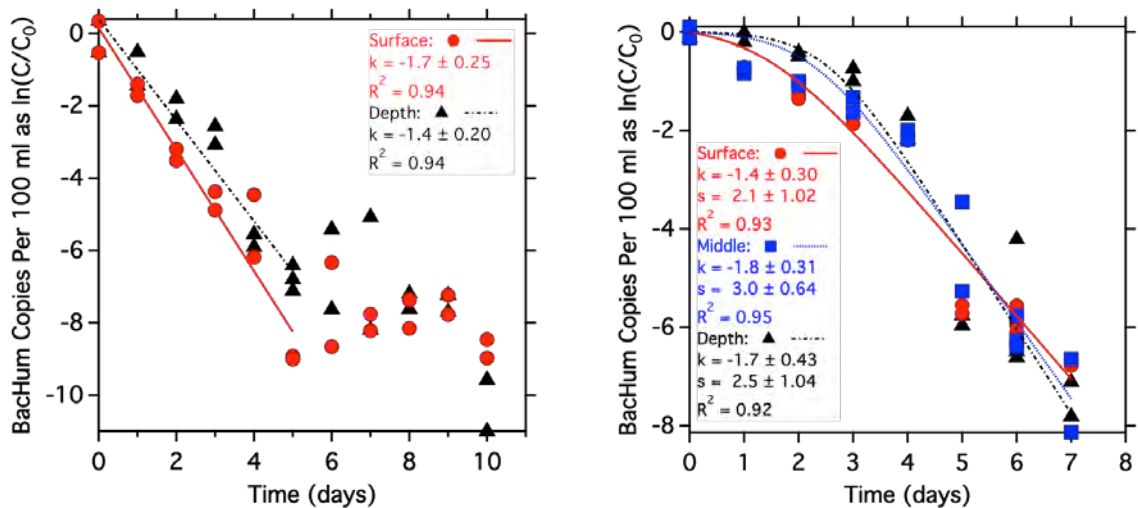


Figure S2. BacHum decay curves for the summer (left) and winter (right) deployments. The modeled decay rate (k , day^{-1}), shoulder (s , d), and model fit (R^2) are displayed for each depth.

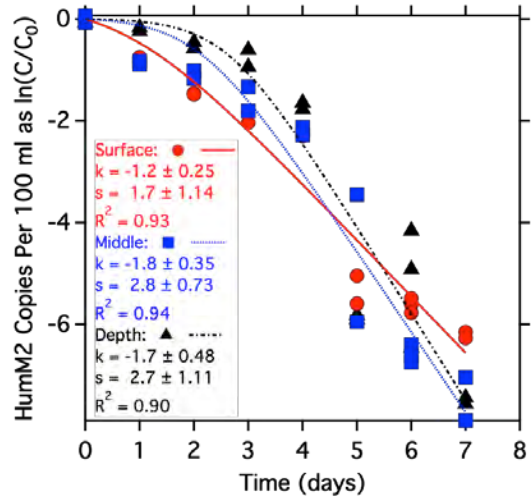
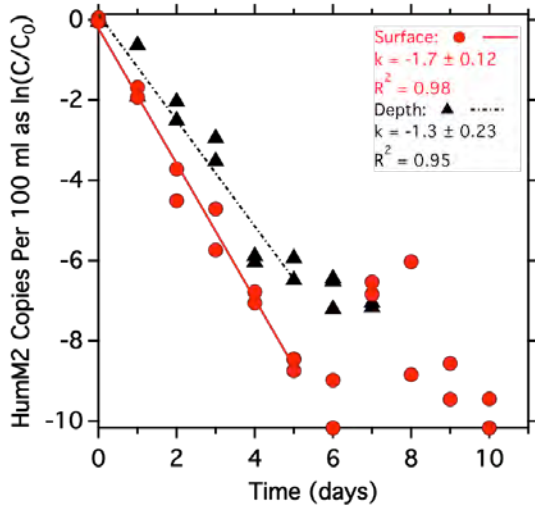


Figure S3. HumM2 decay curves for the summer (left) and winter (right) deployments. The modeled decay rate (k , day^{-1}), shoulder (s , d), and model fit (R^2) are displayed for each depth.

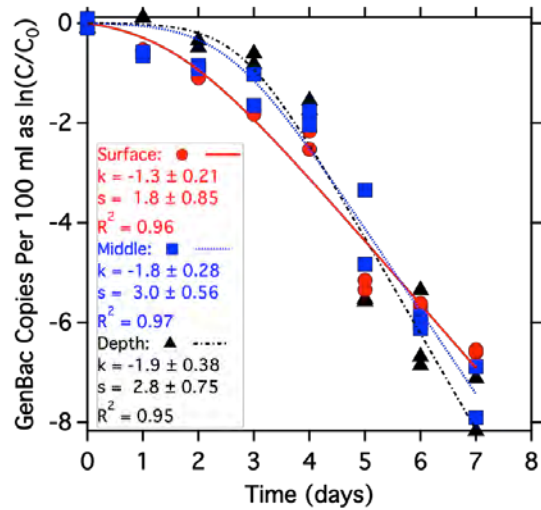
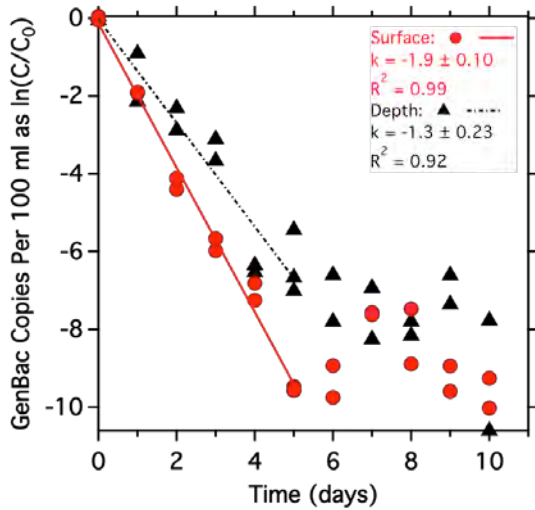


Figure S4. GenBac3 decay curves for the summer (left) and winter (right) deployments. The modeled decay rate (k , day^{-1}), shoulder (s , d), and model fit (R^2) are displayed for each depth.

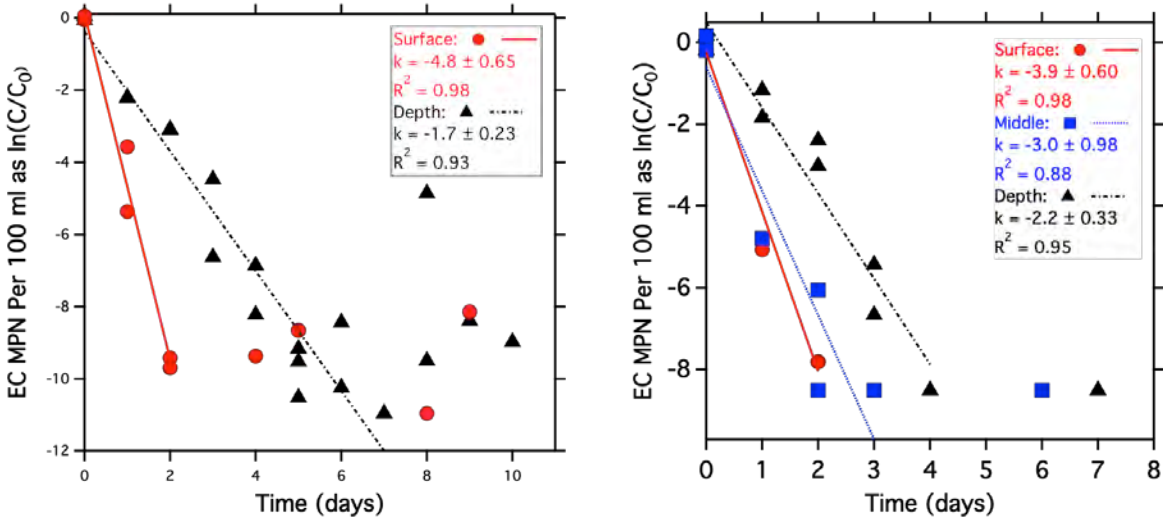


Figure S5. *E. coli* decay curves for the summer (left) and winter (right) deployments. The modeled decay rate (k , day^{-1}), shoulder (s , d), and model fit (R^2) are displayed for each depth.

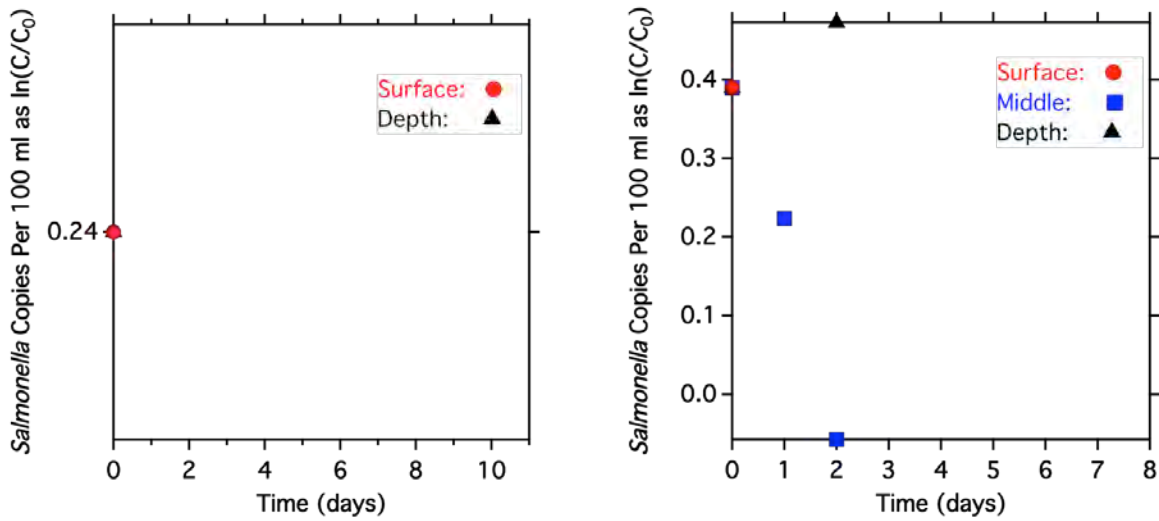


Figure S6. *Salmonella* decay data for the summer (left) and winter (right) deployments.

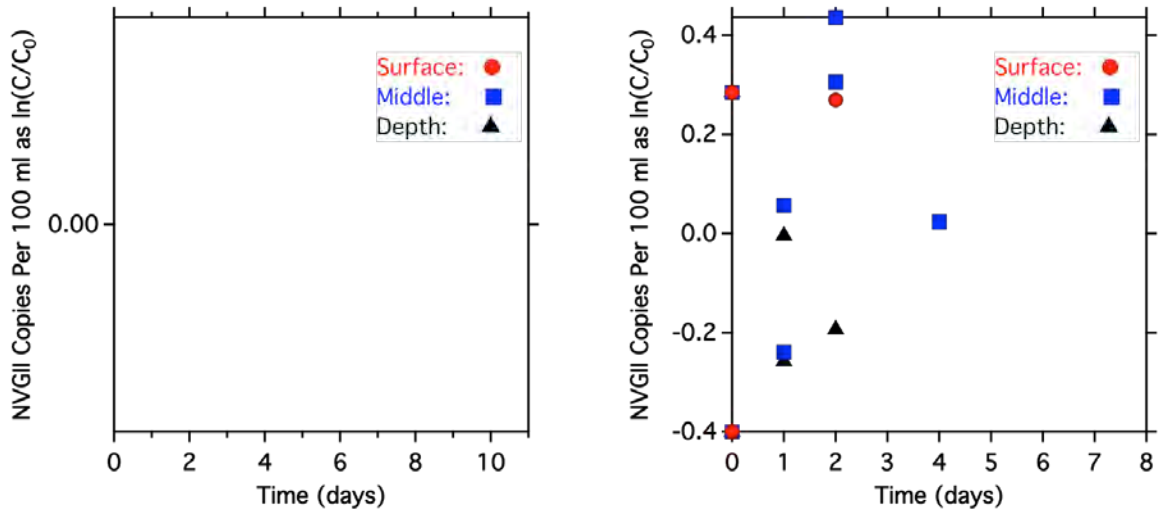


Figure S7. Norovirus GII decay data for the summer (left) and winter (right) deployments.

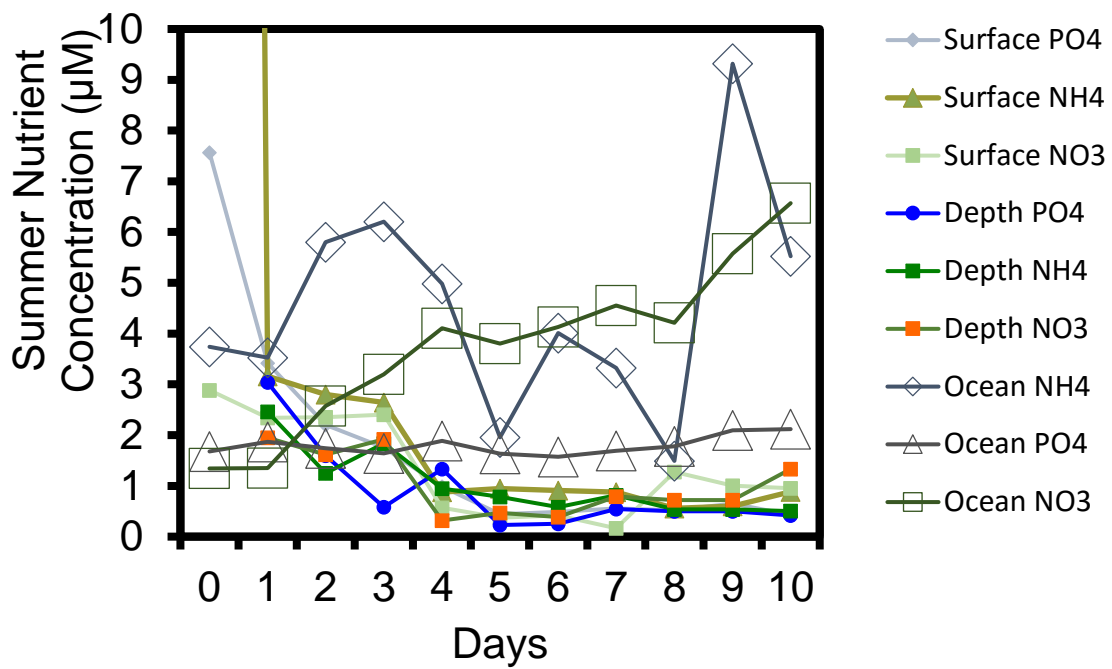


Figure S8. Nutrient concentrations (µM) during the summer deployment.

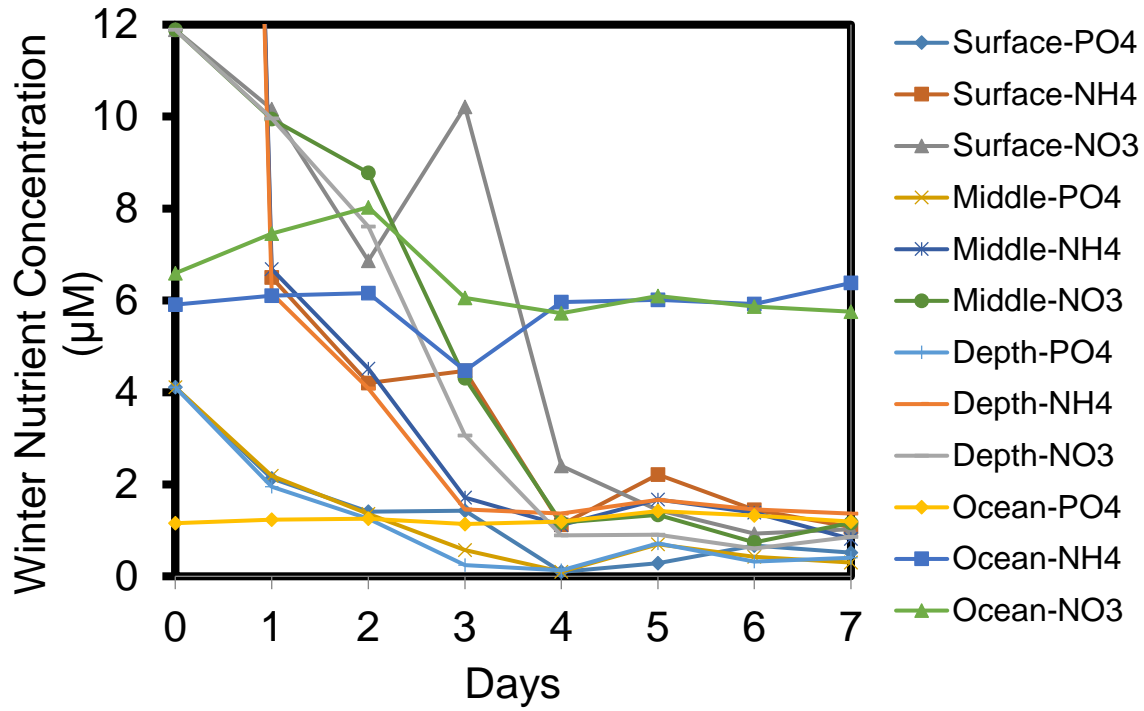


Figure S9. Nutrient concentrations (μM) during the winter deployment.

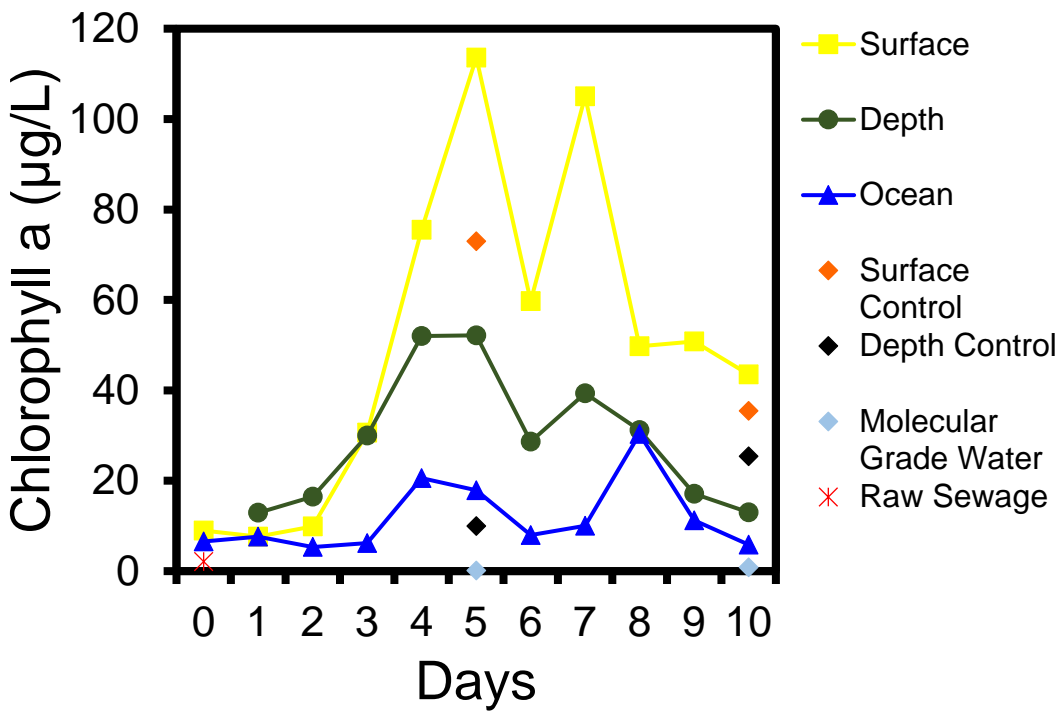


Figure S10. Chlorophyll a concentrations ($\mu\text{g/L}$) during the summer deployment.

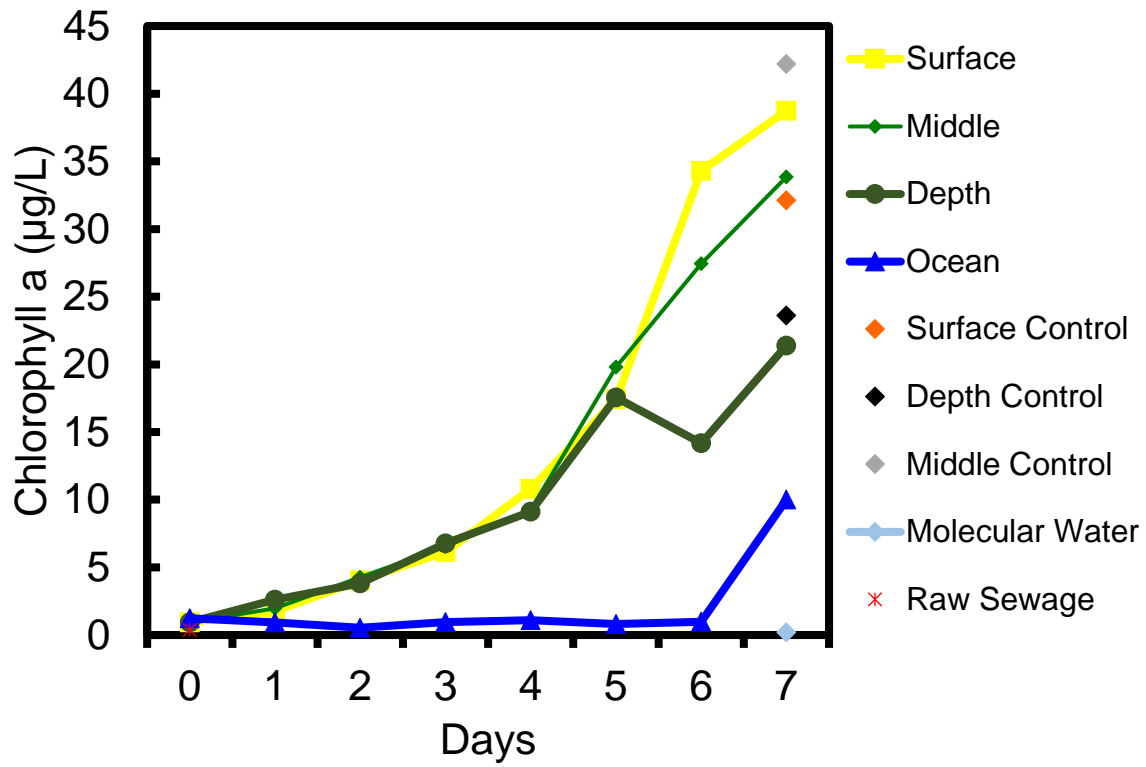


Figure S11. Chlorophyll a concentrations (µg/L) during the winter deployment.

SI References

1. Green, H.C., R.A. Haugland, M. Varma, H.T. Millen, M.A. Borchardt, K.G. Field, W.A. Walters, R. Knight, M. Sivaganesan, C.A. Kelty, O.C. Shanks. Improved HF183 quantitative real-time PCR assay for characterization of human fecal pollution in ambient surface water samples. *Applied and Environmental Microbiology* 2014, 80, (10), 3086-94.
2. Kageyama, T., S. Kojima, M. Shinohara, K. Uchida, S. Fukushi, F.B. Hoshino, N. Takeda, K. Katayama. Broadly reactive and highly sensitive assay for Norwalk-like viruses based on real-time quantitative reverse transcription-PCR. *Journal of Clinical Microbiology* 2003, 41, (4), 1548-57.
3. Kildare, B. J., C.M. Leutenegger, B.S. McSwain, D.G. Bambic, V.B. Rajal, S. Wuertz. 16S rRNA-based assays for quantitative detection of universal, human-, cow-, and dog-specific fecal Bacteroidales: a Bayesian approach. *Water Research* 2007, 41, (16), 3701-15.
4. Malorny, B., E. Paccassoni, P. Fach, C. Bunge, A. Martin, R. Helmuth. Diagnostic real-time PCR for detection of Salmonella in food. *Applied and Environmental Microbiology* 2004, 70, (12), 7046-52.
5. Shanks, O. C., C.A. Kelty, M. Sivaganesan, M. Varma, R.A. Haugland. Quantitative PCR for genetic markers of human fecal pollution. *Applied and Environmental Microbiology* 2009, 75, (17), 5507-13.
6. Siefiring, S., M. Varma, E. Atikovic, L. Wymer, R.A. Haugland. Improved real-time PCR assays for the detection of fecal indicator bacteria in surface waters with different instrument and reagent systems. *Journal of Water and Health* 2008, 6, (2), 225-37.
7. USEPA Method 1611. Enterococci in Water by TaqMan® Quantitative Polymerase Chain Reaction (qPCR) Assay, United States Environmental Protection Agency: Washington, D.C., 2012.

APPENDIX B: RELATIVE DECAY OF SEWAGE FECAL MATERIAL IN BRACKISH WATERS

(Field Site: Arroyo Burro Lagoon)

Introduction

Culturable fecal indicator bacteria (FIB), including *Escherichia coli* and enterococci, are routinely monitored in many coastal areas to assess microbiological water quality and to protect public health at beaches and in other waters with designated recreational uses. Elevated concentrations of FIB have been correlated with an increased risk of gastrointestinal illness to swimmers in waters impacted by wastewater (Cabelli et al. 1982, Wade et al. 2003). However, FIB may come from many human and non-human sources including leaking sanitary sewers (Sercu et al. 2009, 2011), septic systems (Verhougstraete et al. 2015, Viau et al. 2011), domestic animals (Ervin et al. 2014, Wang et al. 2010, Wright et al. 2009), and wildlife (Converse et al. 2012, Meays et al. 2006, Whitlock et al. 2002). FIB may also persist in the environment (Badgley et al. 2011, Imamura et al. 2011) or may be related to non-fecal sources (Goto et al. 2011). The human health risk from non-human sources such as birds has been estimated to be lower than that from human sources (Soller et al. 2010). Therefore, discerning human from nonhuman FIB sources is integral to the informed management of water quality.

Microbial source tracking (MST) is used to identify fecal sources contaminating recreational waters. Results from MST may be used to guide management actions aimed at controlling identified sources or to support the development of alternative water quality criteria through the use of quantitative microbial risk assessment (QMRA) (Ashbolt et al. 2010). To effectively identify sources of fecal contamination, host-associated fecal markers are quantified using DNA-based molecular methods including quantitative PCR (qPCR) and droplet digital PCR (ddPCR). Host-associated markers have been used in many studies to successfully identify sources of fecal contamination with the ultimate goal of identifying the sources of both FIB and pathogens that cause an increased risk of illness. However, using FIB or host-associated markers to reliably assess human health risks from fecal pollution requires a quantitative understanding of how FIB, fecal markers and pathogen concentrations correspond over time.

Studies have investigated the decay of host-associated markers and FIB in laboratory microcosms (Green et al. 2011; Jeanneau et al. 2012) and in environmental waters (Korajkic et al. 2013, 2014), yet the relationships between fecal markers, FIB, and pathogen concentrations are still not well understood. The brackish waters of estuaries and coastal lagoons have been shown to have a dramatic impact on surf zone water quality at many beaches (Grant et al. 2001, Dorsey et al. 2012). Lagoons may be zones of FIB attenuation or amplification, with seasonally-dependent hydrology affecting the dominant process (Steets et al. 2003). However, little is known regarding host-associated marker fates in coastal lagoons, including their persistence and decay patterns relative to FIB. To better understand how lagoons may impact water quality and microbiological risks to beachgoers, the fate of fecal markers, FIB and pathogens in lagoons must be understood.

In this study, dialysis chambers containing diluted sewage were deployed in the Arroyo Burro (AB) Lagoon (Santa Barbara, CA) and sampled daily for ten days under summer (shaded and unshaded) and winter (unshaded) conditions. Samples were analyzed for culturable FIB (*E. coli* and enterococci), host-associated fecal markers for humans (HF183, HumM2, and BacHum) and dogs (DogBact), general fecal markers (EnterolA and GenBac3), bacterial pathogens (*Campylobacter* and *Salmonella*), and viruses (human adenovirus and norovirus). Results showed differential decay rates between culture-based FIB, host-associated fecal markers, and general fecal markers. Except for *E. coli*, decay rate constants were similar in sun or shade during the summer; rate constants in the summer exceeded those in winter for most other assays. Winter rate constants were similar between FIB and the host-associated and general

markers, yet there were marked differences in summer. In particular, human and dog host-associated fecal markers decayed at faster rates than culture-based FIB, general fecal markers, and pathogens. Regardless of season, EnterolA was the most persistent marker and displayed a slower decay rate than the culture-based enterococci. These study results suggest that, in a brackish lagoon environment, host-associated markers may be used as indicators of recent pollution during the summer. However, the use of these markers as alternative indicators of human health risks may be limited due to their more rapid decay compared to the pathogens evaluated herein.

Materials and Methods

Study Area

The Arroyo Burro (AB) Lagoon (Figure S1) is located on California's central coast in Santa Barbara County (34.4045167°N, 119.7405944°W). The upstream watershed area is 25.6 km², with residential, commercial, agricultural, and open space land uses (LaMontagne 2003, Ervin 2014). The outlet of AB Lagoon has a sand berm that periodically breaches, allowing discharge to the surf zone. Lower AB Creek, which carries the combined flow of its upper stem and Las Positas Creek, flows year-round and discharges into the lagoon, as does Mesa Creek.

Field Deployments

Summer and winter field experiments (deployments) were performed in this study. For the summer deployment, two sets of 22 1-L dialysis chambers containing 5% sewage by volume (raw influent sewage collected prior to primary treatment from the City of Santa Barbara's El Estero WWTP on 9/7/14 which was allowed to settle for at 10 minutes to remove settleable solids) mixed with lagoon water (strained using a sterile steel mesh strainer to remove large insects and other debris) were deployed in the AB Lagoon for 10 days from September 8th – 18th, 2014. 50 liters of 5% sewage were mixed in the field on 9/8/14 and chambers were deployed under two treatments (shaded and full sunlight). Chambers consisted of 120mm diameter Spectra/Por 1 dialysis tubing (Spectrum Labs, Rancho Dominguez, CA), which was folded and closed on both ends. The shaded chambers were covered with a single layer of heavy black garden shade cloth. Two control chambers were also deployed for each treatment containing 100% lagoon water. Chambers were secured to a PVC frame using fishing line and submerged 6" below the water surface (Figure S2). Algae growth was manually brushed from the surface each day. Biofilm formation on the inside of the chambers was also controlled through daily manual pinching of the chamber surfaces.

For the winter deployment, one set of 22 1-L dialysis chambers containing 5% sewage (collected on 2/1/15 and treated as before) mixed with strained lagoon water were deployed for 10 days from February 2nd – 12th, 2015. No shading was used in the winter deployment. Two control chambers containing only lagoon water were also included. Two additional chambers containing 5% sewage were deployed for each of the three treatments (summer unshaded, summer shaded, and winter) in case of breakage.

To monitor the experiment, a time-lapse camera was installed in the lagoon (Brinno, TLC100). A photograph of the deployment area was taken every 4 hours during the summer deployment and every 10 minutes during the winter deployment. The primary purpose of this was to ensure that chambers remained intact and undisturbed by animals or people and that a large change in lagoon level did not occur between daily collections without our knowledge. Images were also captured in the weeks before each deployment to determine the frequency and amplitude of lagoon level changes during these two seasons.

Sampling Procedures

Duplicate chambers from each treatment were collected each day and transported back to the lab on ice. A small volume (~50ml) from each chamber was carefully poured into a beaker for dissolved oxygen and electrical conductivity measurements of the chamber contents using a HQ40d multi-parameter meter

equipped with conductivity and luminescent dissolved oxygen (LDO) probes (Hach, Loveland, OH). The remaining chamber contents were thoroughly mixed and poured into a sterile 2-L Nalgene bottle. The following parameters were then analyzed on the contents of each chamber: 1) dissolved oxygen and electrical conductivity using the Hach probe previously described, 2) FIB by IDEXX, 3) nutrients using flow injection analysis 4) dissolved organic carbon (DOC) and total dissolved nitrogen (TDN) by TOC-analyzer 5) DNA markers, pathogens and viruses by qPCR 6) Salmonella & Campylobacter by culture with PCR confirmation. Analytical methods are described in detail in the following section.

On the day of each deployment (day 0), duplicate 1-L samples of the 5% sewage mixture were processed and analyzed in the same way as the chambers for each treatment. On each deployment day, 1-L each of the 100% settled sewage and 100% lagoon water (that was combined to make the 5% sewage mixture) were also processed and analyzed in this way. One control chamber (containing 100% lagoon water) from each treatment was collected and processed on day 7 and the other on day 10.

Analysis was also performed on the ambient lagoon water outside the chambers each day. During chamber collection, the temperature, dissolved oxygen and electrical conductivity was measured directly in the lagoon at the deployment site (same depth as the chambers) with the Hach probe previously described. Continuous (5 minute intervals) temperature and light measurements were collected in situ using two HOBO Pendant temperature/light data loggers (Onset, Bourne, MA). Loggers were mounted to the PVC deployment frame at the same depth as the dialysis chambers. A sample of the ambient lagoon water was transported back to the lab on ice and stored at 4C for turbidity and absorbance analyses. The turbidity of the ambient lagoon water each day was measured using a 2100N Turbidimeter (Hach, Loveland, OH). Absorbance in the ambient lagoon water was measured using a UV-1800 UV Spectrophotometer (Shimadzu, Columbia, MD) by scanning wavelengths from 190 to 1100nm.

Laboratory Analyses

For FIB analysis, samples were analyzed by defined substrate culture methods (IDEXX, Westbrook, ME) for enterococci (Enterolert) and *E. coli* (Colilert) bacteria. Duplicate reactions were performed on all samples for both indicators. Samples were diluted with autoclaved Nanopure water. Two dilutions were run for the first 5 days of the summer deployment and the first 4 days of the winter deployment to ensure that results were generated within the range of quantification.

For nutrient analysis, approximately 30 ml of each sample were filtered through a 0.4 μ M polycarbonate (PC) membrane (EMD Millipore, Billerica, MA) and stored in a 60 ml HDPE bottle at -20°C until analysis was performed. Frozen samples were sent to the Marine Science Institute (MSI) at the University of California, Santa Barbara (UCSB) for analysis using a QuikChem 8000 (Lachat Instruments, Loveland, CO) flow injection analysis system. The following nutrients were analyzed: nitrate + nitrite, nitrite, phosphate, and ammonium. Nitrate concentrations were calculated by subtracting nitrite from nitrate + nitrite.

For DOC/TDN analysis, approximately 30 ml of each sample was also filtered through a 0.4 μ M polycarbonate (PC) membrane (EMD Millipore, Billerica, MA) and stored in a 60 mL HDPE bottle at -20°C until analysis was performed. Samples were then analyzed for DOC and TDN using a TOC-V CSN total organic carbon analyzer with a TNM-1 total nitrogen unit and an ASI-V autosampler (Shimadzu, Columbia, MD).

For DNA fecal marker and bacterial pathogen analysis, triplicate 100 ml samples from each sample were filtered through 0.4 μ M polycarbonate (PC) membranes (EMD Millipore, Billerica, MA). Using sterile forceps, filters were rolled into bead tubes (GeneRite, North Brunswick, NJ), flash frozen in liquid nitrogen, and stored at -20°C until DNA extraction was performed. DNA was extracted from each of three filters using the DNA-EZ ST1 kit (GeneRite, North Brunswick, NJ), and the extracts were pooled.

The total DNA concentration of each pooled extract was quantified using the Quant-iT dsDNA broad-range assay kit (Life Technologies, Carlsbad, CA).

DNA extracts were analyzed by quantitative polymerase chain reaction (qPCR) for the HF183Taqman (Haugland, 2010, Green, 2014), HumM2 (Shanks, 2009), and BacHum (Kildare, 2007) human-associated fecal markers, the Entero1A (Haugland, 2005) and GenBac3 (Siefring, 2008) general fecal markers, and the DogBact (Sinigalliano, 2010) dog-associated fecal marker. Inhibition during qPCR was assessed using an internal amplification control (IAC) that was performed in duplex with the HF183Taqman assay. DNA extracts were also analyzed by qPCR for genes associated with the bacterial pathogens *Campylobacter* (Lund, 2004) and *Salmonella* (Malorny et al. 2004). Filter and extraction blanks were analyzed to assess contamination during sample filtration and DNA extraction, respectively. PCR reactions were performed in triplicate with three no-template controls included in each 96-well plate; separate plasmid DNA standards were PCR amplified in triplicate on each 96-well plate.

Pooled standard curves were generated for each assay including standard concentrations down to the lowest concentration standard in which amplification was detected in at least 80% of replicates. A regression analysis was performed on the pooled standard curve generated for each assay, and outliers were removed based on standardized residual values of $>+3$ or <-3 . The Lower Limit of Quantification (LLOQ) for each assay was calculated by taking the average Ct value of the non-outlier standard replicates at the lowest concentration included in the standard curve. Samples with at least two replicates amplifying within the range of the standard curve were considered to be within the range of quantification (ROQ) and were quantified. Samples with replicates amplifying below the concentration of the lowest standard were considered detected but not quantifiable (DNQ), and samples with one or zero replicates amplifying were considered not detected (ND) (Sinigalliano, 2013).

For viral analysis, duplicate 100 ml samples from each sample were filtered through 0.45 μM mixed cellulose (HA) membranes (EMD Millipore, Billerica, MA). Prior to filtration, each 100 ml sample aliquot was mixed with 2ml of 5M MgCl₂. After filtration, filters were treated with 0.5 ml of RNAlater RNA Stabilization Reagent (Qiagen, Valencia, CA). Using sterile forceps, filters were rolled into 5 ml transport tubes (GeneRite, North Brunswick, NJ) and kept at 4 °C overnight before being stored at -80 °C until extraction was performed. RNA and DNA were extracted together using a modified PowerWater RNA Extraction Kit (Cat. #: 14700-50-NF, MoBio Laboratories, Inc., Carlsbad, CA). Modification of the kit included the removal of the DNase1 treatment in order to extract both RNA and DNA. Norovirus GII was analyzed by reverse transcriptase PCR (RT-PCR) (Viau, 2011). Adenovirus was analyzed by droplet digital PCR (ddPCR). Viral extracts were sent to the Southern California Coastal Water Research Project (SCCWRP) for RT-PCR and ddPCR analysis.

Decay Modeling and Statistical Analyses

The GInaFit modeling add-in for Excel (Geeraerd 2005) was used to compare four common decay models and select the best fitting model to determine decay parameters. Regression models tested included log linear (Bigelow 1920), shoulder (Geeraerd 2000), tail (Geeraerd 2000), and shoulder and tail (Geeraerd 2000). Decay curves and model output parameters were adjusted to natural log based decay. The equations used for each model are shown in the supplemental information (SI). For analytes where an increase in concentration was measured from day 0 to day 1 or day 2 (*E. coli* light, *E. coli* shade, *E. coli* winter, and *Campylobacter* winter), day 0 or day 0 and day 1 data was excluded from the analysis (i.e., modeling was performed beginning with the day in which the maximum chamber concentration was measured). Similarly, for analytes where an increase in concentration was measured after decay had reached a minimum (*Enterococci* winter, *Campylobacter* light, and *Campylobacter* shade), data from days after the minimum concentration was measured were excluded. Data from days where one replicate was quantified and the other was BDL, DNQ, or ND were only included in the analysis if the model fit was improved. Model fit was assessed using the root mean sum of squared error (RMSE) for measured versus

modeled decay. If two models resulted in a similar fit then the simpler model was selected. Modeled decay parameters generated by GInaFiT include k_{max} (natural log based decay coefficient or decay rate constant), SL (shoulder length), and C_{res} (residual analyte concentration), depending on the best-fit model selected. The standard error (SE) was also generated for each of these parameters. The 95% confidence intervals for modeled decay rate constants were calculated using the formula $k \pm t(0.975, df) * SE$, where df is the degree of freedom for the regression decay model.

Summary statistics and statistical analysis including Spearman’s rank correlations and Wilcoxon rank sum tests were performed using JMP 10 (SAS, Cary, NC).

Results

qPCR Quality Assurance and Controls

All master calibration curves were of acceptable quality ($R^2 > 0.99$, $E > 0.91$, Table 1), and no amplification inhibition was detected based on the IAC procedure. DNA contamination was low with 100% of no-template controls below the detection limit ($n = 120$), and 99.4% and 100% of filter blanks ($n = 176$) and extractions blanks ($n = 88$) below detection, respectively.

Table 1. Chemical, nutrient, FIB, DNA fecal marker, and bacterial pathogen concentrations in raw sewage (Sewage), ambient lagoon water (Lagoon) and 5% sewage / 95% lagoon water mixture (Mix) for summer and winter deployments.

Parameter	Units	Summer			Winter		
		Sewage	Lagoon	Mix	Sewage	Lagoon	Mix
DOC	mg/L	90.6	7.02	10.6	65.0	4.29	7.34
TDN	mg/L	34.7	0.52	2.18	64.8	0.50	3.85
Nitrate	μ M	6.31	3.74	3.78	BDL	4.39	3.95
Nitrite	μ M	0.76	0.14	0.20	0.58	0.19	0.25
Ammonia	μ M	2,220	1.24	123	4,200	8.24	234
Phosphate	μ M	60.4	1.14	5.03	91.0	3.11	10.7
E. coli	Log MPN/100ml	7.21	2.95	5.76	6.89	2.90	5.58
Enterococci	Log MPN/100ml	5.99	2.06	4.73	6.15	2.45	4.89
HF183	Log Copies/100ml	7.35	DNQ	6.95	6.93	ND	6.83
HumM2	Log Copies/100ml	6.78	ND	5.99	6.20	ND	5.94
BacHum	Log Copies/100ml	8.10	DNQ	7.37	7.70	ND	7.54
Enero1a	Log Copies/100ml	7.03	DNQ	5.75	6.75	DNQ	6.02
GenBac3	Log Copies/100ml	9.04	5.24	8.16	8.32	4.98	8.26
DogBact	Log Copies/100ml	6.33	DNQ	5.52	5.31	DNQ	5.50
Campylobacter	Log Copies/100ml	4.18	2.73	3.55	3.45	3.22	3.35
Salmonella	Log Copies/100ml	DNQ	ND	DNQ	DNQ	ND	DNQ
Adenovirus	Log Copies/100ml	3.05	ND	2.41	5.17	ND	3.90
Norovirus	Log Copies/100ml	ND	ND	ND	DNQ	ND	ND

BDL = Below Detection Limit, DNQ = Detected but Not Quantifiable, ND = Not Detected

Physical Lagoon and Chamber Characteristics

Physical parameters measured in the ambient lagoon water each day and weather conditions during summer and winter deployments are summarized in Table S2. Air temperature and solar radiation represent the daily average based on hourly measurements acquired from California Irrigation Management Information System (CIMIS) weather station #230 (2.4 km from the AB Lagoon). The median values for all parameters shown in Table 2 were significantly different between summer and winter deployments (Wilcoxon two-sample rank-sum test, $p < 0.05$, $n = 11$). These results show that the physical conditions in the lagoon were dramatically different between summer and winter deployments. These two deployments therefore represent a range of seasonal conditions that are typical of the AB Lagoon.

Table 2. Modeled decay kinetics for FIB, DNA fecal markers and pathogens.

Assay	Treatment	Days	Model	SSE	RMSE	R ²	k _{max} (days ⁻¹)	k _{max} SE (days ⁻¹)	SI (days)	SI SE (days)
E. coli	Light	1-7*	GT	2.57	0.48	0.99	2.61	0.14	-	-
E. coli	Shade	1-10*	GT	3.08	0.43	0.99	1.40	0.05	-	-
E. coli	Winter	2-9*	GT	2.49	0.44	0.98	2.15	0.15	-	-
Enterococci	Light	0-3	GT	0.35	0.26	0.99	3.25	0.16	-	-
Enterococci	Shade	0-6	GST	3.12	0.56	0.98	2.60	0.37	1.69	0.30
Enterococci	Winter	0-7*	GT	9.23	0.84	0.94	1.61	0.18	-	-
HF183	Light	0-3	GST	0.14	0.21	1.00	5.20	0.42	0.56	0.07
HF183	Shade	0-3	GST	0.48	0.35	0.99	4.67	0.46	0.63	0.11
HF183	Winter	0-8	GST	1.33	0.31	0.99	1.65	0.11	1.88	0.24
HumM2	Light	0-2	GS	0.36	0.35	0.99	4.16	0.46	0.82	0.14
HumM2	Shade	0-2	GS	0.25	0.29	0.99	5.32	0.53	1.01	0.11
HumM2	Winter	0-5	GS	1.65	0.45	0.97	1.93	0.19	1.91	0.29
BacHum	Light	0-3	GST	0.92	0.48	0.99	5.64	0.69	0.82	0.13
BacHum	Shade	0-4	GST	2.44	0.64	0.98	4.29	0.74	0.66	0.23
BacHum	Winter	0-9	GST	2.79	0.42	0.99	1.63	0.12	1.85	0.30
Entero1a	Light	0-4	LL	0.97	0.35	0.96	1.09	0.08	-	-
Entero1a	Shade	0-6	LL	1.57	0.36	0.96	0.79	0.05	-	-
Entero1a	Winter	0-9	LL	2.21	0.35	0.96	0.61	0.03	-	-
GenBac3	Light	0-5	GT	2.81	0.56	0.98	2.36	0.14	-	-
GenBac3	Shade	0-7	GT	2.79	0.46	0.98	1.90	0.11	-	-
GenBac3	Winter	0-9	GST	2.36	0.38	0.99	1.56	0.10	1.72	0.29
DogBact	Light	0-2	GS	0.15	0.22	1.00	5.27	0.40	1.01	0.09
DogBact	Shade	0-2	GS	0.30	0.39	0.99	6.81	1.68	1.19	0.22
DogBact	Winter	0-4	GS	1.49	0.46	0.93	1.53	0.30	1.53	0.50
Campylobacter	Light	0-2*	LL	0.26	0.25	0.97	1.44	0.13	-	-
Campylobacter	Shade	0-2*	LL	0.26	0.25	0.97	1.39	0.13	-	-

Campylobacter	Winter	2-4*	LL	1.46	0.70	0.76	1.28	0.42	-	-
Adenovirus	Light	0-2	GT	0.05	0.13	0.95	2.40	1.42	-	-
Adenovirus	Shade	0-3	GT	0.31	0.32	0.78	1.36	0.85	-	-
Adenovirus	Winter	0-3	GT	0.63	0.46	0.88	1.16	0.48	-	-

SSE = Sum of Squared Error, RMSE = Root Mean Sum of Squared Error, SE = Standard Error, SL = Shoulder Length

LL = Log Linear, GS = Geeraerd Shoulder, GT = Geeraerd Tail, GST = Geeraerd Shoulder & Tail, *Data excluded due to growth

Water temperature, dissolved oxygen, electrical conductivity, and lagoon depth were measured in situ at the time of chamber collection each day (approx. 9am) and are shown in Figure S3. Dissolved oxygen and electrical conductivity of collected chambers were measured upon returning to the lab. Results show that within chamber electrical conductivity and dissolved oxygen were consistent with variations seen in the ambient lagoon for both the shaded and unshaded summer deployments. Measured physical parameters were also similar between chambers and the ambient lagoon for the winter deployment with the exception of just after the largest lagoon breach, which occurred prior to chamber collection on day 4. However, by day 5 both dissolved oxygen and electrical conductivity within chambers had returned to that of the ambient lagoon.

Continuous visual monitoring of the deployment site was also conducted through the placement of a time-lapse camera. Captured images were used to evaluate lagoon level and other conditions at the site between sampling events. During the summer deployment, the lagoon level was consistent with daily measurements and no unusual disturbances were observed during the deployment. During the winter deployment, several lagoon breaches were observed which caused large changes in the level of the lagoon between daily sampling events. There was also a rainfall event that occurred on 2/7/15 (0.61 in, CIMIC #230), which caused several of the chambers to become partially exposed to the air for a short period of time (approx. 3 hrs.). Three chambers also ruptured during the winter deployment leaving only a single chamber for collection on day 10.

Nutrient Availability in Raw Sewage, Ambient Lagoon Water and Chambers

Chemical and nutrient analysis results are shown in Table 3 for raw sewage, ambient lagoon water, and the initial 5% sewage / 95% lagoon water mixture for summer and winter deployments. DOC was higher in the summer ambient lagoon sample (7.0 vs 4.3 mg/L in the winter); while TDN was not different between deployments (0.5 mg/L in both summer and winter). Nutrient concentrations (nitrate, nitrite, ammonia, and phosphate) were all lower in the summer ambient lagoon water compared to winter, showing that the winter lagoon water may represent a more nutrient-rich environment which could favor microbial growth or persistence. Analysis of the raw sewage showed that concentrations were higher than that measured for the ambient lagoon water in both deployments for all analytes except nitrate in the winter deployment, which was below the detection limit in raw sewage. Nitrite and nitrate were both relatively low (<1 µM and <10 µM, respectively) for both lagoon water and sewage samples. Sewage concentrations for other analytes ranged from 10X (DOC) to over 500X (ammonia) greater than the ambient lagoon water. Concentrations of these analytes were therefore also greater in the initial sewage / lagoon water mixture compared to ambient lagoon water (Table 3).

Table 3. Chemical, nutrient, FIB, DNA fecal marker, and bacterial pathogen concentrations in raw sewage (Sewage), ambient lagoon water (Lagoon) and 5% sewage / 95% lagoon water mixture (Mix) for summer and winter deployments.

Parameter	Units	Summer			Winter		
		Sewage	Lagoon	Mix	Sewage	Lagoon	Mix
DOC	Mg/L	90.6	7.02	10.6	65.0	4.29	7.34
TDN	Mg/L	34.7	0.52	2.18	64.8	0.50	3.85
Nitrate	μM	6.31	3.74	3.78	BDL	4.39	3.95
Nitrite	μM	0.76	0.14	0.20	0.58	0.19	0.25
Ammonia	μM	2,220	1.24	123	4,200	8.24	234
Phosphate	μM	60.4	1.14	5.03	91.0	3.11	10.7
E. coli	Log MPN/100ml	7.21	2.95	5.76	6.89	2.90	5.58
Enterococci	Log MPN/100ml	5.99	2.06	4.73	6.15	2.45	4.89
HF183	Log Copies/100ml	7.35	DNQ	6.95	6.93	ND	6.83
HumM2	Log Copies/100ml	6.78	ND	5.99	6.20	ND	5.94
BacHum	Log Copies/100ml	8.10	DNQ	7.37	7.70	ND	7.54
Enero1a	Log Copies/100ml	7.03	DNQ	5.75	6.75	DNQ	6.02
GenBac3	Log Copies/100ml	9.04	5.24	8.16	8.32	4.98	8.26
DogBact	Log Copies/100ml	6.33	DNQ	5.52	5.31	DNQ	5.50
Campylobacter	Log Copies/100ml	4.18	2.73	3.55	3.45	3.22	3.35
Salmonella	Log Copies/100ml	DNQ	ND	DNQ	DNQ	ND	DNQ
Adenovirus	Log Copies/100ml	3.05	ND	2.41	5.17	ND	3.90
Norovirus	Log Copies/100ml	ND	ND	ND	DNQ	ND	ND

BDL = Below Detection Limit, DNQ = Detected but Not Quantifiable, ND = Not Detected

Daily measurements of chemicals and nutrients were also made on chamber and ambient lagoon water throughout the winter experiment (Figures S4 and S5 of the SI). Within-chamber TDN concentrations were similar to the ambient lagoon throughout the winter deployment, while DOC concentrations were higher in chambers than in the ambient lagoon, steadily rising from day 2 to day 10. Summer deployment TDN and DOC concentrations were consistent throughout the experiment with TDN similar to the initial ambient lagoon water and DOC higher than the ambient lagoon. In general, within-chamber nutrient concentrations were similar to ambient lagoon levels for the first 3 to 5 days of the experiment before dropping below ambient concentrations in the winter deployment. Daily chemical and nutrient data was not collected from the ambient lagoon during the summer deployment; therefore daily comparisons of chemicals and nutrients cannot be made. Daily within-chamber concentrations of nutrients for the summer deployment are shown in Figure S6 of the SI and are compared to the initial ambient lagoon

concentrations. Within-chamber nutrient concentrations followed the same general trend for the summer deployment compared to the winter deployment with concentrations dropping below the initial ambient measurement after the first 4 to 6 days of the experiment. Ammonia was the exception, which was similar to ambient concentrations throughout both summer and winter deployments. Nitrate concentrations were also much lower throughout the summer deployment compared to winter.

FIB, Fecal DNA Markers, and Pathogens in Raw Sewage and Ambient Lagoon Water

The initial concentrations of FIB, DNA fecal markers, bacterial pathogens, and viruses are also shown in Table 3 for raw sewage, ambient lagoon water and the initial mixture. FIB concentrations in the ambient lagoon water ranged from 2.06 to 2.95 Log MPN/100ml for both *E. coli* and Enterococci, with *E. coli* concentrations higher than Enterococci in both summer and winter deployments. Initial FIB concentrations in raw sewage were 3+ Log higher than that of the ambient lagoon water. Based on initial FIB concentrations, greater than 99.5% of the FIB contained in the initial mixtures originated from the sewage. Initial FIB concentrations were similar between winter and summer for both raw sewage and ambient lagoon water (within 0.4 Log MPN/100ml), suggesting that seasonal variation in the initial FIB concentration may not be significant between deployments.

Human DNA fecal markers (HF183 and BacHum) were detected at the DNQ level in the ambient lagoon water during the summer deployment. The HumM2 marker was not detected in the ambient lagoon water during either deployment. All three human markers were detected at high concentrations in the raw sewage (6.20 to 8.10 Log copies/100mL) and in the initial mixture (5.94 to 7.54 Log copies/100ml) for both deployments. Therefore, nearly 100% of the markers measured in the initial mixture originated from the sewage. Human marker concentrations were slightly higher in the summer sewage sample compared to the winter sample for all three markers. For both raw sewage samples, the BacHum marker was measured at the highest initial concentration, followed by the HF183 marker, and lastly the HumM2 marker (1.3 Log and 1.5 Log difference between BacHum and HumM2 for summer and winter, respectively). The same trend was observed in the initial mixture for both deployments (1.4 Log and 1.6 Log difference between BacHum and HumM2 for summer and winter, respectively).

The Enterol1a and DogBact markers were detected at the DNQ level in the ambient lagoon water for both deployments, while the GenBac3 marker was quantified (5.24 and 4.98 Log copies/100ml for summer and winter, respectively). This result suggests that there may be source(s) of Bacteroidales to the ambient lagoon water other than that of humans or dogs. For the raw sewage, both Enterol1a and GenBac3 markers were measured at high concentrations, with higher concentrations of GenBac3 compared to Enterol1a and higher concentrations of both markers in the summer than in the winter. The DogBact marker was quantified in both raw sewage samples (6.33 and 5.31 Log copies/100ml for summer and winter, respectively). This suggests that dog waste was present in the raw sewage at concentrations of 10% that of the HF183 marker in the summer and 2% in the winter.

The Salmonella DNA marker was not detected in the ambient lagoon water for either deployment and was detected at the DNQ level in both raw sewage samples and in the initial mixtures for both deployments. The *Campylobacter* DNA marker was quantified in the ambient lagoon water for both deployments with a higher concentration in the winter (3.22 Log copies/100ml) compared to the summer (2.73 Log copies/100ml). The *Campylobacter* marker was quantified in the raw sewage samples at a similar concentration to that of the ambient lagoon water in the winter (3.45 Log copies/100ml) and at a higher concentration than that of the ambient lagoon water in the summer (4.18 Log copies/100ml). These results suggest that there is a source of *Campylobacter* marker to the lagoon, which is resulting in ambient lagoon water concentrations that are similar to that of raw sewage, particularly in the winter. *Campylobacter* was also detected by culture in ambient lagoon water from the winter deployment, but

was not detected in the summer or in either sewage sample. *Salmonella* was detected by culture in both sewage samples, but was not detected in the ambient lagoon water for either deployment.

Norovirus was not detected in the ambient lagoon water or initial sewage lagoon water mixture for either deployment and was only detected at a DNQ level in the winter sewage sample. Adenovirus was also not detected in the ambient lagoon water samples, but was quantified in both summer and winter raw sewage samples (3.05 and 5.17 Log copies/100ml for summer and winter, respectively), as well as in the initial sewage lagoon water mixture (2.41 and 3.90 Log copies/100ml for summer and winter, respectively). Adenovirus concentrations were 2 Log higher in the winter sewage sample suggesting that seasonal differences may be important in sewage viral concentrations.

FIB Decay Kinetics

The decay profiles for *E. coli* and Enterococci are shown in Figure S7 of the SI. Complete FIB results for all chambers analyzed are included in Table S1 of the SI. Quantifiable concentrations (>10 MPN/100ml) of *E. coli* persisted longer than Enterococci (up to ten days for *E. coli*, compared to seven days or less for Enterococci), although initial concentrations of *E. coli* were also higher and growth was observed over the first day of the summer deployment. For both *E. coli* and Enterococci, greater persistence was observed in the summer shaded treatment compared to the un-shaded treatment. However, in the winter deployment, *E. coli* decay closely followed the unshaded summer treatment while Enterococci decay more closely followed the shaded treatment. This result suggests that different decay mechanisms may be controlling the degradation of these bacteria during different seasons in the lagoon environment (i.e., sunlight and temperature).

Decay profiles for HF183, Enterol1a, and *Campylobacter* are shown in Figure 1. Modeled decay kinetics for *E. coli* and Enterococci are shown in Table 4. The log linear model including a tail (GT) resulted in the best fit in every case except for Enterococci in the shaded treatment, which the log linear model with shoulder and tail (GST) was the best fit. As observed in the decay profiles, decay rate constants (k_{max}) varied between treatments and ranged from 1.40 to 2.61 days⁻¹ for *E. coli* and 1.61 to 3.25 days⁻¹ for Enterococci.

Table 4. Modeled decay kinetics for FIB, DNA fecal markers and pathogens.

Assay	Treatment	Days	Model	SSE	RMSE	R ²	K _{max} (days ⁻¹)	K _{max} SE (days ⁻¹)	SL (days)	SL SE (days)
E. coli	Light	1-7*	GT	2.57	0.48	0.99	2.61	0.14	-	-
E. coli	Shade	1-10*	GT	3.08	0.43	0.99	1.40	0.05	-	-
E. coli	Winter	2-9*	GT	2.49	0.44	0.98	2.15	0.15	-	-
Enterococci	Light	0-3	GT	0.35	0.26	0.99	3.25	0.16	-	-
Enterococci	Shade	0-6	GST	3.12	0.56	0.98	2.60	0.37	1.69	0.30
Enterococci	Winter	0-7*	GT	9.23	0.84	0.94	1.61	0.18	-	-
HF183	Light	0-3	GST	0.14	0.21	1.00	5.20	0.42	0.56	0.07
HF183	Shade	0-3	GST	0.48	0.35	0.99	4.67	0.46	0.63	0.11
HF183	Winter	0-8	GST	1.33	0.31	0.99	1.65	0.11	1.88	0.24
HumM2	Light	0-2	GS	0.36	0.35	0.99	4.16	0.46	0.82	0.14
HumM2	Shade	0-2	GS	0.25	0.29	0.99	5.32	0.53	1.01	0.11
HumM2	Winter	0-5	GS	1.65	0.45	0.97	1.93	0.19	1.91	0.29
BacHum	Light	0-3	GST	0.92	0.48	0.99	5.64	0.69	0.82	0.13
BacHum	Shade	0-4	GST	2.44	0.64	0.98	4.29	0.74	0.66	0.23
BacHum	Winter	0-9	GST	2.79	0.42	0.99	1.63	0.12	1.85	0.30
Entero1a	Light	0-4	LL	0.97	0.35	0.96	1.09	0.08	-	-
Entero1a	Shade	0-6	LL	1.57	0.36	0.96	0.79	0.05	-	-
Entero1a	Winter	0-9	LL	2.21	0.35	0.96	0.61	0.03	-	-
GenBac3	Light	0-5	GT	2.81	0.56	0.98	2.36	0.14	-	-
GenBac3	Shade	0-7	GT	2.79	0.46	0.98	1.90	0.11	-	-

GenBac3	Winter	0-9	GST	2.36	0.38	0.99	1.56	0.10	1.72	0.29
DogBact	Light	0-2	GS	0.15	0.22	1.00	5.27	0.40	1.01	0.09
DogBact	Shade	0-2	GS	0.30	0.39	0.99	6.81	1.68	1.19	0.22
DogBact	Winter	0-4	GS	1.49	0.46	0.93	1.53	0.30	1.53	0.50
Campylobacter	Light	0-2*	LL	0.26	0.25	0.97	1.44	0.13	-	-
Campylobacter	Shade	0-2*	LL	0.26	0.25	0.97	1.39	0.13	-	-
Campylobacter	Winter	2-4*	LL	1.46	0.70	0.76	1.28	0.42	-	-
Adenovirus	Light	0-2	GT	0.05	0.13	0.95	2.40	1.42	-	-
Adenovirus	Shade	0-3	GT	0.31	0.32	0.78	1.36	0.85	-	-
Adenovirus	Winter	0-3	GT	0.63	0.46	0.88	1.16	0.48	-	-

SSE = Sum of Squared Error, RMSE = Root Mean Sum of Squared Error, SE = Standard Error, SL = Shoulder Length

LL = Log Linear, GS = Geeraerd Shoulder, GT = Geeraerd Tail, GST = Geeraerd Shoulder & Tail, *Data excluded due to growth

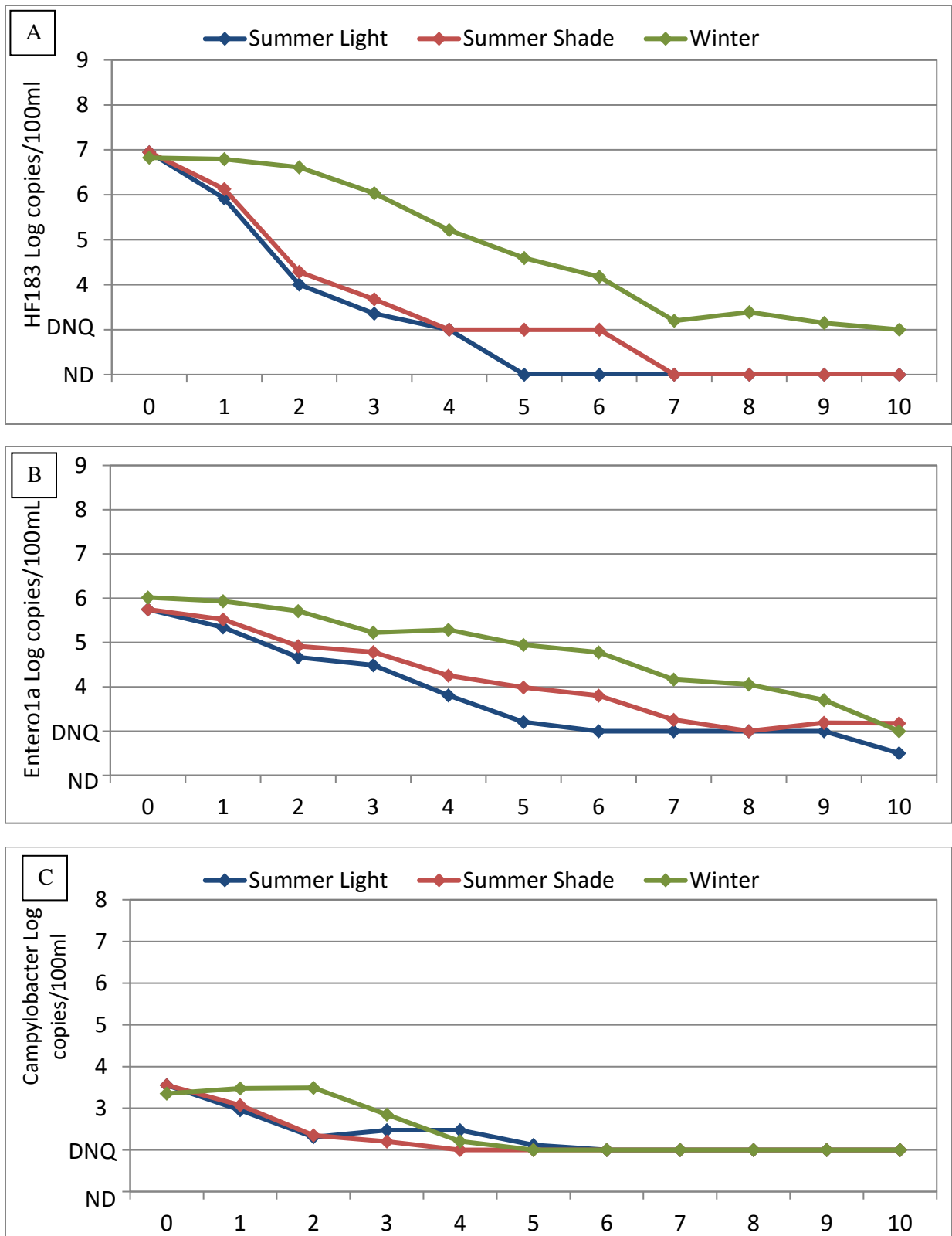


Figure 1. Decay profiles for HF183 (A), Enterotoxigenic E. coli (B), and *Campylobacter* (C).

Based on the modeled decay kinetics, the 95% confidence interval of each decay rate constant was calculated (Figure 2). For *E. coli*, decay for the shaded summer treatment was significantly lower than for the other treatments. For Enterococci, decay for the winter treatment was lower than for the summer unshaded, but the shaded treatment was not significantly different from the other two. While the modelled winter decay rate constant was not significantly different between *E. coli* and Enterococci, both summer shaded and unshaded rates were higher for Enterococci. This result along with the lower initial concentrations suggests that detectable Enterococci would not be expected to persist in the lagoon environment for as long as *E. coli*.

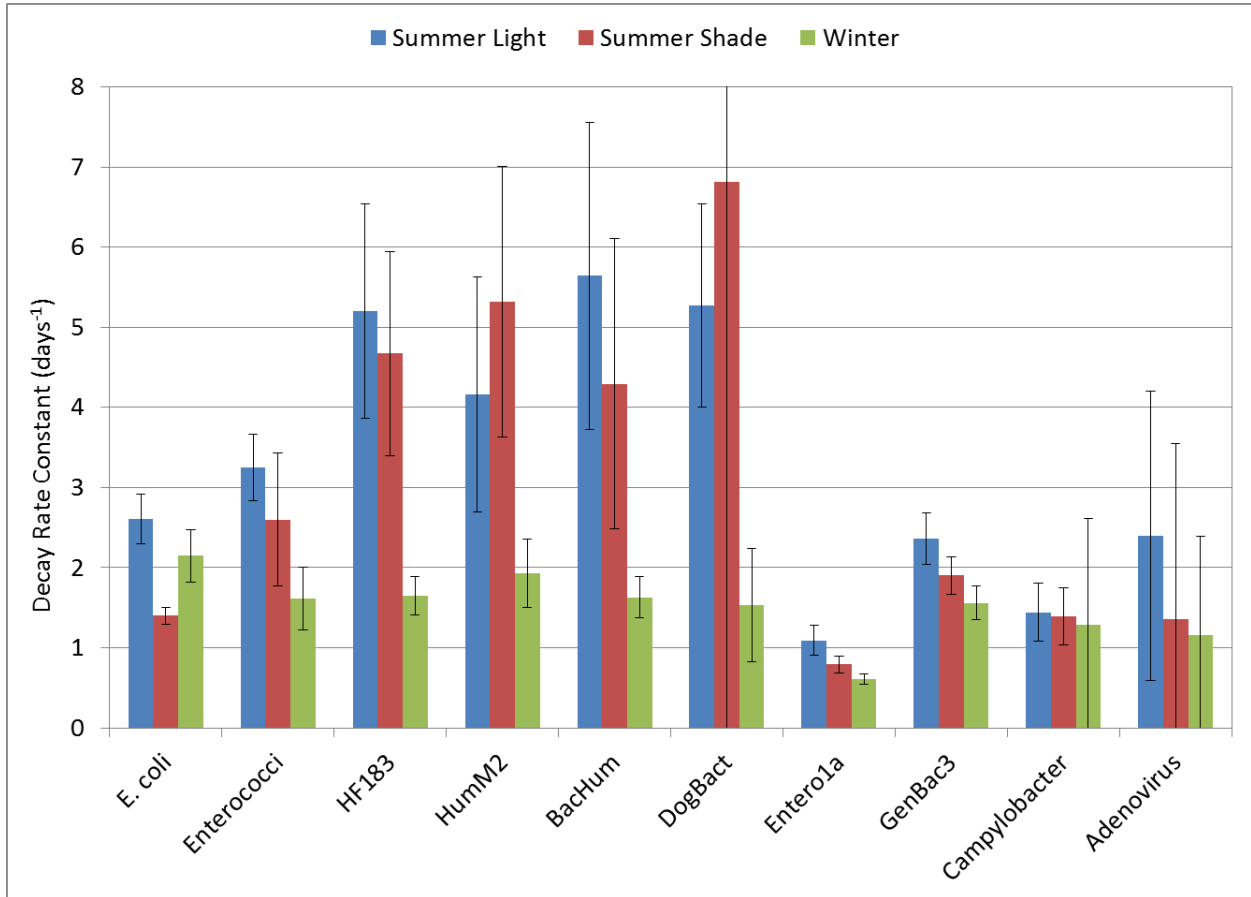


Figure 2. Modeled decay coefficients for FIB, DNA fecal markers, and pathogens. Error bars represent the 95% confidence interval.

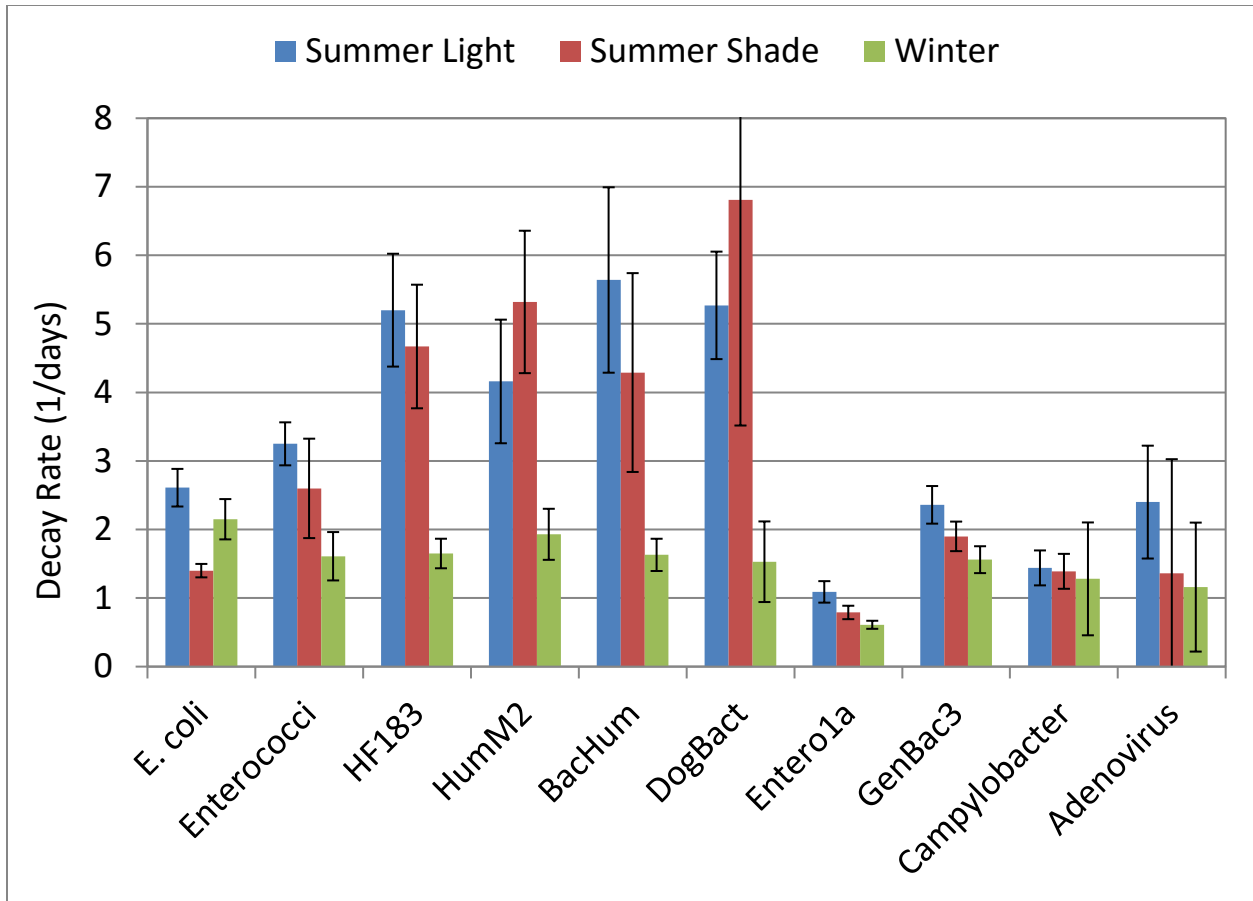


Figure 3. Modeled decay rates for FIB, DNA fecal markers, and pathogens. Error bars represent the 95% confidence interval.

To further explore FIB persistence based on modelled decay parameters, Half-life, T_{90} , and T_{99} values were calculated (Table 5). Values were calculated using the decay rate constant only and using the complete model including shoulder and tail parameters. T_{99} values for *E. coli* ranged from 1.8 days for the unshaded summer treatment to 3.3 days for the shaded summer treatment. T_{99} values for Enterococci ranged from 1.4 days for the unshaded summer treatment to 3.5 days for the shaded summer treatment. These results further support that the persistence of FIB in lagoon or brackish waters depends on both season and sunlight.

Table 5. Half-life, T₉₀, and T₉₉ values for FIB, DNA fecal markers, and pathogens based on the modeled decay rates and on the full model including shoulder and tail parameters.

Assay	Treatment	Based on K _{max} (days)			Based on full model (days)		
		T _{1/2}	T ₉₀	T ₉₉	T _{1/2}	T ₉₀	T ₉₉
E. coli	Light	0.27	0.88	1.76	0.27 ⁺	0.88 ⁺	1.77 ⁺
E. coli	Shade	0.49	1.64	3.29	0.49 ⁺	1.64 ⁺	3.29 ⁺
E. coli	Winter	0.32	1.07	2.14	0.32 ⁺	1.07 ⁺	2.16 ⁺
Enterococci	Light	0.21	0.71	1.42	0.21	0.71	1.43
Enterococci	Shade	0.27	0.89	1.77	1.70	2.54	3.48
Enterococci	Winter	0.43	1.43	2.85	0.43	1.43	2.87
HF183	Light	0.13	0.44	0.89	0.57	0.99	1.46
HF183	Shade	0.15	0.49	0.99	0.64	1.10	1.62
HF183	Winter	0.42	1.40	2.79	1.90	3.21	4.68
HumM2	Light	0.17	0.55	1.11	0.82	1.34	1.92
HumM2	Shade	0.13	0.43	0.87	1.01	1.43	1.88
HumM2	Winter	0.36	1.19	2.39	1.92	3.05	4.29
BacHum	Light	0.12	0.41	0.82	0.83	1.21	1.65
BacHum	Shade	0.16	0.54	1.07	0.68	1.18	1.74
BacHum	Winter	0.43	1.42	2.83	1.88	3.21	4.69
Entero1a	Light	0.64	2.11	4.22	0.64	2.11	4.22
Entero1a	Shade	0.88	2.93	5.85	0.88	2.93	5.85
Entero1a	Winter	1.14	3.80	7.60	1.14	3.80	7.60
GenBac3	Light	0.29	0.98	1.95	0.29	0.98	1.95
GenBac3	Shade	0.36	1.21	2.42	0.36	1.21	2.42
GenBac3	Winter	0.45	1.48	2.96	1.76	3.13	4.68
DogBact	Light	0.13	0.44	0.87	1.01	1.43	1.88
DogBact	Shade	0.10	0.34	0.68	1.19	1.51	1.87
DogBact	Winter	0.45	1.51	3.02	1.59	2.98	4.55
Campylobacter	Light	0.48	1.60	3.21	0.48	1.60	3.21
Campylobacter	Shade	0.50	1.66	3.31	0.50	1.66	3.31
Campylobacter	Winter	0.54	1.80	3.61	0.54 ⁺	1.80 ⁺	3.61 ⁺
Adenovirus	Light	0.29	0.96	1.92	0.60	(-)*	(-)*
Adenovirus	Shade	0.51	1.69	3.38	1.19	(-)*	(-)*
Adenovirus	Winter	0.60	1.99	3.98	0.72	(-)*	(-)*

*Does not include initial growth, *Concentration does not reach value due to tailing.

Literature Cited

- Ashbolt, N.J., M.E. Schoen, J.A. Soller, D.J. Roser. Predicting pathogen risks to aid beach management: the real value of quantitative microbial risk assessment (QMRA). *Water Res.* 2010, 44 (16), 4692–4703.
- Badgley, B.D., F.I.M. Thomas, V.J. Harwood. Quantifying environmental reservoirs of fecal indicator bacteria associated with sediment and submerged aquatic vegetation. *Environ. Microbiol.* 2011, 13 (4), 932–942.
- Bigelow, W.R. and J.R. Esty. The thermal death point in relation to time of typical thermophilic organisms. *J. Infect. Dis.* 1920, 27 (6), 602–617.
- Cabelli, V.J., A.P. Dufour, L.J. McCabe, M.A. Levin. Swimming-associated gastroenteritis and water quality. *Am. J. Epidemiol.* 1982, 115 (4), 606–616.
- Converse, R.R., J.L. Kinzelman, E.A. Sams, E. Hudgens, A.P. Dufour, H. Ryu, J.W. Santo-Domingo, C.A. Kelty, O.C. Shanks, S.D. Siefiring et al. Dramatic improvements in beach water quality following gull removal. *Environ. Sci. Technol.* 2012, 46 (18), 10206–10213.
- Dorsey, J.H., V.D. Carmona-Galindo, C. Leary, J. Huh, J. Valdez. An assessment of fecal indicator and other bacteria from an urbanized coastal lagoon in the City of Los Angeles, California, USA. *Environ. Monit. Assess.* 2012.
- Ervin, J.S., L.C. Van De Werfhorst, J.L.S. Murray, P.A. Holden. Microbial Source Tracking in a Coastal California Watershed Reveals Canines as Controllable Sources of Fecal Contamination. *Environ. Sci. Technol.* 2014.
- Geeraerd, A.H., V.P. Valdramidis, J.F. Van Impe. GInaFIT, a freeware tool to assess non-log-linear microbial survivor curves. *Int. J. Food Microbiol.* 2005, 102 (1), 95–105.
- Geeraerd, A.H., C.H. Herremans, J.F. Van Impe. Structural model requirements to describe microbial inactivation during a mild heat treatment. *Int. J. Food Microbiol.* 2000, 59 (3), 185–209.
- Goto, D.K. and T. Yan. Effects of Land Uses on Fecal Indicator Bacteria in the Water and Soil of a Tropical Watershed. *Microbes Environ.* 2011, 26 (3), 254–260.
- Grant, S.B., B.F. Sanders, A.B. Boehm, J.A. Redman, J.H. Kim, R.D. Mrse, A.K. Chu, M. Gouldin, C.D. McGee, N.A. Gardiner, et al. Generation of enterococci bacteria in a coastal saltwater marsh and its impact on surf zone water quality. *Environ. Sci. Technol.* 2001, 35 (12), 2407–2416.
- Green, H.C., O.C. Shanks, M. Sivaganesan, R.A. Haugland, K.G. Field. Differential decay of human faecal *Bacteroides* in marine and freshwater. *Environ. Microbiol.* 2011, 13 (12), 3235–3249.
- Green, H.C., R.A. Haugland, M. Varma, H.T. Millen, M.A. Borchardt, K.G. Field, W.A. Walters, R. Knight, C.A. Kelty, O.C. Shanks. Improved HF183 quantitative real-time PCR assay for characterization of human fecal pollution in ambient surface water samples. *Appl. Environ. Microbiol.* 2014.
- Green, H. and K. White. Development of Rapid Canine Fecal Source Identification PCR-Based Assays. *Environ. Sci. Technol.* 2014, 48, 11453–11461.
- Haugland, R.A., S.C. Siefiring, L.J. Wymer, K.P. Brenner, A.P. Dufour. Comparison of *Enterococcus* measurements in freshwater at two recreational beaches by quantitative polymerase chain reaction and membrane filter culture analysis. *Water Res.* 2005, 39 (4), 559–568.

- Haugland, R.A., M. Varma, M. Sivaganesan, C. Kelty, L. Peed, O.C. Shanks. Evaluation of genetic markers from the 16S rRNA gene V2 region for use in quantitative detection of selected Bacteroidales species and human fecal waste by qPCR. *Syst. Appl. Microbiol.* 2010, 33 (6), 348–357.
- Imamura, G.J., R.S. Thompson, A.B. Boehm, J.A. Jay. Wrack promotes the persistence of fecal indicator bacteria in marine sands and seawater. *Microbiol. Ecol.* 2011, 77 (1), 40–49.
- Jeanneau, L., O. Solecki, N. Wéry, E. Jardé, M. Gourmelon, P.Y. Communal, A. Jadas-Hécart, M.P. Caprais, G. Gruau, A.M. Pourcher. Relative decay of fecal indicator bacteria and human-associated markers: a microcosm study simulating wastewater input into seawater and freshwater. *Environ. Sci. Technol.* 2012, 46 (4), 2375–2382.
- Kildare, B.J., C.M. Leutenegger, B.S. McSwain, D.G. Bambic, V.B. Rajal, S. Wuertz. S.16S rRNA-based assays for quantitative detection of universal, human-, cow-, and dog-specific fecal Bacteroidales: a Bayesian approach. *Water Res.* 2007, 41 (16), 3701–3715.
- Korajkic, A., B.R. McMinn, V.J. Harwood, O.C. Shanks, G.S. Fout, N.J. Ashbolt. Differential decay of enterococci and *Escherichia coli* originating from two fecal pollution sources. *Appl. Environ. Microbiol.* 2013, 79 (7), 2488–2492.
- Korajkic, A., B.R. McMinn, O.C. Shanks, M. Sivaganesan, G.S. Fout, N.J. Ashbolt. Biotic Interactions and Sunlight Affect Persistence of Fecal Indicator Bacteria and Microbial Source Tracking Genetic Markers in the Upper Mississippi River. *Appl. Environ. Microbiol.* 2014, No. April, 1–32.
- LaMontagne, M.G. and P.A. Holden. Comparison of free-living and particle-associated bacterial communities in a coastal lagoon. *Microb. Ecol.* 2003, 46 (2), 228–237.
- Lund, M., S. Nordentoft, K. Pedersen, M. Madsen. Detection of *Campylobacter* spp. in chicken fecal samples by real-time PCR. *J. Clin. Microbiol.* 2004, 42 (11), 5125–5132.
- Malorny, B., E. Paccassoni, P. Fach, C. Bunge, A.R. Martin, R. Helmuth, S. Aliments. Diagnostic Real-Time PCR for Detection of *Salmonella* in Food. *Appl. Environ. Microbiol.* 2004, 70 (12), 7046–7052.
- Meays, C.L., K. Broersma, R. Nordin, A. Mazumder, M. Samadpour. Spatial and annual variability in concentrations and sources of *Escherichia coli* in multiple watersheds. *Environ. Sci. Technol.* 2006, 40 (17), 5289–5296.
- Sercu, B., L.C. Van De Werfhorst, J. Murray, P.A. Holden. Storm Drains are Sources of Human Fecal Pollution during Dry Weather in Three Urban Southern California Watersheds. *Environ. Sci. Technol.* 2009, 43 (2), 293–298.
- Sercu, B., L.C. Van De Werfhorst, J.L.S. Murray, P.A. Holden. Sewage exfiltration as a source of storm drain contamination during dry weather in urban watersheds. *Environ. Sci. Technol.* 2011, 45 (17), 7151–7157.
- Shanks, O.C., C. Kelty, M. Sivaganesan, M. Varma, R.A. Haugland. Quantitative PCR for genetic markers of human fecal pollution. *Appl. Environ. Microbiol.* 2009, 75 (17), 5507–5513.
- Siefring, S., M. Varma, E. Atikovic, L. Wymer, R.A. Haugland. Improved real-time PCR assays for the detection of fecal indicator bacteria in surface waters with different instrument and reagent systems. *J. Water Health* 2008, 6 (2), 225–237.

- Sinigalliano, C.D., J.M. Fleisher, M.L. Gidley, H.M. Solo-Gabriele, T. Shibata, L.R.W. Plano, S.M. Elmir, D. Wanless, J. Bartkowiak, R. Boiteau, et al. Traditional and molecular analyses for fecal indicator bacteria in non-point source subtropical recreational marine waters. *Water Res.* 2010, 44 (13), 3763–3772.
- Sinigalliano, C.D., J.S. Ervin, L.C. Van De Werfhorst, B.D. Badgley, E. Ballesté, J. Bartkowiak, A.B. Boehm, M. Byappanahalli, K.D. Goodwin, M. Gourmelon, et al. Multi-laboratory evaluations of the performance of *Catellibacterium marimammalium* PCR assays developed to target gull fecal sources. *Water Res.* 2013, 47 (18), 6883–6896.
- Soller, J.A., M.E. Schoen, T. Bartrand, J.E. Ravenscroft, N.J. Ashbolt. Estimated human health risks from exposure to recreational waters impacted by human and non-human sources of fecal contamination. *Water Res.* 2010, 44, 4674–4691.
- Steets B.M., P.A. Holden. A mechanistic model of runoff-associated fecal coliform fate and transport through a coastal lagoon. *Water Res.* 2003, 37, 589–608.
- Verhougstraete, M.P., S.L. Martin, A.D. Kendall, D.W. Hyndman, J.B. Rose. Linking fecal bacteria in rivers to landscape, geochemical, and hydrologic factors and sources at the basin scale. *Proc. Natl. Acad. Sci.* 2015, 112 (33), 10419–10424.
- Viau, E.J., D. Lee, A.B. Boehm. Swimmer risk of gastrointestinal illness from exposure to tropical coastal waters impacted by terrestrial dry-weather runoff. *Environ. Sci. Technol.* 2011, 45 (17), 7158–7165.
- Wade, T.J., N. Pai, J.N.S. Eisenberg, J.M. Colford. Do U.S. Environmental Protection Agency Water Quality Guidelines for Recreational Waters Prevent Gastrointestinal Illness? A Systematic Review and Meta-analysis. *Environ. Health Perspect.* 2003, 111 (8), 1102–1109.
- Wang, J.D., H.M. Solo-Gabriele, A.M. Abdelzaher, L.E. Fleming. Estimation of enterococci input from bathers and animals on a recreational beach using camera images. *Mar. Pollut. Bull.* 2010, 60 (8), 1270–1278.
- Whitlock, J.E., D.T. Jones, V.J. Harwood. Identification of the sources of fecal coliforms in an urban watershed using antibiotic resistance analysis. *Water Res.* 2002, 36 (17), 4273–4282.
- Wright, M.E., H.M. Solo-Gabriele, S. Elmir, L.E. Fleming. Microbial load from animal feces at a recreational beach. *Mar. Pollut. Bull.* 2009, 58 (11), 1649–1656.

Supplementary Information

Equations

Log Linear (LL) Decay Model:

$$C = C_0 * e^{-k_{max}*t}$$

C_0 = Initial Analyte Concentration

C = Analyte Concentration at Time t

k_{max} = Specific Decay Rate Constant (Decay Coefficient)

Log Linear with Shoulder (GS) Decay Model:

$$C = C_0 * e^{-k_{max}*t} * \frac{e^{k_{max}*Sl}}{1 + (e^{k_{max}*Sl} - 1) * e^{-k_{max}*t}}$$

Sl = Shoulder Length

Log Linear with Tail (GT) Decay Model:

$$C = (C_0 - C_{res}) * e^{-k_{max}*t} + C_{res}$$

C_{res} = Residual Analyte Concentration

Log Linear with Shoulder and Tail (GST) Decay Model:

$$C = (C_0 - C_{res}) * e^{-k_{max}*t} * \frac{e^{k_{max}*Sl}}{1 + (e^{k_{max}*Sl} - 1) * e^{-k_{max}*t}} + C_{res}$$

Fecal DNA Marker Decay Kinetics

The decay profiles for HF183 and Enterol1a are shown in Figure 1, decay profiles for the HumM2 and BacHum markers are shown in Figure S8 of the SI, and the decay profiles for the DogBact and GenBac3 markers are shown in Figure S9 of the SI. The complete results for all markers analyzed are included in Table S1 of the SI. All three human markers persisted longer in the winter treatment compared to the summer treatments, with DNQ levels of both the HF183 and BacHum marker still detectable on day ten of the winter deployment. Marker decay for shaded and unshaded summer treatments was similar for all three markers, although DNQ level detections did persist two days longer for both HF183 and BacHum markers in the shaded treatment. The HumM2 marker was initially detected at a concentration 1 Log lower than HF183 and BacHum and degraded to below detection on day 5 for the summer treatments and day 7 for the winter. The DogBact marker was initially detected at a lower concentration than the human markers and persisted at a detectable level until day 3 for the summer treatments and day 6 for the winter. The general fecal markers tended to persist longer than the human markers with both Enterol1a and GenBac3 still detectable at either quantifiable or DNQ levels on day ten for all three treatments. Similar to the human markers, the general markers decayed more slowly in the winter treatment compared to the summer treatments. However, the shaded summer treatment also showed less decay compared to the unshaded treatment throughout the profile for both Enterol1a and GenBac3.

Modeled decay kinetics for the human, dog, and general markers are shown in Table 4. For these markers, the log linear shoulder (GS) or log linear shoulder and tail (GST) models were the best fit for all markers except Enterol1a, which was log linear (LL). Human marker decay constants ranged from 1.6 to 5.6 days⁻¹ across all three markers, while general marker decay constants ranged from 0.6 to 1.1 days⁻¹ for Enterol1a and 1.6 to 2.4 days⁻¹ for GenBac3. Decay rate constants for the dog marker were similar to the human markers. The highest decay rate constant modeled was for the dog marker in the shaded summer treatment (6.8 days⁻¹). Decay rate constants were higher for the summer treatments compared to the winter treatment for all fecal markers. Based on the 95% confidence intervals (Figure 2), decay was significantly lower for all three human markers in the winter treatment compared to the summer treatments, while the shaded and unshaded summer treatments could not be distinguished. For both general markers, there was also a significant difference between decay-rate constants for the winter compared to the unshaded summer treatments, while the shaded treatments could not be distinguished from the winter or unshaded summer treatments. These results further show the impact of season on fecal marker decay in the lagoon environment, particularly for the source-associated markers, which are widely used in MST.

Half-life, T₉₀, and T₉₉ values for the human, dog, and general markers are shown in Table 5. T₉₉ values for the human markers ranged from 1.5 days for HF183 in the unshaded summer treatment to 4.7 days for BacHum in the winter treatment, when the full model including shoulder and tail parameters was used. T₉₉ values were similar across all three human markers within each treatment (range <0.5 days), showing that marker persistence was similar for all human markers investigated in this study. The HumM2 marker was therefore not detected as long as the other markers because the initial concentration was lower than HF183 and BacHum, rather than due to any difference in the decay rate constant or other modeled decay parameters. Dog marker T₉₉ values were also similar to the human markers across all treatments. The largest T₉₉ values in this study were calculated for the Enterol1a marker (4.2 to 7.6 days). The GenBac3 marker showed similar values to the human markers for the winter and only slightly larger values for the summer treatments. T₉₉ values were lower when only the decay rate constant was used in the calculation instead of the full model parameters due to the presence of a shoulder for the modeled human marker decay.

Bacterial Pathogen and Virus Decay Kinetics

The decay profile for *Campylobacter* is shown in Figure 1 and the decay profile for adenovirus is shown in Figure S10 of the SI. The complete bacterial pathogen and viral results are included in Table S1 of the SI. Quantifiable concentrations of *Campylobacter* (>100 copies/100ml) persisted for three to five days depending on treatment, but DNQ levels were detected through day ten in all three treatments. *Salmonella* was only detected at the DNQ level in the initial mixture and was then detected at this level for one day in the unshaded summer treatment and three days in the shaded summer and winter treatments. For adenovirus, quantifiable concentrations were detected up to day three in all three treatments, with the concentration in the winter still one log higher than that of the summer. Chamber samples were not analyzed beyond day three for adenovirus. Although norovirus was detected at the DNQ level in the initial winter sewage sample, norovirus was not detected in any other samples analyzed.

Modeled decay kinetics for the *Campylobacter* DNA marker and adenovirus are shown in Table 4. Concentrations of the *Salmonella* DNA marker and norovirus were too low to model decay kinetics. For the *Campylobacter* DNA marker, a log linear (LL) model resulted in the best fit. For adenovirus, the log linear tail (GT) model was the best fit. Decay rate constants (k_{max}) were not significantly different between treatments for *Campylobacter* or adenovirus based on the 95% confidence intervals (Figure 2) and ranged from 1.28 to 1.44 days⁻¹ for *Campylobacter* and 1.16 to 2.40 days⁻¹ for adenovirus. Although the unshaded summer decay rate constant was higher for adenovirus compared to other treatments, this difference was not significant due to high variability in the modeled decay rate constants. Analysis of

additional data would be needed to determine if seasonal conditions have an effect on adenovirus decay in the lagoon environment.

Half-life, T_{90} , and T_{99} values are shown in Table 5. Like decay rate constants, T_{99} values for *Campylobacter* were similar across treatments ranging from 3.2 days in the summer (unshaded) to 3.6 days for the winter. For adenovirus, T_{99} values could not be calculated when the full model was used. This was because the modeled concentration did not decay to the point where only 1% persisted due to tailing of the modeled data. When only the decay rate constant was used, the T_{99} value ranged from 1.9 days in the summer (unshaded) to 4.0 days in the winter, with the shaded summer value (3.4 days) more similar to that of winter.

Decay Comparison between FIB, Fecal DNA Markers and Pathogens

Modeled decay rate constants for FIB, fecal DNA markers, *Campylobacter* and adenovirus are shown in Figure 2. Decay was highest for the human markers in the summer treatments showing that these markers decay relatively rapidly under summer lagoon conditions. The HF183 marker decay was higher than that of FIB, general markers and *Campylobacter* during the summer deployment for the unshaded treatments. Summer HumM2 decay was higher than all other non-human markers, FIB and *Campylobacter* for the shaded treatment, but was not significantly different from FIB in the unshaded treatment. Summer BacHum decay was higher than all other non-human markers, FIB and *Campylobacter* for the unshaded treatment, but was not significantly different from Enterococci in the shaded treatment. During the winter deployment, human marker decay was not significantly different from FIB. In general, winter decay-rate constants were similar across all nine parameters. Only the Enterol1a winter decay was significantly different than other winter rate constants (lower than all except *Campylobacter* and adenovirus based on the 95% confidence intervals). These results show that FIB, fecal DNA markers, and pathogens all decay at different rates in the lagoon environment, particularly during the summer.

A shoulder in the decay profile, based on modeling, was observed for several of the organisms quantified in this study, including all three human markers. The presence of a shoulder in the modeled decay increases persistence even if the decay rate constant is high. For example, the decay rate constant for HF183 in the unshaded summer treatment was 5.2 days^{-1} compared to 3.25 days^{-1} for Enterococci. However, the T_{99} based on the full model (including the shoulder parameter) was 1.5 days for HF183 and 1.4 days for Enterococci, which did not have a shoulder modeled. This shows that the decay rate constant alone may not fully capture environmental persistence. Initial growth was also observed for *E. coli*, which increases persistence even when a shoulder model was not used.



Figure S1. Satellite Image of the Arroyo Burro Lagoon (shaded blue) with the deployment site indicated (Google Earth, 2016).



Figure S2. Lagoon deployment apparatus with dialysis chamber (inset).

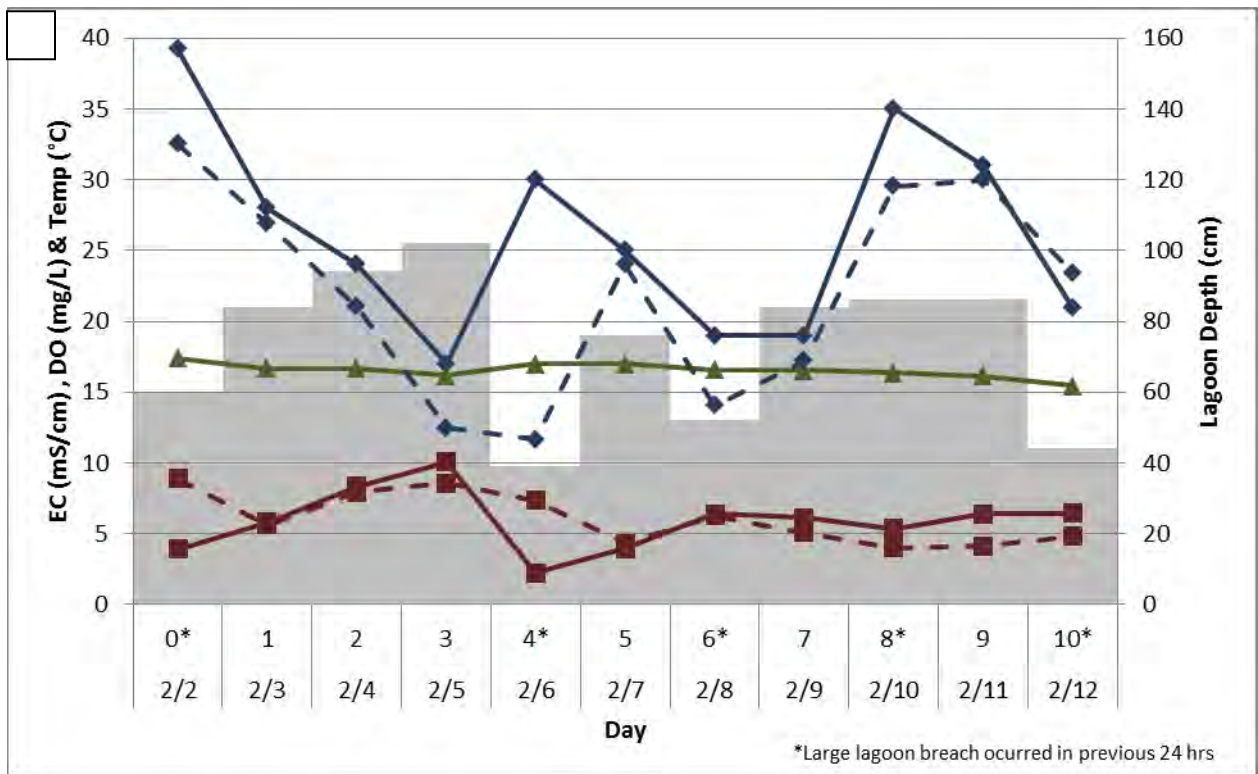
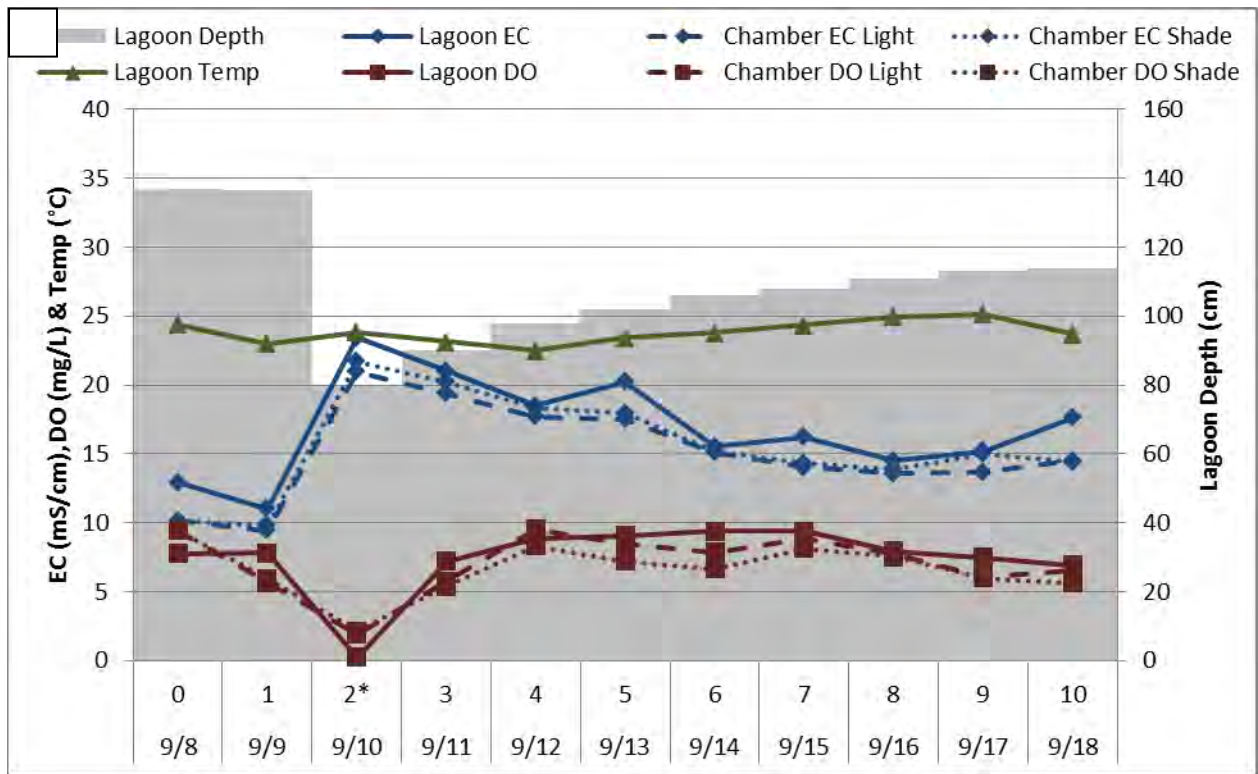


Figure S3. Electrical conductivity (EC), dissolved oxygen (DO), temperature (Temp), and depth of lagoon water; EC and DO of chamber water for summer (A) and winter (B) deployments.

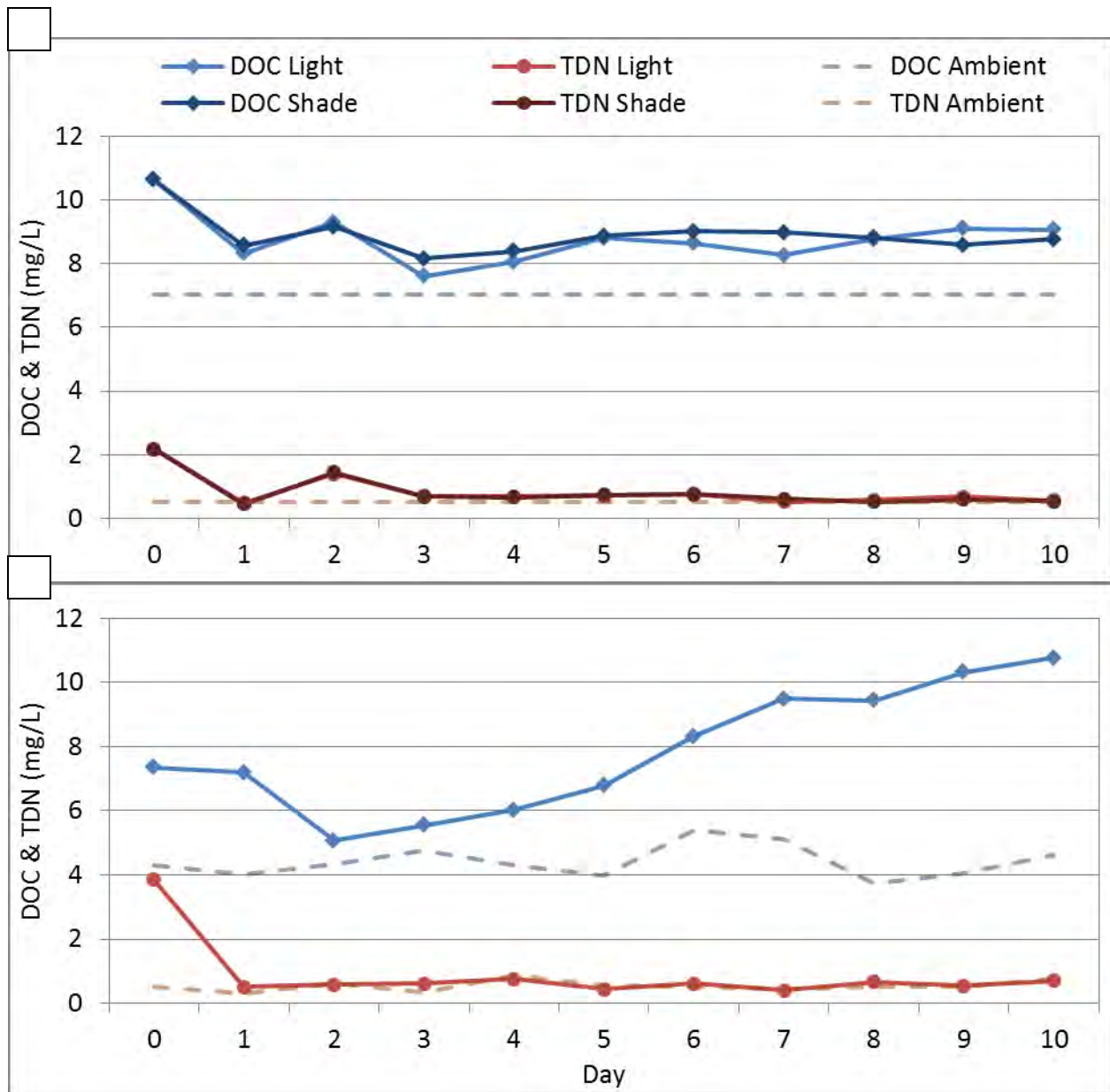


Figure S4. DOC and TDN concentrations within chambers and in the ambient lagoon for the summer (A) and winter (B) deployments. Ambient concentrations for the summer deployment were measured on day 0, while daily measurements were made during the winter deployment.

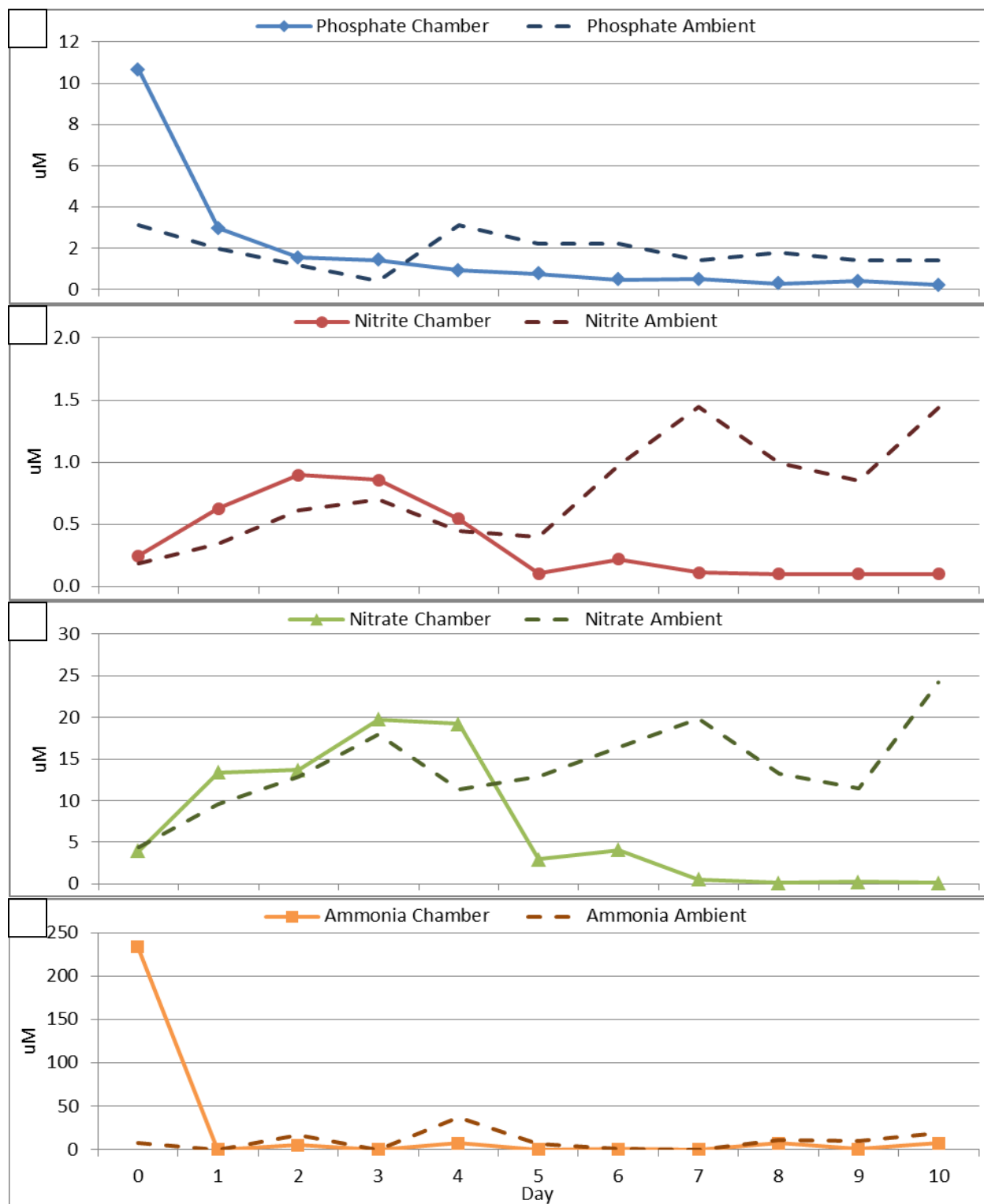


Figure S5. Phosphate (A), nitrite (B), nitrate (C), and ammonia (D) concentrations within chambers (solid lines) and in the ambient lagoon (dashed lines) for the winter deployment.

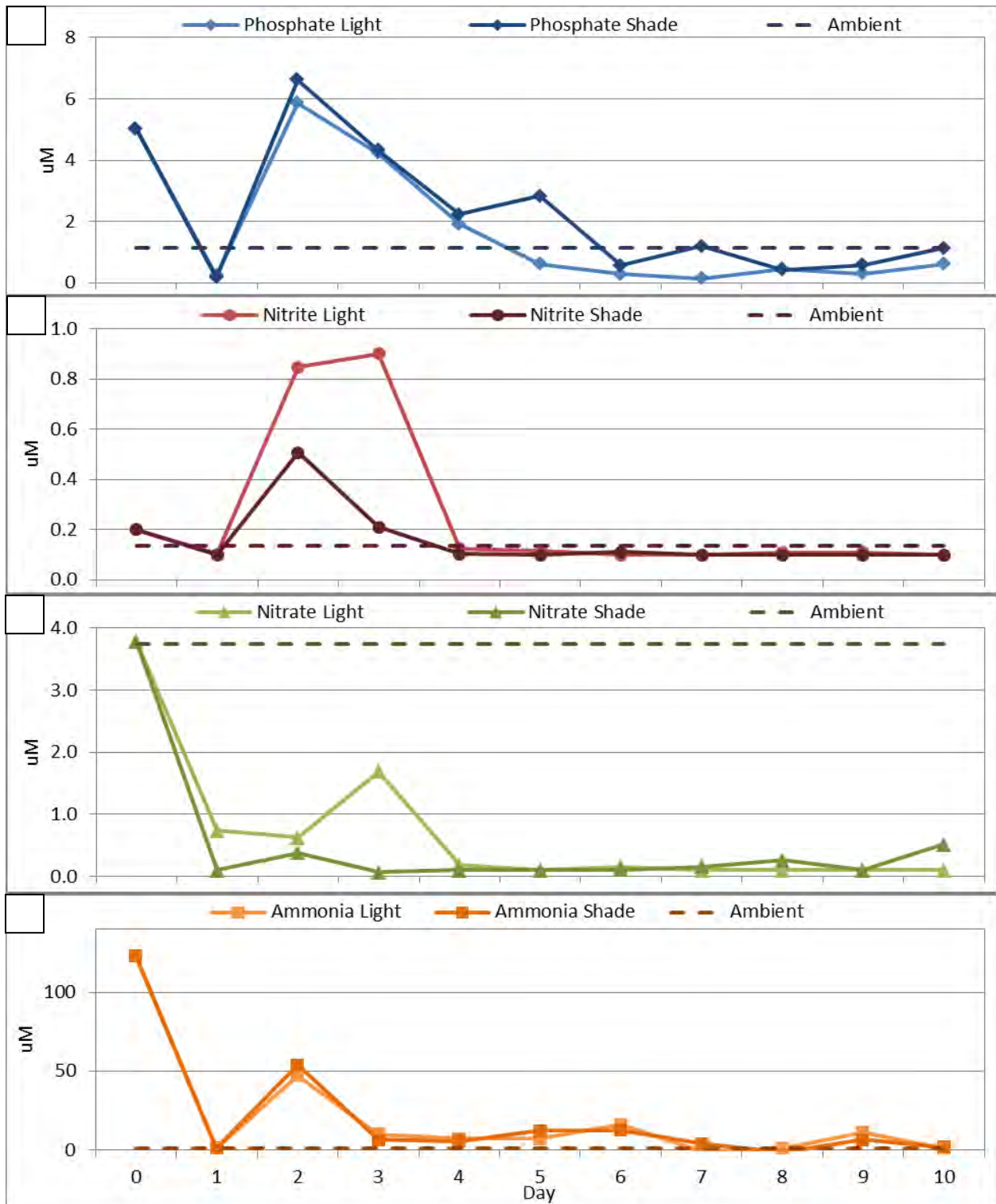


Figure S6. Phosphate (A), nitrite (B), nitrate (C), and ammonia (D) concentrations within chambers (solid lines) and in the ambient lagoon (dashed lines) for the summer deployment.

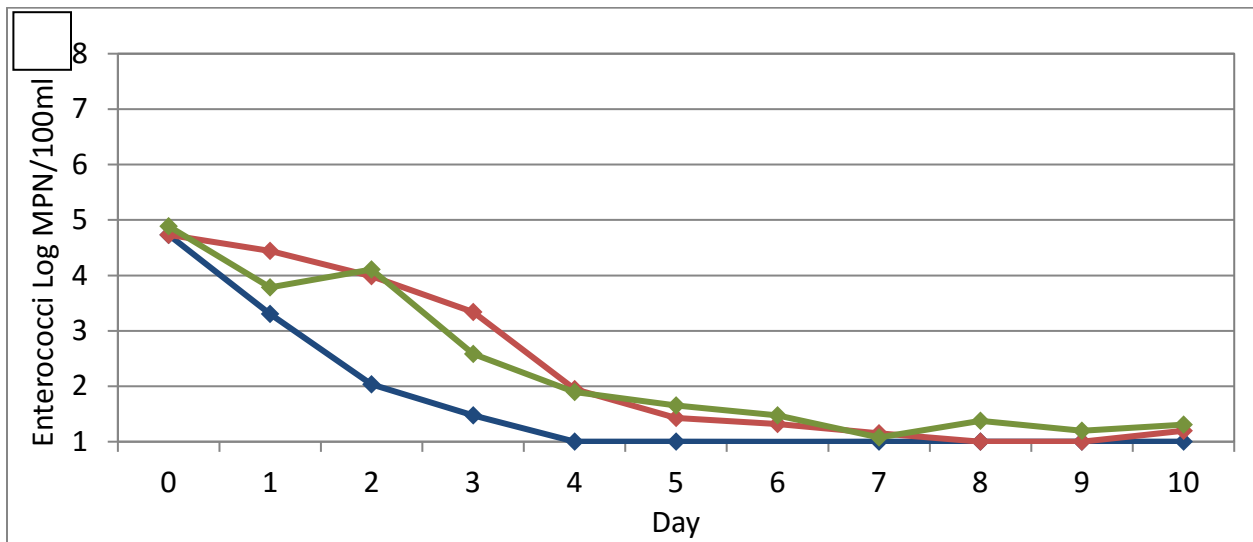
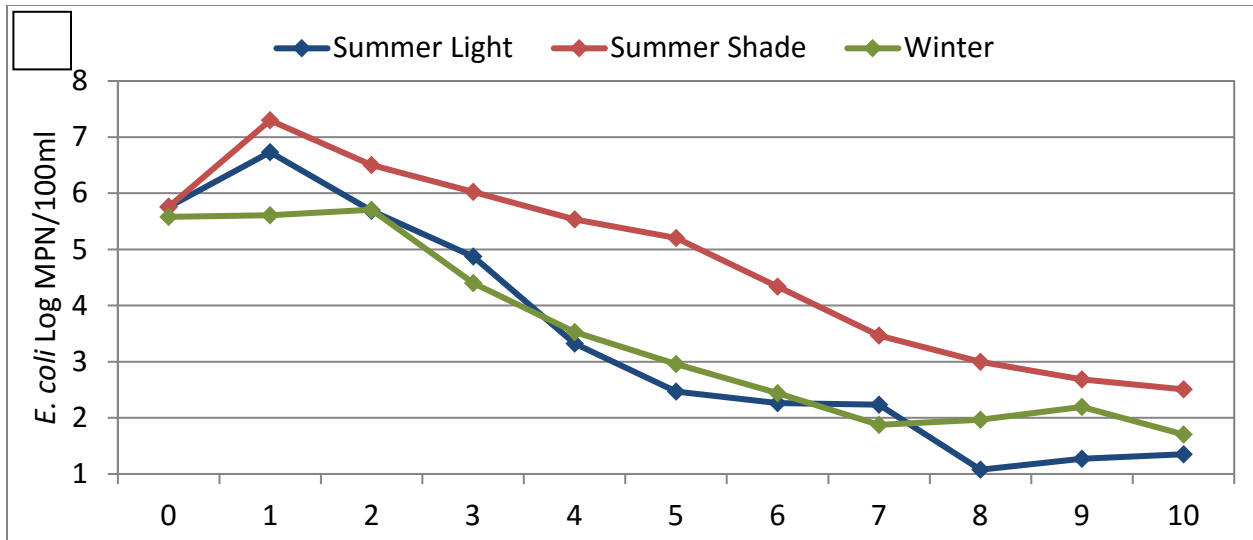


Figure S7. FIB decay profiles for *E. coli* (A) and Enterococci (B).

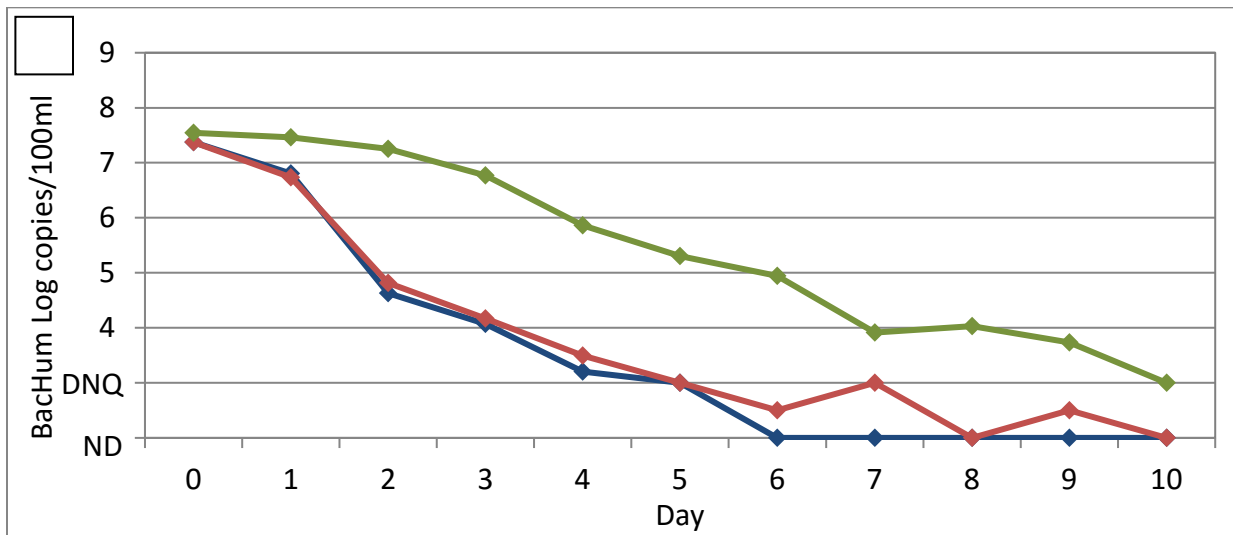
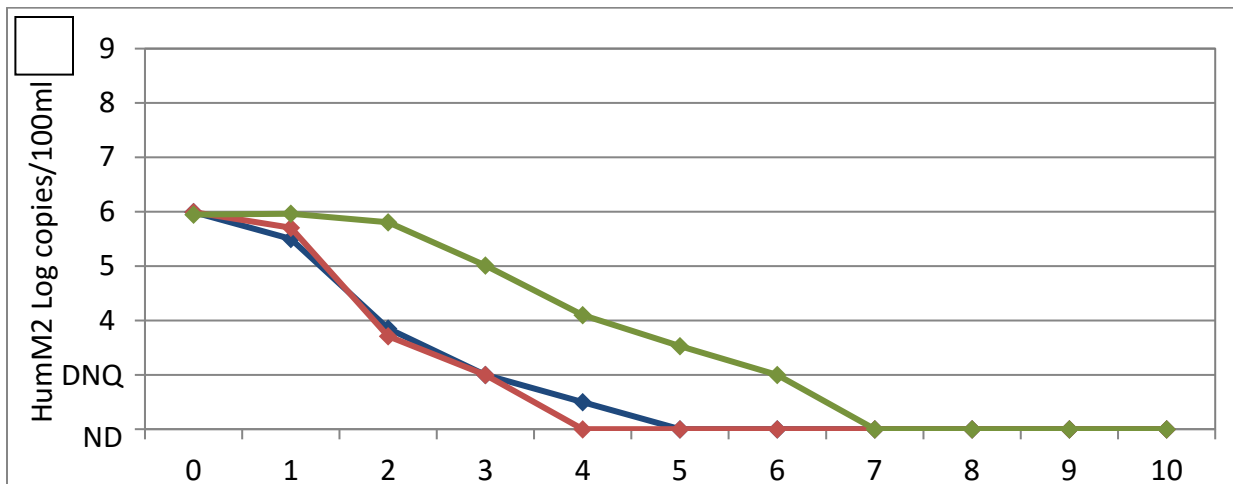
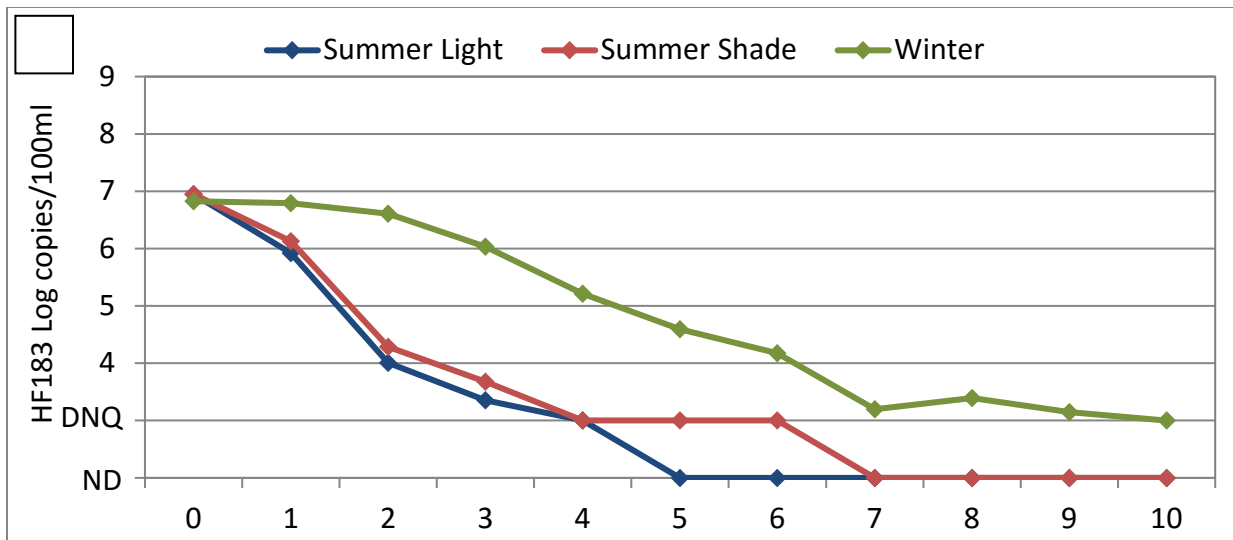


Figure S8. Human fecal marker decay profiles for HF183 (A), HumM2 (B), and BacHum (C).

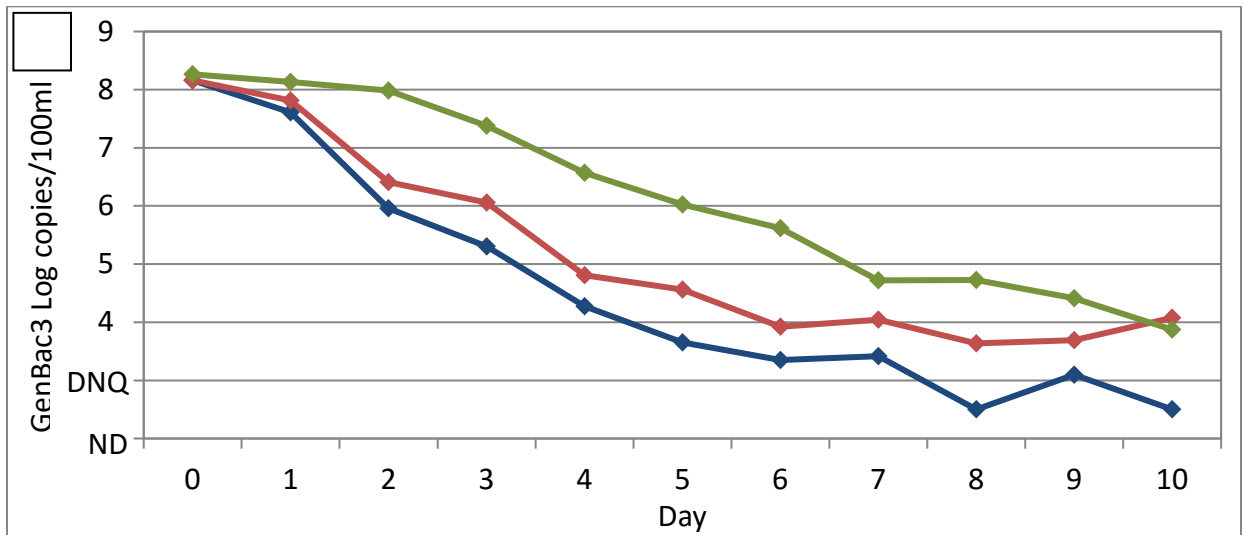
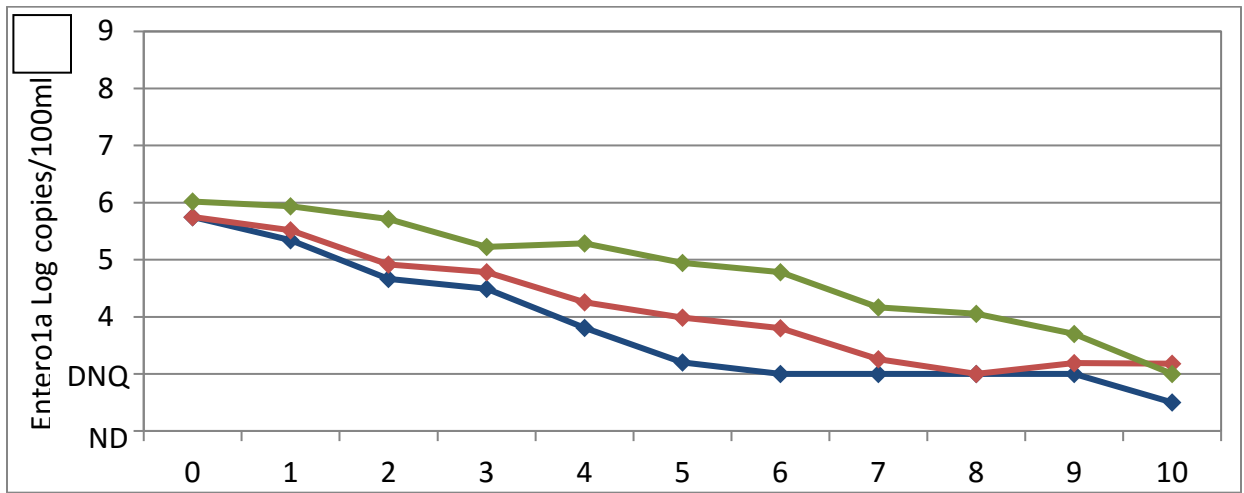
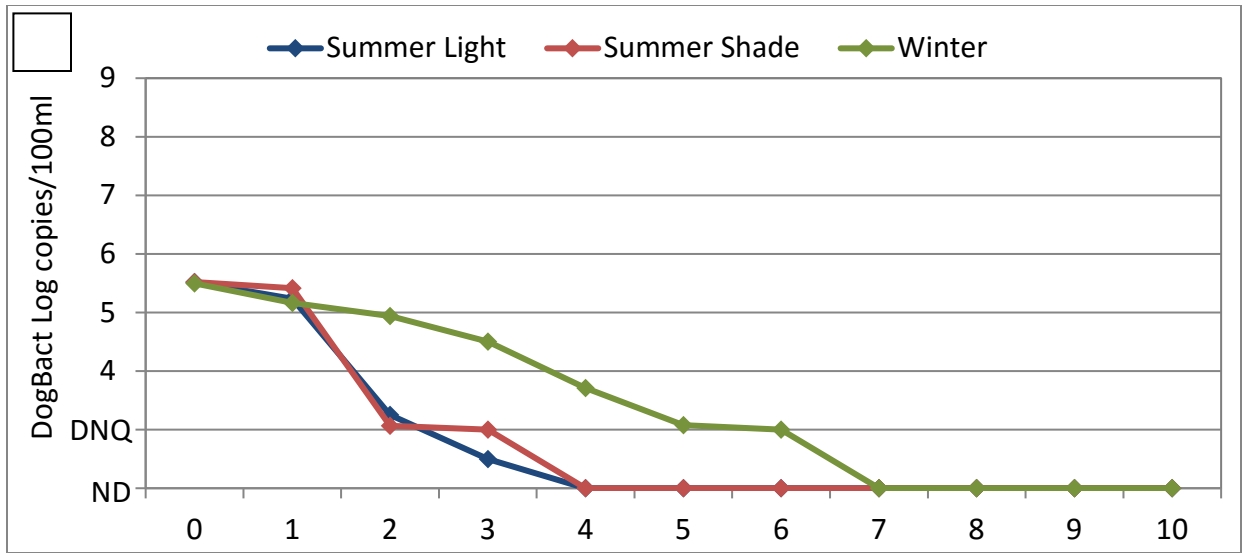


Figure S9. Marker decay profiles for DogBact (A), Entero1a (B), and GenBac3 (C).

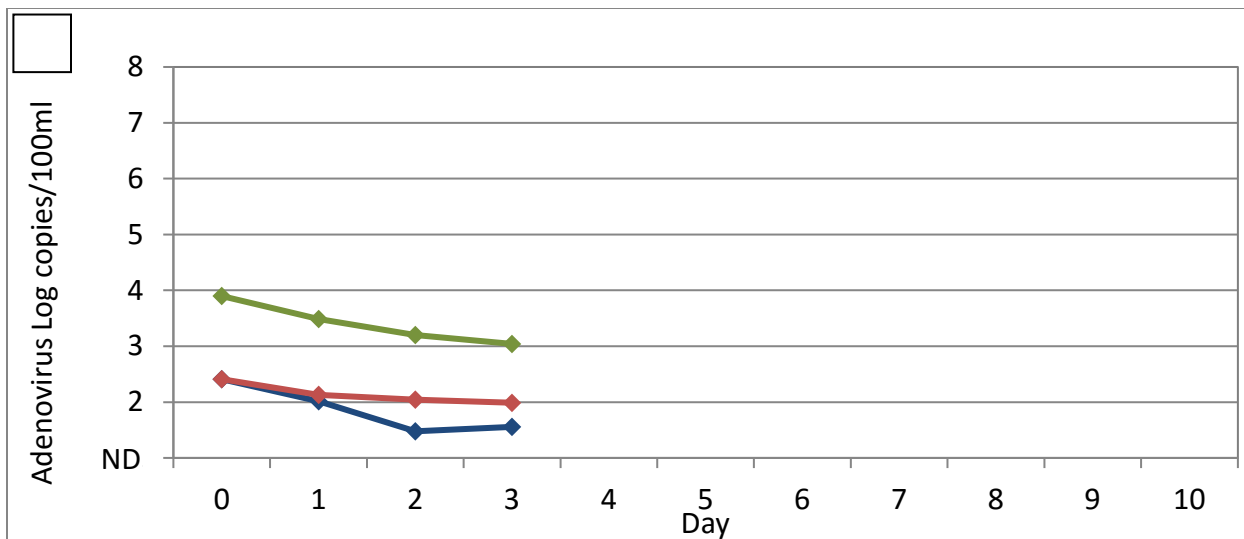
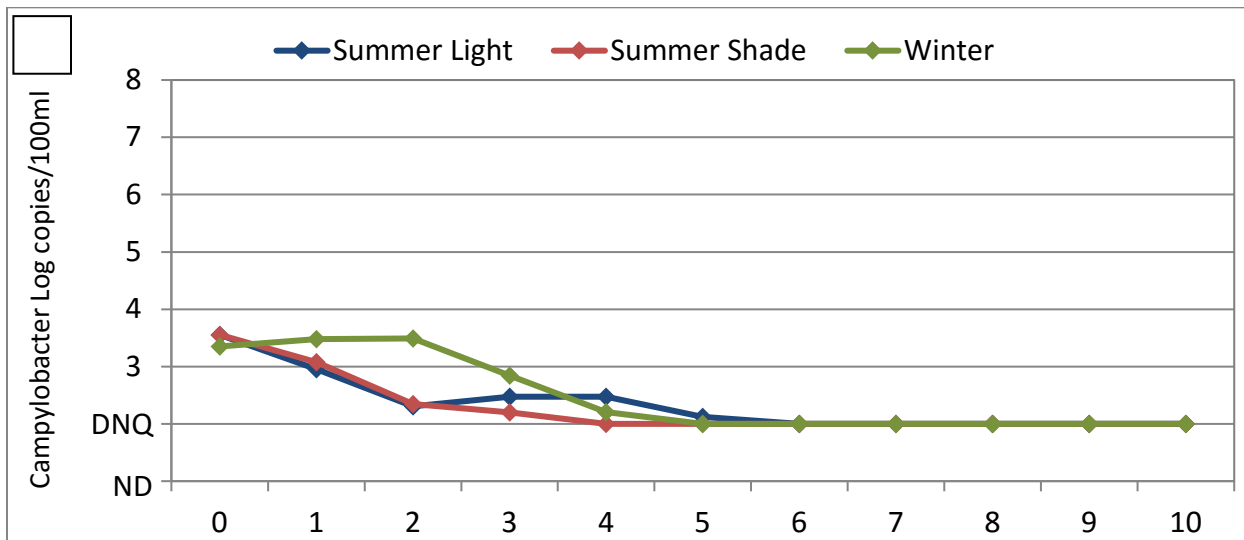


Figure S10. Pathogen decay profiles for Campylobacter (A) and Adenovirus (B).

Table S1. qPCR standard curve statistics for DNA fecal markers and bacterial pathogens. ROQ = Range of Quantification. *Efficiency = $10^{-(1/\text{slope})}-1$.

Assay	Slope	y-intercept	R ²	Efficiency*	ROQ (Log Copies/reaction)
HF183	-3.46	38.7	0.999	0.947	2E01 to 2E07
HumM2	-3.47	40.7	0.998	0.940	2E01 to 2E07
BacHum	-3.36	40.2	0.998	0.985	2E01 to 2E07
Enter01a	-3.46	39.7	0.998	0.946	2E01 to 2E07
GenBac3	-3.55	40.5	0.995	0.913	2E01 to 2E07
DogBact	-3.47	40.5	0.996	0.942	2E01 to 2E07
Campylobacter	-3.38	37.7	0.998	0.978	6E00 to 6E06
Salmonella	-3.30	37.8	0.999	1.007	6E00 to 6E06

Table S2. Physical parameters measured daily in ambient lagoon water and weather conditions during summer and winter deployments. *p-values represent probability $> |Z|$ for the Wilcoxon 2-sample rank sum test.

Parameter	Units	Median		Range		Summer vs Winter
		Summer	Winter	Summer	Winter	p-value*
Water Temperature	°C	23.8	16.6	22.5 – 25.2	15.5 – 17.4	<0.0001
Electrical Conductivity	mS/cm	16.2	25.0	11.0 – 23.4	17.0 – 39.2	0.0018
Dissolved Oxygen	mg/L	7.8	6.1	0.2 – 9.4	2.2 – 10.1	0.0301
Turbidity	NTU	2.2	3.4	0.8 – 3.6	2.3 – 11.7	0.0038
Depth	cm	108	84	80 - 137	39 - 102	0.0009
Air Temperature (Daily Average)	°C	20.5	14.1	19.1 – 25.2	11.7 – 22.7	0.0016
Solar Radiation (Daily Average)	Ly/day	509	325	408 - 560	53 - 394	<0.0001

Table S3. Half-life, T₉₀, and T₉₉ values for FIB, DNA fecal markers, and pathogens based on the modeled decay rate constants and on the full model including shoulder and tail parameters.

Assay	Treatment	Based on k _{max} (days)			Based on full model (days)		
		T _{1/2}	T ₉₀	T ₉₉	T _{1/2}	T ₉₀	T ₉₉
E. coli	Light	0.27	0.88	1.76	0.27 ⁺	0.88 ⁺	1.77 ⁺
E. coli	Shade	0.49	1.64	3.29	0.49 ⁺	1.64 ⁺	3.29 ⁺
E. coli	Winter	0.32	1.07	2.14	0.32 ⁺	1.07 ⁺	2.16 ⁺
Enterococci	Light	0.21	0.71	1.42	0.21	0.71	1.43
Enterococci	Shade	0.27	0.89	1.77	1.70	2.54	3.48
Enterococci	Winter	0.43	1.43	2.85	0.43	1.43	2.87
HF183	Light	0.13	0.44	0.89	0.57	0.99	1.46
HF183	Shade	0.15	0.49	0.99	0.64	1.10	1.62
HF183	Winter	0.42	1.40	2.79	1.90	3.21	4.68
HumM2	Light	0.17	0.55	1.11	0.82	1.34	1.92
HumM2	Shade	0.13	0.43	0.87	1.01	1.43	1.88
HumM2	Winter	0.36	1.19	2.39	1.92	3.05	4.29
BacHum	Light	0.12	0.41	0.82	0.83	1.21	1.65
BacHum	Shade	0.16	0.54	1.07	0.68	1.18	1.74
BacHum	Winter	0.43	1.42	2.83	1.88	3.21	4.69
Entero1a	Light	0.64	2.11	4.22	0.64	2.11	4.22
Entero1a	Shade	0.88	2.93	5.85	0.88	2.93	5.85
Entero1a	Winter	1.14	3.80	7.60	1.14	3.80	7.60
GenBac3	Light	0.29	0.98	1.95	0.29	0.98	1.95
GenBac3	Shade	0.36	1.21	2.42	0.36	1.21	2.42
GenBac3	Winter	0.45	1.48	2.96	1.76	3.13	4.68
DogBact	Light	0.13	0.44	0.87	1.01	1.43	1.88
DogBact	Shade	0.10	0.34	0.68	1.19	1.51	1.87
DogBact	Winter	0.45	1.51	3.02	1.59	2.98	4.55
Campylobacter	Light	0.48	1.60	3.21	0.48	1.60	3.21
Campylobacter	Shade	0.50	1.66	3.31	0.50	1.66	3.31
Campylobacter	Winter	0.54	1.80	3.61	0.54 ⁺	1.80 ⁺	3.61 ⁺
Adenovirus	Light	0.29	0.96	1.92	0.60	(-)*	(-)*
Adenovirus	Shade	0.51	1.69	3.38	1.19	(-)*	(-)*
Adenovirus	Winter	0.60	1.99	3.98	0.72	(-)*	(-)*

*Does not include initial growth, *Concentration does not reach value due to tailing.

APPENDIX C: RELATIVE DECAY OF FECAL MATERIAL IN FRESH WATERS

(Field Site: San Joaquin Marsh)

Introduction

This appendix describes the field studies that investigated relative degradation of fecal organisms in freshwater sites. The studies were conducted in two seasons (summer, winter) with each of the three fecal sources (primary influence sewage, cow fecal material, gull fecal material).

Methods

Field site

The field site (33° 39' 57.9" N, 117° 50' 46.8" W) is located within San Joaquin Marsh (SJM) in Irvine, CA. The SJM, one of Irvine Ranch Water District's natural treatment systems, consists of a series ponds connected by channels. It receives mostly urban runoff from and discharges into the adjacent San Diego Creek. Ambient water at the experiment site is similar to that in the creek, and experiments were conducted at SJM instead of the creek itself because of increased public traffic around the creek leading to potential vandalism to the experimental devices.

Fecal material

Three fecal sources (sewage, cow and gull feces) were used in the experiments. Sewage was primary influent (grab sample) from Orange County Sanitation District (Costa Mesa, CA) collected the night before and stored in 4C before use. Fresh deposits of cow feces were collected within two days (then stored in 4C) leading up to the experiment from August 15-16, 2014 and January 8-9, 2015 during the summer and winter, respectively. Ten and eight individual patties were collected for summer and winter, respectively. In order to obtain enough mass, fresh deposits of gull feces were collected between 6-8 a.m. over four days (then stored in 4C) leading up to the experiment from Surfrider Beach (Malibu, CA) and Doheny State Beach (Data Point, CA) and over two days (then stored in 4C) from Doheny State Beach (Data Point, CA). Approximately 140 and 100 individual droppings were collected from large flocks of gulls for summer and winter, respectively.

***In situ* microcosms**

The 10-day decay experiments were conducted *in situ* using dialysis bags (6-8 kDa, Spectra/Por[®]4, Spectrum Labs, Rancho Dominguez, CA) containing a single fecal source (sewage (5% v/v), cow (1% w/v) or gull (0.1% v/v) feces) seeded into unaltered ambient water from the field site. In the summer, six sets of dialysis bags were used with one set for each fecal source and each treatment (exposed to direct sunlight and shaded from direct sunlight). In the winter, all three sets of dialysis bag (one set for each fecal source) were exposed to direct sunlight. Each set of seeded bags was also accompanied by two control bags containing just the ambient water. All bags contained 1 liter sample or control water. Duplicate bags from each source and treatment were retrieved daily and the contents processed for FIB, MST marker, pathogens and microbial community analysis. On day 7 and day 10, one control bag was retrieved for each source. The treatment and the contents of the control bags were processed the same as the sample bags were processed.

Dialysis bags were made by sealing the two ends of dialysis tubing using buoyant clamps (Spectrum Labs). Each set of dialysis bags were suspended from PVC frames placed in ambient water so that the bags floats at approximately 12cm below the surface of water. In the summer, half of the frames were covered with one layer of the shade cloth (Easy Gardener Heavy Black Sun Screen Shade Cloth, Home Depot) to provide the sunlight vs. shaded treatment contrast.

Microcosm setup summer

The summer experiments occurred August 18 to 28, 2014. Approximately 170L of ambient water were collected from SJM and large debris such as leaves were removed. The water was then premixed in a large carboy on a stir plate and used for creating spiked waters for all sources and treatments and for filling control bags.

Three liters of sewage were pre-mixed (10 min hand shake followed by 10min settling to remove large debris) then mixed into 57L water in a large carboy on a stir plate (continuous mixing, 200 rpm). After 20 min, the spiked water were collected while stirring from a spigot attached to the carboy for filling dialysis bags.

An equivalent mass of cow feces from each of 24 patties was mixed (stirred using spatula) and 600 g of the mixture was added into 10L of PBS (mechanic stir, 20min, 200rpm) to make the initial fecal slurry. Any large particles that floated to the top were skimmed off. The entire volume of the slurry was then mixed into 50L water and used for experiments in the same manner as sewage.

Approximately 80 ml of gull feces were mixed into 1L of PBS (vortex, 10min) to make the initial fecal slurry, which was then mixed into 59L of water and used for experiments in the same manner as sewage and cow feces.

Microcosm setup winter

The winter experiments occurred January 9 to 19, 2015. Approximately 100L of ambient water was collected from SJM and large debris such as leaves were removed. The water was then premixed in a large carboy on a stir plate and used for creating spiked waters for all sources and treatments and for filling control bags.

One and a half liters of sewage were pre-mixed (10 minutes hand shake followed by 10 minutes settling to remove large debris) then mixed into 28.5L water in a large carboy on a stir plate (continuous mixing, 200 rpm). After 20 minutes, the spiked water was collected while stirring from a spigot attached to the carboy for filling dialysis bags.

An equivalent mass of cow feces from each of eight patties was mixed (stirred using spatula) and 360 g of mixture was added into 5.64L of PBS (mechanic stir, 20 minutes, 200 rpm) to make the initial fecal slurry. Any large particles that floated to the top were skimmed off. The 5 liters of the slurry was then mixed into 25L water and used for experiments in the same manner as sewage.

Approximately 40 mL of gull feces was mixed with 40 ml of PBS (vortex, 10 minutes) to make an initial fecal slurry, 60 ml of which was then mixed into 29L of water and used for experiments in the same manner as other fecal sources.

Sample collection

Sampling occurred daily at 8 a.m., and each sample was processed and assayed for FIB, MST marker, pathogens, and the entire microbial community. Dialysis bags were retrieved then placed in capped bucket filled with ambient water for transport from the site and the laboratory. The dialysis bags were shaken gently to mix the sample water before pouring it into acid-cleaned (regular wash followed by 10%HCl >15min) bottles for processing within 6 hours of sample collection.

In the summer, two ambient waters (the composite water used for making spiked water in the dialysis bags, and one ambient grab sample at day one) were collected for analysis each day. In the winter, the composite water used for spiking as well as daily ambient water was also collected for analysis.

Sample processing

Sample water was processed for culture-based analysis within 6 hours of collection. Three sets of filters for bacteria and two sets of filters for viruses were archived for molecular analysis. For bacteria analysis, 100 ml of each sample was filtered directly onto polycarbonate filters (0.45µm pore size), then flash frozen in liquid nitrogen and stored in -80°C until DNA extraction. For virus analysis, 100ml of each sample was mixed with MgCl₂ (final concentration 0.1 µM) and filtered onto mixed nitrocellulose filters (0.45µm pore size), then flash frozen in liquid nitrogen and stored in -80 °C until viral DNA/RNA extraction. For the cow treatments, sample waters were centrifuged (10000g at 4°C, 20min) prior to filtration as described above in order to reduce filtration time. Both the pellets and filters were stored at 80 °C until DNA extraction. Following extraction, DNA from pellets and filters from the same sample was combined for downstream molecular analysis.

About 40ml of sample water or ambient water was also filtered through Sterivex HV 0.45µm filter units (Millipore, SVHV010RS) into nutrient inert containers (FisherSci Nalgene 03-312AA or Glass vials V320-6-1-3360). The container with filtered water were stored in -20°C until shipment to UCSB for analysis of Nitrate (NO₃) + Nitrite (NO₂), Nitrite (NO₂), Phosphate (PO₄), and Ammonium (NH₄), DOC (as non purgeable organic carbon) and total dissolved nitrogen.

Culturable total coliform, e.coli, enterococcus, campylobacter, and salmonella

Each sample was analyzed in duplicate for *Enterococcus*, *E. coli*, and total coliform by Enterolert and Colilert (IDEXX Laboratory) at appropriate dilutions.

In the summer, presence and absence of culturable *Campylobacter* and *Salmonella* was also measured by a modified version (Yamahara et al. 2012) of the method of Khan and Edge (2007). Method and a growth-molecular detection hybrid method, respectively. In the winter, only presence and absence of culturable *Salmonella* was measured.

Briefly, for culturable *Campylobacter*, 100 ml of water sample was filtered through HA filters and then placed in 25 ml of Bolton broth (Remel, Lenexa, KS) supplemented with Oxoid Bolton Broth Selective Supplement (Remel) and Laked Horse Blood (Remel) for enrichment under microaerophilic conditions (42°C for 48 h) using GasPak 100 systems with EZ Campy Container System sachets (BD Diagnostic). Bolton broth enrichments were streaked onto modified Karmali agar (Remel) supplemented with Oxoid *Campylobacter* Selective Supplement Karmali (Remel) and again incubated under microaerophilic conditions (42°C for 48 h). Colonies displaying typical *Campylobacter* morphology (white to gray colonies) were picked as presumptive positives with PCR confirmation targeting *Campylobacter* 16S rRNA (Linton et al. 1996).

Briefly, for culturable *Salmonella* analysis, 50, 50, or 10ml of sample water, for sewage, gull and cow treatments respectively, were filtered onto one polycarbonate filter (0.45µm). The filter was then fully immersed and shaken for a few seconds in 10ml of TSB in falcon tubes. Tubes were then incubated in 37 °C for 24 hours before the culture broth was filtered onto another polycarbonate filter, flash frozen in liquid nitrogen and stored in -80°C till DNA extraction. Droplet digital PCR quantification of *Salmonella* of pre- and post-TSB filter were compared to determine if there was significant growth of *Salmonella*. A pilot study was conducted with 5% sewage in ambient IRWD water and a one-to-two order of magnitude increase in ddPCR results was observed after overnight TSB culturing.

DNA and RNA extraction

DNA was extracted from PC filters for the quantification of bacterial molecular markers using the GeneRite DNA-EZ kit (catalog no. K200-02C-50, GeneRite, North Brunswick, NJ) following

manufacturer's instructions with a 100 µl final elution volume. The eluent from the three replicate PC filter extractions (each with 100 ml of sample filtered) were pooled (300 µl total extract eluent) and then separated into 50 µl aliquots and stored at -80°C for subsequent molecular analyses. DNA concentrations and purities were determined on a Nanodrop[®] ND-1000 UV-Vis spectrophotometer (Nanodrop Technologies, Wilmington, DE).

Total RNA and DNA were extracted simultaneously from the two replicate HA filters for the quantification of norovirus GII using a modified MoBio PowerWater[®] RNA Isolation Kit (Mo Bio Laboratories Inc., Carlsbad, CA) with a final elution volume of 100 µl (see SI for details on modifications)(Mattioli 2014 , Viau et al. 2011). Extraction blanks were run with every seventeen samples. Separate 30 µL aliquots of extracted RNA/DNA were stored at -80°C for subsequent molecular analyses. All RNA and DNA aliquots underwent a maximum of one freeze-thaw cycle prior to molecular analysis.”

PCR-based analysis of genetic FIB, MST markers, and pathogens

All three categories of organisms were quantified by qPCR and/or droplet digital PCR (ddPCR): Enterococcus, E.coli, general Bacteroidales; HF183, BacHum, HumM2, LeeSeagull, CowM2; Campylobacter, Salmonella; Adenovirus, Norovirus. Details of the assays including primer/probe sequences, references, and PCR cycling conditions are presented in Tables 1 and 2.

Master standard curves for qPCR assays were established with outlier removal procedure (Ebentier et al. 2013). Quantification was based on comparison of the C_q to the respective master standard curves. The lower limit of quantification (LLOQ) was defined as the lowest concentration on the standard curves where all replicates were detected. Limit of detection (LOD) was defined as the concentration corresponding to the y-intercept of the regression line representing the master standard curve or the number of cycles run for the qPCR assay, whichever was larger.

Droplet digital PCR data were processed, including threshold setting and determination of detection limit, as described previously (Cao et al. 2015, Cao et al. 2016). All concentrations were reported as log₁₀ MPN or copies per 100ml water.

Dilution (Cao et al. 2015, Cao et al. 2012) and competitive IAC (Green et al. 2014) were used to check for inhibition. Selected samples were analyzed undiluted and 10-fold diluted. For qPCR, if C_q difference between undiluted and 10-fold diluted was less than 2.32 cycles, then inhibition was suspected. For ddPCR, if concentration measured from diluted samples was higher than that from undiluted samples, then inhibition was suspected. No inhibition was indicated.

Table 1. List of all standards or positive controls used in qPCR and ddPCR analyses.

Assay	Forward	Reverse	Probe	ddPCR/qPCR	Reference
GenBac3	GGGGTTCTGA GAGGAAGGT	CCGTCATCCTT CACGCTACT	FAM- CAATATTCCTCACTGCTGCCT CCCGTA-BHQ1	Both	12
HF183	ATCATGAGTTC ACATGTCCG	CTTCCTCTCAG AACCCCTATCC	FAM- CTAATGGAACGCATCCC- MGB	dPCR duplex with Ent	10
Entero	GAGAAATCCA AACGAACTTG	CAGTGCTCTAC CTCCATCATT	FAM-TGGTTCTCT CCGAAATAGCTT TAGGGCTA-BHQ1	dPCR duplex with HF183	13
E. coli	CAACGAACTGA ACTGGCAGA	CATTACGCTGC GATGGAT	FAM- CCCGCCGGAATGGTGATTA C-BHQ1	dPCR (duplex with CowM2)	{Chern, 2009 #356}
HumM2	CGTCAGGTTTG TTTCGGTATTG	TCATCACGTAA CTTATTTATATG CATTAGC	FAM- TATCGAAAATCTCACGGATTA ACTCTTGTGTACGC-BHQ1	qPCR (other labs besides SCCWRP)	EPA Method
BacHum	TGAGTTCACAT GTCCGCATGA	CGTTACCCCGC CTACTATCTAA TG	FAM- TCCGGTAGACGATGGGGATG CGTT-TAMRA	qPCR (other labs besides SCCWRP)	Kildare et al 2007
CowM2	CGGCCAAATAC TCCTGATCGT	GCTTGTTGCGT TCCTTGAGATA AT	Hex- AGGCACCTATGTCCTTTACC TCATCAACTACAGACA-BHQ1	dPCR	EPA Method
Lee Seagull	AGGTGCTAATA CCGCATAATAC AGAG	GCCGTTACCTC ACCGTCTA	FAM- TTCTCTGTTGAAAGGCGCTT- MGB	Both	Lee et al 2013
Adenovir us	GGA CGC CTC GGA GTA CCT GAG	ACI GTG GGG TTT CTG AAC TTG TT	FAM- CTGGTGCAGTTCGCCCGTGC CA-BHQ	dPCR	Cao, in prep
Noroviru s GII	ATGTTCAAGRTG GATGAGRITCT CWGA	TCGACGCCATC TTCATTCACA	FAM- AGCACGTGGGAGGGCGATC G-BHQ1	RTPCR	Loisy et al 2005

Salmonella (TTR)	CTCACCAGGA GATTACAACAT GG	AGCTCAGACCA AAAGTGACCAT C	FAM- CACCGACGGCGAGACCGAC TTT-BHQ1	Both (dPCR duplex with invA)	Malorney et al 2004
Salmonella (invA)	CAACGTTTCCT GCGGTACTGT	CCCGAACGTG GCGATAATT	Hex- CTCTTTTCGTCTGGCATTATCG ATCAGTACCA-BHQ1	Both (dPCR duplex with TTR)	Rahn et al 1992
Campylobacter	CACGTGCTACA ATGGCA TAT	GGCTTCATGCT CTCGAGTT	FAM- CAGAGAACAATCCGAACTGG GACA-BHQ1	Both	Lund et al 2004

Table 2. Thermal cycling conditions used in qPCR and ddPCR analysis.

Assay	RT	Pre-denaturation Temp, Time	Denaturation Temp, Time	Anneal Temp, Time	Cycle number	Extension Temp, Time	Technology (Platform)
Adenovirus	NA	95, 10min	94, 30s	55, 1min	45	98, 10min	dPCR (QX100)
GenBac3, HF183, Enterococcus, E. coli, CowM2	NA	95, 10min	94, 30s	60, 1min	40	98, 10min	dPCR (QX100)
Campylobacter, Salmonella (ttr, invA), LeeSeagull	NA	95, 10min	94, 30s	60, 1min	45	98, 10min	dPCR (QX100)
GenBac3, HumM2, BacHum,	NA	95, 10min	95, 15s	60, 1min	40	NA	qPCR (CFX96 or StepOnePlus)
Norovirus GII	50, 30min	95, 10min	95, 15s	60, 1min	45	NA	RT-PCR (StepOnePlus)
LeeSeagull	NA	95, 10min	95, 15s	60, 1min	45	NA	qPCR (CFX96)

Decay modeling

The GinaFit modeling add-in for EXCEL (Geeraerd et al. 2005) was used to compare six common models (LL, LL+Sh, LL+Tail, LL+Sh+Tail, Biphasic, Biphasic+Sh) and select the best fitting model to determine decay parameters. Best-fit model was selected based on low root mean sum of squared error (RMSE) and absence of parameter redundancy as suggested (Geeraerd et al. 2005). Parameter redundancy is indicated by non-significant parameter estimates for extra parameters in more complex models compared to the simpler ones. As simulation indicated that different models could lead to drastically different k_{max} estimates on the same data, the same model was selected for all analytes to facilitate comparison among analytes if the said model provided only a slightly inferior fitting (based on RMSE) than an alternative model.

All non-detect or data above the quantification limits were excluded from model fitting. Data below the LLOQ were also excluded from model fitting, unless doing so resulted in, on rare occasions, less than a minimum number of time points (e.g. three) needed for model fitting. For analytes where an increase (“growth”) in concentration was observed prior to decay or after concentrations reached minimum, these “growth” data points were excluded from model fitting as well. For each assay, laboratory technical replicates but not field replicates (i.e. two dialysis bags) were averaged, providing two data points per day for model fitting.

Results

Sewage field studies

Majority of the decay curves (32 out of 35) were modeled with LL model, except for three assays during: TC and EC by Colilert-18 both used LL+Tail model while Enterolert used LL+Shoulder+Tail (Table 3).

Comparing across assays, i.e. focus on relative degradation, showed general trends (Figure 1A). Generally, the human markers (3 markers, HF183 measured by both qPCR and ddPCR) had higher decay rates than FIB and pathogens. However, in the winter, human markers had much lower decay rates than in the summer. Human markers had similar decay rates to campylobacter, to GenBac3.q in the winter. Decay rates among the Bacteroidales human markers were mostly similar to each other.

Decay rates of total Bacteroidales FIB marker were generally lower than that of the human Bacteriales markers. GenBac3 markers were also quite abundant in ambient waters, so it was not unexpected the ambient members would decay slower than the human fecal Bacteroidales. For example, for Summer.Shade and Winter, GenBac3.q had significantly smaller decay rates than human markers by qPCR; For Summer.Sun, GenBac3.q decayed at a slower rate than HF183.q and BacHum.q.

PCR-based measurement of organism generally decayed slower than culture-based measurement, although low quality IDEXX measurement in summer experiment was a confounding factor.

Enterolert, as well as E.coli.d, appeared to be conservative markers, exhibiting generally lower (or similar) decay rates than the MST and pathogen groups. Culturable FIB decayed much faster than genetic FIB markers, MST markers and pathogens during the winter.

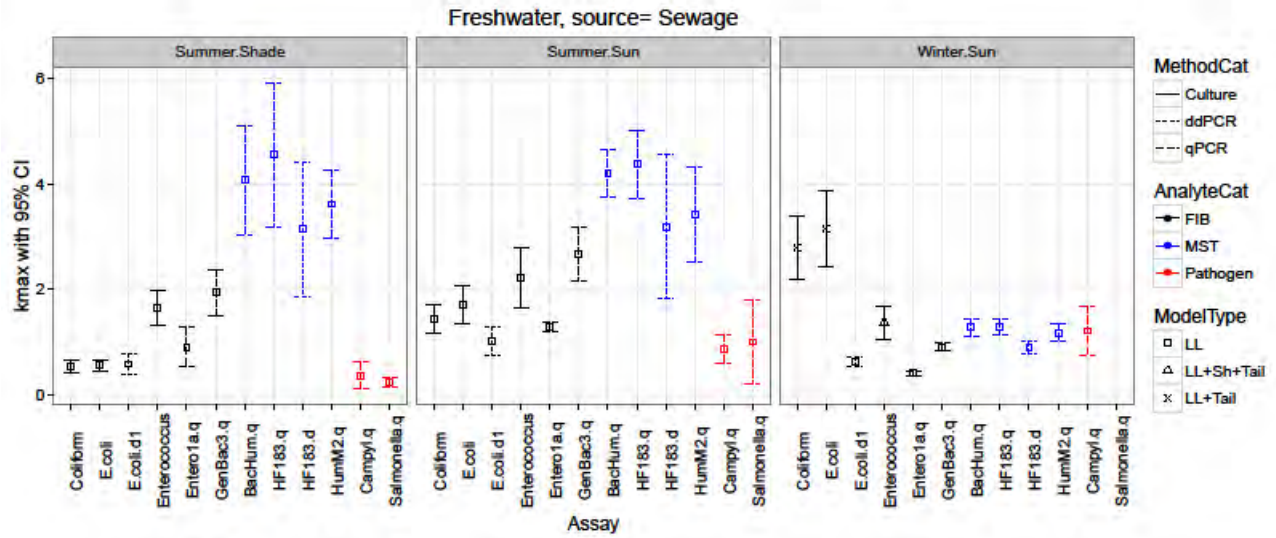
Comparing among the experiments (Figure 1B), a majority of the assays showed the lowest decay rates in winter, although campyl.q did not show a significant difference among the three experiments. Decay rates were generally not significantly different between shade vs. sun treatment in summer, for all human markers, GenBac3.q, Enterolert, E.coli.d, and Enterolert.

Table 3. Decay modeling results for sewage field studies. Three experiments, shade (summer with shading), sun (summer no shading), and winter, were conducted. Assays with suffixes .q and .d indicate measurement by qPCR and digital PCR, respectively, while assays without suffixes were measured by IDEXX. Days indicate time points available for model fitting. IgN0, kmax, SI, IgNres denote model predicted Ig10 initial concentration (log MPN or copies per 100ml), decay rate (day⁻¹), shoulder length (day), Ig10 residual concentration (log MPN or copies per 100ml, applicable to LL+Tail models only). “SE” denotes standard error of the estimated parameter.

Experi	Analyte Category	Assay	Days	Model	RMSE	Adjust R2	IgN0	IgN0.SE	kmax	kmax.SE	SI	SI.SE	IgNres	IgNres.SE	
Shade	FIB	GenBac3.q	0-5	LL	0.5	0.88	7.72	0.31	1.93	0.24					
		Coliform	1-10	LL	0.34	0.8	6.96	0.17	0.53	0.06					
		E.coli	1-10	LL	0.34	0.81	6.36	0.16	0.55	0.06					
		E.coli.d	1-10	LL	0.61	0.58	6.03	0.30	0.57	0.11					
		Enterococcus	0-5	LL	0.42	0.89	4.60	0.25	1.65	0.18					
		Entero1a.q	0-5	LL	0.42	0.67	6.58	0.26	0.90	0.21					
	MST	HF183.d	0-2	LL	0.51	0.82	5.57	0.43	3.14	0.71					
		BacHum.q	0-2	LL	0.42	0.92	6.77	0.35	4.07	0.57					
		HF183.q	0-2	LL	0.55	0.9	6.62	0.47	4.55	0.76					
		HumM2.q	0-2	LL	0.26	0.96	5.57	0.22	3.61	0.36					
	Pathogen	Campyl.q	0-7	LL	0.51	0.28	3.26	0.26	0.36	0.14					
		Salmonella.q	0-10	LL	0.26	0.55	3.43	0.12	0.22	0.05					
	Sun	FIB	GenBac3.q	0-4	LL	0.42	0.93	8.21	0.29	2.67	0.28				
			Coliform	1-7	LL	0.49	0.87	7.57	0.29	1.43	0.15				
E.coli			1-7	LL	0.64	0.85	6.75	0.39	1.71	0.20					
E.coli.d			1-7	LL	0.56	0.78	6.23	0.32	1.01	0.15					
Enterococcus			0-4	LL	0.51	0.89	4.71	0.33	2.21	0.31					

		Entero1a.q	0-4	LL	0.08	0.99	6.91	0.05	1.29	0.05				
MST		HF183.d	0-2	LL	0.55	0.81	5.69	0.46	3.19	0.75				
		BacHum.q	0-2	LL	0.18	0.99	6.92	0.16	4.20	0.25				
		HF183.q	0-2	LL	0.26	0.97	6.72	0.22	4.37	0.36				
		HumM2.q	0-2	LL	0.31	0.94	5.68	0.26	3.42	0.50				
Pathogen		Campyl.q	0-5	LL	0.34	0.76	3.98	0.20	0.86	0.15				
		Salmonella.q	1-3	LL	0.39	0.44	4.20	0.42	0.99	0.45				
Winter	FIB	GenBac3.q	0-10	LL	0.25	0.96	8.39	0.11	0.90	0.04				
		Coliform	2-10	LL+Tail	0.2021	0.95	10.05	0.39	2.79	0.33	5.16	0.06		
		E.coli	2-10	LL+Tail	0.2572	0.94	9.58	0.48	3.15	0.39	3.97	0.08		
		E.coli.d	0-10	LL	0.33	0.86	5.80	0.14	0.61	0.05				
		Enterococcus	0-10	LL+Sh+Tail	0.18	0.97	4.32	0.13	1.35	0.17	1.83	0.54	1.47	0.09
		Entero1a.q	0-10	LL	0.11	0.96	6.48	0.05	0.40	0.02				
MST		HF183.d	0-10	LL	0.39	0.9	6.15	0.17	0.88	0.06				
		BacHum.q	0-6	LL	0.28	0.94	7.07	0.15	1.27	0.10				
		HF183.q	0-6	LL	0.24	0.95	6.82	0.13	1.27	0.08				
		HumM2.q	0-6	LL	0.28	0.93	6.14	0.15	1.17	0.10				
Pathogen		Campyl.q	0-4	LL	0.44	0.73	4.91	0.29	1.21	0.26				

(A)



(B)

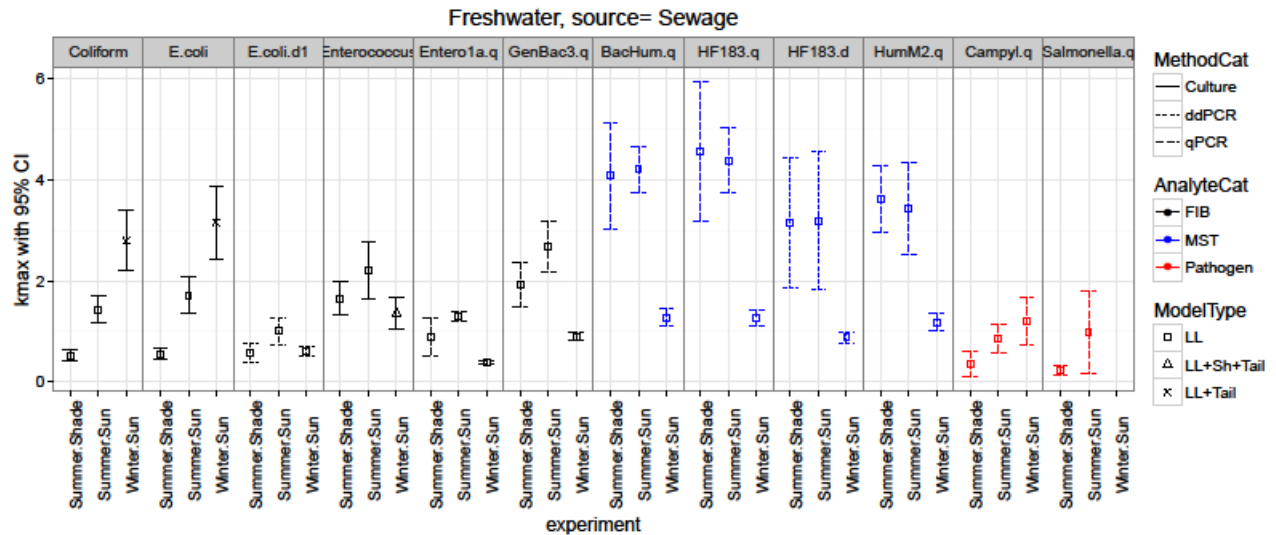


Figure 1. Freshwater water field studies with sewage: Modeled decay rates for FIB (black), MST markers (blue), and pathogens (red) during two seasons. During the summer, a light vs. shade contrast was examined by applying a shade cloth over half of the dialysis bags, while no shade cloth was applied during winter, resulting in three experiments: Summer.Shade, Summer.Sun, and Winter.Sun. Panel A contrasts the assays within each experiment while panel B contrasts the experiments for each assay. Assays with suffixes .q and .d indicate measurement by qPCR and digital PCR, respectively. Assays without suffixes were measured by IDEXX. Error bars represent the 95% confidence interval of decay rates (day⁻¹).

Cow fecal field studies

More than half of the decay curves (20 out of 33) were modeled with LL model (Table 4). Also note that CowM2 marker decay only had limited time points available for modeling in summer (up to day 2 and day 3 for Summer.Sun and Summer.Shade, but all 10 days for Winter). Campyl also remained detectable for the entire 10 days (all available for model fitting) except for Summer.Sun where only up to day 4 results were available for modeling.

Comparing across assays, i.e. focus on relative degradation, there was some general trends (Figure 2A). CowM2 to FIB and pathogen comparison were variable among experiments. This MST marker generally decayed faster than pathogens (Campylobacter measured by qPCR and ddPCR) in Summer.Sun, similar in Summer.Shade, and even slower than pathogens in Winter. CowM2 k rates were significantly higher than E.coli.d, Enterolert (by LL+Tail model), but similar to that of Campyl, for Summer.Shade. CowM2 k rates were significantly higher than Campyl, GenBac.d (but not Genbac.q), Ecoli.d, and Enterolert for Summer.Sun. In winter, there was a little trend reverse: CowM2 had lower k rates than GenBac.d (though CowM2>Genbac3.q), Enterolert, Campyl (both .q and .d). But all winter rates were < 1 day (Yamahara et al. 2012) to begin with.

In most cases, MST Bacteroidales had similar decay rates to that of total Bacteroidales across experiments. This was different from the general trend with sewage where GenBac3 had lower k than human markers.

Whether Enterolert was a conservative marker or not differed among experiments: Enterolert k rates were significantly lower, similar, and higher than Campyl and CowM2 for Summer.Shade, Summer.Sun, and Winter, respectively.

E.coli measured by ddPCR appeared to be a conservative marker across experiments, as it showed significantly lower (Summer.Shade) or similar (Summer.Sun, Winter) decay rates than Campyl and CowM2.

Culturable Enterococcus might be a reasonable conservative indicator for Cow fecal contamination. Enterolert k rates were lower than CowM2 marker, but not significantly different from Campyl (.q and .d) in the summer. In the winter, there were similar k rates among Enterolert, CowM2, and Campyl (both .q and .d).

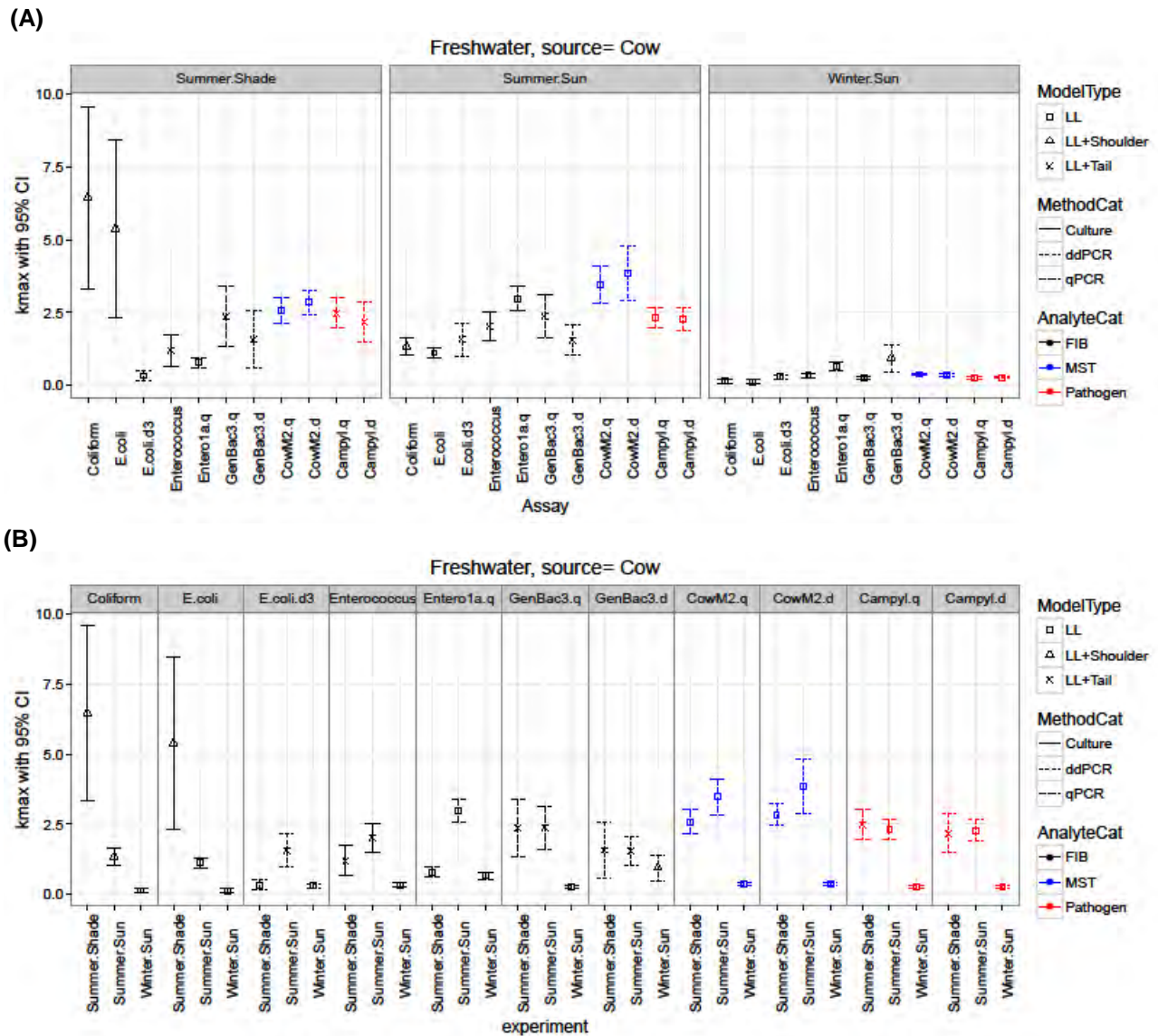
Comparing among the experiments (Figure 2B), nearly all assays showed lowest decay rates in winter, with only the exception of GenBac3.d (unlike GenBac3.q). This could be an artifact resulting from comparing decay rates between different models, as GenBac3.d was modeled by LL+Shoulder in winter vs. LL+Tail in summer. Unlike in sewage experiments (campyl showed similar k rates among three experiments), campyl.q and campyl.d showed significant lower decay rates in winter than in summer.

Decay rates were generally not significantly different between shade vs. sun treatment in summer for nearly all assays: CowM2.q, CowM2.d, Campyl.q, Campyl.d, GenBac3.q, GenBac3.d, and Enterolert. The exception was for E.coli.d and Enterolert, where their decay rates were higher without shading than with shading during the summer.

Table 4. Decay modeling results for cow fecal field studies. Three experiments, shade (summer with shading), sun (summer no shading), and winter, were conducted. Assays with suffixes .q and .d indicate measurement by qPCR and digital PCR, respectively, while assays without suffixes were measured by IDEXX. Days indicate time points available for model fitting. IgN0, kmax, SI, IgNes denote model predicted Ig10 initial concentration (log MPN or copies per 100ml), decay rate (day⁻¹), shoulder length (day), Ig10 residual concentration (log MPN or copies per 100ml, applicable to LL+Tail models only). “SE” denotes standard error of the estimated parameter.

Experi	Analyte Category	Assay	Days	Model	RMSE	Adjust R2	IgN0	IgN0.SE	kmax	kmax.SE	SI	SI.SE	IgNres	IgNres.SE
Shade	FIB	GenBac3.q	1-7	LL+Tail	0.29	0.84	8.91	0.41	2.36	0.58			6.08	0.10
Shade	FIB	GenBac3.d	1-7	LL+Tail	0.29	0.71	8.40	0.39	1.57	0.54			6.46	0.12
Shade	FIB	Coliform	0-10	LL+Sh	0.38	0.76	7.68	0.11	6.46	1.73	8.05	0.23		
Shade	FIB	E.coli	2-9	LL+Sh	0.36	0.69	7.59	0.11	5.38	1.70	8.06	0.27		
Shade	FIB	E.coli.d	1-7	LL	0.34	0.40	6.16	0.21	0.33	0.11				
Shade	FIB	Enterococcus	1-2, 4-9	LL+Tail	0.34	0.80	6.02	0.31	1.20	0.30			3.64	0.14
Shade	FIB	Enter1a.q	1-7	LL	0.31	0.84	5.27	0.19	0.78	0.10				
Shade	MST	CowM2.q	0-3	LL	0.28	0.95	5.45	0.21	2.59	0.24				
Shade	MST	CowM2.d	0-3	LL	0.26	0.96	6.16	0.19	2.85	0.22				
Shade	Pathogen	Campyl.q	0-10	LL+Tail	0.31	0.93	6.73	0.23	2.49	0.29			3.02	0.09
Shade	Pathogen	Campyl.d	0-10	LL+Tail	0.40	0.85	6.24	0.30	2.17	0.38			3.07	0.11
Sun	FIB	GenBac3.q	1-10	LL+Tail	0.40	0.86	8.75	0.40	2.38	0.42			4.77	0.12
Sun	FIB	GenBac3.d	1-10	LL+Tail	0.40	0.84	8.22	0.34	1.55	0.29			4.95	0.13
Sun	FIB	Coliform	2-10	LL+Sh	0.36	0.91	8.09	0.19	1.34	0.16	4.51	0.68		
Sun	FIB	E.coli	2-10	LL	0.52	0.86	9.44	0.31	1.12	0.11				
Sun	FIB	E.coli.d	1-10	LL+Tail	0.34	0.82	7.89	0.32	1.57	0.32			5.07	0.11

Sun	FIB	Enterococcus	1-10	LL+Tail	0.37	0.91	5.80	0.32	2.03	0.28		1.62	0.12
Sun	FIB	Entero1a.q	1-3	LL	0.21	0.97	6.84	0.22	2.98	0.24			
Sun	MST	CowM2.q	0-2	LL	0.26	0.96	5.48	0.22	3.48	0.36			
Sun	MST	CowM2.d	0-2	LL	0.38	0.93	6.20	0.32	3.86	0.53			
Sun	Pathogen	Campyl.q	0-4	LL	0.46	0.93	6.67	0.27	2.33	0.20			
Sun	Pathogen	Campyl.d	0-4	LL	0.48	0.92	6.72	0.29	2.27	0.21			
Winter	FIB	GenBac3.q	0-10	LL	0.14	0.88	8.42	0.06	0.27	0.02			
Winter	FIB	GenBac3.d	0-10	LL+Sh	0.08	0.83	7.79	0.03	0.94	0.26	9.25	0.28	
Winter	FIB	Coliform	3-10	LL	0.15	0.45	8.19	0.12	0.14	0.04			
Winter	FIB	E.coli	3-10	LL	0.16	0.40	8.16	0.12	0.13	0.04			
Winter	FIB	E.coli.d	1-10	LL	0.23	0.73	6.68	0.11	0.29	0.04			
Winter	FIB	Enterococcus	1-2, 4-10	LL	0.21	0.81	4.26	0.12	0.34	0.04			
Winter	FIB	Entero1a.q	1-5	LL	0.13	0.90	4.35	0.10	0.65	0.08			
Winter	MST	CowM2.q	0-10	LL	0.15	0.92	4.31	0.07	0.38	0.03			
Winter	MST	CowM2.d	0-10	LL	0.13	0.93	5.24	0.06	0.36	0.02			
Winter	Pathogen	Campyl.q	0-10	LL	0.20	0.76	3.81	0.09	0.25	0.03			
Winter	Pathogen	Campyl.d	0-10	LL	0.14	0.88	3.75	0.06	0.27	0.02			



Gull fecal field studies

More than half of the decay curves (22 out of 30) were modeled with LL model (Table 5). LL+Tail was used for Enterolert, LeeSeagull.q, LeeSeagull.d, Campyl.d, Campy.q in Summer.Shade, and LeeSeagull.q, LeeSeagull.d in Summer.Sun. LL+shoulder was used for E.coli.d in Summer.Shade.

Comparing across assays, i.e. focus on relative degradation, there were some general trends (Figure 3A). Catellococcus gull marker (qPCR and ddPCR provided nearly identical measurements) had similar decay rates to that of Campyl regardless experiment (season, sunlight). This gull MST marker k rates (<2 /day in summer, <1 /day in winter) were also generally much lower than Bacteroidales MST marker k rates (e.g. cow and human). Additionally, Catellococcus gull marker also had k rates more close to Enterol.a.q than the Bacteroidales MST markers for cow and human fecal material.

PCR-based measurement of organism generally decayed slower than culture-based measurement, although low quality IDEXX measurement in summer experiment was a confounding factor. Enterol.a.q appeared to be a conservative indicator, as its k rates were either similar to or lower than that of Campyl. E.coli.d appeared to be a conservative indicator, as its k rates were lower than both the gull MST marker and Campyl.

Comparing among the experiments, nearly all assays showed lowest decay rates in winter (Figure 3B). The only except was FIB by IDEXX where winter had k rates similar to that from summer. This likely a lab artifact given IDEXX data was of low quality during summer.

Additionally, generally no significant difference observed for shade vs. sun in summer for nearly assays (LeaSeagull.q and .d, Campyl.q and .d, GenBac3.q, E.coli.d). The only exception was Enterol.a.q which had higher k rates for Sun compared to shade.

Table 5. Decay modeling results for gull fecal field studies. Three experiments, shade (summer with shading), sun (summer no shading), and winter, were conducted. Assays with suffixes .q and .d indicate measurement by qPCR and digital PCR, respectively, while assays without suffixes were measured by IDEXX. Days indicate time points available for model fitting. IgN0, kmax, SI, IgNes denote model predicted Ig10 initial concentration (log MPN or copies per 100ml), decay rate (day⁻¹), shoulder length (day), Ig10 residual concentration (log MPN or copies per 100ml, applicable to LL+Tail models only). “SE” denotes standard error of the estimated parameter.

Experi	Analyte Category	Assay	Days	Model	RMS E	Adjust R2	IgN0	IgN0. SE	kmax	kmax.SE	SI	SI.S E	IgNres	IgNres.S E
Shade	FIB	GenBac3.q	1-3	LL	0.36	0.91	6.09	0.39	3.01	0.41				
Shade	FIB	Coliform	2-3, 5-9	LL	0.18	0.60	7.16	0.12	0.21	0.05				
Shade	FIB	E.coli	2-3, 5-9	LL	0.13	0.68	6.89	0.09	0.18	0.03				
Shade	FIB	E.coli.d	1-10 ^a	LL+Sh	0.10	0.89	7.02	0.06	0.47	0.09	5.95	0.87		
Shade	FIB	Enterol1a.q	1-9	LL	0.33	0.90	5.83	0.17	0.83	0.07				
Shade	FIB	Enterococcus	1-3, 5-9	LL+Tail	0.48	0.89	5.59	0.35	1.57	0.26			1.44	0.24
Shade	MST	LeeSeagull.q	0-10	LL+Tail	0.38	0.93	7.03	0.22	1.55	0.16			2.94	0.14
Shade	MST	LeeSeagull.d	0-10	LL+Tail	0.33	0.95	7.17	0.19	1.48	0.13			3.09	0.13
Shade	Pathogen	Campyl.d	0-6	LL+Tail	0.33	0.87	5.02	0.24	1.56	0.31			2.48	0.21
Shade	Pathogen	Campy.q	0-6	LL+Tail	0.31	0.92	5.44	0.24	2.15	0.32			2.38	0.14
Sun	FIB	GenBac3.q	1-3	LL	0.17	0.95	4.83	0.20	2.04	0.24				
Sun	FIB	Coliform	2-3, 5-10 ^b	LL	0.36	0.86	7.60	0.23	0.76	0.08				
Sun	FIB	E.coli	2-3, 5-10 ^b	LL	0.55	0.83	7.59	0.36	1.05	0.12				
Sun	FIB	E.coli.d	1-10	LL	0.27	0.87	7.42	0.13	0.54	0.05				

Sun	FIB	Entero1a.q	1-5	LL	0.09	0.99	6.24	0.07	1.63	0.05		
Sun	MST	LeeSeagull.q	0-10	LL+Tai I	0.28	0.97	7.17	0.15	1.50	0.09	2.53	0.13
Sun	MST	LeeSeagull.d	0-10	LL+Tai I	0.27	0.97	7.28	0.15	1.44	0.09	2.87	0.14
Sun	Pathogen	Campyl.d	0-3	LL	0.27	0.91	4.92	0.20	1.87	0.23		
Sun	Pathogen	Campy.q	0-3	LL	0.26	0.96	5.43	0.19	2.63	0.22		
Winter	FIB	GenBac3.q	0-3	LL	0.17	0.76	4.68	0.13	0.63	0.17		
Winter	FIB	GenBac3.d	0-10	LL	0.43	-0.05	4.86	0.19	-0.02	0.07		
Winter	FIB	Coliform	3-8	LL	0.39	0.70	8.22	0.38	0.79	0.15		
Winter	FIB	E.coli	2-8	LL	0.41	0.87	7.78	0.29	1.15	0.13		
Winter	FIB	E.coli.d	0-10	LL	0.22	0.34	5.62	0.10	0.12	0.04		
Winter	FIB	Entero1a.q	1-10	LL	0.23	0.82	5.38	0.11	0.39	0.04		
Winter	FIB	Enterolert	2, 4-9	LL	0.52	0.88	7.20	0.39	1.37	0.14		
Winter	MST	LeeSeagull.q	0-9	LL	0.38	0.87	7.46	0.18	0.84	0.08		
Winter	MST	LeeSeagull.d	0-9	LL	0.39	0.85	7.08	0.18	0.75	0.07		
Winter	Pathogen	Campyl.d	0-9	LL	0.32	0.91	6.08	0.14	0.80	0.06		
Winter	Pathogen	Campy.q	0-9	LL	0.30	0.93	6.37	0.14	0.88	0.06		

^a(remove d3R1, d8R1)

^b(d1>uloq) removed

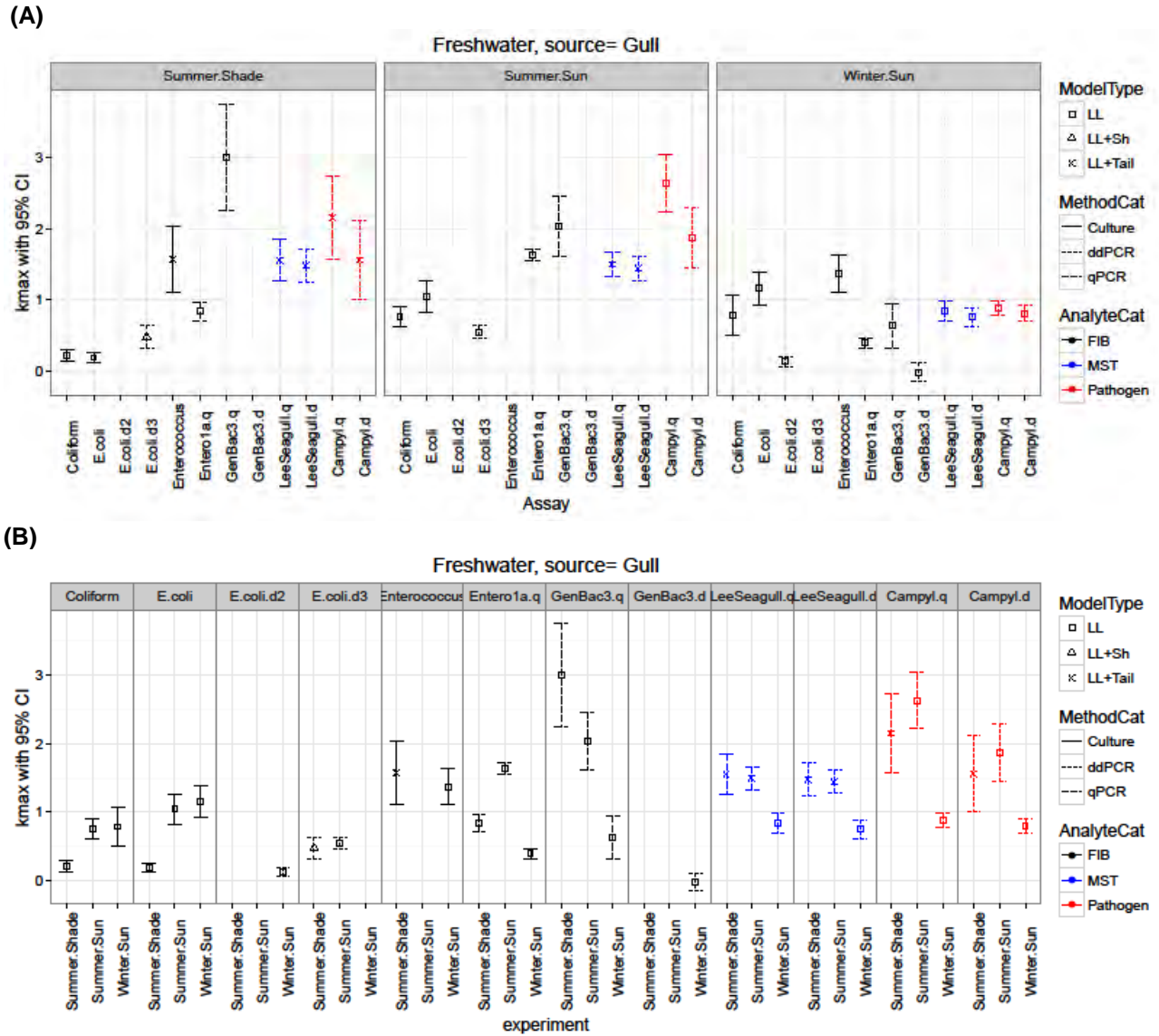


Figure 3. Freshwater water field studies with gull feces: Modeled decay rates for FIB (black), MST markers (blue), and pathogens (red) during two seasons. During the summer, a light vs. shade contrast was examined by applying a shade cloth over half of the dialysis bags, while no shade cloth was applied during winter, resulting in three experiments: Summer.Shade, Summer.Sun, and Winter.Sun. Panel A contrasts the assays within each experiment while panel B contrasts the experiments for each assay. Assay with suffixes .q and .d indicate measurement by qPCR and digital PCR, respectively. Error bars represent the 95% confidence interval of decay rates (day^{-1}).

Literature Cited

- Cao, Y., M.R. Raith, J.F. Griffith. Droplet digital PCR for simultaneous quantification of general and human-associated fecal indicators for water quality assessment. *Water Res.* 2015, 70, 337-49.
- Cao, Y., M.R. Raith, J.F. Griffith. A duplex digital PCR assay for simultaneous quantification of the *Enterococcus* spp. and the human fecal-associated HF183 marker in waters. *Journal of Visualized Experiment* 2016, e53611, doi:10.3791/53611.
- Cao, Y., J.F. Griffith, S. Dorevitch, S.B. Weisberg. Effectiveness of qPCR permutations, internal controls and dilution as means for minimizing the impact of inhibition while measuring *Enterococcus* in environmental waters. *J. Appl. Microbiol.* 2012, 113, 66-75.
- Ebentier, D.L., K.T. Hanley, Y. Cao, B. Badgley, A. Boehm, J. Ervin, K.D. Goodwin, M. Gourmelon, J. Griffith, P. Holden, C.A. Kelty, S. Lozach, C. McGee, L. Peed, M. Raith, M.J. Sadowsky, E. Scott, J. Santodomingo, C. Sinigalliano, O.C. Shanks, L.C.V.D. Werfhorst, D. Wang, S. Wuertz, J. Jay. Evaluation of the repeatability and reproducibility of a suite of PCR-based microbial source tracking methods. *Water Res.* 2013, In press.
- Geeraerd, A.H., V.P. Valdramidis, J.F. Van Impe. GlnaFiT, a freeware tool to assess non-log-linear microbial survivor curves. *Int. J. Food Microbiol.* 2005, 110, 297-297.
- Green, H.C., R.A. Haugland, M. Varma, H.T. Millen, M.A. Borchardt, K.G. Field, W.A. Walters, R. Knight, M. Sivaganesan, C.A. Kelty, O.C. Shanks. Improved HF183 quantitative real-time PCR assay for characterization of human fecal pollution in ambient surface water samples. *Appl. Environ. Microbiol.* 2014, 80, 3086-94.
- Khan, I.U. and T.A. Edge. Development of a novel triplex PCR assay for the detection and differentiation of thermophilic species of *Campylobacter* using 16S-23S rDNA internal transcribed spacer (ITS) region. *J. Appl. Microbiol.* 2007, 103, 2561-9.
- Linton, D., R.J. Owen, J. Stanley. Rapid identification by PCR of the genus *Campylobacter* and of five *Campylobacter* species enteropathogenic for man and animals. *Res. Microbiol.* 1996, 147, 707-718.
- Mattioli, M. C., A.B. Boehm, J. Davis, A.R. Harris, M. Mrisho, A.J. Pickering. Enteric pathogens in stored drinking water and on caregiver's hands in Tanzanian households with and without reported cases of child diarrhea. *PloS one* 2014, 9, e84939.
- USEPA, Method B: Bacteroidales in water by TaqMan® quantitative polymerase chain reaction (qPCR) assay. EPA-822-R-10-003. Office of Water: Washington, DC, 2010.
- USEPA "Method 1611: Enterococci in Water by TaqMan® Quantitative Polymerase Chain Reaction (qPCR) Assay. EPA-821-R-12-008," Office of Water, 2012. Viau, E.J., D. Lee, A.B. Boehm. Swimmer risk of gastrointestinal illness from exposure to tropical coastal waters impacted by terrestrial dry-weather runoff. *Environmental Science and Technology* **2011**, 45, 7158-65.
- Yamahara, K.M., L.M. Sassoubre, K.D. Goodwin, A.B. Boehm. Occurrence and persistence of bacterial pathogens and indicator organisms in beach sand along the California coast. *Appl. Environ. Microbiol.* **2012**, 78, 1733-45.

APPENDIX D: COMMUNITY ANALYSIS OF FECAL MATERIAL DEGRADATION IN MARINE, BRACKISH AND FRESH WATERS

(Field Site: Pillar Point Harbor, Arroyo Burro Lagoon, San Joaquin Marsh)

Introduction

The fields of DNA sequencing and bioinformatics have made tremendous advancements in the last few years, and now enable quantitative tracking of nearly all microorganisms that occur in environmental samples. This part of the project uses two different high-throughput DNA analyses, 16S rRNA Illumina sequencing and PhyloChip microarray, in order to:

1. Study the composition and decay of fecal microbial communities in response to the following conditions: type of fecal material (human sewage, bird feces, and cattle feces), types of receiving waters (freshwater streams, lagoon, ocean), seasons (summer and winter), and light exposure (sun exposed and shaded).
2. Compare the performance of FIB, MST, and pathogen tests used for water quality monitoring.
3. Identifying subsets of the microbial community that correlate with FIB, MST, and pathogen tests, and determining the persistence patterns of different microbial taxa.

Material and Methods

Illumina sequencing

In total, 271 samples were sequenced: 202 samples from the field experiments, 60 samples from the water matrix effect microcosm experiments, and 9 samples from the sediment microcosm experiments. The barcoded library preparation followed the protocol described previously (Caporaso et al. 2012), with some modifications. The amplification, done in triplicate, was tested and optimized for our samples, with the template amount normalized. The samples were pair-end sequenced by MySeq sequencing system from Illumina at the Vincent J. Coates Genomics Sequencing Laboratory at UC Berkeley. The obtained no-demultiplexed sequences were quality filtered, demultiplexed, pair-end joined, identified, and rarefied using QIIME. For the taxonomic identification of the OTUs, the Greengenes 16S rRNA gene database was referenced for closed-reference OTU picking.

PhyloChip array

In total, 176 samples were selected for PhyloChip array analysis: 104 samples from the field experiments, 48 samples from the water matrix effect microcosm experiments, and 6 samples from the sediment microcosm experiments. The samples were processed following the protocol described elsewhere (Hazen et al. 2010). The 16S rRNA amplification was tested and optimized for our samples. After running the chips, the taxonomic identification of the OTUs was assessed using the Greengenes database as reference.

Statistical analysis

In order to study the effects of the experimental treatments over the decay of the microbial community, the relative abundance and the binary data obtained by Illumina sequencing and PhyloChip array analyses were input in software PRIMER v7. Non-Multidimensional Scaling (nMDS) and CLUSTER analysis were used to compare the relative similarities between the type of experiment, samples, and their aging over time. The ANOSIM analysis was used to test for significant differences in microbial community structure among the different experimental treatments and time points.

SourceTracker software (Knights et al. 2011) was used to track the decay of the whole microbial community in each experiment. For this analysis, the binary data showed to be more sensitive tracking the

fecal contamination signal than the relative abundance data. The commonly present and absent OTUs were filtered out in both of the sources (raw water and raw fecal material) for each experiment.

In order to compare the decay of the fecal contamination signal detected by the different methodologies (FIB, MST, and pathogens test, Illumina sequencing, and PhyloChip analyses), the OTUs were down-selected from the high-throughput DNA analyses data related to each subset of microorganisms targeted with FIB, MST, and pathogens tests. For each experiment, the water and fecal material mix in day 0 was assigned a signal of 100%, and the signal for the following days was expressed as the percentage of that first sample.

Results

Effect of environmental conditions over the microbial community:

All the nMDS plots shown in Figure 1 represent the presence/absence data, but similar results were obtained analyzing the relative abundance of OTUs (data not shown). There was a clear evolution over the time of the microbial communities from the raw fecal material to the raw and control water samples of each experiment (Figure 1, y axes), reflecting the decay of the fecal contamination.

The initial mixture (day 0) contained 5% of fecal material calculated by volume. Normalizing the amount of fecal material added by ng of DNA, these proportions correlate with the distance between the mix in day 0 and the fecal source sample. For example, in the experiments with creek water seeded with gull slurry, both mixes (summer and winter) in day 0 contained less than 1% of gull slurry after normalizing by ng of DNA, and their microbial community compositions were dissimilar to the raw gull slurry in the nMDS (Figure 1A). In contrast, the creek water mixes with cow slurry contained around 5% of the raw slurry DNA and were similar to raw cow slurry samples.

The water controls bags sampled in day 7 and 10 grouped closer with the samples seeded with fecal material at the last days of each experiment instead of grouping with the raw water sampled in day 0 (nMDS and CLUSTER analysis). There is an effect caused by the dialysis bag that could be related with the light or nutrients able to pass through the membrane, or even the temperature reached inside the bag. More analyses are required to clarify this effect.

The salinity of the water matrix had the strongest influence on overall microbial community composition, over season or light exposure factors. Figure 1A includes all the samples from the field experiments analyzed by Illumina sequencing. There was a clear salinity gradient from the ocean samples (33.2 ± 0.5 ppt) to the creek water (1.41 ± 3.6 ppt). This trend was also apparent for the PhyloChip array analyses (Figure 1B), and for the water matrix microcosms experiment (Figure 1C). The lagoon water was the only matrix that presented significant differences in salinity between seasons (winter with 19.6 ± 6.5 ppt, summer with 10.2 ± 2.5 ppt) due to the differential influence from the ocean water, considerably affecting the microbial community patterns (Figure 1A). In the ocean and creek water samples, season also significantly affected the microbial community (ANOSIM: $R=0.63$, $p=0.001$), while the light exposure did not affect the microbial community (Figure 1A) (ANOSIM: $R=0.11$, $p=0.001$).

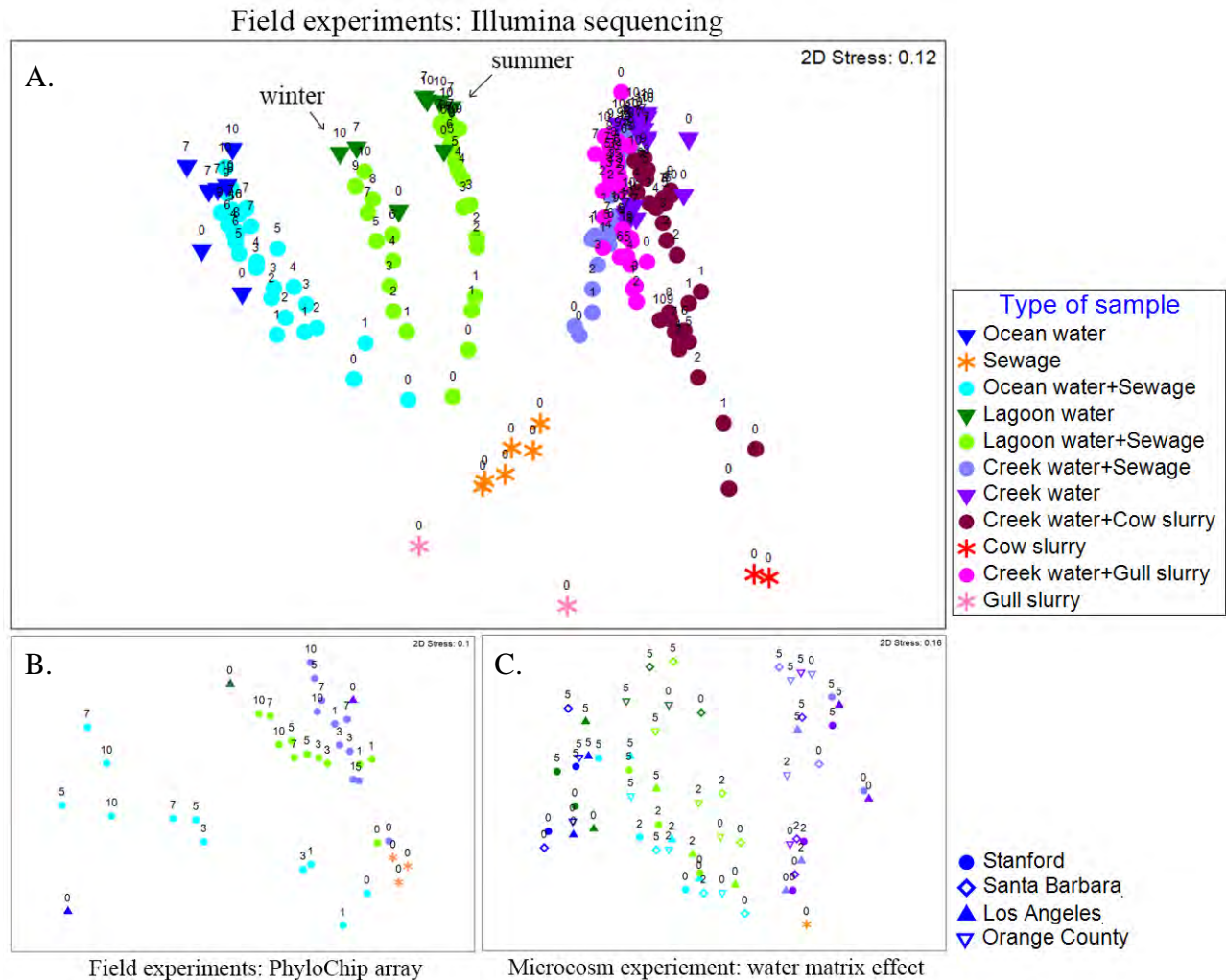


Figure 1. nMDS representing the present/absent data. A. Illumina sequencing data from the field experiments. B. PhyloChip data from the field experiments using sewage and performed in summer. C. Illumina data from the water matrix effect microcosm experiments.

Tracking the decay of the microbial community over time

Figure 2 represents the percentage of fecal signal detected with SourceTracker over the time in the field experiments. Both Illumina sequencing and PhyloChip detected fecal signal in all fecal treatment samples throughout the entire 10 day period of decay. The PhyloChip array was more sensitive than the Illumina sequencing at detecting fecal signals, detecting 1.2 to 83.7% of fecal signal over 10 day period compared with 0.14-65.1% detected by Illumina. In previous studies (Cao et al. 2013) it was demonstrated PhyloChip detection based on probes level analysis was even more sensitive than the OTU level detection results presented here. The analysis will also be conducted at the probe level in future work.

There were some differences of decay rates between light exposures. PhyloChip analysis detected a faster decay under unshaded conditions for the ocean and creek water. The Illumina data detected differences between seasons, being slower during winter. The creek water presented lower decay rates than the

lagoon and ocean water, showing higher fecal contamination signal at the end of the experiments. The analysis of the water matrix effect microcosm will help to clarify this outcome.

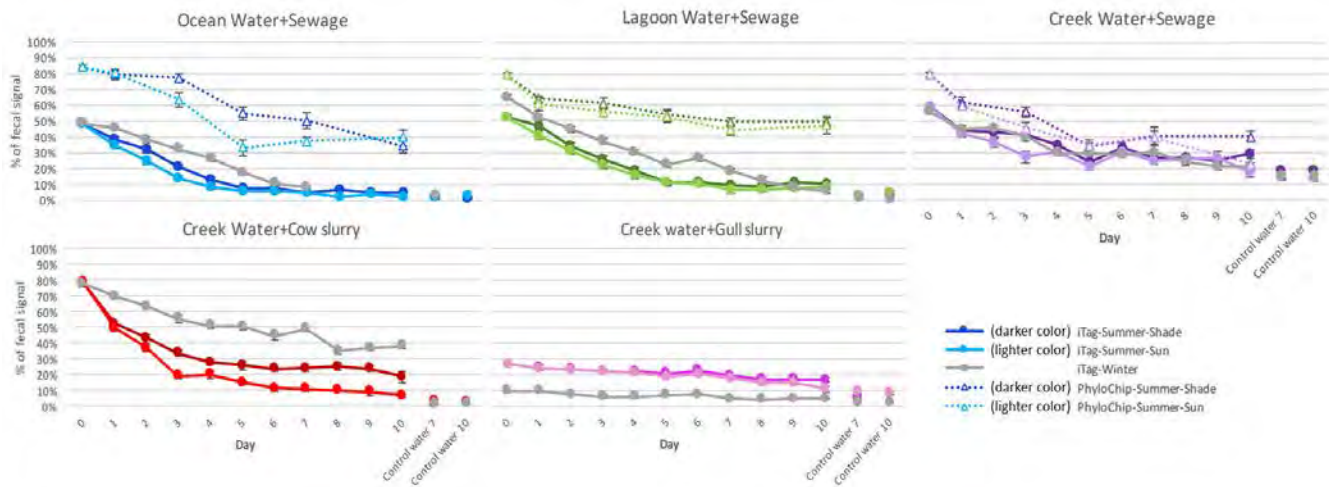
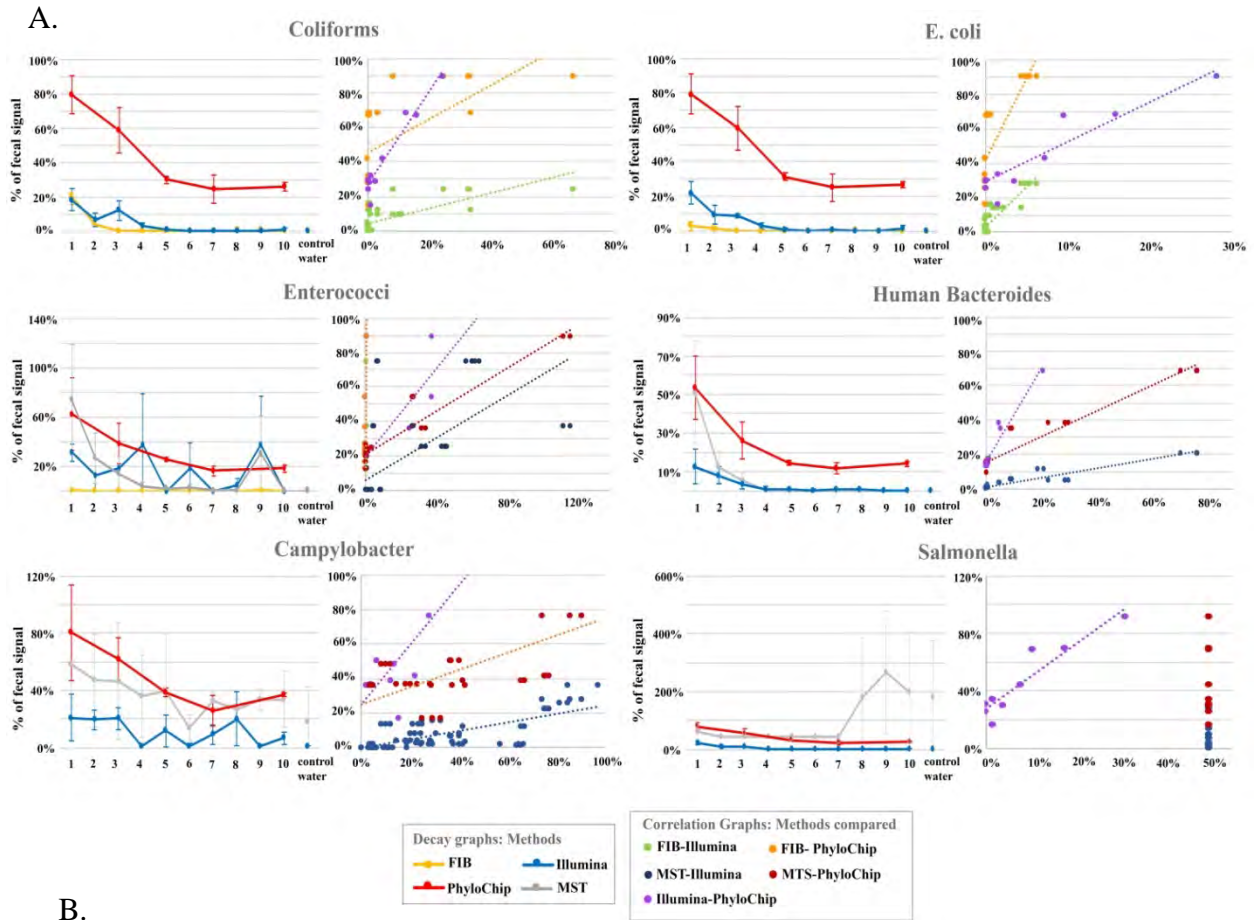


Figure 2. Decay of the fecal signal detected with SourceTracker over the time in the field experiments.

Fecal contamination methodology comparison

Figure 3 represents data from the ocean water field experiment in summer only for subsets of microorganisms that correspond with FIB, MST or pathogen tests. For each subset, the left column graphs show the percentage of fecal contamination signal over the time detected by different methods, and the right column graphs show the correlation between pairs of methods. In each comparison, the results of the method named first in the legend are plotted in the X axis. Human *Bacteroides* tests (BacHum, HF183, HumM12 markers) gave similar results than the total *Bacteroides* assay (tracked by GenBac3 marker), so only one is represented for summary purposes. In Figure 1B are summarized the correlation coefficients (R^2) obtained for pair of method comparison.

Compared to all other methods, PhyloChip was the most sensitive method for tracking decay of specific FIB, MST, and pathogens. For each community subset (Coliforms, *E. coli*, Enterococci, Human *Bacteroides*, *Campylobacter*, *Salmonella*), PhyloChip detected a greater percentage of the starting signal than any other method. The correlation between the Illumina and PhyloChip detection was high ($R^2 \geq 0.8$), except for *Campylobacter* which was not properly identified by Illumina sequencing. The MPN rendered lower correlation coefficients ($0.4 \geq R^2 \leq 0.7$). For enterobacteria (including coliforms and *E. coli* detection tests), the MPN method correlates better with Illumina ($R^2 \geq 0.5$), while it does so with PhyloChip for enterococci ($R^2 = 0.6$). The qPCR methods present much better correlations with PhyloChip ($R^2 \geq 0.9$) for the fecal markers. For the pathogen markers (*Campylobacter* and *Salmonella*) the correlations coefficients in general are much lower ($0.4 \geq R^2 \leq 0.5$), due to the fact that qPCR methods don't reflect the decay of the pathogens.



Microorganisms													
	Coliforms		E. coli		Enterococci			Human Bacteroides		Campylobacter		Salmonella	
Method	FIB	Illumina	FIB	Illumina	FIB	MST	Illumina	MST	Illumina	MST	Illumina	MST	Illumina
Illumina	0.45	-	0.72	-	0.38	0.43	-	0.89	-	0.49	-	-	-
PhyloChip	0.38	0.96	0.56	0.9	0.6	0.91	0.79	0.93	0.94	0.41	0.59	-	0.88

Figure 3. Comparison of the decay of each specific FIB, MST, and pathogens detected by different methods. A. For each group tested, the left plot shows the percentage of fecal contamination signal over the time detected by different methods, and the right column graphs show the correlation between pairs of methods. In each comparison, the results of the method named first in the legend are plotted in the X axis. B. Summary of the correlation coefficients (R²) obtained for pair of method comparison.

Preliminary conclusions

The PhyloChip array was the most sensitive method for tracking the decay of the fecal contamination, under field and lab conditions, over any other method. Among the routine methods used for fecal contamination monitoring, qPCR tracking the enterococci and the human *Bacteroides* is the most reliable protocol.

The salinity of the receiving water was the most significant environmental factor influencing the decay of the fecal signal and was slowest in lower salinity matrices. PhyloChip detection showed that fecal signal persisted at least until day 10. Thus, 10 days is insufficient time to track the complete decay and elimination of fecal contamination signal.

In the more detailed microbial community analysis, different taxonomic groups had distinctly different decay rates. This could help to explain the variable sensitivities of individual FIB tests. Knowledge of the characteristic decay rate pattern of each of multiple members of a fecal microbial community provides a powerful new tool in tracing not only the source of fecal contamination in the receiving waters but also, potentially, the timing of the discharge.

Literature Cited

Cao, Y., Van De Werfhorst, L.C., Dubinsky, E.A., Badgley, B.D., Sadowsky, M.J., Andersen, G.L., Griffith, J.F., and Holden, P.A. Evaluation of molecular community analysis methods for discerning fecal sources and human waste. *Microb. Source Track.* 2013. *47*, 6862–6872.

Caporaso, J.G., Lauber, C.L., Walters, W.A., Berg-Lyons, D., Huntley, J., Fierer, N., Owens, S.M., Betley, J., Fraser, L., Bauer, M., et al. Ultra-high-throughput microbial community analysis on the Illumina HiSeq and MiSeq platforms. *ISME 2012. J* *6*, 1621–1624.

Hazen, T.C., Dubinsky, E.A., DeSantis, T.Z., Andersen, G.L., Piceno, Y.M., Singh, N., Jansson, J.K., Probst, A., Borglin, S.E., Fortney, J.L., et al. Deep-Sea Oil Plume Enriches Indigenous Oil-Degrading Bacteria. *Science.* 2010. *330*, 204–208.

Knights, D., Kuczynski, J., Charlson, E.S., Zaneveld, J., Mozer, M.C., Collman, R.G., Bushman, F.D., Knight, R., and Kelley, S.T. 2011. Bayesian community-wide culture-independent microbial source tracking. *Nat Meth* *8*. 2011. 761–763.

APPENDIX E. SEDIMENT EFFECT INVESTIGATION

Introduction

Recent studies have highlighted health risks associated with exposure to beach sand (Halliday and Gast 2011, Heaney et al. 2012). Sediments can constitute a reservoir for microbial contaminants (Rehmann and Soupir, 2009, Steets and Holden, 2003), leading to confusion about the source. Under some conditions, sediment resuspension can contribute significant microorganisms to the water column (Pandey et al. 2012). Sediments can promote persistence of fecal organisms both by providing protection from ultraviolet radiation, temperature fluctuations, and predation by microorganisms in the overlying water column (Davies et al. 1995, Korajkic et al. 2013, Wanjugi and Harwood 2013, Alm et al. 2003) and by supplying critical nutrients (Craig et al. 2004, Labelle et al. 1980, Mika et al. 2009). Under favorable sediment conditions, fecal indicator bacteria (FIB) exhibit extended survival and even regrowth, which in turn complicates interpretation of FIB levels (Byappanahalli et al. 1998, Byappanahalli et al. 2012). Although *Bacteroidales* do not survive in water due to their anaerobic physiology (Bae and Wuertz, 2012), *Bacteroidales* may persist (Kim and Wuertz, 2015) and there is some evidence for regrowth (Eichmiller et al. 2014) in sediments. Despite this, little research has been conducted evaluating the comparative decay of FIB, DNA-based marker, and pathogens in sediments.

In this study, the relative decay rates of pathogens, DNA-based markers, and FIB were tested in sediment under relevant environmental conditions. Three field sites representing typical coastal habitats in California were selected to compare decay: a baseflow freshwater creek site, a brackish water coastal lagoon site, and an ocean site. The dominant human source, sewage, was evaluated under ambient environmental conditions at two concentrations. Results of this study have direct implications for water quality managers tasked with designing MST studies and interpreting MST results. MST that utilizes DNA-based markers that consistently decay similarly or slower than pathogens will be more protective of public health.

Methods

Sediment Collection and Characterization

Sediments were collected from the same three sites targeted during the dialysis bag experiments representing: 1) a baseflow freshwater site located in Irvine, California (Freshwater South-FW); 2) a brackish lagoon site located in Santa Barbara, CA (Brackish Central-BW); and 3) a marine site located in Stanford, CA (Marine North-MW). 3.5 L of sediment was collected from the top 0-5 cm using sterile sediment cores at each site; putting it into sterile, polypropylene containers. and the samples were immediately placed on ice and shipped to UCLA. Sediment was stored at 4°C in the dark until use- within 72 hours. An additional water sample was collected in a 2 L sterile container. Water parameters, including pH, conductivity, and salinity were taken on site and 200 ml of water was filtered for background levels of DNA markers and pathogens.

On aliquots from each sediment sample, particle size was determined by charging the particles in a sodium metaphosphate solution and taking hydrometer measurements at standardized time increments (Zedler 2001). Organic content was measured through loss on ignition at 55° C for two hours (Clesceri et al. 1998). Sediment was combined from each of the four replicate beakers into a composite sample on days 0, 1, 3, 4, 6, and 7 and extracted for analysis of phosphate, nitrite, ammonium, and nitrate-nitrite. Ammonium, nitrate-nitrite, and nitrite were extracted per standard methods with a KCl extraction solution using an automated shaker (ISO 14256-1, 2003). Phosphate was extracted using the Mechlich 3 extraction method (Mechlich 1984), where Mechlich 3 extracting solution (0.2 N acetic acid, 0.25 N NH₄NO₃, 0.015 N NH₄F, 0.013 N HNO₃, and 0.001 M EDTA) and an automated shaker were used to extract Phosphate. Extractants were filtered through a 0.22 um polycarbonate filter and filtrate stored in the dark

at -20° C for up to three weeks before being shipped to the MSI laboratory at UCSB (Marine Science Institute, Santa Barbara, CA) for nutrient analysis. Dry weights of samples were determined by measuring weight differences before and after drying sediments at 105° C for at least 24 hours or until two measurements stabilized.

Microcosm Setup

Primary influent was collected into sterile polypropylene containers from the Orange County Sanitation District (Fountain Valley, CA) 24 hours prior to microcosm and transported to UCLA on ice. Immediately after arrival at UCLA, the sewage solution was mixed and allowed to settle for 10 minutes. The required volume was then removed from the sample bottle avoiding particles that had settled to the bottom or that had floated to the top and stored at 4°C.

Two sewage dilutions were made, 1:10 and 1:2, in three different artificial waters, artificial freshwater (AFW: distilled water with 0.3 mM MgCl₂, 0.6mM CaCl₂, and 1.4 mM NaHCO₃) conductivity of 1449 us/cm, artificial brackish water (ABW: .3 mM MgCl₂, 0.6mM CaCl₂, 1.4 mM NaHCO₃, Instant Ocean) conductivity of 34 ms/cm, and artificial marine water (AMW: prepared with Instant Ocean Aquarium Systems, Mentor, OH) conductivity of 58.4 ms/cm. Sewage solutions were seeded into their corresponding sediment types and allowed to incubate for two hours. After the two-hour incubation, 400 ml seeded sediment was distributed into each of four replicate beakers and 400 ml of the corresponding artificial water (AFW, ABW, or AMW) was added. A total of 24 microcosms were set up in 2 L glass pyrex beakers. Beakers were covered with plastic wrap secured with Parafilm to limit water loss due to evaporation and to prevent the addition of unwanted particles to the microcosms. Beakers were set up under ambient light conditions in a plexiglass water bath on top of Boelter Hall, UCLA. Throughout the experiment, temperature was maintained at 20 °C using two water chillers, and oxygen content of beakers was maintained by using an airstone in each beaker. Light and temperature were monitored continuously by Hobo data logger deployed in at least one beaker per treatment.

Sampling and Analysis

Microcosms were sampled once a day for eight consecutive days for decay of FIB, DNA-based markers, and pathogens. Prior to sampling the sediment at each time point, water was removed carefully with an automated pipetter. Water from the four beakers was combined at each time point, beginning on day one, and the composite sample was processed for FIB, markers, and pathogens to account for resuspension of bacteria to the water column. 100 ml sample water was filtered through 47 mm, 0.4 µm pore size, HTPP polycarbonate filters (EMD Millipore, Billerica, MA) in triplicate. Each filter was placed in an individual two ml polypropylene screw cap tube, containing 0.3 g, 212 – 300 µm (50 – 70 U.S. sieve) acid washed glass beads (Sigma-Aldrich, St. Louis, MO) and stored at -80°C until DNA extraction.

Following removal of the overlying water, approximately 25 g sediment was collected at each time point using a sterile 15 ml falcon tube core. 20 g sediment was washed per standard protocol (Boehm et al. 2009). Briefly, 20g sediment was hand shaken in PBS in a ratio of 1:10 for 2 min and allowed to settle for 30 sec. Sample wash was processed for FIB and 15 ml wash was filtered in duplicate through 0.45 HAWG membrane filters (EMD Millipore, Temecula, CA) for analysis of culturable *Campylobacter* and *Salmonella*. For analysis of DNA-based markers, 0.25 g sediment was placed into an individual two ml polypropylene screw cap tube with 750 µls of Bead Solution (MoBio Inc., Carlsbad, CA) and 1 g of Power Bead Tubes (MoBio Inc., Carlsbad, CA).

After sediment was collected, beakers were replenished with 400 ml new water corresponding to treatment (AFW, ABW, or AMW) simulating semi-continuous flow conditions.

Culturable Pathogens and Fecal Indicator Bacteria (FIB) Analysis

To obtain FIB concentrations, Total Coliform (TC), *E. coli* (EC), and enterococci (ENT) were measured with Colilert-18™ and Enterolert™ (IDEXX, Westbrook ME) reagents and protocols to determine the most probable number (MPN) of cells per 100 ml⁻¹ or g⁻¹ of dry weight of sediments.

In each sample, the presence/absence of *Salmonella* and *Campylobacter* was measured. 15 ml sediment sample wash was filtered in duplicate through 0.45 HAWG membrane filters (EMD Millipore, Temecula, CA). Following filtration of 15 ml sediment wash, one filter was placed in each 30 ml tryptic soy broth (TSB) and incubated at 37°C for 24 hours for *Salmonella* and into Bolton Broth with *Campylobacter* selective supplement in microaerophilic containers (BBL Campy GasPak Sachet) for 48 hours for detection of *Campylobacter*. Following pre-enrichment, Bolton Broth culture tubes were used to inoculate Modified Karmali Agar plates. After a 48-hour incubation, the plates were examined for putative *Campylobacter* colonies and confirmed with PCR with *Campylobacter* specific primers. For presence/absence assessment of viable *Salmonella*, each TSB culture tube was used to inoculate semi-solid Rappaport Vassiliadis plates (MSRV). After a 42-hour incubation, presumptive *Salmonella* colonies were sub-cultured onto xylose lysine desoxycholate selective agar (XLDA) plates. After 24 hours, the plates were examined for the presence of motility and presumptive colonies were confirmed with PCR with *Salmonella* specific primers (Table 1). For PCR confirmation, DNA was extracted from isolates by adding cells to 25 ul DNase free water, vortexing, and heating the solution to 100°C for at least 10 minutes to lyse the cells.

Marker Analysis

DNA was extracted from water column samples using the DNA-EZ ST1 Extraction Kit (GeneRite, North Brunswick NJ) following the manufacturer's protocol. Eluted DNA samples were stored at -20°C until analysis of molecular host-associated markers with qPCR. Sediment samples were extracted according to manufacturer's protocol with the MoBio Power Soil DNA Extraction Kit (MoBio Inc., Carlsbad, CA) with two modifications: DNA was eluted into 50ul of elution buffer, instead of 100 ul, in order to increase recovery and soil was homogenized in a mini-bead beater (BioSpec Products, Bartlesville, OK) for 2 minutes.

QPCR assays were performed according to previously published protocols (Table 1). Reaction mixtures consisted of 1X Taqman Environmental Master Mix (Applied Biosystems, Foster City, CA), forward and reverse primers and probes, bovine serum albumin fraction, and 2 ul of template DNA (for marker and ENT1A assays) and 6 ul of template for pathogen (*Campylobacter* and *Salmonella* qPCR assays). Triplicate samples were run on a StepOnePlus real-time PCR system (Applied Biosystems, Foster City, US).

Samples and calibration standards were run in triplicate. A five-point standard calibration curve was run alongside samples on each well plate. Standard curves had efficiencies between 88 - 100% and $R^2 > 0.99$. Quantification thresholds (Cq) were converted into units of gene copies using a pooled master standard calibration model. Negative controls (no template controls on well plate), filtration and extraction blanks were included to ensure that contamination of samples did not occur during either the filtration or extraction processes.

Table 1. Primers and probes used in PCR and qPCR assays.

Target	Assay	Assay Ref	Primers	Probe	Dye	Quencher
General	GenBac3	USEPA, 2010a	F: GGGGTCTGAGAGGAAGGT R: CCGTCATCCTTCACGCTACT	CAATATTCTCACTGCTGCTCCCGTA	6FAM	TAMRA
Human	HF183	Green et al., 2014	F: ATCATGAGTTACATGTCCG R: CTTCTCTCAGAACCCTATCC	CTAATGGAACGCATCCC	6FAM	MGB
IAC	HF183 IAC	Green et al., 2014		AACACGCCGTTGCTACA	VIC	MGB
<i>Enterococcus</i>	ENT1A	USEPA, 2010b	F: GAGAAATTCCAAAACGAACCTTG R: CAGTGTCTTACCTCCATCATT	TGGTTC TCT CCGAAA TAGCTT TAGGGCTA	6FAM	TAMRA
<i>Campylobacter</i>	qCamp	Lund et al., 2004	F: CACGTGCTACAATGGCA TAT R: GGCTTCATGCTCTCGAGTT	CAGAGAACAATCCGAACTGGGACA	6FAM	BHQ1
<i>Salmonella</i>	qSalm	Malorny et al., 2004	F: CTCACAGGAGATTACAACATGG R: AGCTCAGACCAAAAAGTGACCATC	CAC CGA CGG CGA GAC CGA CTT T	6FAM	BHQ1
<i>Campylobacter</i>	Camp	Khan et al., 2007	F: GGATGA- CACTTTTCGGAGC R: CATTGTAGCACGTGTGTC			
<i>Salmonella</i>	Salm	Rahn et al., 1992	F: GTGAAA TTA TCGCCACGITC GGC R: TCA TCGCACCGTCAA			

Data analysis and Statistical Analysis

A shoulder-tail log linear decay equation was used to determine the decay rates as well as magnitude (if present) of a shoulder and/or tail (eqn. 1).

$$\text{Eqn. 1: } C_t = \left\{ \left((C_o - N_{res}) e^{-kt} \right) \left(\frac{e^{kS}}{1 + (e^{kS} - 1) * e^{-kt}} \right) \right\} + N_{res} \quad (\text{Geeraerd et al. 2005})$$

where N_{res} is the resulting concentration of residual population and represents the presence of a tail, S is the length of the shoulder preceding decay, t is time (days), C_t is the measured concentration at time t , C_o is the measured concentration at time 0, and k (day^{-1}) is the rate constant for the log linear portion of the inactivation curve after the shoulder region and preceding the tail region.

This decay equation can exhibit log linear behavior with and without tailing or shoulder (Geeraerd et al. 2005). In the case of either no shoulder or tail, the model reduces to either eqn. 2 or eqn. 3 which can be derived by setting S or N_{res} equal to zero.

$$\text{Eqn. 2: } C_t = (C_o e^{-kt}) \left(\frac{e^{kS}}{1 + (e^{kS} - 1) * e^{-kt}} \right); \text{ Eqn 3: } C_t = (C_o - N_{res}) e^{-kt} + N_{res} .$$

In the case of no decay, to avoid overfitting, a first-order decay equation (eqn. 4) was applied:

$$\text{Eqn. 4: } C_t = C_o e^{-kt}$$

Paired t-tests were applied to determine if there was a significant difference in the initial versus final concentration of cells. Differences were considered significant when the p-value was less than 0.05. All analyses described above were completed in STATA 12.0 (StatCorp LP, College Station, TX). Correlations between the time evolution of different marker and FIB levels was quantified in R-3.0.1 (R-Project, Boston, MA)

Results

Sediment Characteristics

Relative aging of DNA-based markers, FIB, and pathogens was evaluated in three sediments, representative of California coastal habitats. Sediment collected from the Marine Northern California site consisted mainly of sand, with very little silt and clay, and a low percentage of organic matter and

relatively low levels of nutrients. In comparison, sediment collected at the Brackish Lagoon site from Santa Barbara, CA contained a higher percentage of silt and clay particles and organic matter and increased levels of ammonia. Sediment collected from the Freshwater site in Southern California contained the highest proportion of fines and organic matter of the three sediments. Phosphate and nitrate levels were also approximately three times as high as levels in sediments from the Brackish and Marine sites (Table 2).

Table 2. Sediment characteristics of unseeded sediment used in the microcosm experiments.

Site	Org Matter	Particle Size Distribution			Nutrients				Moisture Content
		%	%			um/g			
			Clay	Silt	Sand	PO ₄ ³⁻	NH ₃	NO ₃ ⁻	NO ₂ ⁻ + NO ₃ ⁻
Marine North	0.00	4.20	0.30	95.50	0.41	0.26	0.09	0.02	23
Brackish Central	0.20	10.20	8.60	81.20	0.46	1.88	0.06	0.01	42
Fresh South	2.44	13.83	10.25	75.91	1.23	0.18	0.26	0.01	58

Decay in Sediment

Decay dynamics were evaluated for pathogens, FIB, and DNA-based markers over the course of the eight-day microcosm and are shown in Figures 1 and 2.

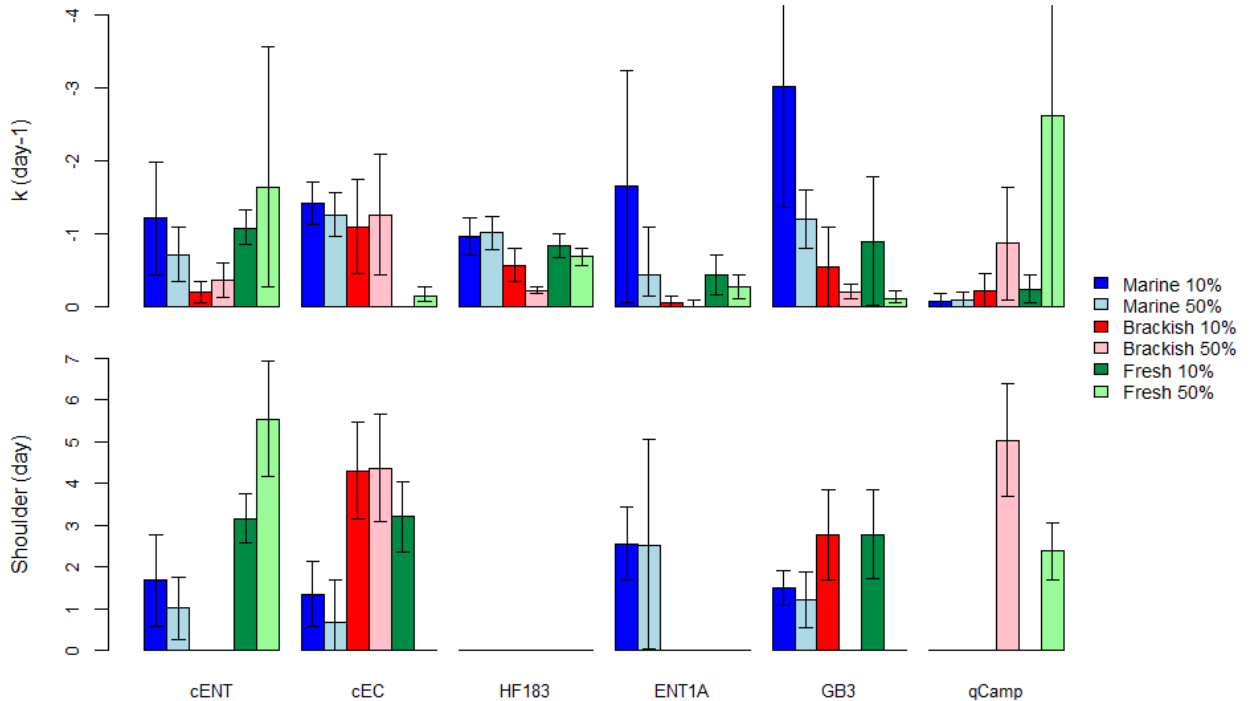


Figure 1. Decay rate and length of shoulder preceding decay given for 10% and 50% treatments. Error bars denote 95% confidence intervals.

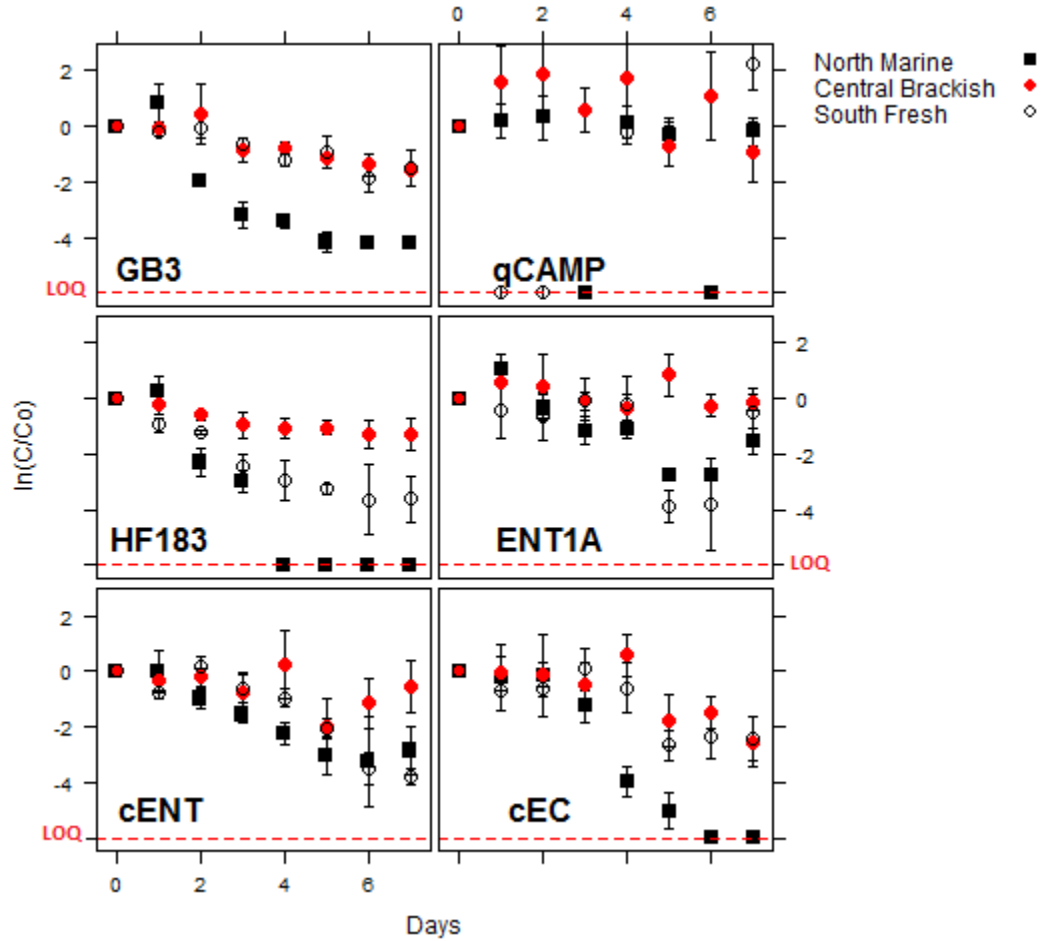


Figure 2. Time series of natural log of concentrations normalized by initial concentration, in marine (black squares), brackish (red circles), and freshwater (white circles) sediments at 10% inoculum. Average concentration and standard error plotted for the four replicate beakers at each time point. Red dashed line indicates where concentrations measured fell below the limit of quantification (LOQ).

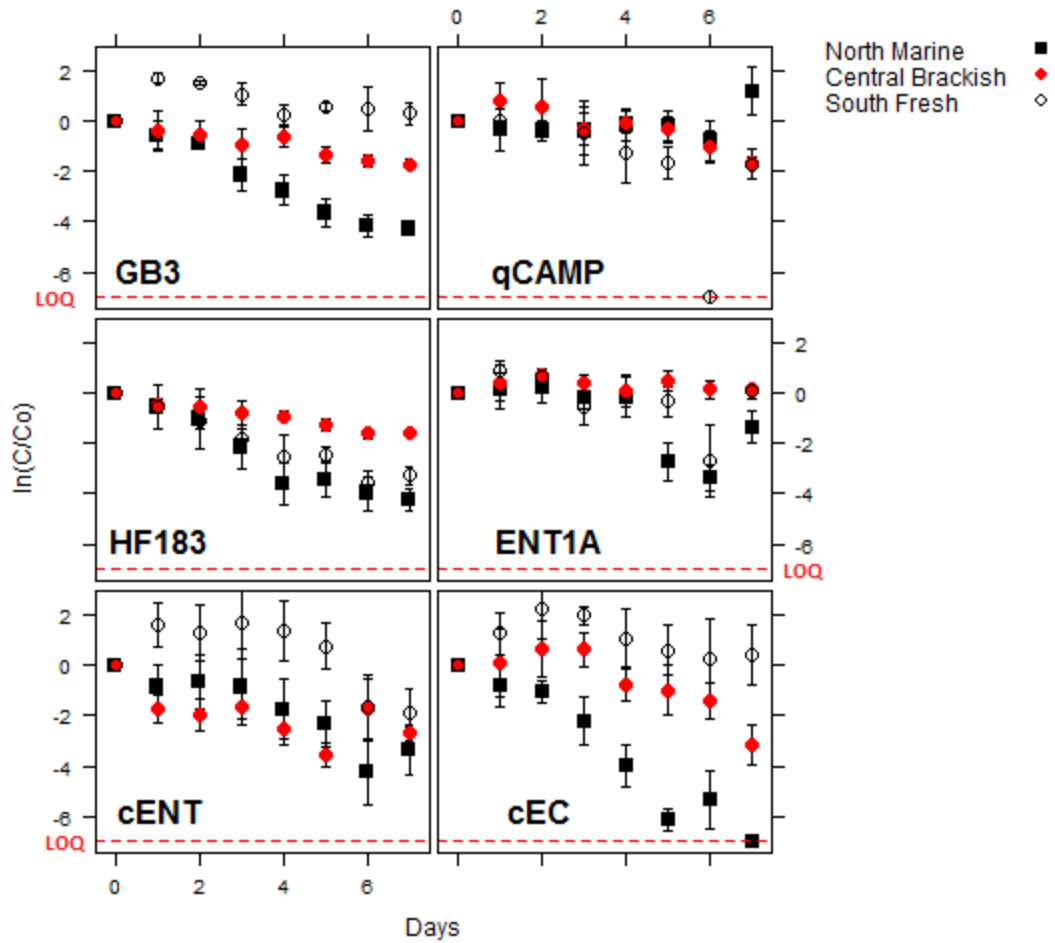


Figure 3. Time series of natural log of concentrations normalized by initial concentration, in marine (black squares), brackish (red circles), and freshwater (white circles) sediments at 50% inoculum. Average concentration and standard error plotted for the four replicate beakers at each time point. Red dashed line indicates where concentrations measured fell below the limit of quantification (LOQ).

Shoulder-tail log linear decay models were used to evaluate decay rate, except in the case of no decay determined by paired t-tests applied to the initial and final indicator levels measured (Table 3). Decay rates and magnitude of tail and/or shoulder are presented in Tables 4 and 5 and illustrated in Figure 1.

Table 3. T test results comparing concentration measured on day 0 versus on day 7. P- values given for microcosms where there was no significant reduction in concentration. **/* indicates a significant reduction in measured concentration at p-value less than 0.01/0.05.

% inoculum	Sediment type	Assay					
		HF183	GB3	ENT1A	qCamp	cEC	cENT
10	MW	**	**	**	0.36	*	**
	BW	**	**	0.43	0.19	**	0.23
	FW	**	**	0.17	*	**	**
50	MW	**	**	**	0.22	*	**
	BW	**	**	0.16	**	**	0.21
	FW	**	**	0.78	*	0.30	**

**p-value<0.01

*p-value<0.05

Table 4. Decay rate (k), length of shoulder (S) and concentration of resistant population (Nres) calculated for markers and FIB at 10% inoculum.

Treatment	C0 copies/ cells	k	95% CI		S	SE	Nres copies/cells	SE	R2
Assay/ Site	(gram ⁻¹)	(day ⁻¹)	LCI	UCI	(day)		(gram ⁻¹)		
cENT									
Marine	2.9E+02	-1.21	-1.99	-0.43	1.68	0.54	6.5	2.5	0.92
Brackish	7.6E+01	-0.20	-0.35	-0.05					0.21
Fresh	4.4E+03	-1.08	-1.32	-0.85	3.16	0.29			0.95
cEC									
Marine	9.5E+02	-1.41	-1.70	-1.12	1.35	0.38			0.95
Brackish	2.6E+03	-1.10	-1.74	-0.46	4.29	0.57			0.67
Fresh	1.4E+04	-5.92	-22.19	10.35	3.20	0.42	1122	291	0.77
HF183									
Marine	2.2E+04	-0.97	-1.21	-0.72					0.80
Brackish	7.5E+04	-0.57	-0.81	-0.34			18413	2441	0.92
Fresh	8.7E+04	-0.84	-1.00	-0.67			1245	444	0.96
ENT1A									
Marine	1.4E+05	-1.65	-3.24	-0.06	2.55	0.43	13700	3434	0.85
Brackish	3.2E+05	-0.05	-0.15	0.05					0.03
Fresh	2.7E+06	-0.44	-0.72	-0.16					0.26
GB3									
Marine	7.1E+06	-3.02	-4.67	-1.37	1.48	0.2	128765	18872	0.97
Brackish	2.0E+07	-0.55	-1.09	-0.01	1.85	0.95	3308472	2E+06	0.93
Fresh	3.0E+07	-0.89	-1.79	-0.02	2.77	0.52	4288429	2E+06	0.87
qCAMP									
Marine	1.9E+03	-0.08	-0.18	0.02					0.09
Brackish	9.7E+03	-0.23	-0.45	-0.01					0.14
Fresh	7.7E+02	-0.24	-0.43	-0.05					0.18

Table 5. Decay rate (k), length of shoulder (S) and concentration of resistant population (Nres) calculated for markers and FIB at 50% inoculum.

Treatment	C0 copies/ cells	k	95% CI		S	SE	Nres copies/ cells	SE	R2
Assay/ Site	(gram ⁻¹)	(day ⁻¹)	LCI	UCI	(day)		(gram ⁻¹)		
cENT									
Marine	1.4E+03	-0.72	-1.09	-0.34	1.01	0.37			0.82
Brackish	5.4E+03	-0.37	-0.60	-0.13					0.26
Fresh	9.7E+03	-1.64	-3.56	-0.28	5.53	0.68			0.33
cEC									
Marine	9.6E+03	-1.26	-1.56	-0.96	0.67	0.5			0.94
Brackish	8.7E+03	-1.26	-2.09	-0.43	4.36	0.63			0.61
Fresh	2.8E+04	-0.14	-0.28	0.07					0.07
HF183									
Marine	7.8E+04	-1.02	-1.23	-0.79			821	251	0.94
Brackish	3.4E+05	-0.23	-0.27	-0.18					0.94
Fresh	4.0E+05	-0.70	-0.81	-0.57			9597	3010	0.97
ENT1A									
Marine	4.3E+05	-0.62	-1.10	0.15	2.54	1.23			0.67
Brackish	7.6E+05	0.00	-0.09	0.09					0.00
Fresh	1.8E+06	-0.27	-0.43	-0.11					0.30
GB3									
Marine	2.4E+07	-1.20	-1.60	-0.81	1.21	0.32	293206	67598	0.98
Brackish	8.5E+07	-0.21	-0.12	-0.31					0.43
Fresh	1.4E+08	-0.11	-0.06	-0.22					0.14
qCAMP									
Marine	2.9E+03	-0.09	-0.21	0.03					0.07
Brackish	1.2E+04	-0.87	-1.64	-0.09	5.03	0.66			0.48
Fresh	7.6E+03	-2.61	-5.52	0.30	2.37	0.34	1022	172	0.87

FIB

In the 10% and 50% seeded microcosms, in most cases, a lag period preceded decay for cENT and cEC. The lag period differed between sediment types, with a longer lag period observed in the FW and BW versus MW sediments. cENT levels did not significantly decrease over the course of the microcosm experiments in either the 10 or 50% treatments in the BW microcosms (Table 3), whereas in the FW and MW cENT levels declined by at least an order of magnitude. An initial increase, indicating potential for regrowth, in cEC was followed by persistence of the indicator in FW; cEC levels measured on day 7 were not significantly different from levels measured on day 0. At 10%, cEC levels decreased by over an order of magnitude (from 11451 to 1175 MPN g⁻¹) but decay rate was not significantly different from 0 and linear decay was observed between day 3 and day 5 only. Decay between cENT and cEC was correlated in the MW sediments at 10 and 50%.

Markers

GB3

In the 10% seeded microcosms, there was a lag period that preceded decay of the GB3 marker in all three sediments. At 50%, a lag period was observed in the MW microcosms. The lag period was similar between sediment types ranging between 1.5 (MW) and 2.8 (FW) days. Faster decay was observed of the GB3 marker in the MW microcosms at both 10 and 50% versus the FW and BW sediments. Persistence of the GB3 marker in FW at 50% was observed as slower decay in both the MW and BW sediments. Levels of the GB3 marker increased between day 0 and 1 in the FW microcosm at 50%, indicating potential for regrowth of the marker in FW sediments.

HF183

The HF183 marker decayed at a similar rate in the MW and FW sediments tested at both 10% and 50%. Increased persistence of the HF183 marker was observed in the BW sediment. In MW microcosms, the HF183 marker was only measured at detectable levels until day four at 10%. At 50%, the HF183 was measured at detectable levels until day seven. Relatively constant levels of the HF183 marker were measured in the MW and FW between day 6 and 7, indicating potential for a tailing effect and increased persistence of low levels of the HF183 marker. However, increased variability between replicates at the later time points was observed making it difficult to discern between an experimental artifact and a true tail.

ENT1A

In the BW and FW microcosms, the ENT1A marker persisted and levels measured on day 7 were not significantly different from levels measured on day 0. A faster decay rate of the ENT1A marker was observed in the MW microcosms, and a significant shoulder was observed, (on average 2.5 days) in both the 10 and 50 % treatments preceding decay.

Pathogens

qCamp

The qCamp marker was detected at mostly quantifiable levels throughout the eight day microcosm experiment in all six treatments. At 50%, there was a significant shoulder observed in the FW (2.4 days) and BW sediments (5.0) preceding decay. In the MW microcosms, qCamp was detected at low levels near the LOQ throughout the experimental time period and at 10% qCamp marker levels fell below the LOQ at several time points.

Culturable *Campylobacter*

Culturable *Campylobacter* was detected sporadically in both the BW and FW sediments and was detected most frequently in the BW sediment microcosms at 10% and in the FW sediment microcosms at 50%. Culturable *Campylobacter* was not detected in the MW sediments at either 10 or 50% (Figure 7).

qSalm

The qSalm marker was detected at levels above the LOD but below the LOQ (658 copies g⁻¹) in all three sediment types at 10 and 50% (Figure 3). Due to the low levels of the qSalm marker observed, decay rates were not able to be quantified.

Culturable *Salmonella*

Culturable *Salmonella* was detected until day seven in FW and MW sediment and until day five in BW sediment in at least one of four replicate microcosms in the 10% seeded sediment. At 50%, *Salmonella* was detected until day seven in FW and BW sediment and until day 3 in MW sediment. At both 10 and 50%, *Salmonella* was detected the most frequently in the FW sediment and the least frequently in the MW sediments for both the 10% and 50% treatments (Figure 4).

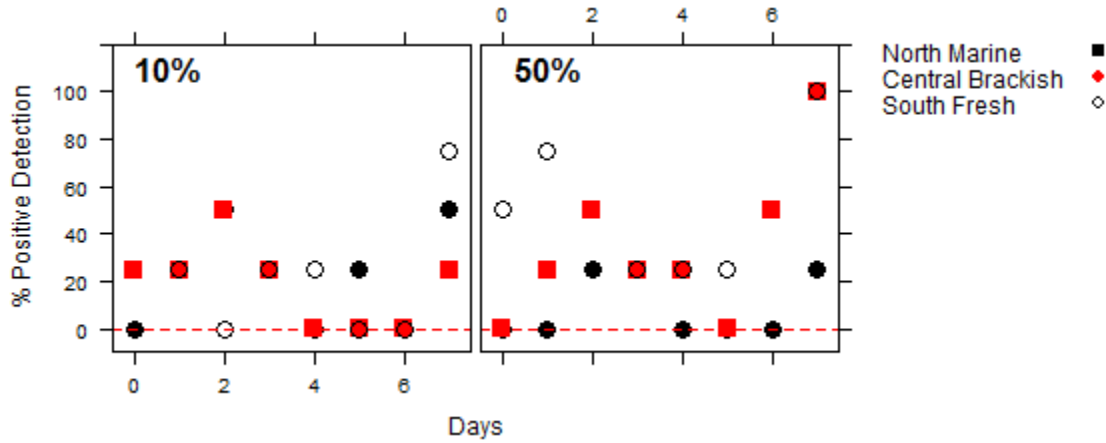


Figure 4. % detection of the *Salmonella* qPCR marker for the four replicate microcosms at each time point. Average marker levels measured in the sediment were detectable but not quantifiable in most cases.

Decay in the Different Sediments

Decay rates of the indicators were compared in each sediment type at 10 and 50% (Figure 5). Temporal evolution of the markers were compared in each sediment type and correlation coefficients are presented in Figures 6 (10%) and 7 (50%).

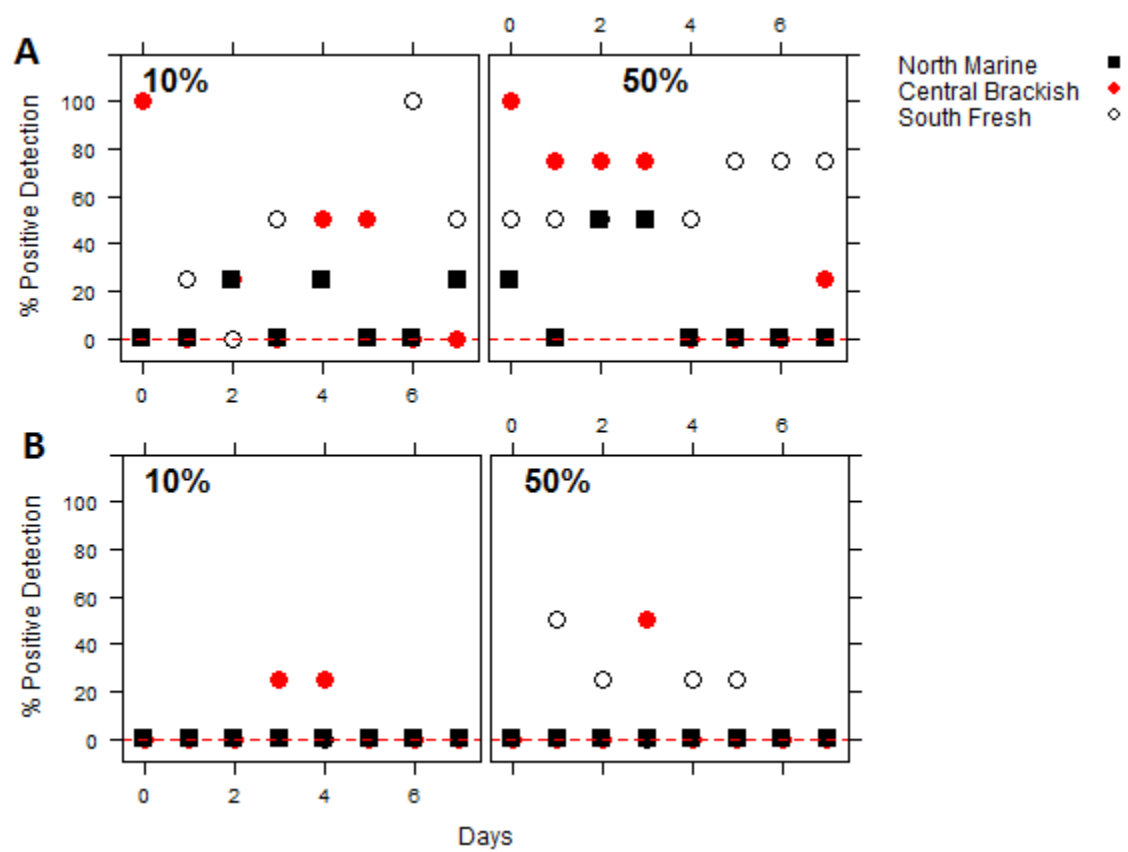


Figure 5. % positive detection of culture-based pathogens for the four replicate microcosms at each time point. A. *Salmonella* Culture-based Presence/Absence. B. *Campylobacter* culture-based Presence/Absence data.

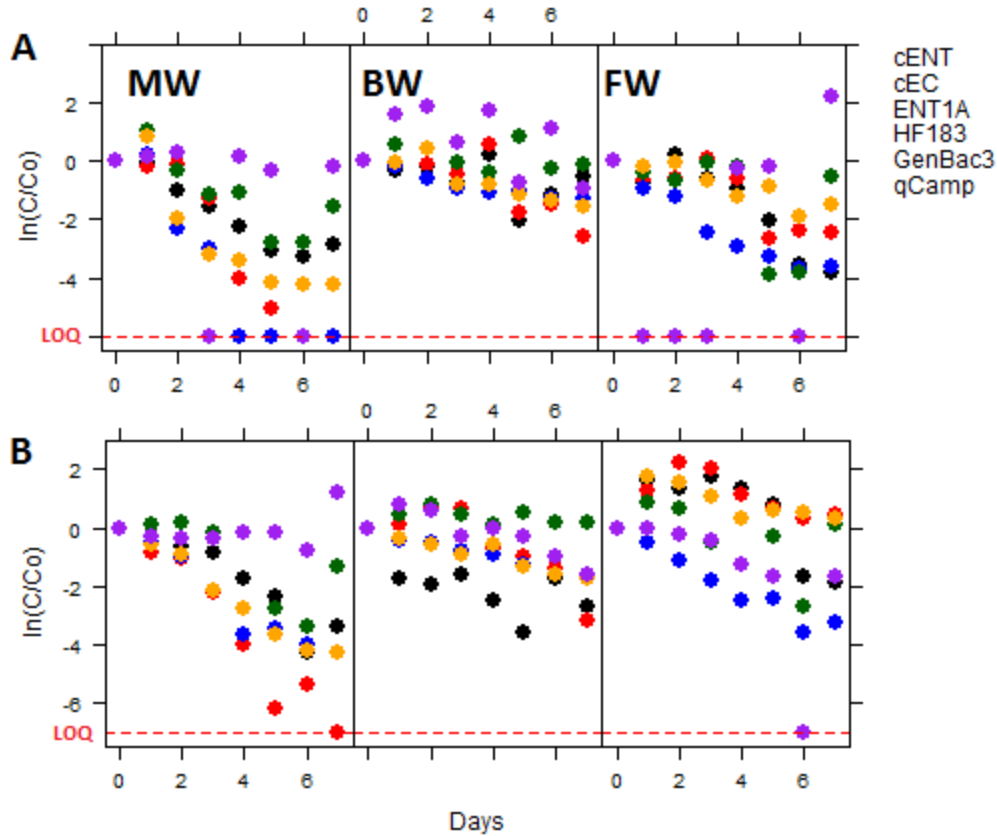


Figure 6. Time series of natural log of concentrations normalized by initial concentration for each marker, in marine, brackish, and freshwater sediments at 10% (A) and 50% (B) inoculum. Red dashed line indicates where concentrations measured fell below the limit of detection (ND=non-detect).

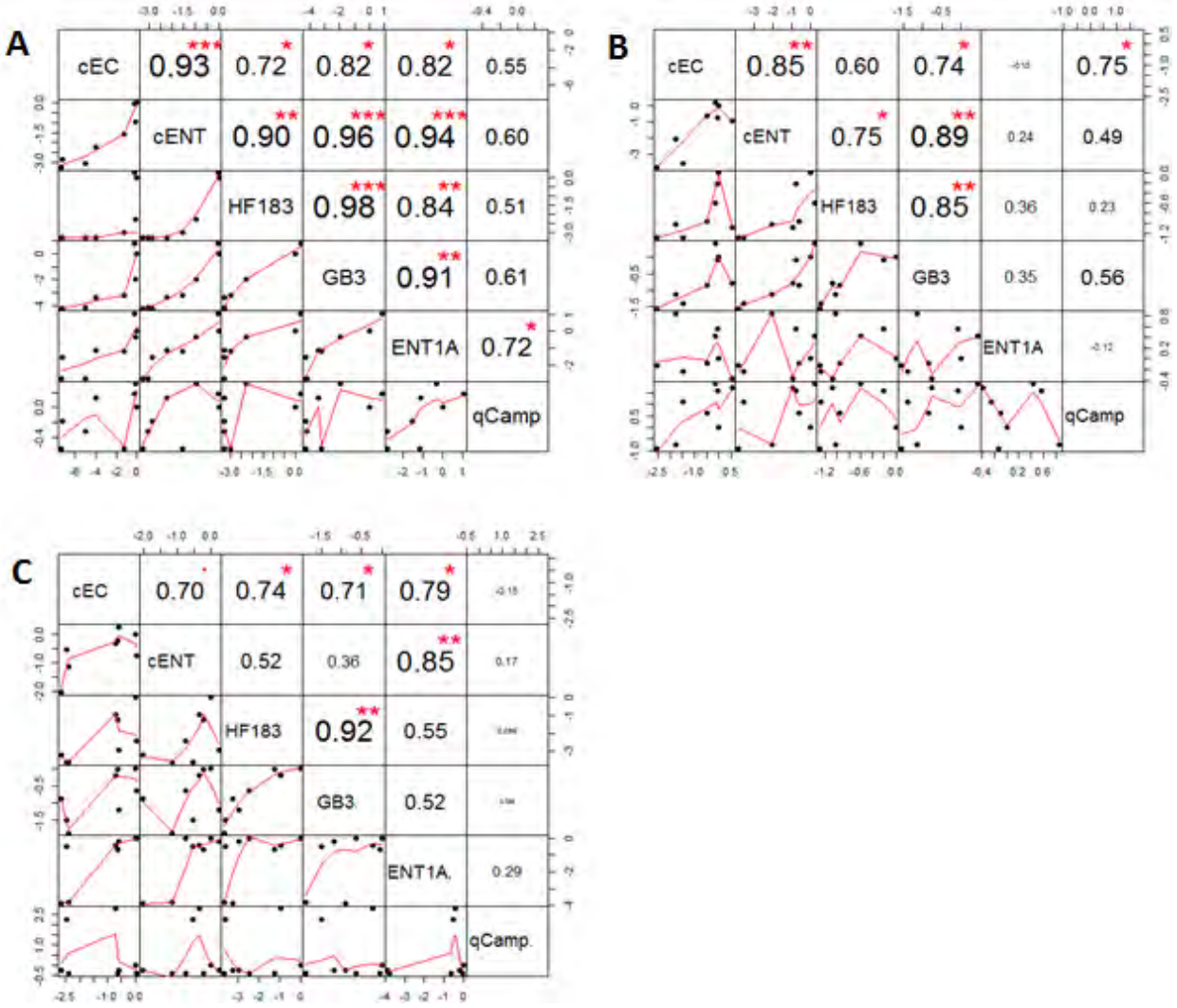


Figure 6. Correlations between decay of each marker in MW (A), BW (B), and FW (C) at 10% inoculum. $\ln(C/C_0)$ plotted against $\ln(C/C_0)$ for each marker. Significant correlations are indicated by a red asterisk at the 0.001(^{***}), 0.01(^{**}), and 0.05(^{*}) levels.

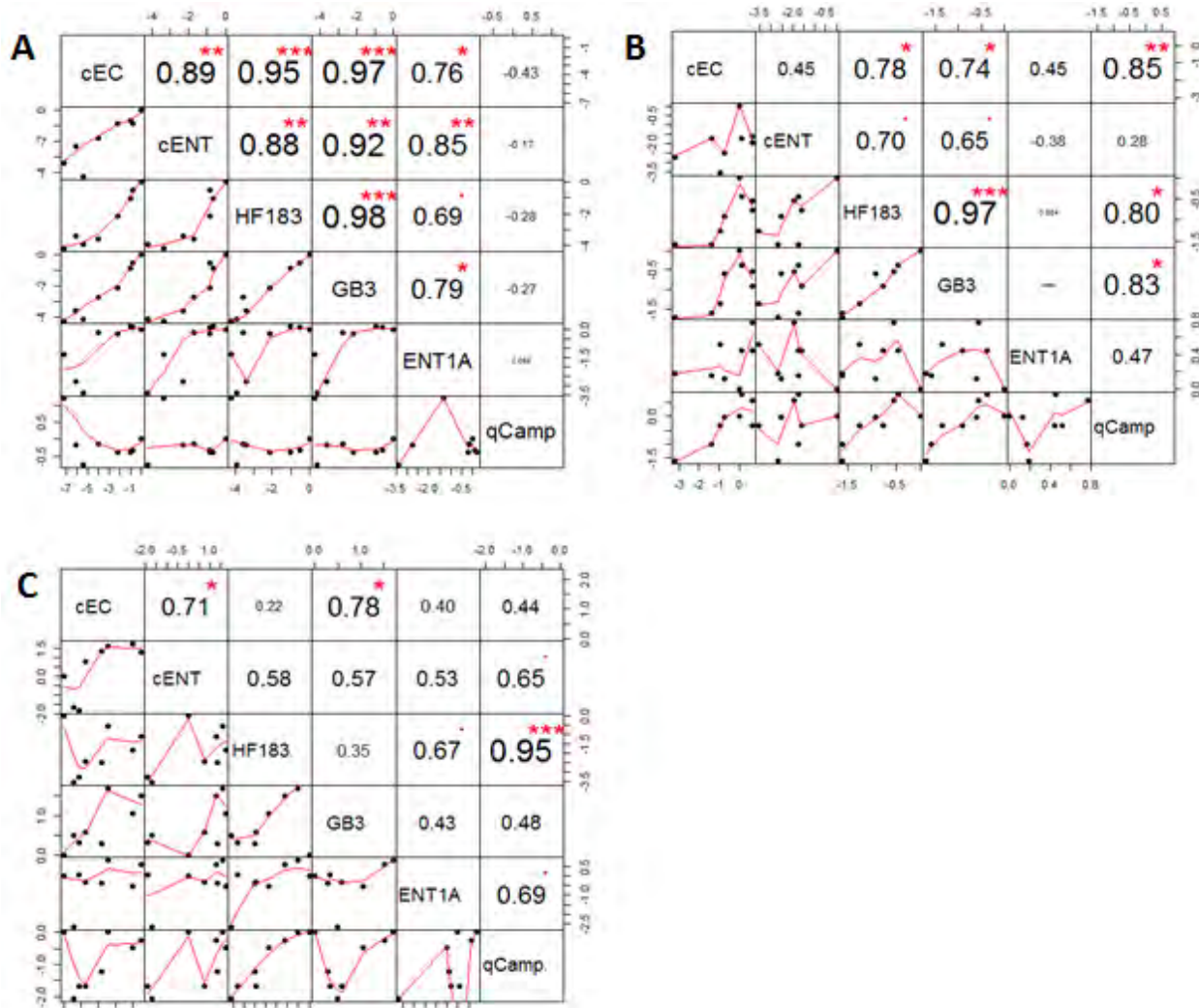


Figure 7. Correlations between decay of each marker in MW (A), BW (B), and FW (C) at 50% inoculum. Ln (C/Co) plotted against ln(C/Co) for each marker. Significant correlations are indicated by a red asterisk at the 0.001(*)/0.01(**), and 0.05(*) levels.**

MW

In the MW sediments, decay rates of the markers (ENT1A, HF183, and GB3) were similar to decay rates observed of culturable EC and ENT and decay was correlated. In contrast, low levels of the qCamp marker persisted in the MW at 10 and 50%. Culturable *Campylobacter* was not observed in the MW at 10 or 50% confounding interpretation of the low qCamp marker levels observed. Despite having similar decay rates, the HF183 marker exhibited log linear decay beginning at day 0 and marker levels fell below the LOQ by day 4 at 10%. All other indicators were detectable until day 7. The GB3 marker exhibited decay most similar to decay of cEC and cENT in the MW sediments; decay rates were comparable as was the magnitude of lag period preceding decay.

BW

In the BW sediment, there was a comparable reduction in concentration of the HF183 and GB3 markers, at 10 and 50%, and the qCamp marker, at 50%, over the course of the eight day study. Decay was correlated between the HF183 and GB3 markers at 10 and 50% and at 50% decay of both the GB3 and HF183 markers was correlated with decay of the qCamp marker. cENT exhibited a similar decay rate to the GB3 and qCamp markers. The ENT1A marker showed increased persistence versus the other indicators; there was not a significant reduction in ENT1A marker levels at either 10% or 50% and ENT1A marker decay was not correlated with decay of any of the other indicators.

FW

In the FW sediment, there was a comparable reduction in levels of the HF183 marker, cENT, and cEC over the eight-day time period. However, there was a difference in decay profile with the HF183 marker exhibiting log linear decaying at similar rate at 10 and 50%, while culturable cEC did not have a decay rate that was significantly different from 0 at 10 or 50%. cENT and the GB3 and HF183 markers had similar decay rates at 10%, although decay of the GB3 marker and cENT was preceded by a significant lag period (2.77 and 3.16 days). The GB3 marker and cEC/cENT exhibited initial growth followed by similar decay at 10% and 50% sewage. The ENT1A marker persisted at higher levels compared to other indicators in FW sediment at 10 and 50%.

Decay in Water Column

A water column sample, the composite of all four replicate beakers, was processed at each time point, starting at day one for FIB, markers, and pathogens in order to account for loss to the water column. The GB3 and ENT1A markers were measured at quantifiable levels until day 7 in all three sediments. Culturable FIB was measured most frequently and at the highest concentrations in the FW microcosms. The FW microcosms were the most turbid (on average turbidity of 418 NTU and 453 NTU in the water column at 10 and 50% versus average turbidity of 5.25 and 3.89 NTU in the BW and 0.66 and 0.62 NTU in the MW microcosms) which may have accounted for increased levels of indicator organisms being resuspended to the water column in the FW microcosms.

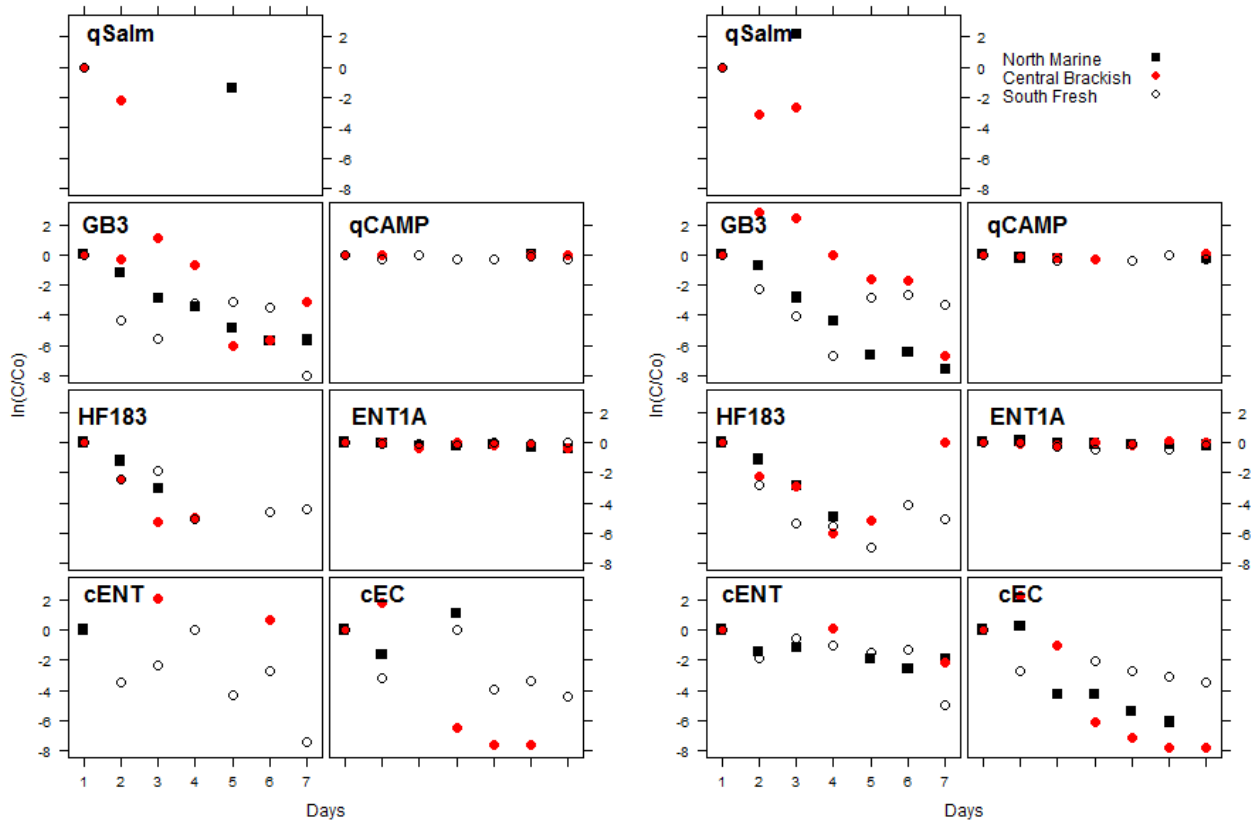


Figure 8. Marker, FIB, and pathogen levels in the water column at A. 10% and B. 50% sewage inoculum.

Literature Cited

- Alm, E.W., J. Burke, A. Spain. Fecal indicator bacteria are abundant in wet sand at freshwater beaches. 2003. *Water research*, 37(16), 3978-3982.
- Bae, S., and S. Wuertz. Survival of host-associated bacteroidales cells and their relationship with *Enterococcus* spp., *Campylobacter jejuni*, *Salmonella enterica* serovar Typhimurium, and adenovirus in freshwater microcosms as measured by propidium monoazide-quantitative PCR. 2012. *Appl. Environ. Microbiol.* 78, 922–32. doi:10.1128/AEM.05157-11
- Boehm, A.B., J. Griffith, C. McGee, T.A. Edge, H.M. Solo-Gabriele, R. Whitman, Y. Cao, M. Getrich, J.A. Jay, D. Ferguson, K.D. Goodwin, C.M. Lee, M. Madison, S.B. Weisberg. Fecal indicator bacteria enumeration in beach sand: a comparison study of extraction methods in medium to coarse sands. 2009. *J. Appl. Microbiol.* 107, 1740–50. doi:10.1111/j.1365-2672.2009.04440.x
- Clesceri, A., A. Greenberg, A. Eaton. *Standard Methods for the Examination of Water and Wastewater*. 20th edition. 1998.
- Craig, D.L., H.J. Fallowfield, N.J. Cromar. Use of microcosms to determine persistence of *Escherichia coli* in recreational coastal water and sediment and validation with in situ measurements. 2004. *J. Appl. Microbiol.* 96, 922–30. doi:10.1111/j.1365-2672.2004.02243.x
- Eichmiller, J.J., A.J. Borchert, M.J. Sadowsky, R.E. Hicks. Decay of genetic markers for fecal bacterial indicators and pathogens in sand from Lake Superior. 2014. *Water Res.* 59, 99–111. doi:10.1016/j.watres.2014.04.005
- Geeraerd, A.H., V.P. Valdramidis, J.F. Van Impe. GInaFiT, a freeware tool to assess non-log-linear microbial survivor curves. 2005. *Int. J. Food Microbiol.* 102, 95–105. doi:10.1016/j.ijfoodmicro.2004.11.038
- Green, H. C., R.A. Haugland, M. Varma, H.T. Millen, M.A. Borchardt, K.G. Field, O.C. Shanks. Improved HF183 Quantitative Real-Time PCR Assay for Characterization of Human Fecal Pollution in Haller, L., E. Amedegnato, J. Poté, W. Wildi. Influence of Freshwater Sediment Characteristics on Persistence of Fecal Indicator Bacteria. 2009. *Water. Air. Soil Pollut.* 203, 217–227. doi:10.1007/s11270-009-0005-0
- Halliday, E. and R.J. Gast. Bacteria in beach sands: an emerging challenge in protecting coastal water quality and bather health. 2011. *Environ. Sci. Technol.* 45, 370–379. doi:10.1021/es102747s
- Heaney, C.D., E. Sams, A.P. Dufour, K.P. Brenner, R.A. Haugland, E. Chern, S. Wing, S. Marshall, D.C. Love, D.C., M. Serre, R. Noble, T.J. Wade. Fecal indicators in sand, sand contact, and risk of enteric illness among beachgoers. 2012. *Epidemiology* 23, 95–106. doi:10.1097/EDE.0b013e31823b504c
- Kim, M. and S. Wuertz. 2015. Survival and persistence of host-associated Bacteroidales cells and DNA in comparison with *Escherichia coli* and *Enterococcus* in freshwater sediments as quantified by PMA-qPCR and qPCR. 2015. *Water Res.* 87, 182–192. doi:10.1016/j.watres.2015.09.014
- Korajkic, A., B.R. McMinn, V.J. Harwood, O.C. Shanks, G.S. Fout, N.J. Ashbolt. Differential decay of enterococci and *Escherichia coli* originating from two fecal pollution sources. 2013a. *Appl. Environ. Microbiol.* 79, 2488–92. doi:10.1128/AEM.03781-12

- Korajkic, A., P. Wanjugi, V.J. Harwood. Indigenous microbiota and habitat influence *Escherichia coli* survival more than sunlight in simulated aquatic environments. 2013b. *Appl. Environ. Microbiol.* 79, 5329–37. doi:10.1128/AEM.01362-13
- Labelle, R.L., C.P. Gerba, S.M. Goyal, J.L. Melnick, I. Cech, G.F. Bogdan. 1980. Relationships Between Environmental Factors , Bacterial Indicators , and the Occurrence of Enteric Viruses in Estuarine. 1980. *Sediments* 39, 588–596.
- Mehlich A. Mehlich 3 soil test extractant: A modification of Mehlich 2. *Comm. Soil Science and Plant Anal.* 15, 1409-1416 .
- Pandey, P.K., M.L. Soupir, C.R. Rehmann. A model for predicting resuspension of *Escherichia coli* from streambed sediments. 2012. *Water Res.* 46, 115–26. doi:10.1016/j.watres.2011.10.019
- Rehmann, C.R. and M.L. Soupir. Importance of interactions between the water column and the sediment for microbial concentrations in streams. 2009. *Water Res.* 43, 4579–89. doi:10.1016/j.watres.2009.06.049
- Steets, B.M. and P.A. Holden. A mechanistic model of runoff-associated fecal coliform fate and transport through a coastal lagoon. 2003. *Water Res.* 37, 589–608. doi:10.1016/S0043-1354(02)00312-3
- Wanjugi, P. and V.J. Harwood. The influence of predation and competition on the survival of commensal and pathogenic fecal bacteria in aquatic habitats. 2013. *Environ. Microbiol.* 15, 517–26. doi:10.1111/j.1462-2920.2012.02877.x
- Zedler, J. 2001. *Handbook for Restoring Tidal Marshes*. CRC Press, Boca Raton.

APPENDIX F. WATER MATRIX EFFECT INVESTIGATION

Introduction

The goal of this task is to understand the attenuation of fecal materials in various representative water matrices from across California using laboratory mesocosm experiments. Field study results were used to determine environmental conditions and sampling times for the laboratory study. Only one representative fecal source, sewage, was tested in this component.

Methods

Field water collection

Waters were collected from three sites from each of the four regions: San Mateo County, Santa Barbara County, Los Angeles County, and Orange County, for a total of 12 different waters for use in the mesocosm experiment (Table 1, Figure S1). Efforts were made to sample a salinity gradient preferably within the same hydrologically connected watershed. However, due to availability of flow at the time of sampling, only the three Orange County sites were hydrologically connected. Arroyo Burro Lagoon, although connected with the upstream creek site, had no surface connection with the ocean (surf zone). Malibu Lagoon was disconnected from both the upstream creek site and the surf zone site. The three northern California sites were not in the same watershed. At each site, 100-120 liter water were collected (in 5 to 6 20-liter cubitainers) and transported on ice in the dark to Kerckhoff Marine Laboratory (Newport Beach, CA) the day before the experiment.

Table 1. Water ID, site description and basic information for the 12 waters used in the experiment.

ID	Site Description	Salinity (ppt)	longitude	latitude
NC01	San Pedro Creek	0.3	122° 30' 19.9434"W	37° 35' 45.5562"N
NC02	Pescadero Marsh Natural Preserve	31.5	122° 24' 42.9012"W	37° 15' 57.564"N
NC03	Pillar Point Harbor	33.6	122° 28' 38.5968"W	37° 30' 7.9524"N
SB04	Arroyo Burro Creek	1.2	119° 44' 24.72"W	34° 24' 17.46"N
SB05	Arroyo Burro Lagoon	6.9	119° 44' 25.404"W	34° 24' 16.164"N
SB06	Surf zone at Arroyo Burro Lagoon Outlet (Outlet closed)	33.1	119° 44' 34.224"W	34° 24' 8.2074"N
LA07	Malibu Creek	1.0	118° 41' 16.8972"W	34° 2' 44.7468"N
LA08	Malibu Lagoon (disconnected from Malibu Creek)	30.1	118° 40' 59.0088"W	34° 2' 4.9992"N
LA09	Surf zone at Malibu pier	33.1	118° 40' 36.9984"W	34° 2' 12.0012"N
OC10	San Diego Creek	1.6	117°51'35.32"W	33°39'37.83"N
OC11	San Diego Creek	18.6	117°50'23.72"W	33°39'5.05"N
OC12	Surf zone at Kerckhoff Marine Laboratory	33	117°52'47.33"W	33°35'48.86"N

Sewage

Sewage used for spiking the mesocosms was primary influent (grab sample) from Orange County Sanitation District (Costa Mesa, CA) collected the day before the experiment. A total 50-60 liter sewage was mixed (200rpm, 25min) then dispensed into 12 portions of 3.5 liter each, and stored in 4 °C until mesocosm setup. Sewage samples were also archived for molecular characterization.

Outdoor mesocosms

A 4-day outdoor experiment (April 23 to April 27, 2015) was conducted using 36 mesocosms on the patio of Kerckhoff Marine Laboratory (Figure 1). For each of the 12 waters, 3 mesocosms were used: two mesocosms contained 30 liter of 5% (v/v) sewage while the third mesocosm was not spike and served as a control.

The mesocosms were constructed from rectangular glass aquariums (dimension, material etc.). Each aquarium was equipped with two airstones for mixing and a sterile siphon tube for sampling. All aquariums were placed in six large trays containing circulating seawater. The seawater flow rate were adjusted and temperature inside the aquarium monitored in preliminary experiments to ensure mesocosm water temperature at ambient seawater temperature during the formal experiments. The aquariums were not covered, but the depth of the water were monitored to account for evaporation. The 30 liter volume was determined so that at least half of the volume will remain in the aquariums after accounting for sampling and evaporation losses.



Figure1. Water matrix mesocosm study on the outdoor patio of Kerckhoff Marine Laboratory.

Mesocosm setup

Mesocosms were setup during the evening of April 22, 2015 (i.e. the night before the experiment) after dark to avoid any potential changes due to high ambient temperature and sun exposure. For each ambient water, 100 liter was mixed (air blow, 20 minutes) in a large sterile tank equipped with an air blower and a spigot at the bottom, for mixing and dispensing sample, respectively. Upon complete mixing, 30 liter mixed water was dispensed to fill the corresponding control mesocosm, and additional 3.5 liter were saved at 4C for arching and sample processing. To the remaining 66.5 liter of mixed water, 3.5 liter

sewage were mixed in (air blow, 20 minutes) to obtain 5% (v/v) sewage-spiked water for the two spiked mesocosms. Each of the 12 sewage-spiked waters was also save at 4C until sampling processing.

Sample collection

Samples were collected at six time points during the 4-day experiment: hour 0 (8am) and hour 6 (2pm) on 4/23/2015, then daily at 8am till 4/27/2015. A 1-liter sample was collected from each mesocosm into an acid-cleaned (regular wash followed by 10% HCl >15min) bottle via the attached siphon tubing after discarding the first 15-20ml (30second) of outflow. All samples were transported on ice in the dark back to the main laboratory (Southern California Coastal Water Research Project Authority) for processing within 6 hours.

Sample processing and analysis

Samples were processed and analyzed for FIB and human fecal-associated markers. Each sample was analyzed in duplicate for *Enterococcus* and *E. coli* and total coliform by Enterolert and Colilert (IDEXX Laboratory), respectively, at appropriate dilutions. Additionally, for bacterial molecular analysis, 100 ml of each sample was filtered directly onto polycarbonate filters (0.45um pore size), then flash frozen in liquid nitrogen and stored in -80C until DNA extraction. *Enterococcus*, total Bacteroidales, and human fecal-associated Bacteroidales (i.e. HF183 marker) were analyzed by droplet digital PCR.

Decay modeling

All data out of quantification range were excluded before decay modeling. FIB and marker concentrations (MPN per 100ml and copy per 100ml) were log10 transformed before analysis. Preliminary analysis indicated a simple log linear model was appropriate to model the decay behaviors of targets measured: $\text{Log}_{10}C = \text{Log}_{10}C_0 - k t$. Decay rates k were reported as per day.

Results

Decay rates

Overall, the duplicate mesocosms were highly consistent in measured target concentration at different time points (Figure 2). Therefore, data from both mesocosms were pooled for decay rate estimates.

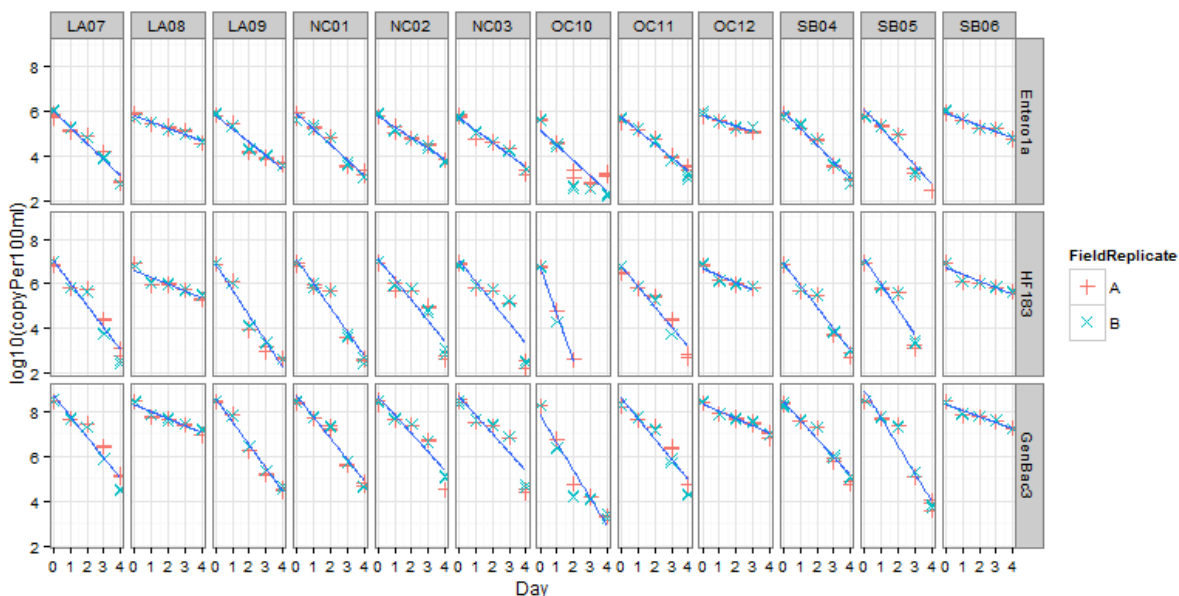


Figure 2. Decay curves and Log-Linear model fitting on genetic targets. Red crosses and green x-crosses indicate data from two replicate mesocosms. Blue lines denote the regression line corresponding to log linear model fit.

Enterococcus and *E. coli* measured by culture-based methods decayed much faster than genetic markers measured by digital PCR (Tables 2, 3). Culture-based *Enterococcus* and *E. coli* signals in all 12 waters disappeared by day 2 and 3, respectively, while all genetic markers were still above detection limits by the end of the mesocosm experiments (i.e. day 4, Figure 2). Because of the fast decay of culturable *Enterococcus* and *E. coli*, decay modeling could not be performed on all waters due to lack of data (Table 2).

Table 2. Decay rates and standard deviation of culturable *Enterococcus* and *E. coli*.

WaterID	Enterococcus	E.coli
	k(sd)	k(sd)
LA07	-3.58 (0.75)	-1.96 (0.68)
LA08	-2.44 (0.38)	-1.29 (0.88)
LA09	-3.02 (0.71)	-2.68 (1.66)
NC01	-3.25 (0.36)	-2.63 (1.42)
NC02	NA*	-2.44 (1.07)
NC03	NA	NA
OC10	NA	-2.23 (0.6)
OC11	-2.23 (0.67)	-1.56 (0.52)
OC12	-1.62 (0.49)	-1.76 (1.11)
SB04	-2.29 (0.3)	-2.1 (0.71)
SB05	-2.51 (0.11)	-1.66 (0.49)
SB06	-2.71 (0.43)	NA

*Decay rate estimates not available due to insufficient data.

Table 3. Decay rates and standard deviation of genetic markers for *Enterococcus*, total Bacteroidales, and human fecal-associated Bacteroidales (i.e. HF183 marker).

WaterID	Entero1a	GenBac3	HF183
	k(sd)	k(sd)	k(sd)
LA07	-0.72 (0.03)	-0.93 (0.05)	-0.99 (0.05)
LA08	-0.28 (0.02)	-0.31 (0.02)	-0.31 (0.03)
LA09	-0.6 (0.04)	-1.04 (0.03)	-1.15 (0.06)
NC01	-0.68 (0.03)	-0.94 (0.05)	-1.07 (0.06)
NC02	-0.48 (0.02)	-0.82 (0.07)	-0.93 (0.08)
NC03	-0.55 (0.03)	-0.83 (0.09)	-0.93 (0.09)
OC10	-0.68 (0.08)	-1.23 (0.08)	-2.12 (0.1)
OC11	-0.6 (0.02)	-0.91 (0.06)	-0.91 (0.06)
OC12	-0.24 (0.02)	-0.33 (0.01)	-0.32 (0.04)
SB04	-0.75 (0.03)	-0.82 (0.04)	-0.98 (0.05)
SB05	-0.83 (0.07)	-1.23 (0.06)	-1.12 (0.11)
SB06	-0.28 (0.01)	-0.27 (0.02)	-0.3 (0.03)

Additionally, decay rates of the different genetic markers were highly correlated (Figure 3), indicating potentially similar water matrix effects on different genetic markers.

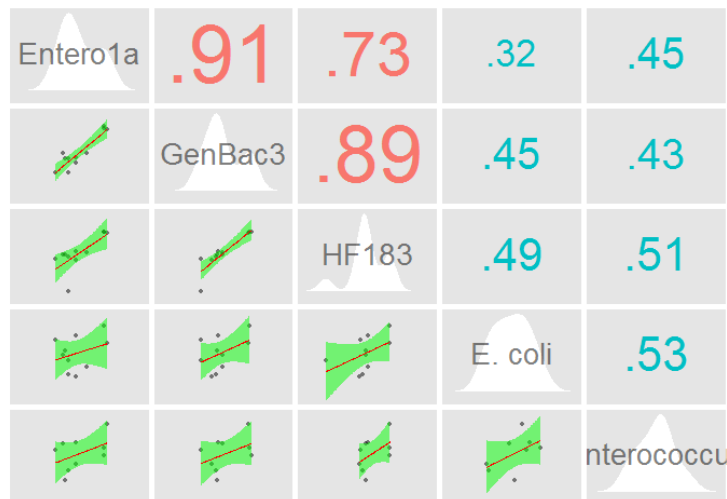


Figure 3. Relationship between decay rates from different fecal targets. Regression lines are in red with green shades indicating 95% CI of the regression. Significant correlations are indicated by red correlation coefficients.

Relationships between decay rates and water matrices

Decay rates were correlated to various environmental parameters (salinity, turbidity of the raw water, turbidity of the spiked water etc.) to explore relationships between decay rates and water matrices. Decay rates appeared to increase with salinity of the water matrices, indicating salinity or some factor correlated to salinity might be influencing decay rates (Figure 4). Further investigation of abiotic (such as UV absorbance of the water, Figure 5) and biotic (such as predation) parameters of the water matrices may shed additional light on this relationship.

Additionally, there is also some evidence that culturable *Enterococcus* and *E. coli* appeared to decay much faster in the three waters from northern California (NC01 to NC03) than in those from southern California.

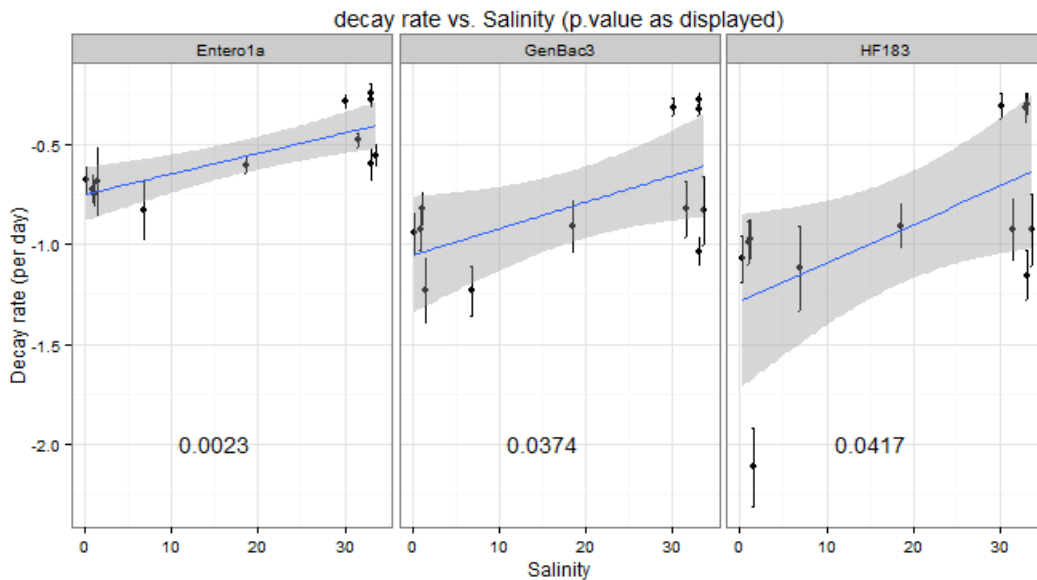


Figure 4. Relationship between decay rates and salinity of the water matrices. P-values are as displayed in each panel.

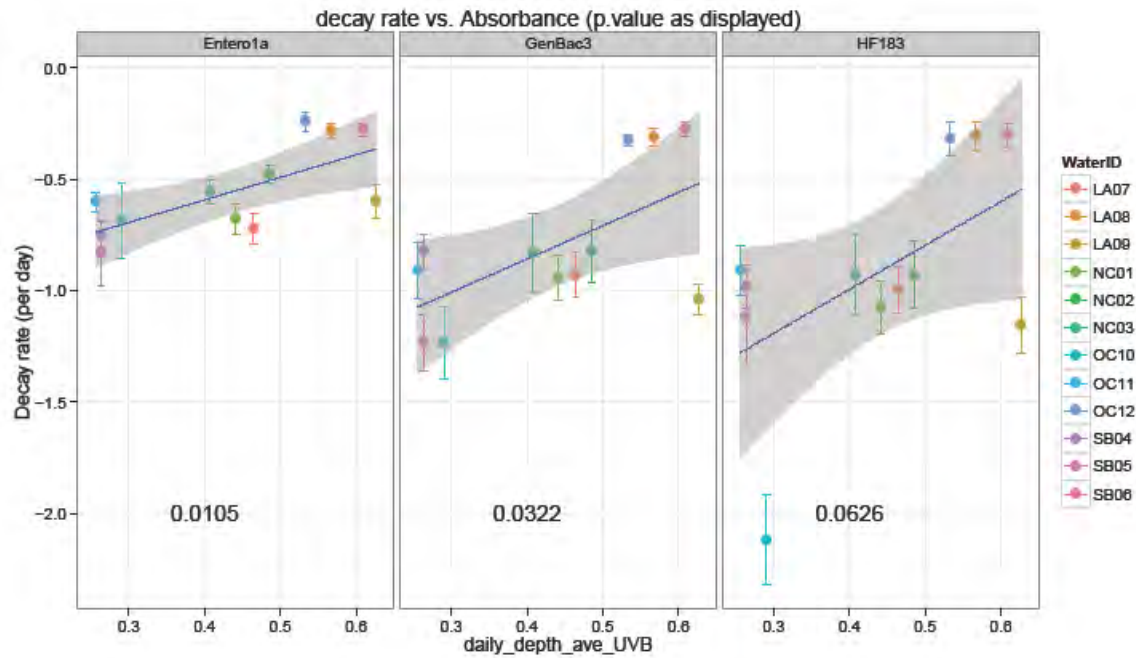


Figure 5. Relationship between LL decay rates and daily averaged UVB absorbance of the waters. p-values are as displayed in each panel.

Supporting Information

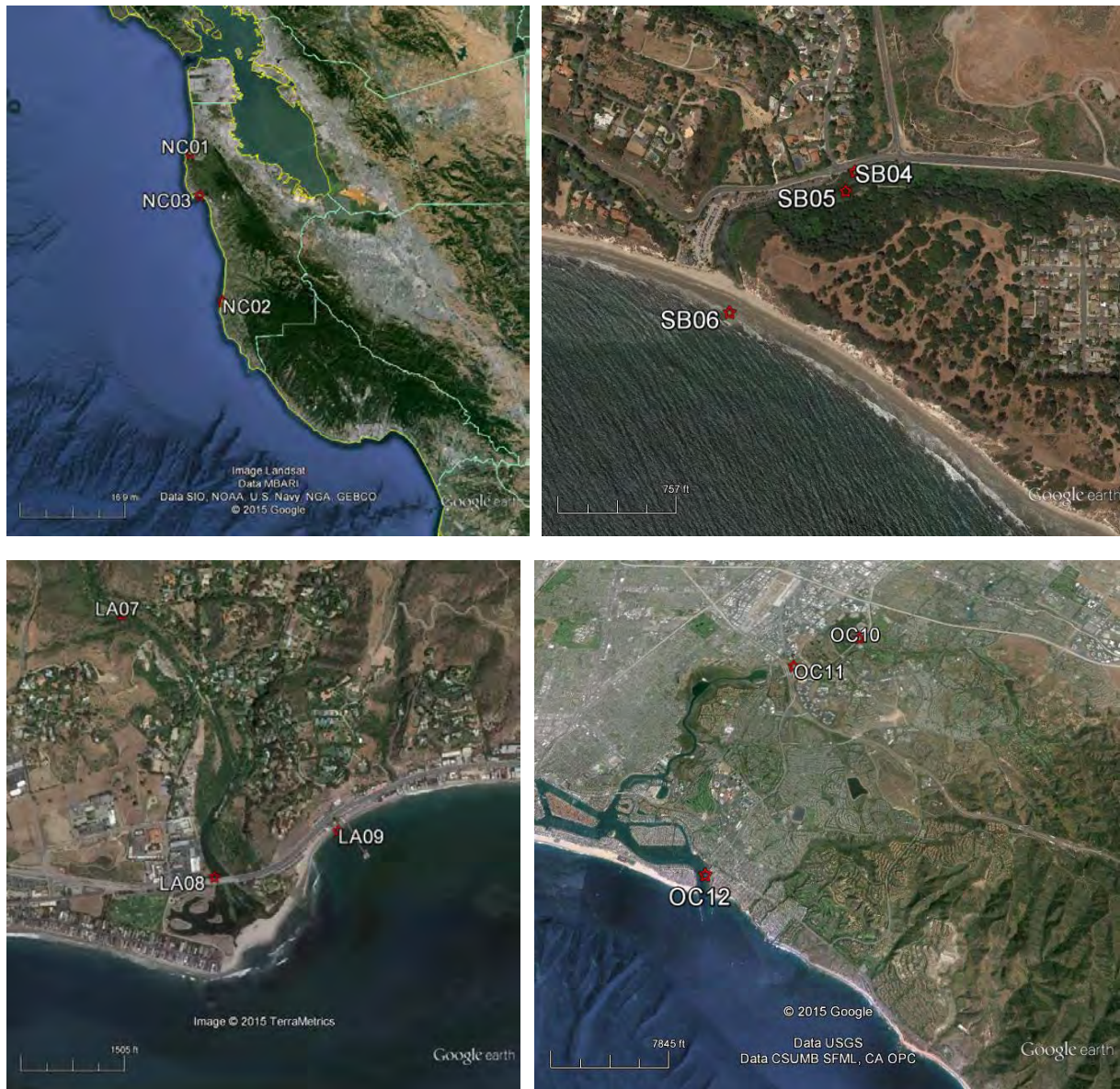


Figure S1. Locations of the water sampling sites in San Mateo County (sites NC01-03), Santa Barbara County (sites SB04-06), Los Angeles County (sites LA07-09), and Orange County (sites OC10-12).

APPENDIX G. RATIO MODEL: THE EFFECT OF AGING ON THE USE OF THE SOURCE ALLOCATION MODEL

Introduction

As part of the SIPP project, a conceptual framework was developed for allocating sources of enterococci and *E. coli* in ambient waters using microbial source tracking (MST) markers (Wang et al. 2013). This model was peer reviewed and is published in *Water Research*.

In brief, in a sample of water, the proportion (P) of enterococci or *E. coli* from a specific fecal source is:

$$P = R_m/R_{feces}(t) \quad (\text{Eqn. 1})$$

where R_m is the ratio of the concentration of MST marker and the FIB being allocated in the ambient water sample and $R_{feces}(t)$ is the ratio of the concentrations of MST marker and FIB in feces aged at time t . The time t is the age of the fecal contamination. $R_{feces}(t=0)$ is the ratio in fresh feces, sewage, or septage.

This method relies on the fact that the MST markers are specific. In the SIPP study, At least two specific human markers were identified in addition to specific animal markers. If there is any cross reactivity between MST markers and non-target fecal sources, this method will not work.

The model for source allocation (equation 1) simplifies if the source of contamination is fresh. It becomes $P=R_m/R_{feces}(t=0)$. If the source of contamination is aged, the model may only be used if the following facts are known: 1) the age of contamination (t), and 2) the ratio R_{feces} at time t . In practice, it may be difficult to know the age of contamination. If the age is known or can be estimated, then knowledge on the decay characteristics of the FIB being allocated and the MST marker in the ambient water matrix can be used to determine $R_{feces}(t)$. In the situation where decay of the FIB being allocated and the MST marker is identical, then their ratio R_{feces} is constant and it is not necessary to know the age of contamination even if the contamination is not fresh.

During the aging study, FIB and MST markers were evaluated to determine whether or not they decay at the same rate in seawater, freshwater and brackish water using field deployments. If they do decay at the same rate, then knowing the age of contamination will not be necessary to use the source allocation model since R_{feces} will be constant regardless of fecal contamination age.

Methods

A comparison between the decay of FIB and human MST markers was conducted at all three field sites. Comparison between FIB and cow marker, and FIB and gull marker was also conducted for the freshwater water site.

UCSB provided their decay models for the brackish sites. Stanford developed decay models for the marine and freshwater sites. Decay models could contain a shoulder (an initial period when no decay occurred), a log-linear decay (during which first order decay kinetics occur), and a tail (during which concentrations were constant at the end of the experiment).

In the present analysis, first order rate constants k (units per day) were compared from the decay models. k describes the decay during the log-linear portion of the decay. The shoulder or tail was not considered (if either was included in the decay models). The shoulder or tail were not included for parsimony. First, the current literature on bacterial decay modeling uses first order decay constants as input, and the presence of a shoulder and tail has not been considered to date in fate and transport modeling. Second, it is not clear whether the shoulder and tail are experimental artifacts or are intrinsic decay characteristics.

Third, not all the models included shoulders and/or tails. While we chose to compare k values herein, future work may consider the entire decay curve obtained from the experiments.

The following hypotheses were tested for each experimental treatment (Table 1):

- H1) Enterococci measured by culture (cENT) has the same k as HF183
- H2) Enterococci measured by culture (cENT) has the same k as HumM2
- H3) Enterococci measured by culture (cENT) has the same k as HumBac
- H4) *E. coli* (EC) measured by culture (cENT) has the same k as HF183
- H5) *E. coli* (EC) measured by culture (cENT) has the same k as HumM2
- H6) *E. coli* (EC) measured by culture (cENT) has the same k as HumBac
- H7) Enterococci measured by QPCR (tENT) has the same k as HF183
- H8) Enterococci measured by QPCR (tENT) has the same k as HumM2
- H9) Enterococci measured by QPCR (tENT) has the same k as HumBac

The following hypotheses were tested in the freshwater treatments:

- H1) Enterococci measured by culture (cENT) has the same k as CowM2
- H2) Enterococci measured by culture (cENT) has the same k as LeeSeaGull
- H3) *E. coli* (EC) measured by culture (cENT) has the same k as CowM2
- H4) *E. coli* (EC) measured by culture (cENT) has the same k as LeeSeaGull
- H5) Enterococci measured by QPCR (tENT) has the same k as CowM2
- H6) Enterococci measured by QPCR (tENT) has the same k as LeeSeaGull

Table 1. Experimental Treatments

1	Marine surface summer
2	Marine depth summer
3	Marine surface winter
4	Marine middle winter
5	Marine depth winter
6	Freshwater shaded summer
7	Freshwater unshaded summer
8	Freshwater unshaded winter
9	Brackish water shaded summer
10	Brackish water unshaded summer

k values were compared using a t-test with $\alpha = 0.05$. Specifically, the difference in k values from the assays was tested in each stated hypotheses to determine if the value was different from 0. The t-statistic was generated using the following equation:

$$t = (k_1 - k_2) / \sqrt{SE_1^2 + SE_2^2}$$

where k_1 and k_2 are the two k values and SE_1 and SE_2 are the standard errors from the model fitting program. If $|t| > 1.96$ when the difference between the k values was deemed different from 0 and the null hypothesis was rejected. No adjustments were made for multiple hypothesis testing.

Results

Marine waters

The decay data from the marine site at Pillar Point Harbor were fit with models to obtain first order decay constants. In some cases (15 out of 30 models, data not shown), a shoulder log-linear model was needed. Tails were not considered in the models. k values from the experimental treatments (2 seasons and the different depths in the water column) are provided in the Table 2.

Table 2. First order decay rate constants k and their 95% confidence intervals (in parentheses) in units d^{-1} for experiments conducted in marine waters at Pillar Point Harbor.

	Summer	Summer	Winter	Winter	Winter
	Surface	Depth	Surface	Middle	Depth
Target	K (per d)				
HF183	1.7 (0.23)	1.4 (0.15)	1.3 (0.32)	1.7 (0.36)	1.7 (0.46)
BacHum	1.7 (0.13)	1.4 (0.20)	1.4 (0.30)	1.8 (0.31)	1.7 (0.43)
HumM2	1.7 (0.12)	1.3 (0.18)	1.2 (0.25)	1.8 (0.35)	1.7 (0.48)
tENT	1.60 (0.27)	0.93 (0.23)	0.75 (0.14)	0.87 (0.23)	0.89 (0.41)
cENT	6.56 (0.85)	2.40 (0.46)	3.92 (0.20)	3.32 (0.37)	1.41 (0.22)
EC	4.8 (0.65)	1.7 (0.23)	3.9 (0.60)	3.0 (0.98)	2.2 (0.33)

The results of the tests determined whether enterococci by culture (cENT), enterococci by QPCR (tENT), and *E. coli* by culture (EC) decayed at different rates than HF813, BacHum, and humM2. The results varied depending on which season and depth the experiments were done, likely due to the diverse response of the targets to photoinactivation (UVB and UVA incident on the experimental bags will vary by season and depth of deployment).

Under the highest light conditions (summer experiments conducted at the surface of the water column), tENT k was the same as k of the three human MST markers while EC and cENT k s were significantly different than k of the three MST markers (FIB decayed more quickly than the markers).

In the summer depth treatment, the human markers and the FIB had significantly different k values with one exception: EC k was the same as BacHum k . cENT and EC had higher k than the MST markers while tENT had a lower k than the markers.

In the winter surface treatment, k of MST markers were significantly different from FIB k values. k s of cENT and EC were higher than those of the MST markers while tENT k was lower than the MST marker k s. The same result holds for the winter middle depth treatment.

Under the lowest light conditions (winter at depth), cENT and EC did not have different k than the MST markers. However tENT k was significantly smaller than MST marker k values.

In marine waters with low transmittance of UVB and UVA, the decay rates of the three human MST markers and fecal bacteria were the same. At higher light levels, the cultivatable organisms decay more quickly than the MST markers.

In terms of the source allocation model, these results suggest the following for marine waters:

1. Allocation sources of cENT and EC using the source apportionment model is only possible when light conditions are low. This could be in turbid or colored waters, or in waters deeper than 1 m that are not well mixed. The precise conditions will be explained in the final report.
2. Allocation of sources of tENT is possible in low light waters, as well as high light waters, but may not be possible at intermediate light levels.

Freshwaters

The decay data from the freshwater site in the Irvine Wetlands were fit with models to obtain first order decay constants. In some cases (3 out of 47 models, data not shown) a shoulder log-linear model was needed.

The first order decay rate constants for targets from the freshwater deployment seeded with sewage are shown in Table 3. We compared whether the k values between general markers of fecal contamination (cENT, EC, and tENT) were different than the k values for the MST markers (HF183, HumM2, and BacHum) among experimental treatments.

Under summer conditions with no shade (summer sun), MST markers and cENT had similar k values; there was no significant difference in ks of cENT and the human MST markers. EC k was the same as humM2 k, but EC k was different from HF183 and BacHum ks (EC k was smaller). tENT had a k value that was significantly different than the MST markers (tENT k was smaller). During the summer shaded conditions, ks of all the MST markers were higher than ks of cENT, EC, and tENT.

During the winter treatment, EC k was the same as MST marker ks. ENT k was the same as HF183 and BacHum ks, but ENT k was different (lower) than HumM2 k. tENT k was different (lower) than all MST marker ks.

Table 3. Decay rates constants (k) of targets listed from the freshwater treatments seeded with sewage. k (\pm 95% confidence interval) are the fitted decay rate constant (per day)

	Summer	Summer	Winter
	Sun	Shade	Sun
	K (per d)	K (per d)	K (per d)
HF183	3.30 (1.15)	4.49 (0.44)	1.11 (0.23)
BacHum	3.88 (1.01)	4.02 (0.85)	1.22 (0.23)
HumM2	2.68 (1.02)	3.55 (0.55)	1.74 (0.54)
tENT	1.59 (0.17)	1.03 (0.34)	0.39 (0.04)
cENT	2.97 (0.99)	1.80 (0.52)	1.08 (0.19)
EC	1.82 (0.32)	0.76 (0.36)	1.82 (0.78)

The decay constant (k) of the cowM2 marker was compared to ks of cENT, tENT, and EC in the treatments seeded with cow feces (Table 4). In the summer sun (unshaded) treatment, cENT and EC had different k values than the MST marker (k was higher for the marker than for the FIB) while tENT k was not different from the MST marker. In the summer shaded treatment, cENT k and cowM2 k were the same, but EC and tENT ks were different than CowM2 k. In the winter treatment, tENT and cENT ks were the same as k of CowM2 but EC k could not be determined during this treatment since it could not be fit with a decay model (no decay was observed for EC).

Table 5. Decay rates constants (k) of targets listed from the freshwater treatments seeded with bird feces. k (\pm 95% confidence interval) are the fitted decay rate constant (per day).

	Summer	Summer	Winter
	Sun	Shade	Sun
	K (per d)	K (per d)	K (per d)
LeeSeaGull	1.58 (0.27)	1.74 (0.46)	0.87 (0.19)
tENT	1.63 (0.11)	0.85 (0.22)	0.39 (0.11)
cENT	2.12 (2.71)	2.70 (0.82)	0.90 (0.39)
EC	2.46 (2.07)	1.29 (0.59)	0.44 (0.26)

LeeSeaGull marker k was compared cENT, tENT, and EC ks in the treatments seeded with bird feces. In the summer sun (unshaded) treatment, ks of the bird marker and FIB were not different. In the summer shaded treatment, cENT and tENT had significantly different ks than the bird marker (cENT k higher and tENT k smaller than the marker). In the winter treatment, cENT and the bird marker did not have different k values, while tENT k was significantly different than k of the marker, and k of EC was significantly different than k of the marker (ks of the FIB were smaller than k of the marker).

Brackish site

The decay data from the brackish site in Santa Barbara were fit with models to obtain first order decay constants (Table 6). In some cases (10 out of 18 models, data not shown) a shoulder log-linear model was needed.

Table 6. First order rate constants k, with units per day and their 95% CI in parenthesis for the brackish site.

Target	Summer	Summer	Winter
	no shade	shade	no shade
	k (per d)	k (per d)	k (per d)
HF183	5.2 (0.82)	4.67 (0.9)	1.65 (0.22)
BacHum	5.64 (1.35)	4.29 (1.45)	1.63 (0.24)
HumM2	4.16 (0.9)	5.32 (1.04)	1.93 (0.37)
tENT	1.09 (0.16)	0.79 (0.1)	0.61 (0.06)
cENT	3.25 (0.31)	2.6 (0.73)	1.61 (0.35)

EC 2.61 (0.27) 1.4 (0.1) 2.15 (0.29)

During the summer sun (unshaded) treatment, k values for the FIB were significantly different (and smaller) than the k values for the three human markers with one exception. The exception was that cENT and HumM2 had k values that were not significantly different. During the summer-shaded treatment, k values for the FIB were significantly different (and smaller) than the k values for the three human markers.

For the winter treatment, the cENT k was not different from those for the three human markers. tENT k was significantly different (smaller) than the k for all three human markers. EC k was not different from humM2 k yet was significantly higher than HF183 and humBac k.

Summary

Tables 7 and 8 summarize the results of the comparison. Overall, the decay of FIB and markers varied. At the marine site, a physical-chemical-biological explanation is available to explain when the FIB and MST markers have the same and different k. The reasons for the differences between FIB and MST k values will be explored within reports by the other researchers on this project.

Taken all together, there are only certain conditions when k values are the same. One cannot assume a priori that they are.

Table 7. Summary of experimental treatments when k was the same between each class of FIB and each MST marker.

	HF183	BacHum	HumM2	CowM2	LeaSeaGull
cENT	marine winter depth, freshwater summer sun & winter sun, brackish winter sun	marine winter depth, freshwater summer sun & winter sun, brackish winter sun	marine winter depth, freshwater summer sun, brackish winter sun & summer sun	fresh summer shaded & winter sun	fresh summer sun, fresh winter sun
tENT	marine summer surface	marine summer surface	marine summer surface	freshwater summer sun & winter sun	freshwater summer sun
EC	marine winter depth, freshwater winter sun	marine winter depth & summer depth, freshwater winter sun	marine winter depth, brackish winter sun, freshwater summer sun & winter sun		freshwater summer sun & summer shade

Table 8. Percent of within treatment comparisons where k of the FIB and MST marker were the same.

	HF183	BacHum	HumM2	CowM2	LeaSeaGull
cENT	36%	36%	36%	67%	67%
tENT	9%	9%	9%	67%	33%
EC	18%	27%	36%	0%	67%

To determine how a difference in k might affect the results of the source allocation model, the following question was asked:

How does the proportion of contamination as measured by cENT from human vary with the age of contamination using the source apportionment model?

For this hypothetical example, HF183 is used to allocate enterococci to a raw sewage source. In this example, the initial concentration of enterococci and HF183 in the ambient water, as well as their concentrations in raw sewage must be specified. It is assumed that concentrations of enterococci and HF183 in the ambient water were 4000 CFU/100 ml and 100 copies / 100 ml, respectively. In the raw sewage, concentrations of 1.54×10^6 CFU/100 ml and 10^7 copies / 100 ml, are assumed respectively. The values from sewage were taken from the SIPP study and a paper by Shanks et al. (2010). It is assumed that the ambient water is marine and that the decay rates measured in the summer at surface and at depth apply. Equation 1 can be rewritten as:

$$P = [R_m/R_{feces}(t=0)] * \exp(t*(k_{hf}-k_{ent}))$$

where R_m is the ratio in ambient water, $R_{feces}(t=0)$ is the ratio in fresh raw sewage, and k_x is the first order decay of target x (either HF183 (HF) or enterococci (ENT)). To be clear, R_m and R_f are equal to the concentration of MST marker divided by the concentration of the fecal bacteria in the appropriate matrix.

As illustrated in Figure 1, the source allocation model predicts that given the concentrations of enterococci and HF183 MST markers in the ambient waters, raw sewage derived enterococci accounts for 0.4% of the enterococci if the contamination is fresh. If the contamination is not fresh (i.e., it is aged), the model predicts even lower contributions of raw sewage-derived enterococci to the ambient enterococci.

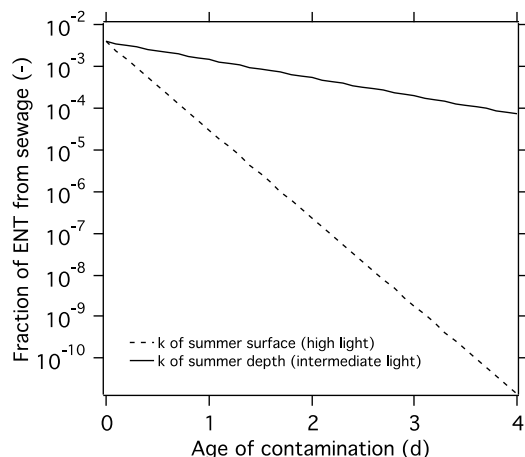


Figure 1. The proportion (P) of enterococci from raw sewage (labeled as fraction here) using the source apportionment model as a function of the age of contamination. Here we have used the decay rates of enterococci and HF183 from the ocean site in summer at the surface and at depth in the water column.

For this example, of the contamination at the beach cannot be determined, so it is assumed to be fresh. Under high light conditions, if assume the contamination is assumed to be fresh, but it is really aged, the proportion of enterococci from raw sewage will be over-predicted. This over-prediction could be significant. For example, if the contamination is 4 days old, but it is assumed to be fresh, then the prediction is that 0.4% of the enterococci are from raw sewage, when really, 10^{-8} are from raw sewage. The over-prediction is 7 orders of magnitude.

Under lower light conditions (where enterococci and HF183 still decay at different rates), there is still an over-prediction of the contribution of raw sewage to the total enterococci if the pollution is assumed to be fresh. However, the over-prediction is not as severe as the case for high light conditions. As above, if the pollution is assumed to be fresh, then 0.4% of the enterococci are predicted to be from raw sewage. If the pollution is really 4 days old, then the true proportion of enterococci from raw sewage would be 0.007%. So the over-prediction is 2 orders of magnitude.

This example illustrates that when the decay rates of the source tracking marker (here HF183) and the fecal bacteria being allocated (here enterococci) diverge, the source allocation model will likely not be useful.

Literature Cited

Wang, D., A.H. Farnleitner, K.G. Field, H.C. Green, O.C. Shanks, A.B. Boehm. Enterococcus and Escherichia coli fecal source apportionment with microbial source tracking genetic markers--is it feasible? *Water Research* **2013**, *47*, (18), 6849-61.

APPENDIX H. HUMAN FECAL SCORE (HFS)

Human fecal contamination is a major issue for beach water quality because human fecal material generally poses much greater public health concern than non-human fecal sources. To effectively allocate resources for contamination remediation and to effectively evaluate the success of clean up, managers need tools to assess the extent and certainty of human fecal contamination at a site. SIPP study has identified sensitive and specific human markers for identifying human fecal contamination. However, data interpretation remains a hurdle for managers because lack of standardized approach for integrating human marker results from multiple samples from a given site.

This report describes the development of a human fecal score and recommendations in using it for site prioritization for remediation.

Background

Assessing the extent and certainty of fecal contamination has been mostly approached via best profession judgement (BPJ) available within the premise of each individual project. As a way to investigate the consistency and viability of such BPJ approaches, the SIPP project organized a group of 10 experienced MST researchers from academia, federal and local regulators, and local sanitation districts who were given an identical human MST marker data set from 26 ‘fake’ beaches and asked to rank them according to the extent of human fecal pollution at the 26 beaches. The ranking outcomes demonstrated tremendous variability/uncertainty/inconsistency in the BPJ approaches used for interpreting MST marker results.

This work was published in 2013 and the team concluded that a mathematically defined standardized algorithm is needed for integrating MST marker results from multiple samples across a site (Cao et al. 2013). As a result, a probabilistic-based framework was conceptualized in the SIPP project to establish such an algorithm called the human fecal score (HFS). It is also recognized that marker degradation would play an important role in interpreting such a score.

The aging project team therefore has been tasked to further develop and refine this model (along with the ratio model in addressing question #1) and provide recommendation to management (regulators and beach managers) for how to use this quantitative MST models in solving real world problems.

Three major tasks have been completed on the probabilistic model during the aging study. These tasks were completed through collaboration with USEPA researchers. Such collaboration not only leverages resources from federal government but also adds to the applicability of the HFI across the nation.

1. Completion of further developing and refining the mathematical formula of the human fecal score (HFS)
2. Completion of model sensitivity analysis to investigate the effects of sample size (how many samples to take per beach site), number of qPCR replicates per water sample, and different site pollution characteristics on the value and variance of the HFI
3. Completion of demonstrating initial use of the HFI for ranking sites based on their extent of human fecal pollution

Completed Work Task 1: Model description

The HFS takes into account all data from a given site in order to reliably characterize its extent of human fecal contamination (Figure 1). All data include human marker results that are non-detect and detected but not quantifiable (i.e. MPN range in Figure 1), and quantifiable (i.e. ROQ range in Figure 1). Previously,

the MPN range could not be integrated and utilized to characterize a site in a quantitative fashion. The HFS utilizes the Poisson probabilistic distribution to combine data from both MPN and ROQ ranges to provide a weighted average of all measurements.

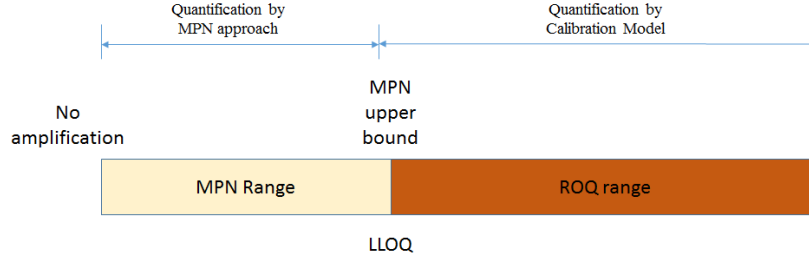


Figure 1. The HFS takes into account all MST data from a site, including non-detects, detected but not quantifiable, and quantifiable results. MPN: most probable number. ROQ: range of quantification. LLOQ is the lower limit of quantification.

The HFS is calculated via Bayesian statistics as a weighted average from all HF183/BacF287 (the human marker assay that is set to become the nationally standardized human fecal MST assay) qPCR measurements from a series of samples collected at a particular site over a designated period of time. The measurements are \log_{10} -transformed prior to the calculations.

Let the number of water samples collected at a beach in ROQ range be r and the number of replicates per sample be n . Suppose the average C_q and the standard deviation of the i^{th} sample are \bar{C}_{qi} and s_i , respectively where $i = 1, 2 \dots r$. Then the standard deviation s of the overall mean \bar{C}_q of all \bar{C}_{qi} is $\sqrt{(s_1^2 + s_2^2 + \dots + s_r^2)/(n \cdot r^2)}$. A normal distribution with mean \bar{C}_q and variance s^2 is assumed for true C_{q0} (i.e. $C_{q0} \sim N(\bar{C}_q, s^2)$). The posterior distribution of

$$\log_{10} C_1 = (C_{q0} - \alpha) / \beta \quad (1)$$

is used to estimate the mean concentration C_1 (in \log_{10} base), where α and β are the intercept and slope parameters of the master calibration curve.

Out of the remaining m samples with n replicates per sample, which are in the MPN group, let the total number of negative C_q measurements be n_0 and $N = n \cdot m$. The following Bayesian model is used to estimate the concentration C_2 in the MPN range:

$$\begin{aligned} n_0 &\sim \text{Bin}(N, p) \\ p &= e^{-C_2} \\ C_2 &\sim \text{Poisson}(e^\mu) \\ \mu &\sim N(0, 10^3) \end{aligned} \quad (2)$$

Note that the above approach provides an estimate for $\log_{10} C_2$, even if $n_0 = 0$ or N .

The HFS (in log₁₀ base) is defined as the weighted average of log₁₀ C₁ and log₁₀ C₂ and is given by:

$$\log_{10} \text{HFS} = W \cdot \log_{10} C_1 + (1 - W) \cdot \log_{10} C_2 \quad (3)$$

where, $W = r/(r+m)$.

Thus, HFS is given by:

$$\text{HFS} = 10^{W \cdot \log_{10} C_1 + (1-W) \cdot \log_{10} C_2} \quad (4)$$

Therefore, the posterior distribution of HFS can be used to estimate the mean human fecal score, as well as a 95% Bayesian credible interval (BCI).

In summary, the HFS can be interpreted as the mean concentration of human fecal marker at a beach site and be used to rank beaches with respect to their human fecal contamination.

Completed Work Task 2: Sensitivity analysis results

Sensitivity analyses using simulated datasets were conducted to evaluate the influence of sample size, number of qPCR replicates per sample, and site data distributions on HFS. A total of 975 scenarios were evaluated representing different combinations of sample size (N; 7 to 105 by increment of 7), qPCR replicate number (j; varied from 2 to 14 per sample by increment of 1) and site (Esco, Esco:Mcyn, Mcyn, Mcyn:Topa, or Topa). For each scenario, a new dataset was created from the respective site simulated dataset by randomly selecting N samples and j qPCR replicates per sample. Each scenario dataset was used to calculate HFS scores with variability. This process was repeated for 100 iterations for each scenario.

Sensitivity analysis results answered the following question that the management community needs to answer in order to effectively use HFS for practical applications: *How reliable are HFS estimates when different sample size (number of samples to take from a site) and effort of analysis per sample (number of qPCR replicates to run per sample) are invested for MST studies at different sites?*

This question was answered by examining how the mean and variance of HFS changed under the 975 scenarios. The main findings are as following:

- Increasing sample size reduced the bias of HFS and increased stability of HFS. Increasing the number of qPCR replicates had minimal effects on bias and stability (Figure 2).

Here, bias of HFS refers to how the estimate HFS differs from true value; stability refers to how narrow the range of HFS estimates are among the 100 iterations under each scenario. Stability is important because even though 100 iterations of “sampling” could be performed on a computer, real field application would be based on a single iteration and the range of possible HFS (i.e. stability of HFS) across the 100 iteration is important.

- Increasing sample size and number of qPCR replicates per sample both reduced the variance in HFS (Figure 3).

The influence of sample size on standard deviations and coefficients of variance was much stronger when sample sizes were smaller than when sample sizes were larger. Similarly, incremental increases in number of qPCR replicates lead to higher reduction in standard deviation and coefficients of variance of HFS when number of qPCR replicates were smaller than when number of qPCR replicates were larger.

- The extent sample size and number of qPCR replicates per sample affected mean and variance of HFS varied by site (Figures 2, 3).

As details of the site condition (relating to human fecal contamination) are generally unknown prior to initial MST marker sampling, the choice of sample size and number of qPCR replicates per sample must be made to accommodate the most conservative assumptions appropriate to the specific management application.

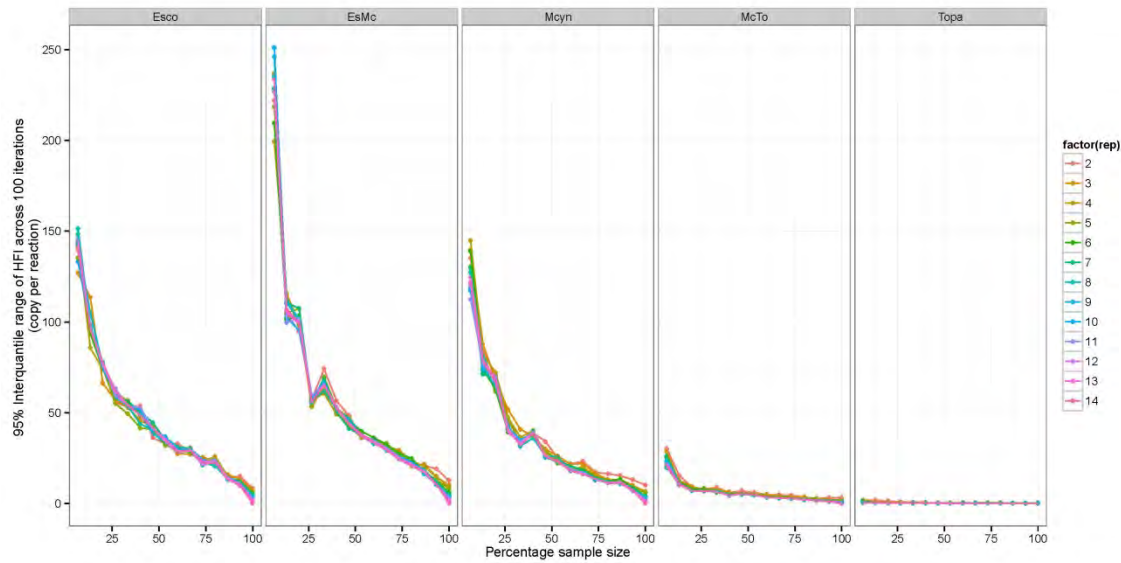


Figure 2. Effect of sampling depth and number of qPCR replicates (denoted by different colors) on the 95% inter-quantile range of HFS values across 100 iterations, for the five simulated field sites (Esco, EsMc, Mcyn, McTo, and Topa). Sampling depth was presented as the proportion of all 105 samples for a respective scenario.

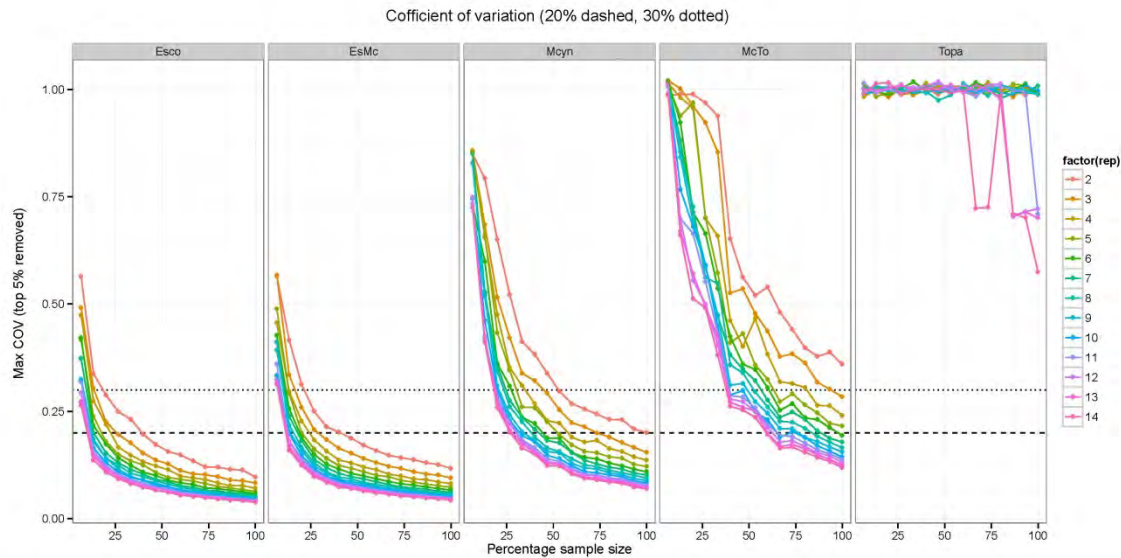


Figure 3. Effect of sampling depth and number of qPCR replicates (denoted by different colors) on coefficient of variation of HFS across the simulated field sites (Esco, EsMc, Mcyn, McTo, and Topa). Sampling depth was presented as the proportion of all 105 samples for a respective scenario. Y-axis represents the HFS maximum coefficient of variation (top 5% removed) for each site and scenario. Dotted and dashed lines indicate COV = 0.3 and 0.2, respectively.

Completed Work Task 3: Model use recommendation for site ranking

HFS was used to rank five simulated sites with expected pollutant gradient (sites were simulated based on real environmental data from 3 Los Angeles county sites) regarding their extent of human fecal contamination. HFS from the sites ranged from 50 to 0 (copy per 100 ml water) and the sites were correctly ranked from more polluted to clean.

To examine how sampling design choices (i.e. sampling depth and qPCR replication) affect the utility of HFS to rank field sites with different human fecal pollution levels, a maximum range derived from 100 iterations of HFS \pm 95% BCI scores was calculated for each sampling depth and qPCR replicate combination. In the best case scenario (14 qPCR replicates at 100% sampling depth), sites could be ranked as follows: (Esco and EsMc) > Mcyn > (McTo, and Topa), where maximum 95% BCI interval ranges do not overlap between site groups. Site ranking outcomes were then determined for each qPCR replicate and sampling depth combination to identify the minimum number of qPCR replicates at each sampling depth required to achieve the same ranking groups as the best case scenario with 5%, 10%, 15%, 20%, and 25% (corresponding to 95%, 90%, 85%, 80%, and 75% probability) of extreme HFS \pm 95% BCI scores removed (Figure 4). Figure 4 can help beach managers and regulators make informed decisions on field implementation of HFS to rank sites for pollution remediation. For example, if a manager requires 95% probability of obtaining the best scenario ranking (Figure 4, bottom panel), he/she can choose to sample 86.7% of the days with 3 qPCR replicates per sample or to sample 66.7% of the days with 8 qPCR replicates per sample.

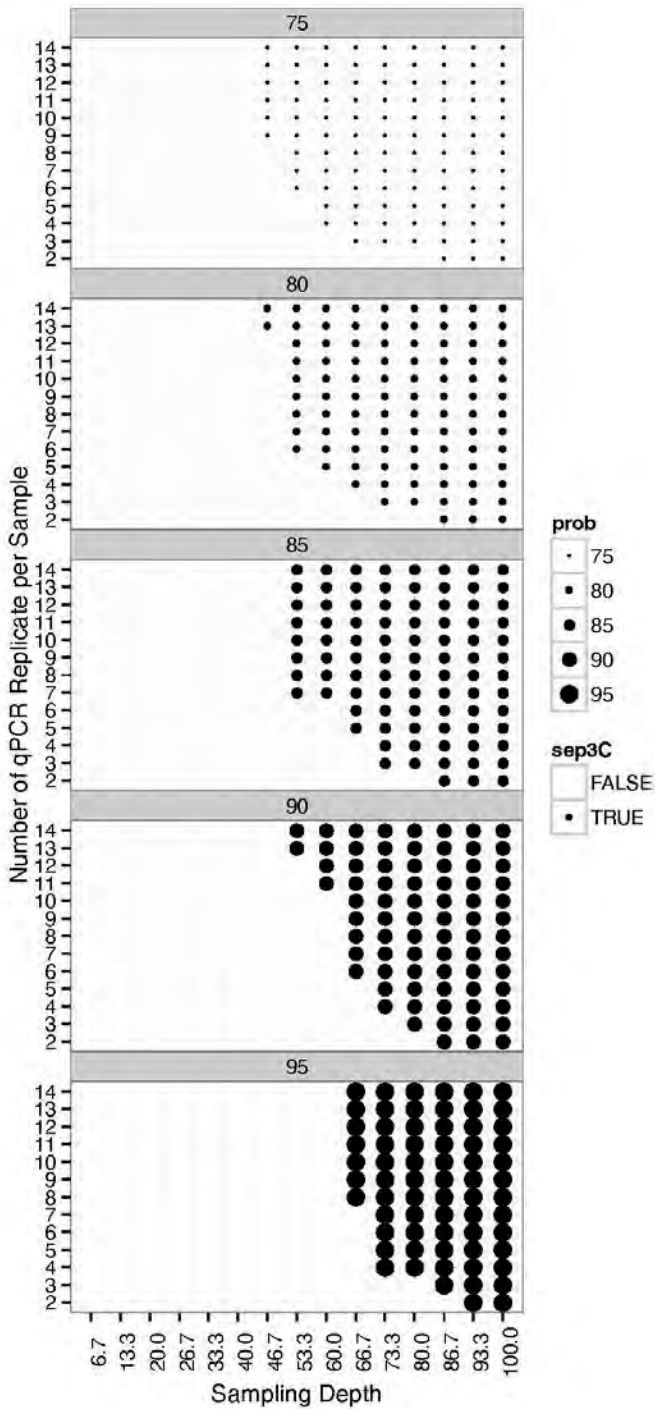


Figure 4. Recommendations on sample size (x-axis, sampling depth, i.e. % of days sampled out of available days within a given time period of interest) and number of qPCR replicates (y-axis) choices when using HFS for site ranking. Back symbols (i.e. “TRUE”) indicate site ranking under the selected combinations of sample depth and qPCR replication is the same as best case scenario, i.e. when all days were sampled (100% sampling depth) and 14 qPCR replicates per sample were run per sample. Size of symbols (i.e. “prob”) indicates the chance/probability managers would obtain such ranking.

Effect of Marker Degradation

However, it is important to consider how HF183 marker degradation may affect application of HFS. A wide range of decay rates ($k = <1 \text{ day}^{-1}$ to 6 day^{-1} , in $C = C_0 e^{-kt}$) were observed for the HF183 marker in this project: marine waters ($k = 1-2$), brackish waters ($k = 1-6$), freshwater ($k = 1-5$), water matrix laboratory study ($k = <1 - 5$), sediment ($k = <1-2$). These rates translate to <0.5 to $<3 \log_{10}$ reduction per day. Assuming a starting concentration of HF183 from fresh sewage input to be $6 \log_{10}$ copy per 100ml (5% sewage measured in this project averaged $6.7 \log_{10}$ copies of HF183 per 100ml), the HF183 signal would disappear in two days under the fastest decay rates observed in this project.

If the sewage fecal source is introduced locally at the beach, with a daily sampling scheme, the HFS would be integrating both the fresh and aged HF183 signals under most decay conditions. Nevertheless, with a less frequent sampling scheme (e.g. only once every two days), it would be possible to miss the HF183 signals under environmental conditions enabling the highest decay rates. It is therefore important for managers to consider the extent of potential HF183 marker decay at their site and compare that to the spectrum of rates observed in this project based on similarities of the field conditions, and adjust sampling design accordingly.

If the sewage fecal source is introduced upstream and needs to travel down before reaching the beach, the length of time required for the source to reach the beach would need to be ascertained in order to anticipate the impact of marker degradation on application of HFS at the beach. Estimating the travel time might be difficult, and loss of marker might be beyond just decay processes. In such situations, measuring markers upstream (or from beach to upstream) might be needed to provide more relevant information regarding extent of human fecal contamination.

Literature Cited

Cao, Y., C. Hagedorn, O.C. Shanks, D. Wang, J. Ervin, J.F. Griffith, B.A. Layton, C.D. McGee, T.E. Riedel, S.B. Weisberg. Towards establishing a human fecal contamination index in microbial source tracking. *Int. J. Environ. Eng. Syst.* **2013**, 4, 46-58.